CONDITION ASSESSMENT OF BRIDGE STRUCTURES USING STATISTICAL ANALYSIS OF WAVELETS

Thèse

Vahid Shahsavari

Doctorat en génie civil
Philosophiae Doctor (Ph. D.)

Québec, Canada

CONDITION ASSESSMENT OF BRIDGE STRUCTURES USING STATISTICAL ANALYSIS OF WAVELETS

Thèse

Vahid Shahsavari

Sous la direction de :

Josée Bastien, directrice de recherche

Luc Chouinard, codirecteur de recherche

RÉSUMÉ

La surveillance à distance des structures a émergé comme une préoccupation importante pour les ingénieurs afin de maintenir la sécurité et la fiabilité des infrastructures civiles pendant leur durée de vie. Les techniques de surveillance structurale (SHM) sont de plus en plus populaires pour fournir un diagnostic de "l'état" des structures en raison de leur vieillissement, de la dégradation des matériaux ou de défauts survenus pendant leur construction. Les limites de l'inspection visuelle et des techniques non destructives, qui sont couramment utilisées pour détecter des défauts extrêmes sur les parties accessibles des structures, ont conduit à la découverte de nouvelles technologies qui évaluent d'un seul tenant l'état global d'une structure surveillée. Les techniques de surveillance globale ont été largement utilisées pour la reconnaissance d'endommagement dans les grandes infrastructures civiles, telles que les ponts, sur la base d'une analyse modale de la réponse dynamique structurale. Cependant, en raison des caractéristiques complexes des structures oeuvrant sous des conditions environnementales variables et des incertitudes statistiques dans les paramètres modaux, les techniques de diagnostic actuelles n'ont pas été concluantes pour conduire à une méthodologie robuste et directe pour détecter les incréments de dommage avant qu'ils n'atteignent un stade critique. C'est ainsi que des techniques statistiques de reconnaissance de formes sont incorporées aux méthodes de détection d'endommagement basées sur les vibrations pour fournir une meilleure estimation de la probabilité de détection des dommages dans des applications in situ, ce qui est habituellement difficile compte tenu du rapport bruit à signal élevé. Néanmoins, cette partie du SHM est encore à son stade initial de développement et, par conséquent, d'autres tentatives sont nécessaires pour parvenir à une méthodologie fiable de détection de l'endommagement.

Une stratégie de détection de dommages basée sur des aspects statistiques a été proposée pour détecter et localiser de faibles niveaux incrémentiels d'endommagement dans une poutre expérimentale pour laquelle tant le niveau d'endommagement que les conditions de retenue sont réglables (par exemple ancastrée-ancastrée et rotulée-rotulée). Premièrement, des expériences ont été effectuées dans des conditions de laboratoire contrôlées pour

détecter de faibles niveaux d'endommagement induits (par exemple une fissure correspondant à 4% de la hauteur d'une section rectangulaire équivalente) simulant des scénarios d'endommagement de stade précoce pour des cas réels.

Différents niveaux d'endommagement ont été simulés à deux endroits distincts le long de la poutre. Pour chaque série d'endommagement incrémentiel, des mesures répétées (~ 50 à 100) ont été effectuées pour tenir compte de l'incertitude et de la variabilité du premier mode de vibration de la structure en raison d'erreurs expérimentales et du bruit. Une technique d'analyse par ondelette basée sur les modes a été appliquée pour détecter les changements anormaux survenant dans les modes propres causées par le dommage. La réduction du bruit ainsi que les caractéristiques des agrégats ont été obtenues en mettant en œuvre l'analyse des composantes principales (PCA) pour l'ensemble des coefficients d'ondelettes calculés à des nœuds (ou positions) régulièrement espacés le long du mode propre. En rejetant les composantes qui contribuent le moins à la variance globale, les scores PCA correspondant aux premières composantes principales se sont révélés très corrélés avec de faibles niveaux d'endommagement incrémentiel. Des méthodes classiques d'essai d'hypothèses ont été effectuées sur les changements des paramètres de localisation des scores pour conclure objectivement et statistiquement, à un niveau de signification donné, sur la présence du dommage. Lorsqu'un dommage statistiquement significatif a été détecté, un nouvel algorithme basé sur les probabilités a été développé pour déterminer l'emplacement le plus probable de l'endommagement le long de la structure.

Deuxièmement, se basant sur l'approche probabiliste, une série de tests a été effectuée dans une chambre environnementale à température contrôlée pour étudier les contributions relatives des effets de l'endommagement et de la température sur les propriétés dynamiques de la poutre afin d'estimer un facteur de correction pour l'ajustement des scores extraits. Il s'est avéré que la température avait un effet réversible sur la distribution des scores et que cet effet était plus grand lorsque le niveau d'endommagement était plus élevé. Les résultats obtenus pour les scores ajustés indiquent que la correction des effets réversibles de la température peut améliorer la probabilité de détection et minimiser les fausses alarmes.

Les résultats expérimentaux indiquent que la contribution combinée des algorithmes utilisés dans cette étude était très efficace pour détecter de faibles niveaux d'endommagement

incrémentiel à plusieurs endroits le long de la poutre tout en minimisant les effets indésirables du bruit et de la température dans les résultats. Les résultats de cette recherche démontrent que l'approche proposée est prometteuse pour la surveillance des structures. Cependant, une quantité importante de travail de validation est attendue avant sa mise en œuvre sur des structures réelles.

Mots-clés : Détection et localisation des dommages, Poutre, Mode propre, Ondelette, Analyse des composantes principales, Rapport de probabilité, Température

ABSTRACT

Remote monitoring of structures has emerged as an important concern for engineers to maintain safety and reliability of civil infrastructure during its service life. Structural Health Monitoring (SHM) techniques are increasingly becoming popular to provide ideas for diagnosis of the "state" of potential defects in structures due to aging, deterioration and fault during construction. The limitations of visual inspection and non-destructive techniques, which were commonly used to detect extreme defects on only accessible portions of structures, led to the discovery of new technologies which assess the "global state" of a monitored structure at once. Global monitoring techniques have been used extensively for the recognition of damage in large civil infrastructure, such as bridges, based on modal analysis of structural dynamic response. However, because of complicated features of real-life structures under varying environmental conditions and statistical uncertainties in modal parameters, current diagnosis techniques have not been conclusive in ascertaining a robust and straightforward methodology to detect damage increments before it reaches its critical stage. Statistical pattern recognition techniques are incorporated with vibration-based damage detection methods to provide a better estimate for the probability of the detection of damage in field applications, which is usually challenging given the high noise to signal ratio. Nevertheless, this part of SHM is still in its initial stage of development and, hence, further attempts are required to achieve a reliable damage detection methodology.

A statistical-based damage detection strategy was proposed to detect and localize low levels of incremental damage in an experimental beam in which the level of damage and beam restraint conditions are adjustable (e.g. fixed-fixed and pinned-pinned). First, experiments were performed in controlled laboratory conditions to detect small levels of induced-damage (e.g. 4% crack height for an equivalent rectangular section) simulated for early stage damage scenarios in real cases. Various levels of damage were simulated at two distinct locations along the beam. For each sate of incremental damage, repeat measurements (~ 50 to 100) were performed to account for uncertainty and variability in

the first vibration mode of the structure due to experimental errors and noise. A modal-based wavelet analysis technique was applied to detect abnormal changes occurring in the mode shapes caused by damage. Noise reduction as well as aggregate characteristics were obtained by implementing the Principal Component Analysis (PCA) into the set of wavelet coefficients computed at regularly spaced nodes along the mode shape. By discarding components that contribute least to the overall variance, the PCA scores corresponding to the first few PCs were found to be highly correlated with low levels of incremental damage. Classical hypothesis testing methods were performed on changes on the location parameters of the scores to conclude damage objectively and statistically at a given significance level. When a statistically significant damage was detected, a novel Likelihood-based algorithm was developed to determine the most likely location of damage along the structure.

Secondly, given the likelihood approach, a series of tests were carried out in a climate-controlled room to investigate the relative contributions of damage and temperature effects on the dynamic properties of the beam and to estimate a correction factor for the adjustment of scores extracted. It was found that the temperature had a reversible effect on the distribution of scores and that the effect was larger when the damage level was higher. The resulted obtained for the adjusted scores indicated that the correction for reversible effects of temperature can improve the probability of detection and minimize false alarms.

The experimental results indicate that the combined contribution of the algorithms used in this study were very efficient to detect small-scale levels of incremental damage at multiple locations along the beam, while minimizing undesired effects of noise and temperature in the results. The results of this research demonstrate that the proposed approach may be used as a promising tool for SHM of actual structures. However, a significant amount of challenging work is expected for implementing it on real structures.

Key-words: Damage Detection and Localization, Beam, Mode Shape, Wavelet, Principal Component Analysis, Likelihood Ratio, Temperature

TABLE OF CONTENTS

LIST OF TABLES

LIST OF FIGURES

LIST OF ABBREVIATIONS

ANN	Artificial Neural Network
ARTBA	American Road and Transportation Builders Association
AR	Auto-Regressive
CRIC	Canadian Infrastructure Report Card
CMIF	Complex Mode Identification Function
CWT	Continuous Wavelet Transform
COMAC	Coordinate Modal Assurance Criterion
COMSF	Coordinate Modal Scaling Factor
DWT	Discrete Wavelet Transform
EMD	Empirical Mode Decomposition
FEA	Finite Element Analysis
FHWA	Federal Highway Administration
FD	Fractal Dimension
FT	Fourier Transform
FFT	Fast Fourier Transform
FRF	Frequency Reference Function
GDF	Girder Distribution Factor
HHT	Hilbert-Huang Transform
LR	Likelihood Ratio
MAC	Structural Health Monitoring
MCS	Monte Carlo Simulation
MSF	Modal Scaling Factor
MSC	Mode Shape Curvature
MUSIC	Multiple Signal Classification
NDT	Non-Destructive Test
PP	Peak-Picking
PCA	Principal Component Analysis

PC	Principal Component
RC	Reinforced-Concrete
SHM	Structural Health Monitoring
STFT	Short-Time-Fourier-Transform
SUV	Singular Value Decomposition
WT	Wavelet Transform
WPT	Wavelet Packet Transform

LIST OF SYMBOLS

Mathematical Symbols

ω	Angular frequency
i	Imaginary unit
e	Euler's number
$( )^{*}$	Function complex conjugate
$[ ]^{T}$	Matrix transpose
{ }	Vector
$\int$	Integral
$\sum$	Summation
$\sqrt{}$	Square root
| |	Absolute value
#	Number
%	Percent
$\leq$	Less than or equal to
$\geq$	Greater than or equal to
=	Equality
~	Approximately equal
π	Pi constant
$(.)^{H}$	Complex conjugate transpose
∞	Infinity

Statistical Symbols

$\bar{x}$	Sample mean
N	Sample size
μ	Population mean
σ	Standard deviation
ν^2	Variance

P	P-value
H	Hypothesis testing
H0	Null hypothesis
H1	Alternative hypothesis
α	Type I error and/or significance level
β	Type II error
R	Sum of ranks
T	t-test statistic
Z	z-statistics
Dof	Hypothesis testing degree of freedom
U	Test statistic for the U-test
T	Test statistic for the t-test

Data Analysis Symbols

r	Mode shape number (subscript)
ω_r	Natural frequency of the r^{th} mode
h	Distance between two nodes
u	Undamaged (subscript)
d	Damaged (subscript)
$\{\phi\}$	Mode shape displacement vector
MAC(*u*,*d*)	MAC value between two mode shapes
MSC(*x*)	Mode shape curvature at location *x*
f(t)	Time-domain function
t	Time variable
F(ω)	Fourier Transform of *f*(t)
f(*x*)	Space-domain function
x	Spatial coordinate
$\Psi(x)$	Wavelet function
$\Psi(\omega)$	Fourier Transform of $\Psi(x)$
u	Wavelet function position parameter
s	Wavelet function scale parameter

j	Positive integer
k	Positive integer
D_j	j^{th} level of the Detail coefficient
A_j	j^{th} level of the Approximation coefficient
CWT(x)	Wavelet coefficient at location x
m	Number of observations
n	Number of variables/nodes
[X]	Wavelet coefficients matrix
[U]	Left-singular values of [X]
[Λ]	Singular-values of [X]
[V]	Right-singular values of [X]
[C]	Covariance matrix of [X]
PC_i	i^{th} principal component
λ_i	i^{th} eigenvalue
η_i	Percentage of variance for the i^{th} PC
[S]	Score matrix
$[S_1]$	Scores for the 1st set of measurements
$[S_2]$	Scores for the 2nd set of measurements
pc	Selected component (subscript)
$\{V\}_{pc}$	Selected eigenvector or PC
$\{S\}_{pc}$	Score vector for the selected component
$\{S_R\}$	Scores for the reference model
$\{S_i\}$	Scores for the alternative model
$LR(x_i)$	Likelihood Ratio at i^{th} location
$L(S_R \mid \mu, \sigma)$	Likelihood of reference scores
$L(S_i \mid \mu_i, \sigma_i)_i$	Likelihood of alternative scores at i^{th} node
Ru	Input covariance matrix
$\{\nu_i\}$	i^{th} mode shape
$S_y(s)$	Output spectrum matrix in the Laplace domain
λ	Variance of a white noise sequence
ξ	Modal damping ratios

ω_i	ith eigenfrequency
α_i	Scale factor

DEDICATION

To my lovely wife, Sara

ACKNOWLEDEGMENTS

First and foremost, I wish to express my sincere thanks to my advisors Prof. Josée Bastien and Prof. Luc Chouinard. Undoubtedly, without your consistent support, valuable guidance, critical feedback, and encouragement this dissertation would not have been possible. I would also like to thank Dr. Antoine Clément for his great ideas and contribution throughout this study.

I would like to thank thesis committee members, Prof. Josée Bastien, Prof. Luc Chouinard, Prof. Charles Darwin Annan, Prof. Laurent Molez, and Prof. James Goulet, for their valuable time in evaluating and improving the quality of this work.

I also would like to extend my appreciation to all the members of the CRIB Research Center at Université Laval, who have been incredibly supportive colleagues. I am very thankful to Mr. René Malo and Mr. Mathieu Thomassin Mailhot, CRIB structural laboratory technicians, for their technical assistance and availability to supply testing facilities.

I gratefully acknowledge the funding received through a CREATE grant from the Natural Sciences and Engineering Research Council of Canada (NSERC) and the CRIB Research Center.

I would like to acknowledge Dr. Shirin Panahi for English proof reading of the thesis.

I wish to extend my gratitude to my friends and family who played an integral role in the successful achievement of this thesis. My special thanks to my parents for their unflagging love and never ending support throughout my life.

At the end, but certainly not least, no words can describe how grateful I am to my lovely wife, Sara Kazemiha, for her unconditional love and support over the entire period of my Ph.D. studies.

FOREWORD

This dissertation is written in an manuscript-based format composed of seven chapters. In this thesis, the aim is to demonstrate *how the efficiency of damage detection techniques may be improved for small levels of damage on bridge-type structures*. Chapter 1 is a general introduction to Structural Health Monitoring (SHM) techniques and includes the problem, challenges of the research, overall objective and hypothesis of this work. The importance of global monitoring techniques for vibration-based assessment of structures is highlighted and reviewed according to the literature reviewed in Chapter 2. The methodology of this work is discussed in Chapter 3. Chapters 4-6 report the main findings of this research which are the subject of three publications. The author of this dissertation is the main author of all papers. The first draft of the papers including experimental work and data analysis was performed by the main author which are revised by all co-authors.

The publications are as follows:

Chapter 4

- **V Shahsavari**, J Bastien, L Chouinard, A Clément, (**2017**), "Likelihood-based testing of wavelet coefficients for damage detection in beam structures", Journal of Civil Structural Health Monitoring, 7(1), 79-98.

In this chapter, for the first time, the combined application of the Continuous Wavelet Transform (CWT), the Principal Component Analysis (PCA), and a series of statistical tests based on an adaptation of the Likelihood Ratio (LR) test are discussed and compared with current SHM techniques for damage detection in an instrumented beam. The experiments were performed under steady-state or controlled conditions of the laboratory where the main objective was to detect incremental damage at low levels of damage despite high noise to signal ratios. Furthermore, in addition to the above publication, some results of this work were published previously in an international conference proceeding, reporting the de-noising application of the PCA in the context of SHM.

- **V Shahsavari**, J Bastien, L Chouinard, A Clément, (**2015**), "A Novel Response-Based Approach to Localize Low Intensity Damage of Beam-Like Structures", The 5th International Conference on Smart Materials and Nanotechnology in Engineering, Vancouver, BC, Canada.

Chapter 5

- **V Shahsavari**, L Chouinard, J Bastien (**2017**), "Wavelet-Based Analysis of Mode Shapes for Statistical Detection and Localization of Damage in Beams Using Likelihood Ratio Test", Journal of Engineering Structures, 132, 494-507.

Given the promising results achieved from chapter 4, further investigations were performed in chapter 5 to examine the efficiency of the proposed likelihood-based approach for damage localization at different limit conditions, implying various levels of noise. Chapter 5 is a continuation of the work presented in chapter 4 to further validate the robustness of the approach for damage detection under steady-state condition of the laboratory.

Chapter 6

- **V Shahsavari**, L Chouinard, J Bastien (**2016**), "Detection of Structural Damage under Varying Environmental Conditions", Structural Health Monitoring, under review.

This chapter addresses challenges given by the reversible effects of temperature change on damage detection with a primary goal to expand the contribution of the proposed technique in real field tests. The experiments were performed in a climate-controlled room under two different temperature degrees. While the same methodology as in previous chapters was used in this chapter, a novel mathematical algorithm was established to obtain a temperature correction factor and minimize the reversible effect of the temperature on the likelihood result.

Finally, in Chapter 7, the overall conclusions, novelty of this work and future directions are discussed. Recently, an additional article has been submitted to the Journal of Structural Control and Health Monitoring as a natural continuation of this work. However, this article is not included in this thesis:

- L Chouianrd, O Baptista, **V Shahsavari**, J Bastien, (**2017**), "Objective Performance Measures of SHM for the Early Detection of Damage in Beams", Journal of Structural Control and Health Monitoring, under review.

CHAPTER 1

1. Structural Health Monitoring (SHM)

1-1 Introduction

According to recent surveys of the assets of civil infrastructure in the United States, the average age of the nation's 607,380 bridges is currently 42 years. In total, one in nine of the US bridges are rated as structurally deficient and require pressing replacement or rehabilitation of at least one major component. It has been estimated that $20.5 billion is needed annually to eliminate the nation's bridge deficient backlog by 2028, while there are nearly over two hundred million daily crossings across deficient bridges in the nation's 102 largest municipal regions (Herrmann, A. W. 2013). According to the American Road and Transportation Builders Association (ARTBA) most recent analysis on the raw 2015 bridge inspection data which was released by the Federal Highway Administration (FHWA) department, more than 9% of the nation's bridges are in poor condition rating, meaning that 58,495 bridges are currently classified as structurally deficient (ARTBA, 2016). The 2016 Canadian Infrastructure Report Card (CIRC) also indicates that approximately 30% of bridges in Canada are at risk of rapid deterioration, representing a call for immediate action before a catastrophic failure event occurs (CIRC, 2016).

Bad design, faulty construction, and extraordinary loads may introduce substantial change of stress/strain distributions in structural elements and cause damage or unexpected failures of structures. In December 1967, the Silver bridge suddenly collapsed into the Ohio River due to a defective eyebar that experienced a cleavage fracture in the lower part of its head. This disaster killed 46 people while only 9 survived (Bosela, Brady et al. 2013). Bridges are generally rated and largely monitored by the predominance of visual inspection and nondestructive evaluation techniques (Moore, Phares et al. 2001). In general, nondestructive techniques can be used for

variety of purposes such as investigating mechanical properties of subsurface layers in structures and/or detecting defects and discontinuities on small portions of structures (Shahsavari 2011).

Table 1-1 lists some of the main nondestructive techniques frequently used in engineering fields. The critical changes experienced in structural parameters are commonly investigated by non-destructive inspection techniques, such as acoustic emission methods, X-ray methods, and thermal field methods. These methods are based on a local evaluation in easily accessible surfaces of the structure and are, therefore, referred to as "local monitoring methods". Furthermore, they are passive and costly methods, since a large amount of human intervention is required to obtain prior knowledge of the damage distribution in order to perform inspection (Robertson, Farrar et al. 2003, Sahin and Shenoi 2003, Han, Ren et al. 2005, Perera and Huerta 2008).

Table 1-1: Most frequently used nondestructive methods.

Method	Standard Code
Visual inspection	ASTM C832
Sonic test	ASTM C597
Impact-echo	ASTM C1383
SASW	ASTM D6758
Impulse response	ASTM C740
Acoustic emission	ASTM STP 571
Radar	ASTM 4748
Infrared thermography	ASTM D4788
X-ray	ASTM CI723
Schmidt hammer	ASTM C805

The limitations of local monitoring techniques raise the need to introduce global monitoring methods. The need of nondestructive and global techniques leads to the development of damage diagnostic techniques by measuring global parameters of structures at a few easily accessible points on the structure. An ideal Structural Health Monitoring (SHM) technique is expected to remotely monitor the structure with almost no human interventions (Salawu and Williams 1995, Alvandi and Cremona 2006, Curadelli, Riera et al. 2008). Research on the potential of damage

detection and localization on the basis of vibration-based analysis techniques date back to the late 1970s from studies in various fields. In the past decade, vibration-based analysis techniques have evolved to the remote monitoring of structures based on observable changes in the dynamic characteristics of structures (e.g. natural frequencies and mode shapes) as a result of localized structural damage (Taha, Noureldin et al. 2006).

In the last thirty years, the number of studies that attempted to evolve SHM to more sensitive and quantifiable methods for damage detection has increased considerably. In contrast with the application of SHM to mechanical systems (e.g. rotating machinery industry), which has been accomplished with the transition from a research topic to successful implementation by practicing engineers, the application of SHM for civil infrastructure on larger scales, such as bridges, has not been particularly effective. This can be explained due to a combination of different factors, including the relatively large size of civil infrastructure, the greater amount of uncertainties inherently existing in material properties, support conditions, system connectively, and variability in operational and environmental conditions. The vibration-based damage assessment of bridge structures was initiated by the civil engineering community since the early 1980s. It was motivated by a number of unexpected bridge failures which resulted in a great deal of attention to the need for early detection of damage or structural change, as well as the desire to minimize life cycle costs of such structures (Harik, Shaaban et al. 1990, Wardhana and Hadipriono 2003).

To build on this research, a large proportion of this study is allocated to the damage monitoring of bridge or beam-like structures as a means to argue and/or overcome the shortcomings of current local Non-Destructive Tests (NDT).

1-2 Objectives of SHM

In this project the industrial interests of SHM as well as scientific originality and contribution required for a Ph.D. project were considered. These two aspects included both challenges and opportunities. For most SHM systems in the field of civil engineering, the industrial objectives maybe expressed as follows (Balageas, Fritzen et al. 2006):

- To reduce the repair costs of civil infrastructures (economical aspect).
- To improve safety and ensure the reliability of civil infrastructures before it reaches a critical state.
- To specify the weak zones of construction and prevent the destruction of structures.
- To prolong the life time of structures by the early detection of damage.
- To increase safety factor of global monitoring techniques of structures.

In order to fulfill our desire for the purpose of precise diagnosis of damage in structures, continuous remote monitoring of structures could be a promising approach in the field of civil infrastructures. Damage detection based on dynamic monitoring of structures can be designed to reach four different levels (Rytter 1993):

1) Detection of the existence of damage
2) Location of the damage plus level 1
3) Extent of the damage severity plus level 2
4) Estimation of the remaining service life of the structure which is usually uncoupled from other three levels.

In this case, the term damage is defined as reduction in stiffness for steel girder bridges. To this end, incremental damage scenarios are introduced into the system connectivity of an experimental beam, which is an assembly of three bolted sections. Since any modification on the connection system relative to its initial or fully bolted configuration state weakens the rigidity of the beam at the location of joint assembly, different patterns of incremental damage can be introduced by removing sequentially a set of stiffeners at each joint. More detailed explanations are found in the Sections 3-2-1 and 3-2-2 of this dissertation.

1-3 SHM Solution Steps

Like nondestructive techniques, SHM can use two approaches: a) passive and b) active. The two possible attitudes in which both experimenter and examined structures are involved is indicated

in Figure 1-1. Passive monitoring refers to an operation in which the structure is being monitored based on evaluations received from embedded sensors. Conversely, if the experimenter has equipped the structure in such a way that both sensors and actuators are used to monitor the response of the structure, the monitoring becomes active (Balageas, Fritzen et al. 2006).

The active monitoring of a highway bridge with a high volume of traffic would be nearly impractical. Indeed, it would require the entire closure of the bridge in order to perform the required vibration test and a high energy shaker. Instead, to ensure a continuous monitoring of the bridge, the passive approach is preferred. The latter will greatly facilitate the remote access for data processing and continuous evaluation of the structure (Olund and DeWolf 2007). For real field tests, the use of free excitation sources (e.g. ambient vibrations due to traffic loads, wind, human activities, etc) is encouraged to retrieve data.

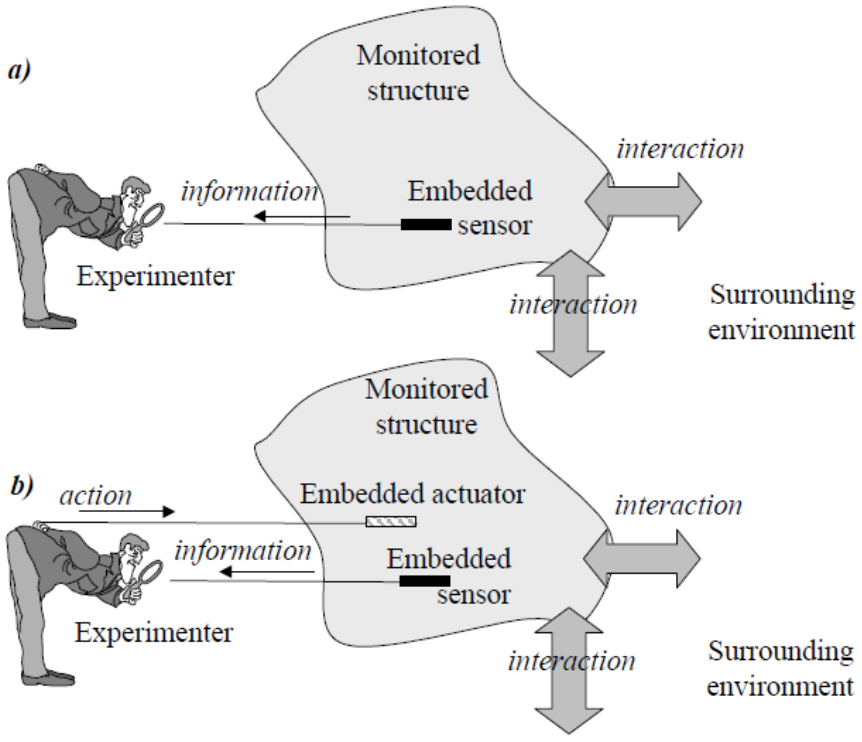

Figure 1-1: The two possible situations of SHM: a) passive and b) active monitoring (Balageas, Fritzen et al. 2006).

Recently, damage detection has been treated more as a classification problem of different patterns formed by the damaged and undamaged response of structures. Thus, it can be included into the statistical pattern recognition paradigm. This paradigm can be explained as the following four-part process for the development of SHM solutions (Farrar, Doebling et al. 2001, Sohn, Farrar et al. 2001, Sohn, Farrar et al. 2004):

1) Operational evaluation
2) Data acquisition
3) Feature extraction
4) Statistical model development for feature classification.

Operational evaluation is the first step of the SHM solution process which answers four questions concerning the implementation of a SHM system: 1) What are the economic justifications and/or life safety for the monitoring process of a system? 2) How is damage defined for the system that is going to be monitored? 3) What are the operational and environmental conditions for performing the monitoring? and 4) What are the data acquisition limitations in the operational environment?

The data acquisition portion consists of selecting different quantities to be measured such as excitation methods, data acquisition/storage/transmittal hardware, the type of sensors, locations, numbers, and bandwidth. Once the data is collected, they must be analyzed to reveal the information related to the existing damage. This is done by extracting damage-sensitive features from the measure vibration response (Farrar, Doebling et al. 2001, Sohn, Farrar et al. 2004). A damage-sensitive feature is a certain quantity derived from the measured vibration response that is correlated with the presence of damage in a structure and allows one to distinguish between the undamaged and damaged states. This process is based on fitting a variety of methods to identify features for damage detection. Several features (e.g. the resonance frequencies of a structure and mode shapes) are often selected for a structure that can be assembled into a feature vector for further analysis.

The last portion of statistical pattern recognition, statistical modeling for feature classification, is concerned with the implementation of the algorithms that operate on the extracted features for their classification and de-noising. However, the least attention in the literature has been given to the development of statistical models, which are essential to enhance the efficiency of damage detection techniques and decision making rules. The statistical models are used to answer, in an unambiguous and quantifiable manner, different questions about the damage state such as the existence, location, type, and extent of damage. The testing of these models on actual data is the important stage of the statistical model development process used to establish the sensitivity analysis of the selected features to damage and to study the possibility of false indications. More information on this paradigm may be found in cited reviews (Farrar, Doebling et al. 2001, Sohn, Farrar et al. 2004, Figueiredo, Park et al. 2009).

1-4 Problem Statement

In large scale civil structures subjected to environmental variations and noisy conditions, the determination of damage without filtering the undesired effects of these factors on global characteristics of structures is not reliable. This occurs particularly when damage-induced modifications in modal parameters at low levels of damage are at the same order of magnitude due to environmental conditions (Farrar and Worden 2012).

Environmental and operational variations can often conceal slight structural changes caused by damage that are not easily discernible by standard testing methods and may cause false indications of damage (Sohn, Farrar et al. 2004). The latter implies the need to develop statistical pattern recognition paradigms with an effort to minimize the effects of environmental variability on the measurements obtained from real-time monitoring of structures. The values obtained from statistical predictions on thermal gradients in a steel box-girder over multiple years in France, were found to be outside the guidelines proposed by the Eurocode at the time (Lucas 2003, Olund and DeWolf 2007).

In contrast to large civil engineering infrastructures that environmental variations have higher negative effects on measurements, the mechanical systems are, in most cases, mounted in a relatively confined environment and perform under relatively constant conditions. This and the uniqueness of each civil structure, are the main reasons that explain the difference of maturity in vibration-based SHM technology between mechanical and civil engineering (Farrar and Worden 2012). Until now, there is little literature describing the application of this technology to bridge damage detection studies. The availability of mechanical parts in large inventories with data available from both damaged and undamaged systems is another fact that discriminates the application of SHM in mechanical engineering from civil engineering. However, civil structures, in general, such as highway bridges are irreplaceable items with little or no data available from the damaged structure. In mechanical engineering the number of damage scenarios is often limited and the possible positions of damage are restricted to fairly small partial regions. However, one of the primary challenges of many damage detection studies in civil engineering research is to define either the damage type or the areas where damage can occur. In general, the response of mechanical systems are exhibited to harmonic-like inputs that are stationary, while measured inputs produced by external loads in civil structures (e.g. traffic trends) are often non-stationary and assumed to be random in nature. On the other hand, data acquisition equipment for mechanical pieces may consist of a single sensor and single channel analyzer. In contrast, in large scale civil monitoring systems, since the approximate location of damage is not generally known, several channels distributed over a relatively large spatial zone are required to complete the setup (Farrar and Worden 2012).

For damage detection at low levels, one of the most important challenges is to increase the sensitivity of SHM methods to detect slight changes of structural characteristics due to damage in an early stage without obtaining false alarms and distinguish between the effects of the damage from the environmental variations (Balageas, Fritzen et al. 2006). Most SHM approaches rely mainly on the features extracted from modal-based techniques alone, which are found poor indicators of localized damage in the presence of noise or environmental variations (Wahalathantri, Thambiratnam et al. 2010, Beskhyroun, Wegner et al. 2012).

The portion of the SHM that has received the least attention is the development of statistical modeling for feature classification which represents one of the crucial points of this research (Farrar, Doebling et al. 2001, Sohn, Farrar et al. 2004). Conceptually, the current vibration-based damage detection methods more or less use the pattern recognition/classification techniques which can discriminate features that are extracted, classified, and monitored. In almost none of several studies reported by Doebling et al. (1996) and Burton et al. (1998), the statistical methods have not been used to assess if changes in selected features are statistically significant for damage decision making (Sohn, Farrar et al. 2004). Lately, few researchers have tried to discriminate between irreversible changes in natural frequencies due to structural damage to those from reversible thermal effects. Comparatively very little attention has been devoted to investigate the variations in air temperature on the vibration modes of structures. For a bridge with small levels of incremental damage and prone to varying environmental conditions, damage detection through changes in natural frequencies and mode shapes can get masked due to adverse impacts of environmental conditions on modal parameters (Doebling, Farrar et al. 1996, Xu and Wu 2007). Current studies are mostly based on either pure statistical approaches or machine learning algorithms to detect the existence of damage under temperature variations only and fail to provide local information about the location and/or extend of damage (Sohn, Dzwonczyk et al. 1999, Cury, Cremona et al. 2012). For both cases, to derive a robust damage detection decision rule training data sets are required from undamaged states of a given structure in different environmental conditions, which are rarely available for real structures (Sohn, Farrar et al. 2004).

In several studies, the damage detection techniques have been encountered with serious problems to localize damage in case of simultaneous and multiple damage scenarios. Considering the economic aspects and human interventions, in in-situ cases, localization of damage has required for too many sensors to measure the structural response (Alvandi and Cremona 2006, Alvandi, Bastien et al. 2009).

Although the idea of using modal parameters was attractive for engineers in many years, these indices cannot be used as directly reliable and effective damage indicators (Sun and Chang 2004). In many existing vibration-based approaches temporal signals measured from the structure are analyzed via traditional Fourier Transform (FT), whereas it is not able to preserve

both the time and frequency information of the signals (Sun and Chang 2002, Law, Li et al. 2005). Wavelet transform (WT) is another approach that has recently been developed as an extension of FT with adjustable window locations and sizes (Sun and Chang 2002, Law, Li et al. 2006). Over the past 10 years, because of the time-frequency multi-resolution property and the ability of WT to perform local analysis of a signal, this method has become one of the most fast-evolving mathematical and signal processing tools to reveal some hidden aspects of the data that other signal processing tools fail to detect (Sun and Chang 2002, Law, Li et al. 2005, Law, Li et al. 2006). This study deals with wavelet analysis in order to expand successful applications of this technology for SHM of real structures.

Despite powerful assets of the wavelet analysis in the processing of signals, it cannot provide clear or consistent patterns in noisy conditions and complicated damage scenarios at small levels of damage. To overcome the limitations of WT, a robust statistical pattern recognition technique has to be developed in order to recognize and extract the features that are highly correlated with damage and are less sensitive to environmental noise.

1-5 General Objectives of the Research

The objective of the ongoing research is to improve the feasibility of vibration-based damage detection techniques to identify the existence and location of damage in bridge structures. Statistical models are developed to further evolve the processing of signals obtained from dynamic measurements in the presence of noise and environmental/operational variations. In particular, since temperature is the most important factor influencing the dynamic characteristics of structures, this study aims to overcome the difficulties associated with previous studies for damage detection under temperature variations.

Aside from the points discussed above, another goal of this research is to discuss the sensitivity of damage localization in noisy conditions which may reduce the ability to detect damage where there are low levels of damage (Farrar, Baker et al. 1994, Taha, Noureldin et al. 2004). In addition, due to insufficient attention on the statistical modeling for damage detection studies reviewed herein (Sohn, Farrar et al. 2004, Farrar and Worden 2012), this research will further

discuss the important contribution of the statistical techniques to accurate identification of structural damage.

To comply with the aforementioned objectives of this project, the implementation of special algorithms that can operate on the extracted feature has become essential on the successful application of the wavelet analysis for health monitoring of bridge-type structures. In order to achieve these goals, an experimental program was planned in the laboratory that will be described in detail in the chapters that follow.

1-6 Originality

The amount of research that has been considered thus far is neither sufficient nor promising to study the effect of environmental variations in beam-like structures (Cross, Koo et al. 2013, Grosso and Lanata 2014). This project has raised various challenges in order to improve the dynamic response analysis of such structures subjected to thermal variations. However, the most fundamental challenge of this project was that the dynamic response of the structures due to environmental and operational variations (e.g. ambient temperature, moisture, wind, and loading conditions) may not be overlooked (Sohn, Farrar et al. 2004). Considering the importance and difficulties related to this subject, a mathematical algorithm was established to correct for the reversible effect of temperature on measured data obtained from different surveys subject to different temperatures.

To address issues related to the limitations of the WT for damage detection in high noise to signal ratio environments, a de-noising algorithm based on a statistical method called the Principal Component Analysis (PCA) method was developed to introduce new features that explained most of the information contained in the observations and were sensitive to changes in the structural dynamic response due to damage. In addition, since experimental errors and environmental noise are important obstacles to gain pure information of the structure to be monitored, a large number of repeated measurements were performed for each state of structure in order to minimize statistical uncertainty and variability in experimental measurements.

Another novelty of this project was to set a statistical level of significance to attain a reliable damage decision making. This significance level obtained from statistical procedures may have enhanced the accuracy of results where different false alarms existed for damage detection as a result of varying factors such as experimental noise. For this purpose, a set of statistical procedures were proposed to perform damage detection for a given significance level. Given statistical detection of damage, a novel statistical approach based on an adaptation of the Likelihood Ratio (LR) test is proposed to localize clearly small levels of damage.

1-7 Thesis Outline

This thesis contains seven chapters based on three manuscripts. The current chapter introduces the project definition, motivations, objectives, and the problem to be face.

Chapter 2 includes a review of the literature as a basis for understanding the subsequent research. A state-of-the-art is presented in this chapter, which reviews the evolution of vibration-based damage detection techniques in global monitoring of bridge-type structures. The details of the problem, principle of current and traditional techniques as well as their advantages and limitations are provided.

Chapter 3 defines the methodology and rationale for technical specifications in the experimental program required for a complete formation of the test configuration setup.

Chapter 4 covers the results of the first article published in the Journal of Civil Structural Health Monitoring. A comparative study is conducted to highlight the limitations of conventional techniques and evaluate the sensitivity of the proposed approach for damage detection in low signal to noise ratio. In this chapter, a set of different statistical tests are explored to detect damage statistically and minimize false indications of damage due to experimental noise with the raw data presented. Moreover, a novel statistical pattern recognition technique is developed to locate different levels of incremental damage gradually evolving from the lowest to highest level of damage. The methodology is tested in an experimental beam restrained at two ends. The results and discussion are presented in the same chapter.

Chapter 5 contains the results of the second article published in the Journal of Engineering Structures. In chapter 5, the proposed methodology was tested and validated with a new set of sensors network implemented on a beam with different boundary conditions (e.g. pinned-pinned and fixed-fixed). The experiments were performed in controlled laboratory conditions to detect small levels of induced-damage simulated for early stage damage scenarios in real cases. In this chapter, a good understanding of the concept behind the proposed methodology was achieved which indicate that the results are in agreement with the results obtained in the previous chapter.

Chapter 6 describes the results of the third article submitted to the Journal of Structural Health Monitoring. In this chapter, given the validity of the proposed approach for damage detection in the laboratory-controlled conditions from chapters 4 and 5, a novel mathematical algorithm was developed to investigate the effect of temperature changes in damage detection. The purpose of this chapter was to minimize the probability of false alarms due to undesired effects of temperature in damage detection and provide a reliable protocol to discriminate between the effect of damage and temperature change in measured data. The experiments were performed in a climate-controlled room and the discussion of the results are presented in the same chapter.

Lastly, chapter 7 provides final conclusions and original findings of this study with suggestions for future work.

CHAPTER 2

2. Literature Review

2-1 Introduction

This chapter provides an overview of the different studies based on the vibration-based assessment of bridge-type structures. The state-of-the-art aims to highlight the originality of the present study and tries to outline how the proposed approach departs from previous studies in this field. As illustrated in the previous chapter, global monitoring methods have developed broadly in different studies because of their advantages over conventional local monitoring methods. Over the past years, numerous attempts have been made by many researchers to assess the efficiency of different techniques through a wide variety of parameters. Modal parameters such as natural frequencies and mode shapes are the most popular global parameters that are closely related to each other for damage detection.

2-2 Introduction to Natural Frequencies and Mode Shapes

The theoretical explanation begins with the introduction of the Fourier Transform (FT) before presenting the identification of modal parameters. The Fourier analysis is defined as a method of decomposition of a function into a set of basic sinusoid functions of various frequencies and phases (Kim and Melhem 2004, Bajaba and Alnefaie 2005). The process of FT can be explained as the sum over all the times of the signal multiplied by a complex exponential. The FT results in many Fourier coefficients which yield the sinusoidal components of the original signal through selection of a sinusoid function with appropriate frequency, ω, multiplied by Fourier coefficients (Misiti, Misiti et al. 1996). To go beyond the colloquial conversation, the mathematical expression of the FT for a periodic function $f(t)$ using a complex exponential over an infinite range $(-\infty , +\infty)$ can be expressed as:

$$F(\omega) = \int_{-\infty}^{+\infty} f(t)e^{-i\omega t}\, dt \tag{2.1}$$

where $F(\omega)$ is the Fourier transform of the function $f(t)$, $i = \sqrt{-1}$ is the complex number, ω is the angular frequency, and t is the time variable. The equation below shows the inverse Fourier transform that produces a function of time:

$$f(t) = \frac{1}{2\pi} \int_{-\infty}^{+\infty} F(\omega)e^{i\omega t}\, d\omega \tag{2.2}$$

More details about the FT can be found in (Kreyszig 2007). The function $F(\omega)$ allows us to visualize the frequency contents of the function $f(t)$. Therefore, Fourier analysis of the periodic function $f(t)$ able to one to go through either the time or frequency domains of the function (Figure 2-1).

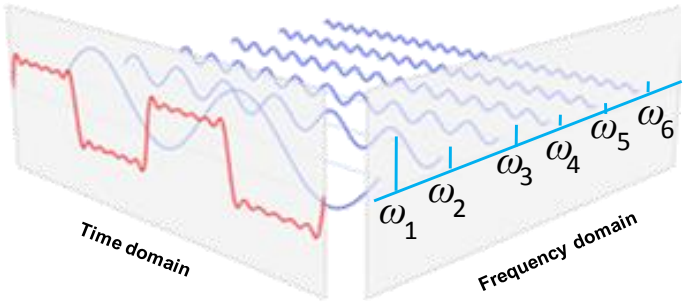

Figure 2-1: Graphical representation of the FT (adapted from http://pgfplots.net).

The FT has made possible the development of modal analysis as the study of the natural characteristics of structures. To become better acquainted with the basic premise behind this theory, a constant sinusoidal force is applied with varying frequency of oscillation on a freely supported flat plate. This excitation is applied in a manner where the peak force will always be the same value. Using an accelerometer attached to one corner of the plate, if the time-history response of the plate is drawn due to the excitation, it will be noticed that the amplitude changed while corresponding to the different rates of oscillation of the input force (Figure 2-2). As time passed, it will be observed that the response function amplifies at different points where the rate

of oscillation of the input excitation gets closer to the natural frequency of the system. By transforming the measured time data from time-domain to the frequency-domain, we can compute the so-called Frequency Response Function (FRF). As shown in Figure 2-3, by overlaying the time trace with the FRF, it will be noted that the peak values of the FRF, which occurr at the resonance frequencies of the system, correspond to the input frequency at which the time response is observed to reaches its maximum value (Avitabile 2001).

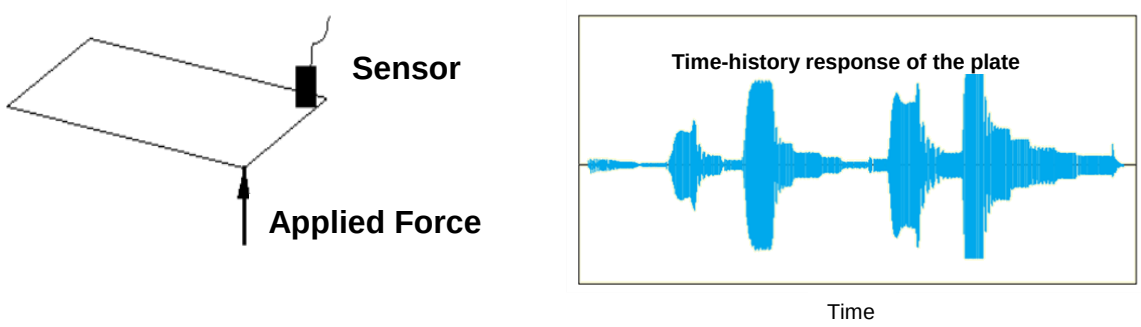

Figure 2-2: Left: Plate excitation, Right: Time-history response of the plate (adabted from Avitabile 2001).

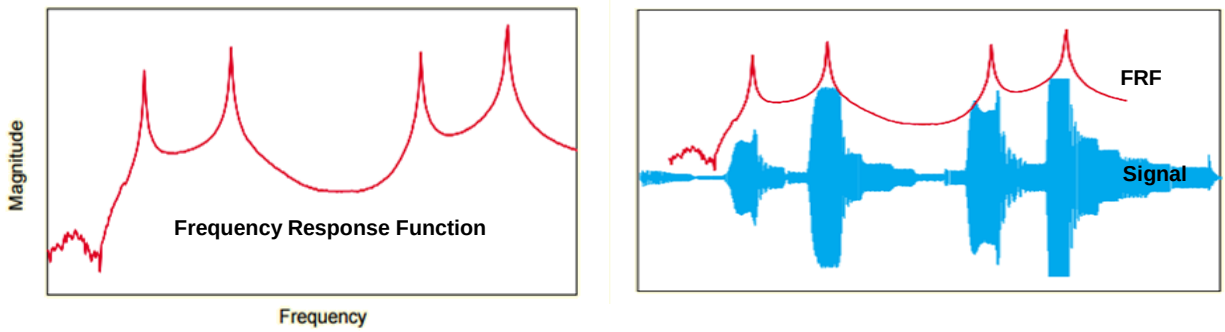

Figure 2-3: Left: Frequency response function (FRF), Right: Superposition of the time and FRF (adabted from Avitabile 2001).

In the latter case, when the frequency of external excitation coincides with natural frequencies of the system the deformation pattern of the structure will be different for each frequency mode. The term "mode shape" is introduced as one of the deformation patterns of a structure that occur at a particular resonance frequency. As an example, for a plate covered with 45 evenly distributed accelerometers it will be seen that a deformation pattern (mode shape) exists at each

one of the natural frequencies of the structure. The above explanation is well identified in Figure 2-4 (Avitabile 2001). Nonetheless, depending on the type of excitations (impact, ambient, sine), there are various modal analysis algorithms to estimate the mode shape in either time-domain requency-domain analyses with different degrees of reliability (Liou and Jeng 1989, Banejad and Ledwich 2002, Peeters and Ventura 2003, Wu, Lu et al. 2013).

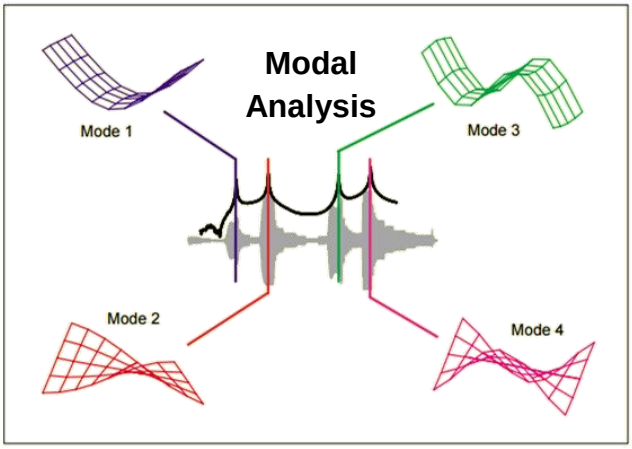

Figure 2-4: Extraction of mode shapes associated with natural frequencies of the plate (adabted from Avitabile 2001).

In general, the type of excitation is very important for accurate measurement of structural responses. In many mechanical engineering systems, dynamic loads can be represented by simple harmonic characteristics of rotating machinery. These excitations are sometimes induced by vibrating machines on industrial installation and supporting foundations (Tedesco, McDougal et al. 1999). The extrapolation of traditional input devices used in mechanical engineering to civil engineering is an important issue in the excitation of large structures. Creative solutions have been found in some papers for the excitation of large structures. Cunha et al. (1999) reported the vibration tests on a cable-stayed bridge by a sudden release of a heavy mass that was suspended from the bridge. Delaunay et al. (1999) described a way to horizontally excite a bridge by a sudden release of a tension cable that connected the bridge to a tug-boat. For the above excitations methods the input is impact-like and the responses are free vibrations. In the last ten years, more attention has been paid to measure the structural response due to ambient excitations originated from freely available "natural" sources. Although these sources cannot be measured exactly, the advantage of using ambient sources is to reduce significantly the cost of

dynamic tests implementation (Peeters 2000, Peeters, Maeck et al. 2001). The excitations can emanate from many different sources which differ in their characteristics, such as pedestrian traffic-induced loads (live loads), ground motion due to construction activities, blast loading and explosion, impact loads, earthquake loads, wind, and waves (Tedesco, McDougal et al. 1999).

The principal mechanical properties that influence the modal parameters, notably natural frequency and the mode shapes, are the mass and stiffness of the system. For a simple supported beam with uniform mass and stiffness, the analytical solution of dynamic equations can be used to determine the value of natural vibration modes (φ) and frequencies (ω_r) depending on the mode number (r), beam length (L), modulus of elasticity (E), inertia (I), and mass (m).

$$\omega_r = \frac{\pi^2 n^2}{L^2}\sqrt{\frac{EI}{m}} \tag{2.3}$$

$$\varphi_r(x) = C_1 \sin\frac{n\pi x}{L} \tag{2.4}$$

where $C_1 = 1$ gives the maximum value of $\varphi_r(x)$ equal to unity (Chopra 2007).

However, the above equations are only valid when there are constant mechanical properties over the entire length of the beam. For simple structures this analysis can be done manually, but for complex structures where the presence of any local variations in the mass or rigidity makes the quick analysis impossible, Finite Element Analysis (FEA) can be performed (Chopra 2007).

Abnormal events due to existence of damage in the structure can be identified as some irregularities in the form of vibration modes. However, mode shapes do not always manifest these irregularities clearly for the case of small abnormalities (Liew and Wang 1998, Grégoire 2011). The proposed methodology in the present study allows the clear identification of such minor deviations in the mode shape that cannot be easily evident from visual inspection of observed changes in this indicator.

2-3 Global Picture of SHM

Early detection of damage may provide many opportunities for prolonging the life of a structure. High attention in the improvement of vibration-based damage detection of structures has resulted

in introducing several techniques to monitor the global behaviour of structures (Doebling, Farrar et al. 1998, Balageas, Fritzen et al. 2006). Figure 2-5 shows the global classification of SHM methods.

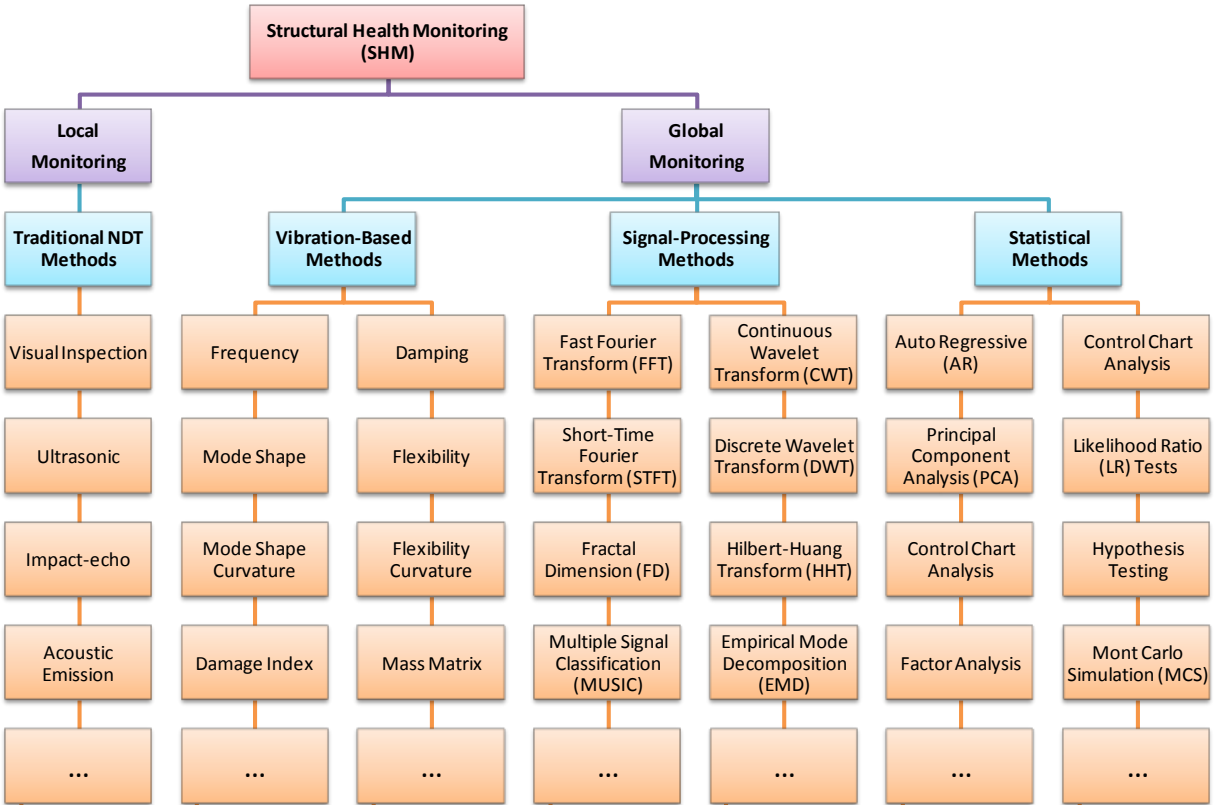

Figure 2-5: Global classification of SHM techniques.

In this figure, the SHM systems are divided mainly into two groups, namely, "local" and "global" monitoring methods. Local methods are referred to NDT used for local evaluation of the structure at the portions that are easily accessible. As it was discussed in the first chapter, these methods involve in a large amount of human intervention to obtain prior knowledge of the damage distribution (Robertson, Farrar et al. 2003, Sahin and Shenoi 2003, Han, Ren et al. 2005, Perera and Huerta 2008). Thus, the priority of this research is to improve techniques with global inherent characteristics.

Given that global parameters of structures are correlated to damaged-induced changes in dynamic characteristics of structures, they can be used as an inductive of structural damage using

a few sensors remotely to monitor the dynamic behaviour of structures (Pandey and Biswas 1994). However, the core issue of most vibration-based methods is to choose damage features that are sensitive to structural damage and immune to noise or environmental variations (Han, Ren et al. 2005).

Global monitoring methods represent the second group of SHM systems which have been recently introduced to overcome the shortcomings of local techniques. Global methods are divided themselves into three subgroups: a) those mainly representing different types of vibration-based based methods used for damage detection alone, b) those exploring combined applications of both signal processing tools and vibration-based damage detection techniques to enhance the efficiency of monitoring methods, and c) those introducing the contribution of statistical pattern recognition algorithms to address issues related to uncertainty and variability due to noise or varying environmental conditions. The next section summarizes the results and findings of previous studies in the literature.

2-4 Global Monitoring Methods

2-4-1 Vibration-Based Damage Detection Methods

Damage detection through changes in the natural frequency of structures is one of the most utilized and oldest methods for SHM owning to the fact that this parameter can be investigated easily and provides an inexpensive assessment technique. However, in any attempts to apply this technique to civil engineering structures special care must be taken into account to filter out the impact of varying environmental conditions, especially temperature, on this parameter. In this instance, the vibration tests on the I-40 Bridge over the Rio Grande in New Mexico, USA, was carried out by Farrar et al. (1994) to determine if the natural frequencies of the bridge can be implemented in order to identify induced structural damage. Damage was introduced to the bridge by gradually cutting one of the bridge girders at four levels. Given the fact that the stiffness of the bridge is proportional to the magnitude of its natural frequencies, the progress of damage was expected through reduction of the frequencies. However, the authors found that the measured natural frequencies do not vary consistently compared to the size of damage. In this case, the increment of the frequency for the first two damage levels was attributed to the possible

effects of ambient temperature that could reversibly affect the bridge's dynamic characteristics (Sohn, Farrar et al. 2004).

To study further the behaviour of structures under short/long-term exposure to environmental variations, the researchers have tried to consider more case studies in recent years and concluded that the natural frequencies of bridges decrease generally by increasing temperatures (Huth, Feltrin et al. 2005, Liu and DeWolf 2006, Olund and DeWolf 2007, Cornwell, Farrar et al. 2008). Cross et al. (2013) investigated the effect of environmental and operational variations on the first five modal frequencies of a suspension bridge during a three year period. They reported that temperature and traffic loading are the dominant environmental factors affecting the modal frequencies of the bridge deck while no clear conclusion has been made for the effect of wind loadings. In contrast, the conclusions drawn by Kim et al. (2003) found that changes in modal frequencies of long span bridges can be barely detected due to traffic-induced loads. In general, the change in temperature is the predominant factor affecting dynamic characteristics of structures.

A further drawback of frequency-change based methods is attributed to their limitations in identifying the location of damage. Therefore, techniques based on local changes in the mode shapes have been developed to detect the presence and location of damage. However, mode shapes are not very good indicators of low-level damage and cannot be used as stand-alone. Comparisons of pre-damage and post-damage fundamental mode shapes of a cracked bridge indicate that the damage was discernable only for the most severe case of damage (Figure 2-6) (Kim and Stubbs 2003). In this case, the first level of damage corresponds to a 0.06 m long cut through the mid-height of the web of the bridge girder (3.048 m cross-section depth) and it spreads eventually into the bottom mid-height of the web and the entire flange to reach the highest level of damage.

Different damage detection criteria such as Modal Assurance Criterion (MAC) and Coordinate Modal Assurance Criterion (COMAC) are adopted to indicate the existence of any changes between two modes due to damage. The MAC and COMAC factors were used to measure the correlation between two mode shapes derived from damaged and undamaged states of a

Reinforced-Concrete (RC) beam having a constant rectangular cross-section of 250×200 mm (Ndambi, Vantomme et al. 2002). The damage was simulated as a progressive cracking process through six different steps of static loadings (ranging from 4 kN to 25 kN applied symmetrically on two points along the beam), while the last step led to the failure of the beam. However, the authors illustrated that the MAC and COMAC factors are poor indicators of the state of health of the structure and a large number of measurement points is often required for an accurate estimate of these factors.

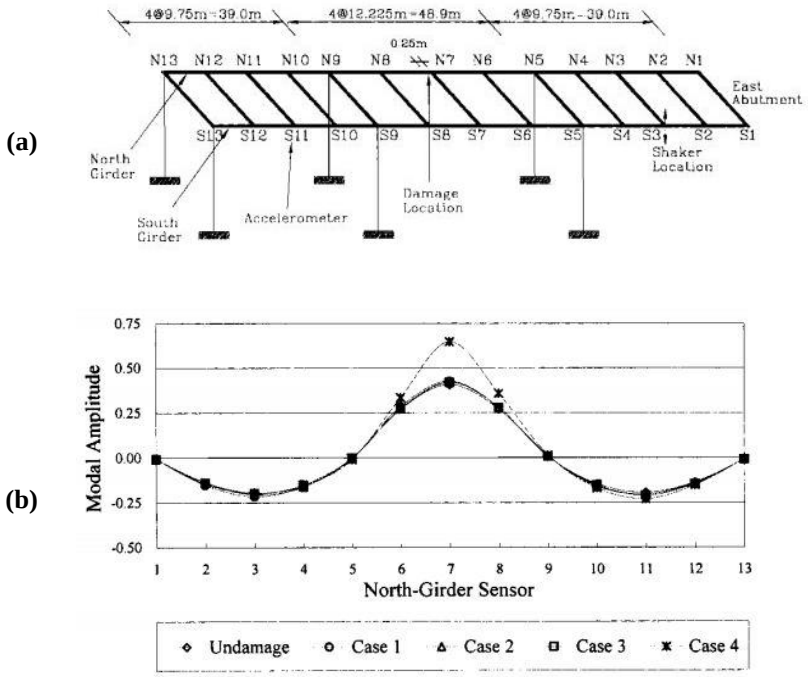

Figure 2-6: Schematic representation of the test bridge and its vibration modes; a) the locations of sensors and the damage introduced to the middle span, b) extracted mode shapes for the first mode (Kim and Stubbs 2003).

The MAC value is known as a scalar-based measure between two mode shapes, which varies between 0 and 1. A MAC value greater that 0.98 demonstrates that the two modes are perfectly correlated, thus indicating the full correlation between two modes, while a MAC value lower than 0.98 can be attributed to the existence of damage (Huth, Feltrin et al. 2005). Based on the same theory behind MAC, COMAC is defined as a point-by-point comparison of the mode shapes from two sets of measurements. However, a reliable approximation of COMAC coefficients relies on the combination of the information obtained from the first few modes of the structure. When processing the coefficients, since the level of variability and uncertainty on

extracted mode shapes increases for higher modes, this method may lead to a wrong interpretation of the results proportional to the actual location of damage (Ndambi, Vantomme et al. 2002, Reynders 2012).

Zhang (1994) developed the analytical model of a constructed highway bridge according to the experimental modal parameters to assess the structural integrity using Modal Scaling Factor (MSF) and Coordinate Modal Scaling Factor (COMSF). The information derived from COMSF was used to provide the magnitude difference at all locations of one set of mode shapes with respect to other sets of modes and it was found that MSF-based methods appear to be useless as damage indicators. These methods follow a same principle as MAC and COMAC with little modifications in their formulations and suffer from a same drawback as MAC-based methods. In another attempt, Perera and Huerta (2008) noticed that the MAC and MSF values do not undergo very significant changes when they are calculated from the mode shapes in RC beams. The beam was subjected to progressive cracking process at two symmetrical points nearly located at the mid-span by applying three stages of static loadings ranging from 8 kN to 52 kN and adding external masses of 100 Kg and 160 Kg. The authors made significant effort to introduce a novel indicator to better predict the existence of changes in the state of the beam based on what was referred to as local modal stiffness. This parameter not only depended on the mode shapes but also the frequencies. However, the results indicated that the proposed approach could not be served as a robust and simple way to locate damage in structures. As cited by Zhang and Aktan (1995), a reason for which the aforementioned detection criteria cannot be used effectively to detect damage resulted from the fact that the differences between two sets of data were averaged over all of the measurement points (MAC, MSF) or all of the mode shapes (COMAC, COMSF).

Unlike natural frequency and mode shape, there is less literature evaluating the sensitivity of modal damping for damage assessment in structures. In general, the experiences obtained from previous studies in the past years recommend precluding of its usage in structure integrity assessment. The latter can be attributed to the lack of enough accuracy in computing damping ratios from modal analysis techniques (Zhou 2006).

The variations of the first two damping modes of reinforced concrete beams were estimated by means of two dynamic channels and an impact-based dynamic excitation to record damped-free vibrations of the beam before and after inducing damage (Casas and Aparicio 1994). Cracking

was simulated by inducing different levels of notch ranging from 30% to 92% of the beam depth at the middle point of the beam. However, experimental results indicated that the system damping ratio did not consistently increase or decrease with an increase in the level of damage. Similarly, Farrar and Jauregui (1998) measured the modal damping ratio for the purpose of damage detection in a steel plate girder of a highway bridge subjected to four levels of damage simulated by various torch cut in the web and in the flange of the girder. Again, no significant and consistent change between system damping and damage growth was found until the final level of damage (cutting the mid-height of the section) was introduced. On the other hand, further investigations indicated that the shifts in the natural frequencies corresponding to the first six modes of the structure are not able to disclose clear information for the detection of damage.

Curadelli et al. (2008) used changes in the modal damping as an indicator to detect structural damage by correlating instantaneous changes in the damping coefficient to damage. The authors assessed the performance of their approach using acceleration time-history data obtained from a reinforced concrete beam (6.50 m length) under five steps loading cycles at two discrete points along the beam. According to the results only when the maximum loading cycle (7.5 kN) was considered, the correlation between instant damping coefficient and the amplitude of vibration for the healthy and damaged conditions indicated a pronounced variation in the damping.

Modal updating methods have been introduced based on accurate development of a finite element model of the structure in which the residual difference between numerical and experimental modal data has to be minimized in order to detect, localize and quantify the damage on the basis of the tuned model. Hu et al. (2001) adopted a model updating method to locate and identify the magnitude of the damage in the mode shape of a fixed-fixed end aluminum beam and demonstrated the capability of the proposed algorithm to identify damage along the beam. However, in their study the damage was induced by a very significant saw-cut extending through half of the cross-section of the intact specimen.

Vakil-Baghmisheh et al. (2008) described the efficiency of a generic algorithm technique to identify crack location and depth in an aluminum cantilever beam through comparison of updated frequency-based numerical modal parameters of the beam with those obtained from the original beam. The optimization problems were formulated by means of a cost function based on the minimum residual difference of measured and calculated natural frequencies. The first four

natural frequencies of the numerical simulations of the beam, which were functions of location and depth, were measured for various patterns of damage location and depths to generate a genetic algorithm. The real frequencies computed from the cracked beam were considered as the cost function input value. The experiments were done in a beam with a length of 0.82 m and a uniform cross-section. However, in complex structures for which the difficulty and uncertainty in simulating accurate analytical models will be increased, the effectiveness of this approach becomes limited.

A frequency-domain method was introduced by Lee and Shin (2002) based on the structural dynamic stiffness equation of motion applied to a beam structure. The extraction of an exact dynamic stiffness matrix was formulated for intact and damaged conditions of a beam. The feasibility of the proposed method was evaluated through numerically and experimentally damage tests. However, as stated by the authors, the applicability of this method is limited to structures for which exact dynamic stiffness matrix is available. To address damage detection in beam-like structures, Rosales et al. (2009) used the power series algorithm in conjunction with the application of Artificial Neural Networks (ANNs) with a training set of data simulating more than four hundred damage scenarios. The ANN algorithm was trained by the numerical experiment data obtained from a finite element model of the beams and the measured natural frequencies of the damaged beam were then introduced to the trained ANN. Several experiments were carried out and small errors were observed in the detection of damage presence using the power series technique. In this study, although neural networks were trained to resolve issues related to the prediction of damage, the latter yielded on average rather large errors in the results and no conclusive evidence was observed to locate damage as clearly.

A new parameter called Mode Shape Curvature (MSC), functions of the second derivatives of the deflected shapes, was proposed by Pandey et al. (1991) to improve damage detection and identify the location of damage in a cantilever and a simply supported analytical beam. In principle, the changes in the curvature modes extracted from both intact and damaged states of the beam are associated with the changes in the flexural stiffness of the structure in the region of damage and hence, it can be used as an inductive to damage location. In this paper, the damage was considered by the change in the stiffness of the beam with 50% reduction in the modulus of elasticity. The authors compared the results obtained from the curvature-based approach with

those derived from changes in the displacement mode shapes in their original forms and reported that mode shape curvatures are more efficient than simple modes for damage detection.

Sahin and Shenoi (2003) investigated numerically the curvature difference for the first three modes of a cantilever beam subjected to incremental reduction in thickness as 2.5% up to 80% localized damage at different locations along the beam. Nevertheless, the results demonstrated that damage detection could not be easily visible at small levels of damage (e.g. less than 40%) using mode shape curvatures alone. The authors also proposed a neural-based experimental study to predict the location and severity of damage on a beam with a length of 0.45 m subjected to 66% reduction in stiffness at nearly the middle of the beam. To generate the input models of the neural networks the finite element analysis was implemented to obtain free vibration dynamic behaviour of intact and damaged beams. However, the results of the ANN regarding the prediction of the severity of damage were not promising as the ones obtained to determine the location of damage.

A noise-free numerical study was carried out by Brasiliano et al. (2004) to identify the damage in beam-like structures using modal key input parameters such as natural frequencies and mode shapes. The damage localization procedure was performed by observing the residual error present in the movement equation of a continuous beam and the highest error value was expected to indicate the location of damage along the beam. The beam was modeled using the finite element analysis and the damage was simulated as much as a 3% to 15% reduction in stiffness at three structural elements. To investigate the efficiency of the method, MAC, COMAC, and MSC methods were considered as comparative techniques and it was shown that the changes in the curvature of mode shapes are reasonably acceptable to locate the damage besides the proposed approach. However, a drawback of the proposed method is that it must be computed in terms of several parameters such as stiffness and mass matrices of the structure in the reference condition as well as the natural frequencies and mode shapes of the damaged state. In real cases where the dynamic baseline data of the intact structure is not usually available any uncertainty in obtaining an accurate estimation of these parameters may affect the results.

Pandey and Biswas (1994) demonstrated numerically that the evaluation of changes in the flexibility matrix may lead to locate damage in simple beam models. The damage was modeled by a reduction in the modulus of elasticity (E) of the section over the range from 10% to 90% E.

However, the results corresponding to less than 50% E were not able to localize damage. In another study, Bernal (2000) discussed the sensitivity of the modal flexibility matrix for damage detection on the analytical model of a beam with the fixed-fixed end conditions. Damage was simulated as a 25% and 50% reduction in the flexural stiffness of the structural elements and it was shown that the absolute difference in the modal flexibility displacements between reference and damaged states of the beam can be used as an indicator for damage detection. However, the authors stated that the capacity of the proposed method to operate consistently under experimental and noisy conditions is uncertain and depends on the accuracy of the extracted flexibility matrices derived from measured data.

Using similar principles as MSC method, Catbas et al. (2007) investigated the applicability of the flexibility method and its curvature for damage detection in a an experimental steel grid bridge model. The damage was induced as a significant reduction in the structural stiffness by loosening the connection between a cross-member and a girder at one joint along the structure. For a better understanding of the model, Figure 2-7 shows the experimental setup along with the modifications related to the induced damage. Given the damage, the authors illustrated that the curvatures of the displacement shapes are advantageous for certain cases when the results derived from deflations do not provide substantial changes caused by damage.

(a) **(b)**

Figure 2-7: The steel grid model in the laboratory, a) instrumentation of the model, b) loss of stiffness by removing cover plate from the top and bottom of the girder (Catbas et al. 2007).

A new approach based on mode shape sensitivities to changes in mass or stiffness of beam-like structure was presented by Parloo et al. (2003) using the mode shapes obtained from the two states (damaged, undamaged) of the structure. This study was performed on a series of modal

data obtained from 26 accelerometers mounted on a highway bridge girder subjected to a single-location damage evolving incrementally through four steps ranging from a small cut in the centre of the web to a larger one that cleaved entirely the bottom flange and half of the web. Comparisons were also added to evaluate the sensitivity of MAC, COMAC, MSC, modal strain energy and flexibility based methods and it was found that all of these methods are strongly affected by the presence of measurement noise since they were only able to localize the damage for the most severe damage cases. For this study, it should be noted that the proposed approach imposes certain limitations to assess the structural condition of bridges since the sensitivity matrix introduced herein relied on a linear combination of a several number of estimated mode shapes while a reliable estimation of higher modes is costly and cannot be derived easily for large-scale structures (Reynders 2012).

Maia et al. (2003) revealed the results of their comparative study to assess the efficiency of different techniques based on changes observed in mode shapes displacement, mode shapes slope, mode shapes curvature, and square curvature of mode shapes to detect damage in a beam and concluded that mode shapes with higher-order derivatives (modal strain energy) are more sensitive to damage. However, further studies (Alvandi and Cremona 2006, Cao and Qiao 2008, Perera and Huerta 2008) report that curvature methods at the same time that are magnifying the effect of damage in the mode shapes can amplify small noise in the measured data, which can mask minor changes in the mode shapes due to small levels of damage.

A comparative study of detection methods performed on RC beams subjected to symmetric and asymmetric damage scenarios concludes that changes in natural frequencies, flexibility matrices, MAC and COMAC factors are less significant than those observed from the modal strain energy method (Ndambi, Vantomme et al. 2002). Alvandi and Cremona (2006) used the strain energy method based on the theory behind the curvature techniques to detect damage using the first three mode shapes of a numerical model of a beam in the presence of added noise. This method is often referred to as damage index method in the literature. The authors compared the results of their studies with those obtained from the flexibility and the flexibility curvature methods and found mode shapes curvature techniques are more conclusive to indicate the location of damage.

Recently, Wahalathantri et al. (2010) indicated that existing strain energy-based method indices either present false alarms or fail to detect some damage locations at or near nodal points. Hence,

the authors developed a novel approach through an adjustment in the formulated damage index to detect damage in a numerical model of a simply supported beam subjected to various levels of damage (ranging from 10% to 40% of the beam height) at single or double locations along the beam. Unlike modal strain energy damage indices that require the first few modes to be measured, the proposed strain energy method was modified to localize the damage using any one of the modes numerically measured. However, the authors never resolved issues related to undesired impacts of noise presence in experimental mode shapes.

2-4-2 Vibration-Based Signal Processing Techniques

The continuous advances in the field of structural health monitoring have been led to the development of vibration-based signal processing techniques aiming to detect slight changes in the dynamic response of structures due to damage.

Fourier analysis is one of the oldest signal processing techniques that has been used in many types of simple structures to detect damage based on measuring dynamic response of structures. Lee and Kim (2007) used the FFT to detect damage in a scaled bridge model using a novel signal anomaly index to express the amount of FRF variation proportional to the spatial location of embedded sensors distributed along the girders. As shown in Figure 2-8, it should be note that in transforming the time domain to the frequency domain of a signal the time information is lost and it is impossible to determine when a particular event took place (Kim and Melhem 2004, Bajaba and Alnefaie 2005).

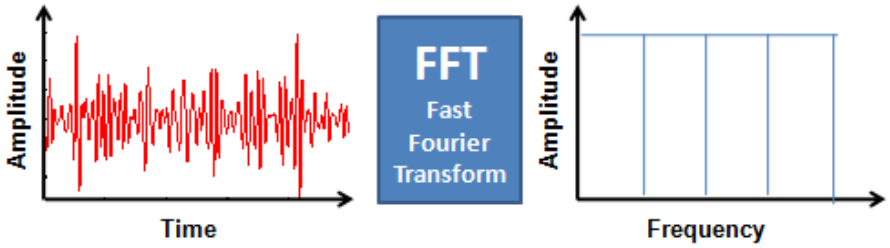

Figure 2-8: FFT representation, indicating its capability to exhibit the frequency contents only.

Based on the same theory behind the Fourier analysis, Osornio-Rios et al. (2012) applied the Multiple Signal Classification (MUSIC) algorithm for health monitoring of a five-bay truss-type

structure subjected to forced excitations. Truss elements were damaged by inducing corrosion and a crack in the elements. The external corrosion was introduced by immersing both ends of a bar element in hydrochloric acid whereas the internal corrosion was simulated by substituting a hollow tube element instead of a solid bar. In this paper, a damage index value was suggested to automate structural damage detection based on the comparison of the energy distribution change in the natural frequencies. Although, the results demonstrated that the proposed algorithm was potentially an effective tool for distinguishing between healthy bar elements and damaged bar elements in this particular case, it could not provide spatial information for the localization of damage. The algorithm was first introduced for health monitoring of high rise buildings and therefore, it has not been quite popular in the field of SHM (Jiang and Adeli 2007).

To address the limitations of FFT to depict spectral changes of time signals over time, the Short-Time Fourier Transform (STFT) was proposed by Gabor (1946). Yesilyurt and Gursoy (2013) presented an application of the STFT for predicting modal damping ratios of a composite beam subjected to vibration by an impact hummer. This technique utilizes a moving window function that is multiplied by the input signal before computing FFT and analyzes only a small section of the signal at a time. Moreover, it contains both time and frequency information of the signal. However, the major drawback of the STFT is attributed to the fixed width of the sliding window (Figure 2-9). In theory, a tradeoff exists between the time and frequency resolution of a signal since a large window represents low frequency components of the signals and, therefore, transient signals cannot be observed effectively, whereas high frequency components could be detectable by a small window (Robertson, Camps et al. 1996).

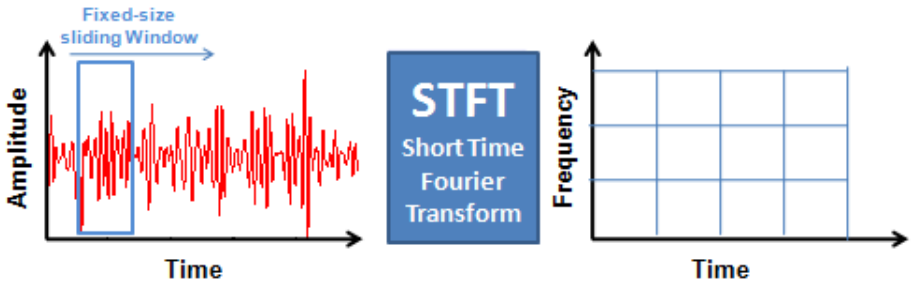

Figure 2-9: STFT representation, indicating its capability to exhibit time-frequency information of a signal simultaneously.

Hadjileontiadis et al. (2005) used the Fractal Dimension (FD) algorithm as an inductive of sudden changes in the spatial variation of the mode shape of a 0.30 m long plexiglas cantilever beam with a relative crack depth of 30% at 0.06 m from the clamped end. A total number of 39 measuring points were used to record the dynamic response of the beam under harmonic excitations. Since direct implementation of the FD algorithm may detect many points in sample data as singularities, the authors performed an over-sampling procedure using cubic spline interpolation to smooth the transition from one point to another. In addition, given that the FD estimate increases with increasing crack depth, the authors generated a curve correlating estimated FD coefficients versus different depths of crack for an analytical model of the beam. The latter was used to propose an alternative for the prediction of damage size in real cases by relating the estimated FD obtained from experimental analysis to the size of crack. The FD is also based on a fixed-size moving window across the signal to be analyzed and its delectability mainly depends on an appropriate determination of the length of the sliding window.

Banerjee and Pohit (2014) also implemented the FD analysis into the first three mode shapes of a numerical model of a 0.5 m long cantilever beam subjected to transverse open cracks with relative depths of 30% and 50% of the beam depth. Attempts were made to examine the efficacy of this technique to detect multiple cracks along the beam. Two cracks were simulated at 0.25 m and 0.45 m from the fixed end of the beam. However, only when the most severe case of damage was considered the results were informative as to the locations of damage. For the other case, the damage was detectable only for one location using the first mode. It was also shown that the use of higher modes may lead to misleading information at other regions along the beam.

Wavelet analysis is one of the most acknowledged techniques for processing of structural vibration data. The Continuous Wavelet Transform (CWT) is one of the most-widely used forms of the WT which provides a time-frequency representation of the signal using a variable-size windowing technique simultaneously (Figure 2-10). The CWT decomposes the signal into many basic functions called "wavelets" and are used to assess sequentially the similarity between the wavelet and a portion of the signal to be analyzed at all times or locations (in case of signals at space-domain) of the signal. Wavelets with finer scales are an indicator of high frequency information of the signal while wavelets with coarser scales are appropriate to capture low frequency components. As a result, any irregularity or discontinuity in the signals that are not

visible easily by visual inspections or conventional methods may exhibit themselves as high values or coefficients through CWT (Liew and Wang 1998).

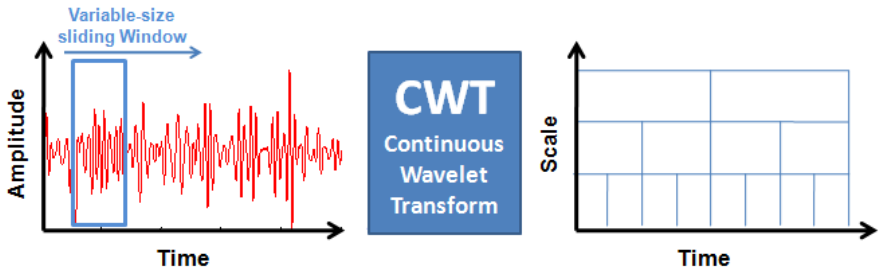

Figure 2-10: CWT representation, indicating its capability to exhibit multi-resolution characteristics of a signal using a size varying wavelet.

The literature on the use of the application of the CWT for damage identification in structures is vast. Melhem and Kim (2003) examined the effectiveness of the FFT and CWT in the analysis of the time-series data obtained from the vibration of a simply supported concrete beam and a portland cement concrete slab subjected to incremental fatigue loads. The results demonstrated that the CWT method not only yielded a clear difference between the initial and damaged states of both structures, but was also capable of determining when a particular change of frequency took place in the signal due to damage. In this study, the wavelet analysis was found as a useful means to analyze non-stationary signals, which are usually the case of real inspections. However, the authors only demonstrated an application of the wavelets for the detection of the existence of damage.

It has been remarked that the use of the CWT on spatial data (such as mode shapes and deflection curves) provides also a useful means to detect and to localize small changes in modal parameters (Cao and Qiao 2008). Liew and Wang (1998) presented the first attempt of an application of the CWT to illustrate how the wavelet theory can be used as a means to locate damage in beams when mode shapes could not exhibit alone trivial changes caused by damage. Investigations were performed on the mode shapes of a numerical simply supported beam subjected to an open crack and it was indicated that the wavelet analysis can precisely locate damage, though the conclusions were derived only for a severe case of damage (e.g. crack depth of 50%).

Another example of an application of the CWT is found in the studies of Salgado et al. (2006) to determine the location of damage for a small-scale model of a composite simply supported bridge fabricated by two steel I-beams and a concrete slab. Damage was modeled as open cracks located in the mid-length regions of the beam while inducing through four stages starting from the bottom flange of the beam (e.g. a transverse open crack with depth of 0.008 m) and propagating to the half of the total depth. In this case, the experimental measurements were used to calculate the updated mode shapes of the beam through numerical simulations. The results could successfully indicate damage location when the crack was propagated to 0.017 m along the bottom flange of the beam. However, the authors noticed that for all damage cases the results were evidently affected when only 1% noise was added to the measured dynamic responses to simulate errors during the acquisition of the data.

A study for crack identification in a double-cracked cantilever beam was carried out both analytically and experimentally through an application of the CWT on the first measured fundamental vibration mode (Loutridis, Douka et al. 2004). Sudden changes in the spatial variation of the bending mode shape were considered in order to locate the two transverse surface cracks along the beam. Experimental measurements were performed using 30 measuring points on a small-scale plexiglass beam with a length of 0.03 m and two cracks of relative depths 20% and 30% of rectangular cross-section. Nevertheless, the experimental results were not smooth as in the case of the simulated response, resulting in significant coefficients beyond the locations of damage along the beam. Pakrashi et al. (2008) performed a numerical study for damage detection in single and multi-span beams with an open crack using CWT. Simulations were considered for damage models of different levels of complexity and different crack depths and positions in the presence of Gaussian white noise. It was noted that the noise could lead to a significant decrease in the performance of CWT to locate accurately damage in all cases.

A numerical study was carried out on static deflection profiles of a single damaged-induced fixed beam under a concentrated load of 500 kN at different points along the beam (Umesha, Ravichandran et al. 2009). The analysis was performed to compute sequentially the deflection profiles at a particular point along the beam and to use them as signals for the CWT. Finally, the results indicated that the clarity and detectability of the location of damage increases as the measuring point approaches the damage point.

Due to inherent properties of the wavelet analysis for post-processing of signals, the combined form of structural vibration modes has been examined experimentally for damage detection in a beams (Grégoire 2011). A CWT was applied to the sum of the first three mode shapes of steel beams with simply supported end conditions. Different patterns of damage were taken into account by introducing a saw-cut as to 30% up to 50% of the beam height for estimating the sensitivity of the wavelet analysis for damage detection at different locations. Although the proposed approach was able to highlight hidden irregularities in the mode shapes caused by damage in significant cases of damage, no clear and consistent evidence was observed to determine damage at small levels and multiple locations simultaneously occurred along the beam.

Discrete Wavelet Transform (DWT) is another form of the WT that has drawn the interest of researchers to decompose the measured vibration data into their low frequency (Approximation) and high frequency (Detail) components. As shown in Figure 2-11, the data contained in the approximation part, iteratively, is split into higher levels of approximation and detail until covering a desired level of decomposition. Lastly, the information extracted from high level decompositions of signals can be used as an indicator of damage (Misiti, Misiti et al. 1996).

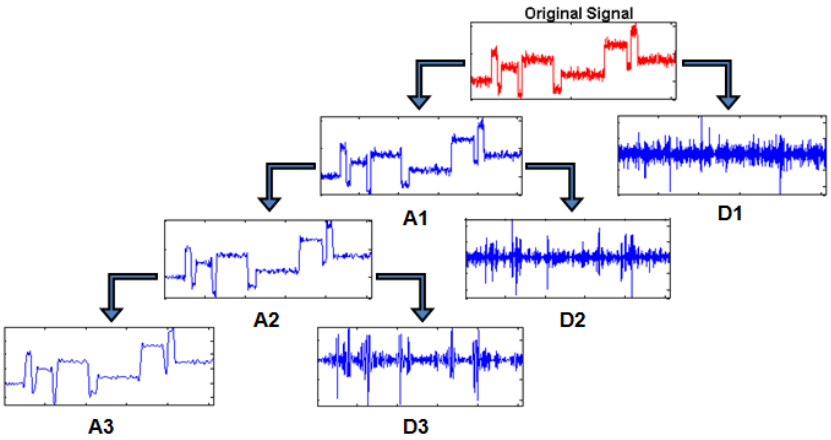

Figure 2-11: Schematic diagram of the third level of decomposition of a signal using DWT.

Jaiswal and Pande (2015) performed a numerical study for damage detection in a free-free boundary condition beam through discrete wavelet analysis of the first five mode shapes of the beam which were converted into their curvatures to be treated as space-domain signals for the

wavelet analysis. The damage was simulated as a transverse rectangular cut at 0.1 m from one end with a small relative depth of 17% of the beam thickness. Although visual inspections of the mode shapes numerically obtained for this level of damage could not reveal any discontinuity caused by damage, the detailed part of the wavelet coefficients indicated relatively large magnitudes at the damage location, though they were disturbed also by significant values near extremities of the beam.

Cao and Qiao (2008) introduced a new approach which examines the synergistic advantages of the DWT and CWT to improve the robustness of abnormality analysis of mode shapes in damage detection. The mode shape was measured from the numerical finite element analysis and experimental testing of a cantilever beam with a through-width crack. The proposed method was performed in two stages. First, a discrete wavelet analysis was applied to decompose sequentially the original mode shape into low frequency and high frequency components. Assuming that the low frequency components of the mode shapes are correlated with damage, the latter was used to decompose the original mode shape into several levels and to select a mode that exhibits better existing defects or discontinuities in the mode shape due to damage. Second, a continuous wavelet analysis was performed on the refined mode shape to determine the location of damage. For this approach, however, the filtering procedure may produce also some deviations in the actual patterns of variations of the original mode shape and results in false indications of damage at other locations along the beam.

A neuro-based discrete wavelet technique was proposed by Vafaei et al. (2015) to locate and quantify damage in a rectangular cantilever beam of a length of 0.625 m subjected to three different locations of damage and severities corresponding to 7%, 14%, and 21% of the beam height. In this experiment, damage localization was accomplished by decomposition of the mode shapes obtained from measured data at 30 locations along the beam. However, it was indicated that the decomposition of mode shapes using DWT cannot be utilized effectively to detect substantial changes of experimental mode shapes, though the mode shapes were obtained for a relatively simple setup in which the homogeneity of the beam and the large number of measuring points could result in less uncertainty in the extraction of mode shapes. In this paper, a neural network was further developed for damage quantification. To this end, a finite element model of

the beam was developed to provide the training samples via simulating different scenarios of damage to the model.

Zhong and Oyadiji (2007) presented a new discrete-based wavelet approach through numerical simulations of cracked simply supported beams to determine damage using the difference in the detail coefficients between two halves of the mode shape. In the latter, the modal data of the left half of the damaged mode shape were considered as the baseline for the modified right half of the beam and vice versa. However, in real field tests in which the actual location of damage is initially unknown, the baseline modal parameter may contain the damage information and thus, restricts the applicability of the proposed method for damage detection in real cases.

To extend the applicability of the wavelet theory to real structures, some researchers place their efforts in analyzing deflection profiles of bridge-type structures captured from high resolution laser-based measurements. Okafor and Dutta (2000) explored the use of laser-based optical systems combined with an application of the discrete wavelet analysis for the detection of damaged-induced changes in the mode shape of a 0.3 m long cantilevered aluminum beam due to damage. The damage was induced as a notch of width 0.02 m with a relative depth of 20% beam thickness and the measurements were performed with an overall optimal number of 100 scan points. The displacement data corresponding to the first three modes of the beam were analyzed by the wavelets. However, in this case, only the results obtained from the first and third mode shapes were able to detect damage.

Poudel et al. (2005) continued with the same technique using a high-speed digital video camera (up to 40000 frames/s) to provide vibration measurement data for a simply supported prismatic steel beam of length 1.1 m with a rectangular cross-section. The image processing was performed to capture digital motion images by recording free vibration motions of the beam in the vertical direction for further processing using the CWT. Two damage states were introduced at 0.3 m and 0.7 m from the left support, respectively, indicating relative crack depths of 16% and 14% beam height. Although the proposed approach was promising in detecting damage locations along the beam, exhibited results derived from the wavelet analysis were not quite satisfactory to detect precisely and clearly such a small levels of damage in the presence of experimental noise.

Pakrashi et al. (2008) performed an experimental study to study the validity of their numerical results previously described in this review. Experimental validations were carried out on a 1 m long phenolic beam subjected to an open crack at different sizes relative to the height of the section (16%, 33%, 50%). The beam was subjected to a static load on its surface and its deflected shape was recorded for wavelet analysis by using a digital camera. In this case, the experimental investigations were performed to indicate the sensitivity of the wavelet coefficients maxima in terms of the size of damage. The authors concluded that the wavelet-based methods are able to detect damage in the deflected shape as long as the damage can introduce itself as singularities in the space signals; however, the presence of noise can cause major difficulties and mask the effect of damage.

Wu and Wang (2011) reported the results of their studies for damage detection in a cantilever aluminum beam of length 0.55 m using a high resolution laser profile sensor to determine invisible perturbations in the static deflection profile of the beam subjected to static displacements at its free end. Although the CWT was successfully used to detect damage location despite noise in the measured data, this study was also conducted on a very small-scale test object subjected to a severe level of damage which corresponded to 50% of the beam thickness.

Law et al. (2005) tried to evaluate the sensitivity of the Wavelet Packet Transform (WPT) energy components with respect to local change in system parameters based on dynamic responses resulting from numerical and experimental analysis of a beam with simply supported end conditions. In this approach, the WPT was accomplished in order to compute the equivalent energy for each component, which was obtained from discrete decomposition of the measured signals, corresponding to each sensor at a particular point along the beam. The relative energy contained in the selected components was computed sequentially for each individual channel covering the length of the beam. Experimental measurements were carried out on a homogenous steel beam of dimensions 2, 0.50, 0.009 m subjected to a single damage scenario by saw-cutting a region of the beam at one-fourth of its length. The damage in this case corresponded to an 11.5% reduction in the flexural rigidity of the beam. Although the numerical equations resulted in a good estimation of damage location, the high noise to signal ratio in the experimental measurements caused false alarms appear significantly at other locations along the beam and

hinder accurate identification of damage. The investigations were performed on both acceleration and strain-gauge time history responses of the beam and it was found that the sensitivity of acceleration responses compared with the local change of parameters could be much better than that from strains. However, the applicability of this technique becomes difficult in practice since the identification of an appropriate level of signal decomposition requires many trial-error sensitivity analyses.

It is worth to note that the WPT is a generalization of the DWT and can be defined as a complete level by level decomposition of signals. Conceptually, WPT decomposes the signal into approximations (A) and details (D). Compared with DWT, in WPT these two parameters (A and D) are separately split into a new level of decomposition (Figure 2-12) (Misiti, Misiti et al. 1996, Salgado, Cruz et al. 2006).

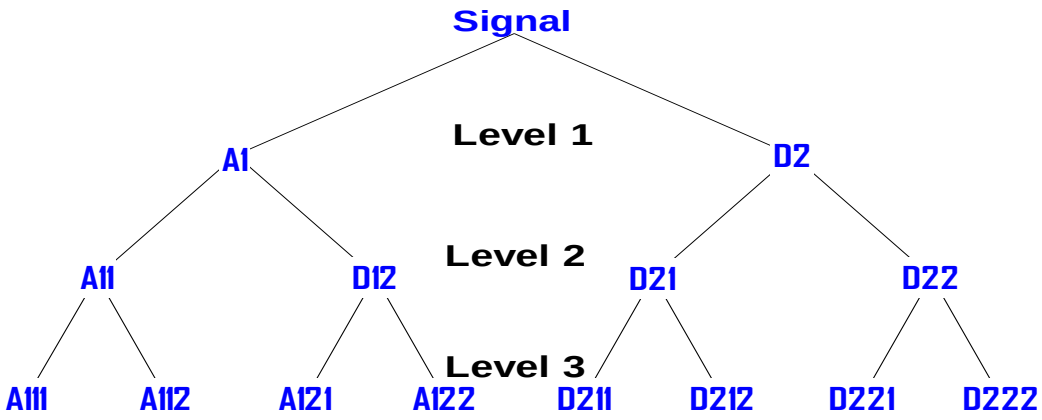

Figure 2-12. Schematic representation of WPT three.

Sun and Chang (2002) published the results of their study using a combined application of the WPT in conjunction with neural networks to assess structural integrity for a numerical simulation of a three-span continuous bridge under impact excitation and rigidity reduction of 10%, 20%, and 30%. The basic concept behind this method was to obtain the energy components obtained from the decomposition measured from acceleration signals using the WPT and use them as inputs to the neural models for various levels of damage assessment. It was shown that the developed models were not capable to identify reasonably damage at all severities, except the most severe cases in this study. This study was performed under a repeated constant pulse force and no attempt was made to extend the methodology for various types of service loads such as

ambient excitations. To extend the application of such methods in real bridges, a mechanical shaker may be required to excite the structure, which can impose practical difficulties for using this technique in in-situ cases.

The Empirical Mode Decomposition (EMD) energy damage index has been introduced as a means to detect and quantify cracks in a simple cantilever beam with a short length of 0.35 m and subjected to a mid-span notch size varying from 15% to 75% of the beam thickness (Rezaei and Taheri 2010). However, in this paper the authors did not propose any solutions to locate damage. The beam vibration was monitored via three sensors bounded adjacent to the notch and the acquired signals were decomposed to derive the proposed damage index for both healthy and damage states of the beam. Given that this indicator is based on the decomposed signal energy before and after the occurrence of damage, this methodology may encounter difficulties in real field measurements. This can be explained by the variation in the dynamic loading conditions on the structure that could be registered potentially as damage signals.

Based on the principal theory behind the EMD, Quek et al (2003) favored the application of the Hilbert–Huang Transform (HHT) to localize abnormal events and slight distortions in time signals measured from two beams. The HHT is an innovative energy-frequency-time distribution of the signals that decompose a signal into a set of basic functions called the Implicit Mode Functions (IMF). In the first case, HHT was implemented to the experimental wave signals of a 0.65 m long aluminum beam subjected to a single damage location with relative depth of 17%. The second analysis was performed to detect the damage of a sandwiched beam formed by two wide aluminum strips with length of 0.8 m which were glued together throughout their lengths. In the latter case, the damage was simulated as delamination in a portion at the mid-center of the beam. Finally, it was noticed that the relative errors corresponding to the location of damage estimated by HHT are not quite significant. However, the main concern of this method is that the first IMF can fail to reflect the true frequency pattern of the signal since it covers a wide range of frequencies and therefore, may cause misinterpretation in the results.

2-4-3 Statistical Pattern Recognition Techniques

Statistical pattern recognition techniques have not developed as rapidly to improve the efficiency of SHM systems. They are mostly confined to the indication of the damage existence in

structures rather than their locations and quantities in structures. An important contribution of the present study is to address objectively and statistically experimental uncertainties relevant to real field measurements and to propose a reliable damage localization criterion in structures.

Deraemaeker et al. (2006) used factor analysis in combination with multi-variate control charts to indicate whether or not the structure has deviated from its normal condition. This methodology was illustrated through a numerical example of a three-span bridge relying on a long-time monitoring of the intact structure using large arrays of sensors. During the monitoring, environmental effects were assumed as temperature gradients varying from -15°C to 45°C. For each temperature sample, modal features were computed for both reference and damaged states of the structure using a modal filtering technique combining linearly the output of the sensors network into one single output, resulting in a total number of 61 features for each state of structure. The control chart analysis was proposed to create threshold limits based on location parameters of the reference features and to detect unusual sources of variability such as damage from the normal conditions. Finally, results indicated that the use of factor analysis can improve the capabilities of the statistical quality control chart tools by eliminating the effects of random quantities or factors correlated with temperature.

A statistical time-series model based on the Auto-Regressive (AR) moving average model together with a statistical classifier has been used to detect damage in a three-span reinforced concrete and a post-tensioned box girder bridge under sinusoidal and ambient dynamic excitations respectively (Carden and Brownjohn 2008). In the latter case, the results demonstrated that the model cannot adapt to non-linear variations where the effects of in-service operational conditions (e.g. wind, traffic) causes the amplitude of ambient dynamic excitations to vary in time, resulting in the variation of the frequency spectrum. For continuous, long-term, and remote monitoring of structures developing an innovative damage detection technique that could rely only on ambient excitation of structures rather than dynamic excitations is very important and cost effective.

Sun and Chang (2004) developed a time-domain statistical pattern classification method based on an experimental study performed on a steel cantilever beam with different damage sizes at one location near the mid-span. The investigations were done only to detect and classify damage-related abnormality of time signals directly measured from one accelerometer attached to the

free-end of the beam. The core idea of this study was to calculate energy components of the signals based on the WPT, and then discard those components that were small in signal energy and define the remaining dominant component energies as a novel condition index for damage detection. To determine the abnormality in the new data an X-bar control chart was established based on the statistical properties of the measured damage indicator under healthy conditions. This chart was proposed as a threshold method to enclose variation of the extracted damage indicator due to damage and measurement noises. The beam considered for this study was excited under a repeated consistent pulse load acting at a fixed location along the beam. However, for real cases subjected to various loading conditions due to changes in both magnitude and location of the excitations the effect of measurement noise becomes important to be removed or quantified. This is because the temperature can affect on the damage indicator even when the structure condition is unchanged.

As an extension of the work done by Sun and Chang (2004) and for the purpose of localization of damage, Han et al. (2005) calculated the WPT energy rate index for each individual channel recording the acceleration time-history dynamic response of four I-section beams. The beams were restricted with simply supported ends and equipped with 26 accelerometers evenly distributed over the entire length of each one. For this study, a threshold algorithm based on the statistical process control method (Bentley 1999) was used for alarming possible abnormality in the damage indicator. Finally, the location of sensors whose damage indicator energy values were fallen outside the enclosure was considered as outliers and possible indication of damage location along the beam. However, an important drawback of the current technique is that it relies on a reliable reference (undamaged) model of the structure to be analyzed, which restricts its applicability for damage localization in real structures.

Uncertainty associated with the structural model and measured vibration data reflected in the mode shape curvature damage factor of a finite element model of a cantilever beam was the scope of a statistical approach performed by Chandrashekhar and Ganguli (2009). To alleviate uncertainty in structural damage detection, the authors developed a fuzzy logic approach using Monte Carlo Simulation (MCS) to study the variation in the damage indicator due to randomness in structural parameters. The conventional MCS is one of the traditional methods for a probabilistic analysis which uses randomly generated samples of the input variables and

estimates response statistics after numerous repetitions. The main disadvantage of this method is that it requires an enormously large amount of computation time (Cheng and Xiao 2007). For this study, the structural damage was simulated by stiffness reduction of 20%, 40%, and 60% into five different segments along the beam. In addition, the modeling uncertainty was originated from randomness in geometric property of the beam through 1% coefficient of variation of the thickness at the free end of the beam as well as 10% noise added in vibration data. Although large overlaps in the minimum and maximum values of the measurement data was observed for the defects with different levels of damage at same location due to uncertainty in the physical parameter itself, results demonstrated an average success rate of 80% to classify damage patterns in each case. However, no comparisons were made to investigate the sensitivity of the proposed approach through experimental or field test measurements.

Reiff et al. (2016) proposed a hypothesis testing framework to introduce a novel decision-oriented approach for condition monitoring of a three-span continuous bridge using the Rank-Sum or Mann–Whitney U test. The latter is a statistical non-parametric test often used to determine the probability of equality between two independent samples coming from two groups of data (e.g. damaged and undamaged) with non-normal distributions. The authors developed a hypothesis test using bridge Girder Distribution Factors (GDFs) to determine whether there is enough evidence to conclude statistically damage potentially existing in the bridge. Because the bridge studied was new with almost no significant changes in its dynamic properties due to damage, a calibrated finite element model was simulated alternatively to provide GDF samples for the damaged bridge through four scenarios of damage and the results were employed to develop a damage index providing a warning of the likelihood of potential damage. It is worth to note that the term GDF used herein was the ratio of the live load applied to each girder, which was computed by measured strain data recorded during traffic events at the bridge over the course of 14 months. During this time, however, no strategies were considered by the authors to determine a correction for seasonality effects (e.g. temperature) on baseline data and to investigate the uncertainty in collected strain-data.

In recent years, techniques based on multivariate statistics such as Principal Component Analysis (PCA) (Pearson 1901) have been applied for dimensionality reduction, noise removal, and feature extraction in large dimensional data sets. In an effort to enhance the discrimination

between features from the undamaged and damaged structures Sohn et al. (2000) introduced a combined statistical procedure based on coupling of PCA with the X-bar control chart technique. The proposed method was applied to AR coefficients corresponding to vibration test data acquired from a laboratory specimen of a RC bridge column. The column was subjected to static load cycle testing in order to accumulate various amounts of damage and the excitation for the vibration tests was provided using an electromagnetic shaker. In order to maximize the mean differences between the data sets obtained from the undamaged and damaged classes, the PCA was used for spatial dimensional reduction prior to feature selection. The latter was performed by projecting multidimensional time-history responses from 39 accelerometers into a single channel. This corresponded to the first Principal Component (PC) of the sample covariance matrix mapping the maximum overall variance associated with damage in the observed data. Finally, the authors demonstrated that performing the control chart analysis after PCA projection captures a clearer distinction between undamaged and damaged vibration responses than by applying a statistical control chart alone.

Hu et al. (2012) applied the PCA to a large amount of data continuously collected by the dynamic monitoring of a footbridge to eliminate environmental effects from measured natural frequencies over three years. The authors used the PCA to eliminate effectively the temperature effects and proposed further a novelty analysis based on the residual errors of the PCA reconstruction of the input data to provide a statistical indication of damage. The PCA was performed on the frequencies for the eight vertical bending modes of the bridge measured under maximum variations of 35°C. To determine the threshold limits, an X-bar control chart was constructed based on distribution parameters of the samples observed in the reference condition with normal environmental conditions. In this study, since the bridge was newly constructed the methodology could not be validated for damage detection. However, finite element simulations of the bridge indicated that with raising damage levels the average novelty index deviates clearly from the reference state, which can be attributed to the presence of damage.

Similarly, Kerschen et al. (2005) used the PCA to address uncertainties and variability due to changing environmental conditions in the distribution of the first four natural frequencies of a concrete box girder bridge subject to inducing damages incrementally added under a one year period. The PCA models were trained for the undamaged state of the bridge for varying

environmental conditions. Here again, assuming that the residual error of PCA model remains small in the presence of no damage, the presence of damage was determined with a significant increase beyond the outlier limit of the introduced novelty index.

2-5 Concluding Remarks

A review of the research using different methods has been presented through a variety of numerical, analytical and experimental studies for condition assessment of bridge-type structures. The shortcomings of local nondestructive techniques led to the development of modal/structural based methods which are global in nature.

Damaged-related shifts in natural frequencies have been addressed by several researchers to monitor the integrity of structures and to detect the potential damage existing in structures. However, frequency shifts have been proven to be reliable only for significant levels of damage and are not able to provide spatial information to determine the location of damage (Salawu 1997, Perera and Huerta 2008). Moreover, natural frequencies are found to be more sensitive to environmental variations than damage at small levels. Indeed, reversible effects of ambient temperature on natural frequencies appear to be a significant obstacle to the application of this technique for damage detection in real cases. Frequency-based detection algorithms (e.g. frequency reference function methods) have been mostly developed based on attempts to find discrepancies between a validated finite element model and some damaged specimens (Thyagarajan, Schulz et al. 1998). In general, the damage detection algorithms developed based on finite element models are sophisticated and do not produce always a good agreement between a real structure and its analytical counterpart (Osornio-Rios, Amezquita-Sanchez et al. 2012). Therefore, these types of methods are still in a developmental stage and remain a very challenging research topic for implementation in complicated structures.

Unlike frequencies, damping-based damage detection techniques have been seldom considered for evaluating the integrity of structures. The latter can be explained due to large variability in determining damping ratios and the apparent lack of consistent correlation between structural damage and system damping (Farrar and Jauregui 1998). On the other hand, mode shapes have been found to be more sensitive indicators of damage than natural frequencies and modal

damping. Since damage is expected to induce localized decrease in stiffness, subtle changes in displacement mode shapes caused by damage have been used to detect the presence and the location of damage. The comparison of changes in mode shapes between the damaged and undamaged states of the structure has been considered with many researchers to identify the location of damage (Salawu and Williams 1995). MAC and COMAC, MSC, COMSC have been used for comparison of mode shapes through the literature. However, it has been shown that these methods are relatively insensitive to small perturbations of mode shapes, unless a significant reduction in stiffness occurred at the location of damage (Zhang and Aktan 1995, Parloo, Guillaume et al. 2003, Salgado, Cruz et al. 2006, Perera and Huerta 2008).

The changes in structural parameters such as flexibility and stiffness matrices have been investigated to detect damage in structures. However, these indicators are only reliable to detect damage in severe cases and fail to operate consistently in noisy conditions (Alvandi and Cremona 2006, Perera and Huerta 2008). To overcome the shortcomings of modal/structural based methods, several studies (Pandey, Biswas et al. 1991, Zhang and Aktan 1995, Maia, Silva et al. 2003, Catbas, Gul et al. 2007) have been performed to better exhibit the location of damage in structures using the concept behind the modal curvature methods. However, it was remarked that curvature techniques could not typically provide a good indication of damage using experimental data (Salawu and Williams 1994). Although curvature-based methods have been useful to magnify substantial changes of modal parameters caused by damage, at the same time, they amplify the effect of noise contained in the data (Alvandi and Cremona 2006).

The vibration-based damage detection methods reviewed above suffer from common drawbacks to resolve difficulties associated with experimental noise presented in vibration data and to detect damage at small levels of severity. Therefore, due to the complex features of damage mechanisms, more than one method is usually required to assess effectively damage-induced modifications in structural vibration response. ANNs have been widely presented in correlation with other techniques to assess accurately damage in structures. Although having a well-trained neural model can reasonably increase the accuracy of prediction of damage location and severity, reliable healthy and damaged structural models for training models are not always available in real cases, particularly for aging structures (Sun and Chang 2002, Sun and Chang 2004).

To improve the performance of vibration-based damage detection techniques, modal-based updating methods (e.g. generic algorithms) have been introduced based on modification of structural modal parameters (e.g. natural frequency, damping) in a numerical model so as to find a perfect match with the measured dynamic/static response of the structure. The main advantage of these techniques is their ability to estimate the location and the severity of damage without the baseline of an undamaged state. However, since the core solution of these techniques is on the basis of numerical simulation of a real structure, the development of an accurate analytical model is required to correspond as closely as possible to the structure to be analyzed and to minimize the residual difference between the experimental and analytical modal properties (Hu, Wang et al. 2001).

In recent years, a variety of techniques based on using signal processing tools have been developed as a complement to global-monitoring methods. FFT has been one of the initial mathematical tools primarily used by engineers involved in SHM in order to exhibit abnormal events in measured signals (Sun and Chang 2002). MUSIC algorithm is another type of vibration-based signal processing method that has been used on occasion to increase the detestability of conventional FFT algorithm. However, both algorithms suffer from the fact that they are not able to preserve both the time and the frequency information of the signal (Jiang and Adeli 2007). The methods based on using FD and STFT have been developed to overcome the limitations of previous techniques. However, because of the fixed size of the moving window the proposed algorithms cannot achieve simultaneously a high resolution in time and frequency domain of a signal (Robertson, Camps et al. 1996, Hadjileontiadis, Douka et al. 2005). EMD and HHT are another class of signal processing tools that have been developed recently to detect slight distortions and abnormal events in time signals caused by damage. However, these techniques are inefficient to extract accurately the true frequency pattern of signals in detail which may cause misinterpretation of the structure behaviour (Quek, Tua et al. 2003).

WT and its derivatives have received wide attention through the literature that has been spurred the publication of several papers in the field of SHM (Cao and Qiao 2008). An arbitrary time-frequency resolution characteristic of WT using a variable sized-windowing technique has been yielded the popularity of this tool for the analysis of signals in both the time and the space domains (Sun and Chang 2004). Another advantage of WT is its ability to provide a large

selection of decomposition functions which would make it a suitable tool for different applications. Discrete-based derivatives of WT such as DWT and WPT have been mostly proposed for the analysis of the structural response using time-domain data. These techniques often require several levels of decomposition as well as large computational processing time. In addition, their applications on space-domain data experimentally obtained from real measurements such as mode shapes lead to the loss of information contained in the low frequency components of the signals. In contrast, CWT has emerged as a simple, fast and powerful method to continuously monitor the structural mode shape along the entire length and to reveal small irregularities and perturbations due to trivial damage (Sun and Chang 2002, Sun and Chang 2004).

The result of the CWT procedure is a set of coefficients that correspond sequentially to each location or measurement points along the mode shapes. The bigger the size of damage, the larger the magnitude of the coefficient in the vicinity of the location of damage and therefore, it can be used as an indicator of the severity of the damage. Nevertheless, current studies demonstrate that CWT alone is not able to address the difficulties related to false indications of damage at small levels and in the presence of experimental noise. To extend the applications of wavelets in real structures, efforts have been made to capture either free vibration motions or deflection curves of structures using high-speed image processing tools. Even so, these techniques are not immune to experimental noise since the quality of images obtained from laser-based scanning techniques is highly dependent on exposure conditions and any deviations from the initial position in the camera due to ambient vibrations result in poor extraction of the real displacement data (Poudel, Fu et al. 2005).

In summary, the methods described in the literature demonstrate a comprehensive historic development of vibration-based damage detection methodologies with limited degree of success to detect damage effectively in complicated cases. Promising results have been concluded mostly for either numerical case studies without the presence of noise or simple experimental setups with small-scale test objects or significant cases of damage. Furthermore, attempts for damage detection in real field applications have not been found quite efficient to localize damage in bridges, except for extreme cases. Vibration-based statistical techniques have been rarely developed to overcome the current limitations of existing methods through the applications of

statistical pattern recognitions algorithms. However, most of these approaches address only the difficulties associated with the first stage of damage diagnosis (detection of damage existence) and are not able to provide an efficient approach for damage localization.

Statistical tools have recently gained increased attention to minimize uncertainties associated with experimental noise and to increase the probability of detection by setting an appropriate level of threshold. Classical hypothesis testing methods (e.g. t-test, U-test) have been developed to provide an acceptable area of fidelity for the decision-making process of potential damage in structures (Reiff, Sanayei et al. 2016). The main advantage of these techniques is their simplicity to work for engineers with basic knowledge of probability and statistics. Different methods based on pure statistical approaches (e.g. AR, PCA) and outlier detection algorithms (e.g. control chart analysis) have been developed to classify and extract features obtained from dynamic tests.

There are several obstacles that remain unresolved for AR methods. Examples include the lack of sufficient accuracy and reliability in their results for large-scale structures as well as the difficulties in dealing with large volumes of data, inherent noise-contaminated structural response measurements, and lack of reliable feature extraction tools (Zang, Friswell et al. 2004, Osornio-Rios, Amezquita-Sanchez et al. 2012). However, PCA-based methods have emerged as promising to reduce dimensionality of large sample data to a lower-dimensional space in such a way that the dominant patterns of variations of the data are maximized in the low-dimensional representation space. To discriminate between the effects of environmental variations and induced damage in modal frequencies, different authors have employed the PCA-based damage detection novelty analysis approaches based on coupling of the PCA with statistical control chart techniques. In spite of promising results, these techniques have only accounted for the difficulties associated with the detection of damage existence in structures. Aside from the dimensionality reduction property, PCA can also be used for the purpose of different applications such as noise reduction and feature extraction in the data experimentally measured from structures. The latter is very useful to minimize statistical uncertainties and variability in vibration data due to experimental errors and environmental noise (Shahsavari, Chouinard et al. 2017).

2-6 Wavelet Transform (WT)

Since the results obtained from the WT are used to feed the statistical models in this work, this section describes briefly the principle of WT. However, more comprehensive explanations can be found in the cited references (Daubechies 1992, Misiti, Misiti et al. 1996).

2-6-1 Introduction to Wavelets

From the historical point of view, wavelet analysis has initially been a common tool for analyzing localized variations of power within a time-series. Using the wavelet analysis, one is able to decompose a time-series into a time-frequency space in order to determine how dominant modes of variability vary in time (Torrence and Compo 1998, Wang and Deng 1999). Since mode shapes are typically more sensitive to local features than natural frequencies and due to inefficiency of time-domain techniques to localize damage, the attention of researchers has been gradually turned the use of WT from the time-data to the space-data (Wang and Deng 1999, Allen and Aguilar 2009, Grégoire 2011). In this study, the information contained in the spatially detailed mode shapes measured from a set of accelerometers equally-spaced along the structure is also used to develop a wavelet-based statistical damage detection methodology.

Unlike sine waves (the basis of FT) which are smooth and predictable functions, wavelets are defined as oscillatory, real or complex-valued functions with zero mean value and finite length. Moreover, the irregular and asymmetric shape of the wavelets might lead to better analysis of the signals with sharp changes than smooth sine waves (Misiti, Misiti et al. 1996). The WT can be simply defined as a method of decomposition of an arbitrary signal into a series of local basic functions, also known as mother wavelets (Bajaba and Alnefaie 2005). The mother wavelet, $\psi(t)$, should comply with the following two conditions: it integrates to zero and it is square integrable (see Eq. 2.5 and 2.6). The latter implies the oscillatory shape of the mother function in which most of its energy is restricted to a finite duration (Kim and Melhem 2004, Staszewski and Robertson 2007). It is important to note that in order to perform the analysis on spatial signals as is the case in this study, the time t in all equations can be replaced by the spatial coordinate x, indicating the location (or sampling node) of the displacement mode shape.

$$\int_{-\infty}^{+\infty} \psi(t)\, dt = 0 \tag{2.5}$$

$$\int_{-\infty}^{+\infty} |\psi(t)|^2\, dt \; < \; \infty \tag{2.6}$$

From mother function $f(t)$, the analyzing wavelets can be obtained as function of scale (s) and position (u) parameters and must be positive real numbers (Daubechies 1992).

$$\psi(t) = \frac{1}{\sqrt{s}}\psi\left(\frac{t-u}{s}\right) \tag{2.7}$$

Scaling a wavelet means basically to change its width through either compression or extension of the wavelet. Figure 2-13 indicates that higher scales correspond to the most stretched wavelets (lower frequencies).

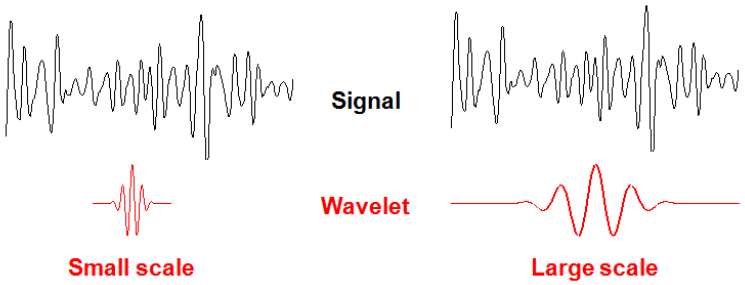

Figure 2-13: Low scale and large scale wavelets correspond to rapidly and slowly changing details of the signal respectively.

A larger portion of the signal, and thus coarser features will be measured using a stretched wavelet and vice versa. Shifting a wavelet means delaying the wavelet onset along the length of the signal (Misiti, Misiti et al. 1996).

An advantage of the WT is its diversity in terms of the type of the wavelets that allows using them for various applications in a wide domain of sciences such as in Geotechnical Engineering (Ding and Ding 2006, Ohkami, Nagao et al. 2006), in Geophysical sciences (Foufoula-Georgiou and Kumar 1994), in Oceanography and Meteorology (Liu 1994), in Earthquake Engineering

(Iyama and Kuwamura 1999) (Amiri, Bagheri et al. 2009), in Mechanical Engineering (Lin and Zuo 2003) (Ocak, Loparo et al. 2007), etc.

Figure 2-14 shows different types of wavelets (Misiti, Misiti et al. 1996). Depending on the type of the features present in the signals, the shape of the wavelet function has to be chosen in a manner that can perfectly reflect these features. One would choose a boxcar-like function (e.g. Haar wavelet) to reflect a signal with sharp jumps or steps, while a smooth function (e.g. Gaussian wavelet) can be a good idea to reflect the detailed changes of smoothly varying signals (Torrence and Compo 1998, Rucka and Wilde 2006). The study reported by Torrence and Combo (Torrence and Compo 1998) provides a practical guide to wavelets and their selection.

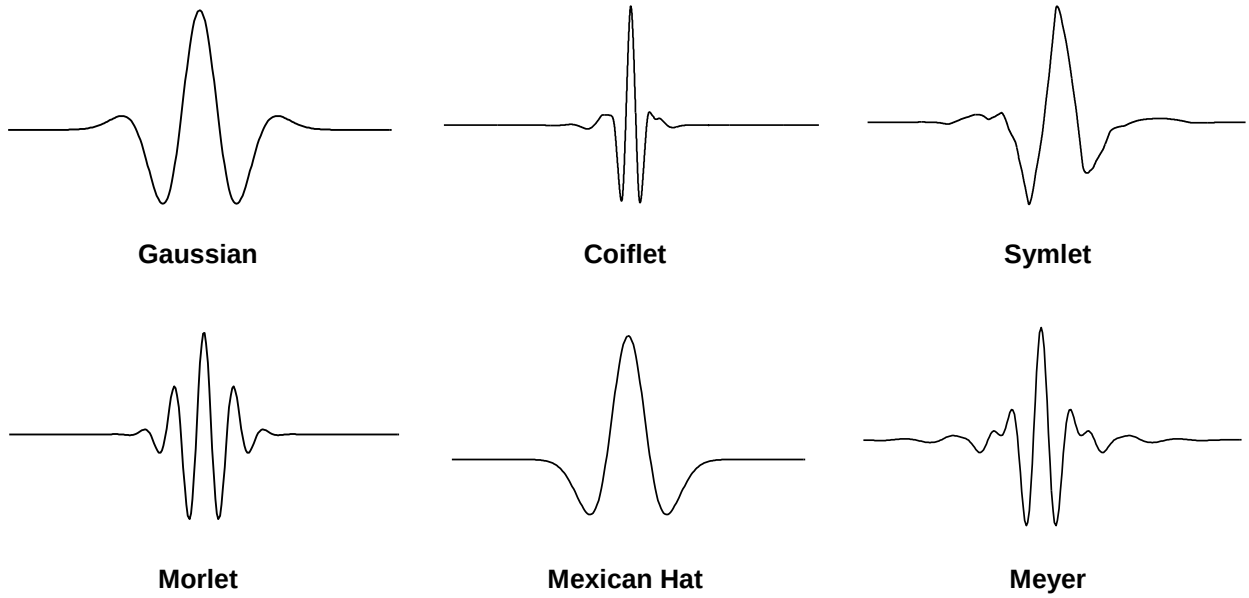

Figure 2-14: Examples of different types of wavelets.

In view of the literature, Gaussian wavelet (Gentile and Messina 2003, Messina 2004, Rucka and Wilde 2006, Rucka and Wilde 2006) and Symlet wavelet (Douka, Loutridis et al. 2003, Douka, Loutridis et al. 2004, Loutridis, Douka et al. 2004, Loutridis, Douka et al. 2005, Umesha, Ravichandran et al. 2009) are reported as the most promising functions for damage detection in several studies. The advantages of the Gaussian and Symlet wavelets have been previously discussed (Gentile and Messina 2003, Loutridis, Douka et al. 2004).

Indeed, a sized-windowing technique allows the use of long time intervals where more precise low frequency components are required, and a short time interval when high frequency information are favorable (Figure 2-15). In contrast with other signal processing tools (e.g. FT, STFT), the WT does not look like neither the frequency nor time-frequency domains, but rather a time-scale region (Misiti, Misiti et al. 1996). The results of the WT are the so-called "wavelet coefficients". Its calculation represents how closely the wavelet is correlated with the selected section of the signal. High values of this coefficient show strong similarity between the wavelet and the localized portion of the signal that is analyzed (Misiti, Misiti et al. 1996). The specific properties of wavelet functions such as orthogonality, make it possible to calculate the coefficient with efficiency (Kim and Melhem 2004, Staszewski and Robertson 2007).

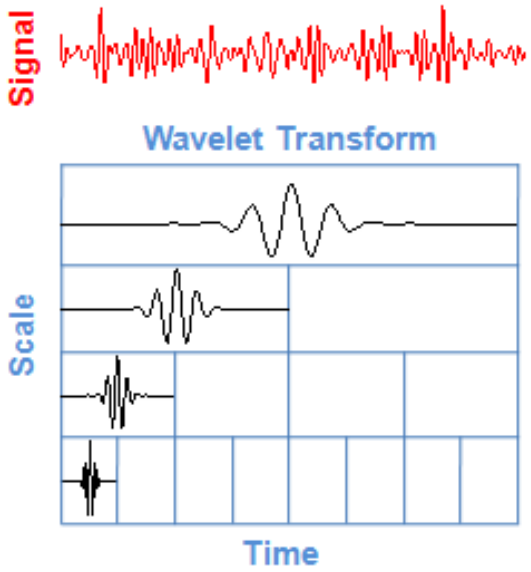

Figure 2-15: A scalogram representing of wavelet transform (WT).

WT results in many wavelet coefficients which are functions of scale and position. In space-domain signals such as mode shapes, the magnitudes of the wavelet coefficient at the damage location can be an indicator of the severity of damage (Bajaba and Alnefaie 2005). WT is classified in two categories. In the context of SHM, the CWT is considered more suitable for local analysis of mode shapes in the space domain whereas the DWT is found to be suitable for decomposition, compression and feature selection of time-series measured from dynamic analysis of structures.

2-6-2 Continuous Wavelet Transform (CWT)

In the most simple form, the CWT is represented by the sum over the entire time of the signal multiplied by scaled and shifted versions of the wavelet function $\psi(t)$ (Misiti, Misiti et al. 1996). The mathematical expression of the CWT for the function $f(t)$ can be defined as:

$$CWT = \frac{1}{\sqrt{|s|}} \int_{-\infty}^{+\infty} f(t)\, \psi^*\left(\frac{t-u}{s}\right) dt \tag{2.8}$$

where s and u are the scale and translation indices respectively, CWT is the calculated wavelet coefficient for the mother function $\psi(t)$ and it calculates the variation of the signal in the vicinity of u whose size is proportional to the scale of the wavelet. $\psi^*(t)$ is the complex conjugate of the mother function (Bajaba and Alnefaie 2005, Rucka and Wilde 2006). The complete process of CWT yields many wavelet coefficients as functions of scale and position. Multiplying each coefficient by a suitably scaled and shifted wavelet may lead to the construction of the original signal $f(t)$ (Misiti, Misiti et al. 1996). The overall procedure to compute the CWT coefficient is performed within five steps:

1) Choose an appropriate wavelet and compare it in a section close to the start point of the original signal (here in the form of a sine function with a small discontinuity or breakdown point along its length).

2) Calculate the wavelet coefficient "CWT" (Figure 2-16).

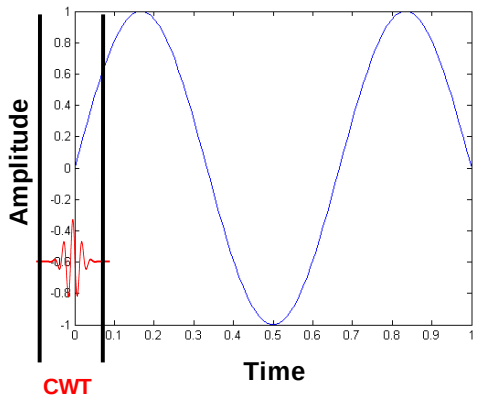

Figure 2-16: Calculation of wavelet coefficient for the first section of the original signal.

3) Shifting the wavelet to the next section (toward right) and repeat the second step until complete coverage of the whole length of the signal (Figure 2-17).

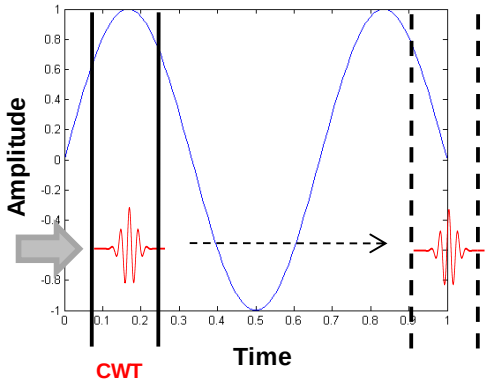

Figure 2-17: Shifting the wavelet and repeat step 1 and 2 for the whole signal.

4) Scaling the wavelet and do the same as that of steps 1 to 3 (Figure 2-18).

5) Repetition of all of the above steps (steps 1 through 4) for the entire scales (Misiti, Misiti et al. 1996).

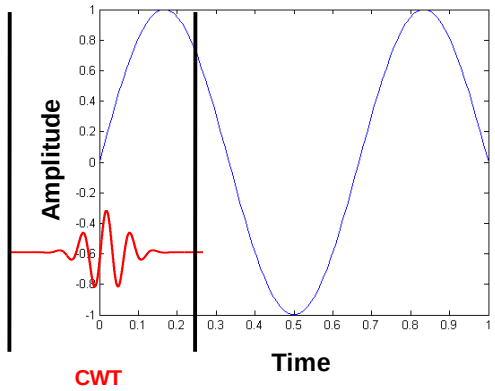

Figure 2-18: Scaling the wavelet and repeat steps 1 to 3.

By doing so one may have many coefficients at different scales corresponding to dissimilar sections of the signal. Finally, providing a plot on which the x-axis and y-axis represent the position (along the time of the signal) and scale parameters respectively, the color at each x-y

point corresponds to the magnitude of the wavelet coefficient which will make a sense of all these coefficients.

As show in Figure 2-19, wavelets with larger scales display oscillatory patterns observed in the signal where the oscillation in the wavelet correlates best with the signal feature. However, wavelets with smaller scales produce relatively large wavelets coefficients around the discontinuity, indicating that smaller scales are more useful for detecting abrupt transitions or breakdown points in the signal (Misiti, Misiti et al. 1996).

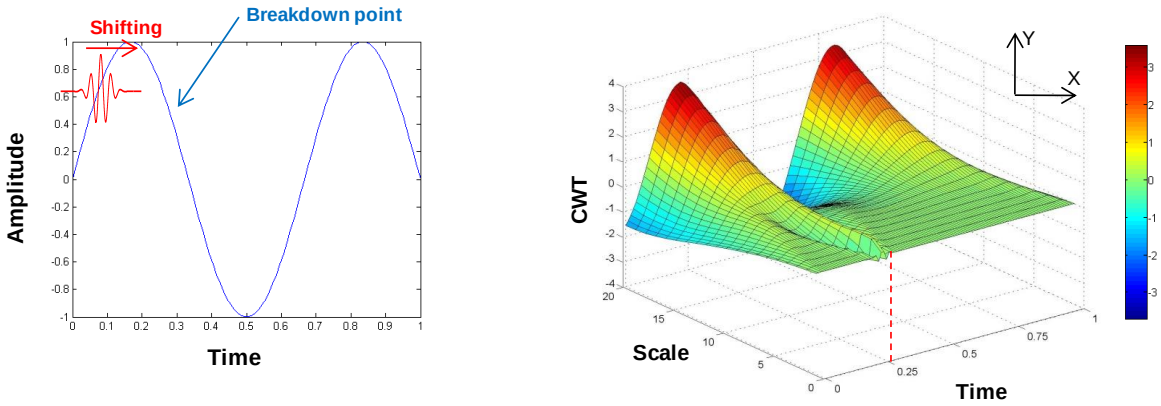

Figure 2-19: Applying the CWT on a sine wave with a small discontinuity along its length.

In order to ensure the existence of the inverse WT, an admissibility condition should be satisfied with the mother wavelet (Kim and Melhem 2004):

$$\int_{-\infty}^{+\infty} \frac{|\psi(\omega)|^2}{|\omega|} d\omega < \infty \tag{2.9}$$

where $\psi(\omega)$ denotes the FT of $\psi(t)$. Moving the wavelet along the time axis implies examining the signal $f(t)$ in the vicinity of the current location of the moving window. Thus, unlike the FT where the frequency domain is used, time domain information remains through wavelet analysis (Moyo and Brownjohn 2001).

2-6-3 Vanishing Moment

As the smoothness and concentration of the wavelet functions is defined and identified by their numbers of vanishing moments. The number of vanishing moments (also known as order) is an

important tool for detecting signal singularities. A wavelet with *n* vanishing moments must satisfy (Rucka and Wilde 2006):

$$\int_{-\infty}^{+\infty} t^k \psi(t)\, dt = 0 \qquad k = 0,\ 1,\ 2,\ ...,\ n-1 \tag{2.10}$$

To explain the concept behind the vanishing moment, lets consider the following Taylor series at x = 0:

$$f(x) = f(0) + \frac{f'(0)}{1!}x + \frac{f''(0)}{2!}x^2 + \frac{f'''(0)}{3!}x3 + ... + \frac{f^n(0)}{n!}x^n. \tag{2.11}$$

Using the presented Taylor series in Eq. 2.11, the CWT formula can be rewritten as:

$$CWT(0,s) = \frac{1}{\sqrt{s}} f(0)\int \psi\left(\frac{t}{s}\right)dt + \frac{f'(0)}{1!}x\int \psi\left(\frac{t}{s}\right)dt... \tag{2.12}$$

$$+ \frac{f''(0)}{2!}x^2\int \psi\left(\frac{t}{s}\right)dt + \frac{f'''(0)}{3!}x^3\int \psi\left(\frac{t}{s}\right)dt + ...\ ]$$

By considering the wavelet moment (M_p) as expressed below:

$$M_p = \int x^p \Psi(t)dt \tag{2.13}$$

and substituting Eq. 2.13 in Eq. 2.14, Eq. 2.12 can be given by:

$$CWT(0,s) = \frac{1}{\sqrt{s}}\left[f(0)M_0 s + \frac{f'(0)}{1!}M_1 s^2 + ... + \frac{f^n(0)}{n!}M_n s^{n+1} + ... \right] \tag{2.14}$$

where x^p denotes for the p^{th} derivative of *f*. Hence, since the zeroth moment equals zero as M_0=0, as a result, the first term of Eq. (2.14) equals to zero. If attempts are made in a way that make the moments up to M_n equal to zero, the CWT coefficients will decay as fast as s^n+2. The latter allows us to write Eq. 2.14 for different number of moments, which is known as a number of vanishing moments. Therefore, when a signal is not differentiable in a certain point due to a singularity at that point, the wavelet transform will result in a relatively large value at that location (Alvandi, Bastien et al. 2009).

2-8 Conclusions

An up-to-date review of the state-of-the-art was considered in this review to outline the contribution of global monitoring methods on vibration-based assessment of bridge-type structures. The significant competencies and restrictions of these techniques were highlighted in the different sections. For the cases reviewed herein, however, the proposed approaches were unable to achieve a high degree of confidence and reliability to detect and localize damage under varying environmental conditions, particularly uncertainties due to reversible effects of changes in ambient temperature. Despite successful applications and inherent merits of CWT for damage detection in structures, it still encounters some shortcomings to conclusively resolve challenges given due to a high noise to signal ratio at low levels and multiple locations of damage.

In light of the literature, this study has been performed to resolve the difficulties associated with previous studies. The latter has been resulted in the formation of the primary objective of this research, which is to set up a simple, robust, and energy efficient approach to locate small levels of damage in mode shapes.

In summary, the specific objectives of this research are to:

- Reduce uncertainty and variability in mode shapes due to experimental errors/noise
- Increase the efficiency and reliability of damage detection and localization algorithms
- Set adjustments in order to eliminate reversible effects of temperature change on damage detection
- Introduce statistically a decision making rule to minimize false indications of damage
- Improve signal to noise ratio commonly observed in experimental vibration data
- Determine the most likely locations of incremental damage at low levels of structural damage
- Expand the application of wavelets for damage detection and condition assessment of real bridges
- Highlight the importance of statistical pattern recognition paradigms in SHM.

To meet with the objectives described above, a novel detection approach has been proposed based on compiling a set of statistical techniques to detect low levels of incremental damage in

an experimental beam. Since spatially detailed mode shapes are typically sensitive to localized variations of the structures caused by damage and because of inherent characteristics of CWT to determine local anomalies or discontinuities in signals, the CWT has been favored over other existing methods to analyze vibration modes of an experimental beam. Thereafter, a PCA has been performed to generate new features by substituting the wavelet coefficients with new variables capturing most of the variability in the coefficients with noise immunity properties proportional to the original raw-data. A statistical detection criterion has been implemented to noise-isolated features to conclude damage statistically and objectively at a given significance level for low levels of incremental damage. Finally, a novel likelihood-based algorithm has been proposed to account for the most likely locations of damage along the structure. Given the promising results due to the proposed approach, statistical investigations have been extended by setting an optimization solution to eliminate the reversible effects of temperature in extracted features and to minimize false indications of damage under varying temperature conditions. Detailed explanations and conceptual formulations of the proposed approach will be discussed in the next chapters of this dissertation.

CHAPTER 3

3. Methodology

3-1 Experimental Program

This project consists of two main phases:

- Tests performed under steady-state or controlled conditions of the laboratory
- Tests performed in a climate-controlled room

The first phase of this methodology examines the efficiency and validity of the proposed approach for the detection and localization of induced-damage in an instrumented beam in which the size of damage and the support conditions of the beam can be modified. The second phase aims to investigate the effect of temperature change in the measured dynamic response of the beam and to provide a temperature correction factor to minimize the reversible effect of the temperature in the extracted scores obtained from PCA.

Experimental tests are affected by uncertainties associated with many factors such as measurements noise, human errors, ambient excitations, material properties, boundary conditions, and etc. The latter makes an experimental study more challenging than a numerical study since it is very difficult to control and isolate the impact of each type of these uncertainties in the experimental results. Hence, the results obtained from experimental tests are expected usually to be closer to those obtained from measurements for an actual structure (Zhou 2006).

The next section describes the configuration of the experimental setup and the specifications required to meet the objectives of this study. To ensure that the results obtained from this study conform as closely as possible to those obtained from actual structures; the experimental setup is designed in a way that can be adapted to real tests circumstances.

3-2 Test Setup Configuration

3-2-1 Test Object

Numerous studies have been undertaken to investigate the applicability of different techniques for damage detection in beam-like structures. However, most of previous experiments were conducted on small-scale specimens such as small steel or aluminum beams (e.g. 0.5 m of length), which exhibits less uncertainty in the results compared to those obtained from large-scale models. Hence, the tested specimen is chosen as a relatively large-scale bolted-beam of length L = 3m and uniform cross-section (W 150×37). Figure 3-1 indicates that the beam is an assembly of three sections joined together (only on the top-half depth of the section) using several sets of bolt-plate suppliers.

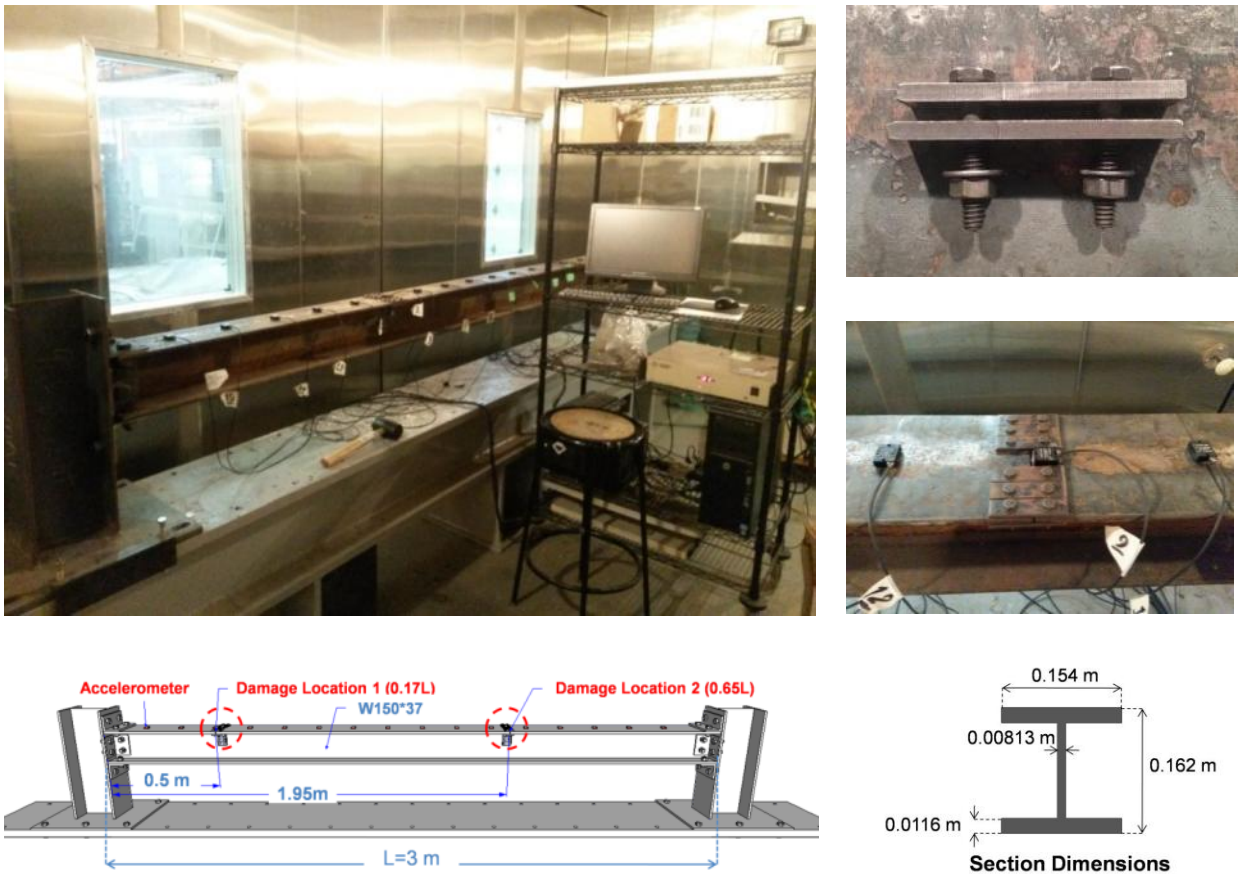

Figure 3-1: A schematic representation of the beam showing the beam in its fully bolted configuration state.

Each joint contains a notch or saw-cut of width 0.002 m across the top-half portion of the beam cross-section and the entire top flange. These joints are located approximately at 0.5 m (0.17L) and 1.90 m (0.65L) from the left end of the beam which are chosen to compare the sensitivity of the method for damage detection at two distinct locations of damage. The beam in its fully bolted configuration system is considered as the reference or initial state of the beam.

3-2-1 Definition of Damage

In comparison to most case studies in which a limited number of specimens are available to represent specific states of structural conditions, the fabricated setup is designed in such a way that not only it allows to make different patterns of incremental damage, but also it allows the inspector to modify the two end conditions of the beam. Various patterns of incremental damage can be simulated as a reduction in both the mass and the stiffness of the beam cross-section at each joint assembly. It may be noted that the incremental damage scenarios are induced by removing sequentially a set of bolts and plates at the locations of damage along the beam. The damage levels are sorted in ascending order from the initial state (E0) to the most severe state (E4) in Figure 3-2. In the latter case, an increase in the size of damage is reversible to the previous state/states. One has to note that the beam is not homogenous in its reference (initial) state. As shown in Figure 3-2, a portion of the beam at damage locations remains unconnected for each location of damage along the beam. It is worth mentioning that the latter has not been the case for most experimental studies dealing with a homogenous beam and an intact section. The presence of such discontinuities in the initial state of the beam may cause noise and irregularities in the mode shapes and subsequently can affect damage detection at a distinct location of damage.

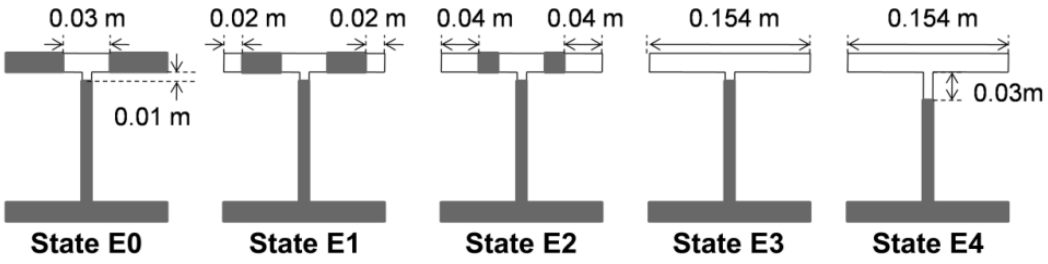

Figure 3-2: Damage evolving from the initial state E0 to the state E4.

3-2-3 Stiffening Tool

To apply precisely a specific torque to the fasteners, a torque wrench has been used for fastening the bolts on their places. In this case, the maximum torque capacity for which the bolts have been able to tolerate was 27.4 N-m (Figure 3-3).

Figure 3-3: Use a torque wrench to apply a same tightening torque to the fasteners.

3-2-4 Boundary Conditions

The two ends of the beam are connected to a beam (W 200×3) vertically fixed on the ground. As shown in Figure 3-4, by removing the L-shape corners mounted on the two surfaces of the beam one can evaluate the impact of different boundary conditions (pinned or fixed) for damage detection. In this case, the fixed-end support enforces restraints on all translational and rotational directions in the coordinate system while the pinned-end support restricts only the movements proportional to translational directions.

(a) Fixed-End **(b) Pinned-End**

Figure 3-4: The setup allows to make different boundary conditions at the end of the beam.

3-2-5 Excitation Method

Since ambient excitations are random in nature and due to the ease of implementation of impact testing methods, random force excitations have been applied manually by an impact hammer (Figure 3-5). It may be noted that the excitation required to vibrate the structure should be sufficient enough to extract the mode shapes properly. However, in a large-scale structure where a huge amount of energy is required to vibrate the structure, ambient excitations are mostly favored to excite the structure. **Error! Reference source not found.** provides a detailed discussion of most commonly used excitation techniques for real field testing of bridges. In this case, excitations are applied in a random manner at different points along the structure, which is important to provide a broad range of frequencies for an accurate estimation of the desired mode shape.

Figure 3-5: Impact hammer used to induce dynamic random excitations on the beam.

3-2-6 Accelerometers

For the complete formation of the setup and to measure the dynamic response of the structure subjected to non-constant force excitations, data acquisition has been performed using sixteen accelerometers equally spaced along the length of the beam. The setup comprises of three types of accelerometers with relatively similar specifications, namely, the KISTLER model 8305B2SP4M, KISTLER model 8310A25A1M11SP15M, and KISTLER model 8315A010B0AC06 (Figure 3-6). The first type of accelerometer, model 8305B2SP4M, measures

the accelerations in the range of $\pm 2g$ with a nominal sensitivity of 500 mV/g and a wide operating temperature ranging from -40°C to 85°C. The second type of accelerometer, 8310A25A1M11SP15M, operates under the same temperature range with acceleration range of $\pm 25g$ and sensitivity of 80 mV/g. The third type of accelerometer, 8315A010B0AC06, is defined by a maximum acceleration range of $\pm 10g$, sensitivity of 200 mV/g, and an operating temperature range between -53°C to 85°C.

(a) **(b)** **(c)**

Figure 3-6: The types of the sensors used in the setup, a) 8305B2SP4M, b) 8310A25A1M11SP15M, c) 8315A010B0AC06

3-2-7 Mounting Method

In general, numerous accelerometer mounting options are available to secure mounting of accelerometers to a test object. To ensure the replication of motion, especially at higher frequencies, the mounting surface of the test object must be prepared carefully before the installation of the sensors. Although the stud mount methods achieve the most accurate results, they often lead to a more demanding preparation such as drilling and tapping a mounting hole and can cause detrimental changes to the structure under study. Magnetic mounting bases provide a wider flexibility; however, they restrict the acceleration amplitude due to higher mass of the sensor and require a ferromagnetic surface. In this study, an adhesive mounting base using a synthetic wax is used due to its simplicity to install light weight sensors (Figure 3-7). To keep the mounting stiffness as high as possible and maximize high frequency transmissibility to the accelerometer it is recommended to spread a light coating of the adhesive wax/glue onto the base of the accelerometer before mounting on the test object. The standard guides for determining the

main characteristics of mounting methods and practical instructions for an optimal use can be found in ASTM E976 (E976).

Figure 3-7: The adhesive mounting method used to fix the accelerometers on the beam surface.

3-2-8 Acquisition System

The data acquisition hardware system is designed by Vishay Precision Group, Inc. to incorporate all the features required for precision strain measurement under a variety of loading conditions. The StrainSmart Software supports the acquisition system and meets the requirements required to acquire, display, and store measurement data in different formats. It is also able to perform a real-time monitoring of the temporal data received from the accelerometers and to extract the peak frequencies relative to vibration modes of the structure. In the present work, the System 6000's model 6100 Scanner is used to record data while maintaining 16 input cards (one channel per card) during measurements and providing data acquisition rates of 5000 samples per second per channel (Figure 3-8).

The model 6100 Scanner operates with a temperature range between -10 ^{o}C to 50 ^{o}C and it is compatible with various models of input cards (e.g. High-Level, Thermocouple, Strain-Gage, Piezoelectric). In this case, the Model 6030A High-Level and the Model 6010A Strain-Gage input cards are used per channel to apply a low-pass anti-aliasing filter during the acquisition of data. Figure 3-9 is a back view representation of the acquisition system using an interface card to connect the extremities of the accelerometers cable to the input card (Micro-Measurements).

Figure 3-8: StrainSmart® data acquisition system, model 6100.

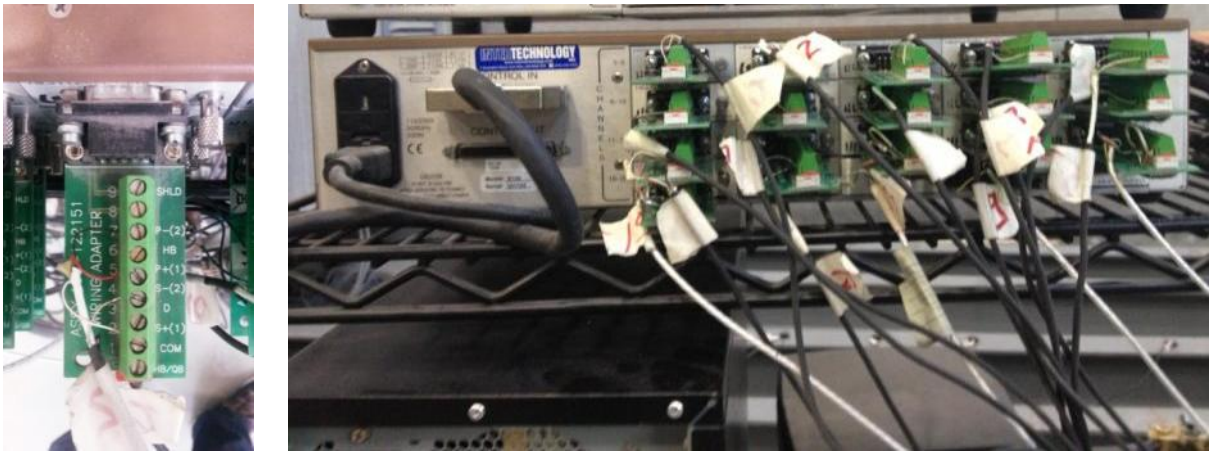

(a) Interface card **(b) Back view representation of the acquisition system**

Figure 3-9: The connection of the cables of the accelerometers to the acquisition system using an interface card.

3-2-9 Climate-Controlled Room

Among all types of environmental and operational factors, the variations in temperature can cause the most pronounced changes in structures. These changes depend on material properties such as Young's modulus, Poisson's ratio, and thermal expansion coefficient. The latter has led

to the investigation of the effect of temperature on the extracted PCA scores obtained from statistical procedures performed in this study. Given the thermal variation, its range must be identified around a temperature that does not make any interruption in the performance of the instruments (e.g. monitoring system, data acquisition system, and accelerometers) when performing the tests in the climate-controlled room.

A freezing-thawing room, Model WM-3800-MP4-15-SCT/WC, equipped with an electronic thermometer, has been used to handle varying degrees of temperature. The interior dimensions of the room in terms of width, length, and height are defined by 3.62 m, 6.25 m, and 4.22 m respectively. The maximum range in which the temperature can alter in the room is between -42.8^{o}C to 65^{o}C. After stability, the situation in which the temperature is controlled may vary at around $\pm$1℃. Figure 3-10 shows the step-by-step moving process of the beam in the climate controlled-room.

Figure 3-10: Step-by-step moving process of the beam in the climate-controlled room.

To measure how the mode shapes extracted from the beam can be affected due to thermal variations two temperature values (5^oC and 25^oC) are chosen to investigate the effect of temperature for the two smallest levels of damage in this case (E0 and E1). Since the primary results in Chapter 6 of this study indicated that the effects of a temperature differential of 20^oC on the mode shapes are distinguishable from those obtained due to damage, the measurements are not performed further beyond the selected range of temperature. More detail and explanations about the experimental setup and protocol are found in Chapter 6.

3-3 Signal Processing

The experimental tests are started by random dynamic excitations of the beam at different points along the beam. To minimize identification problems associated with the extractions of mode shapes and to improve signal strength relative to noise in the measured data, records were performed during 60 seconds with a sampling frequency of 5000 Hz for each set of measurements. Table 3-1 shows a typical representation of a time-series obtained from sixteen accelerometers embedded on the beam surface.

Table 3-1: A typical representation of an acceleration time-history output for an array of sixteen accelerometers.

ID	Elapsed Time (sec)	[1]	[2]	[3]	[4]	…	[16]
1	0.0002	1.1252804	1.3856672	1.4340412	1.5183965		1.1850363
2	0.0004	1.1607344	1.356672	1.5061267	1.5183965		1.2582252
3	0.0006	1.1268219	1.2483213	1.4953905	1.4509122		1.2846977
4	0.0008	1.0589968	1.1140276	1.3895629	1.3466183		1.264454
5	0.001	0.9757568	0.9995727	1.2300546	1.2177847		1.2130661
6	0.0012	0.8786436	0.8988524	1.07208	1.1088896	…	1.0900466
7	0.0014	0.7815304	0.8286534	0.9493813	1.0444728		0.9872708
8	0.0016	0.7260371	0.8057624	0.875762	1.0291354		0.8938382
9	0.0018	0.7167882	0.8317055	0.8680934	1.0736137		0.8829377
10	0.002	0.7553252	0.9263216	0.9309765	1.1303619		0.9763703
11	0.0022	0.8524384	1.0743499	1.0306692	1.2085823		1.0807033
⋮	⋮	⋮	⋮	⋮	⋮	⋮	⋮

As described in the previous chapter, by transforming signals from a time-domain to the frequency-domain different patterns of displacement mode shapes can be derived to each

frequency mode of the structure. The fundamental mode corresponds to the lowest frequency response of the beam with less measurement errors compared to those obtained from high frequencies, thus requiring a smaller range of frequency bandwidth to form the vibration mode corresponding to the first resonance frequency. To this end, data retrieving was performed via the MATLAB computing platform to compute the frequency response spectrum and therefore, to extract the desired mode shape for further processing by the CWT and the proposed statistical procedures. Figure 3-11 shows the flowchart of the methodology proposed in this study. It should be noted that the experimental protocol is explained separately through Chapters 4 and 6 of this thesis with a primary focus on the main objectives of each chapter. The next sub-sections provide a detailed review regarding the theoretical background behind the data analysis.

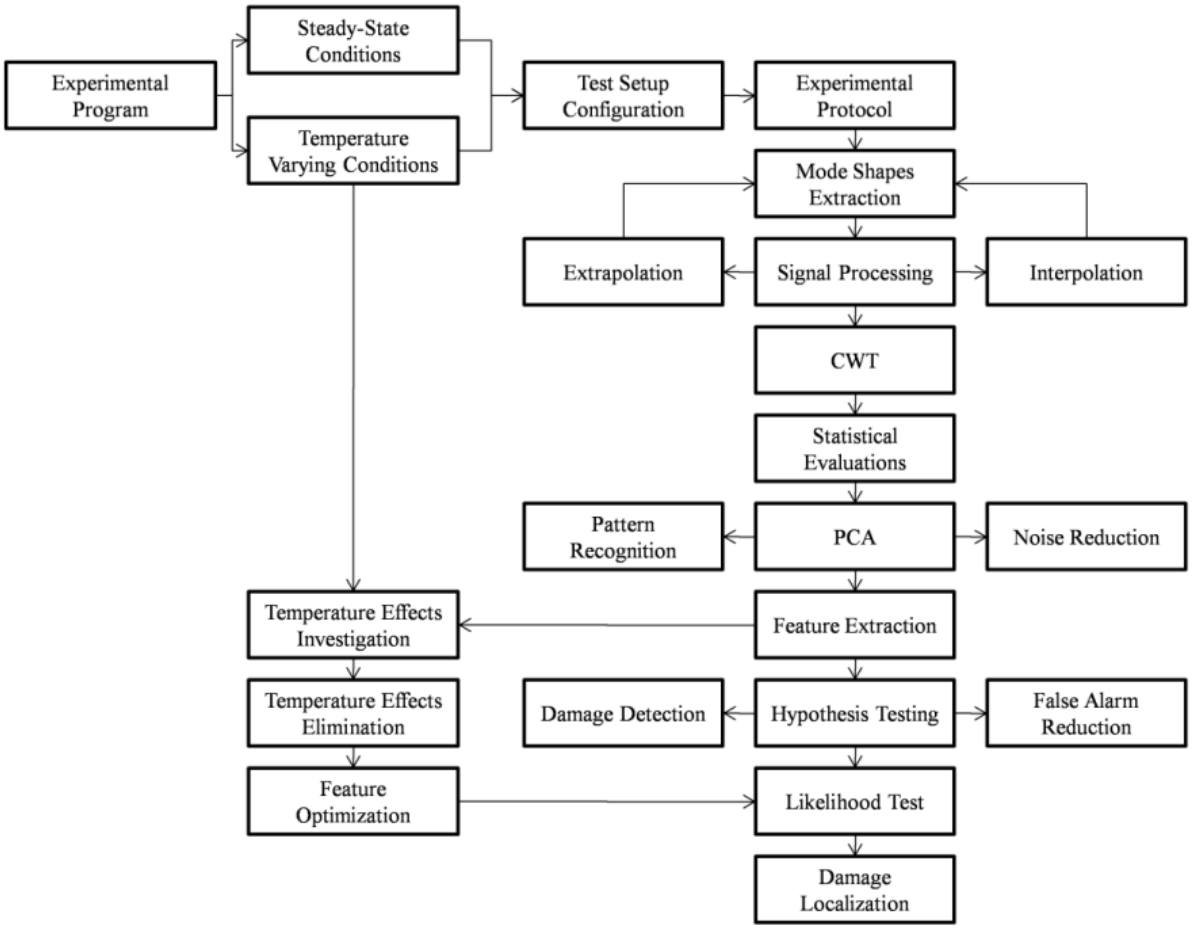

Figure 3-11: Flowchart of the proposed approach for detection and localization of damage.

3-3-1 Mode Shape Extraction

Stochastic system identification methods are usually referred to the techniques that are used for extraction of the modal parameters in a structure excited by an unmeasurable input force and that only output measurements (e.g. accelerations). Theoretical explanations of this section are provided from the cited references (Peeters and Roeck 2001, Peeters 2000). In the context of civil engineering, structures such as bridges and towers are known as the "systems", the estimation of the modal parameters is the "identification" in a particular type, and "stochastic" means that the input excitation force is unmeasurable. System identification starts by adapting a certain model that is aligned well with the system. Next, a range of values are assigned to the parameters as to match the acceleration measurements. Probably the most widely used and simplest approach to estimate the modal parameters of a structure is the so-called Peak-Picking (PP) method. The key step in this method is the identification of the eigenfrequecnies as the peaks of a spectrum plot. The modal identification used in this dissertation is based on the implementation of the so-called Complex Mode Identification Function (CMIF) method, which is consist of computing the Singular Value Decomposition (SVD) of the spectrum matrix obtained through PP method. A theoretical justification of the two methods is given below.

In case of acceleration measurements, the output power spectrum matrix of a system can be obtained by applying the Laplace transform of a continuous-time model and introducing the modal parameters:

$$S_y(s) = \left(\sum_{i=1}^{n} \frac{1}{s-\lambda_i} \{\nu_i\} \left\langle l_i^T \right\rangle \right) R_u \left(\sum_{i=1}^{n} \frac{1}{s^*-\lambda_i} \{l_i\} \left\langle \nu_i^T \right\rangle \right) \Bigg|_{s=j\omega} \tag{3.1}$$

where s is the Laplace variable, $\{\nu_i\}$ denotes the ith modal vector, $\left\langle l_i^T \right\rangle$ defines the ith modal vector, m is the number of inputs, and R_u is the input covariance matrix. In PP method, when eigenfrequencies are well-separated and damping is low, the spectrum around an eigenfrequency (ω_i) can be approximated as follows:

$$S_y(j\omega_i) \cong \alpha_i \{\nu_i\} \left\langle \nu_i^H \right\rangle \tag{3.2}$$

$$\alpha_i = \frac{1}{(\xi_i \omega_i)} \left\langle l_{c_i}^T \right\rangle R_u \left\{ l_{c_i}^* \right\} \tag{3.3}$$

where α_i , ξ_i , and $\{\nu_i\}$ represent the complex scale factor, the ith damping ratio, and the ith mode shape. The interpretation of this equation is that each column or row of the spectrum matrix at an eigenfrequency (resonance) can be considered as an estimate of the mode shape at that frequency. The CMIF method is a more advanced technique for the extraction of mode shapes based upon the diagonalization of the spectral density matrix using the SVD algorithm:

$$S_y(j\omega_i) = U(j\omega)\sum(j\omega)U^H(j\omega) \tag{3.4}$$

where U is a complex unitary matrix containing the singular vectors as columns, and $\sum$ is a diagonal matrix containing non-zero positive singular values in descending order. The CMIF method is based on the fact that the number of significantly contributing modes at a certain frequency determines the rank of the spectrum matrix. The rank of the spectrum is typically estimated by performing the SVD, where the number of non-zero singular values corresponds to the rank. Therefore, plotting the singular values of the spectrum matrix as a function of the frequency yields the eigen-frequencies as local maxima, which could be used to detect spaced modes Figure 3-12 shows a typical representation of the CMIF plot. In other words, the first singular value at resonance frequency is inductive of the first mode shape at that frequency. The second singular value corresponds to the second mode shape and so on. Figure 3-13 shows the first vibration mode of the beam corresponding to the first singular value.

For each state of damage, the measurements are repeated several times to reduce uncertainty and variability in the experimental mode shapes. For each case, in order to remove mode shapes corrupted by experimental errors, the Modal Assurance Criterion (MAC) is used to estimate deviations of each mode relative to the mean of entire modes for the corresponding state of damage. A strong correlation between two modes results in a MAC values close to one, whereas MAC values close to zero represents poor correlation. Since MAC values greater that 0.98 indicates a high correlation or similarity between two modes, the mode shapes corresponding to MAC values greater than 0.98 are used only to ensure the quality of experimental mode shapes for damage detection (Huth, Feltrin et al. 2005).

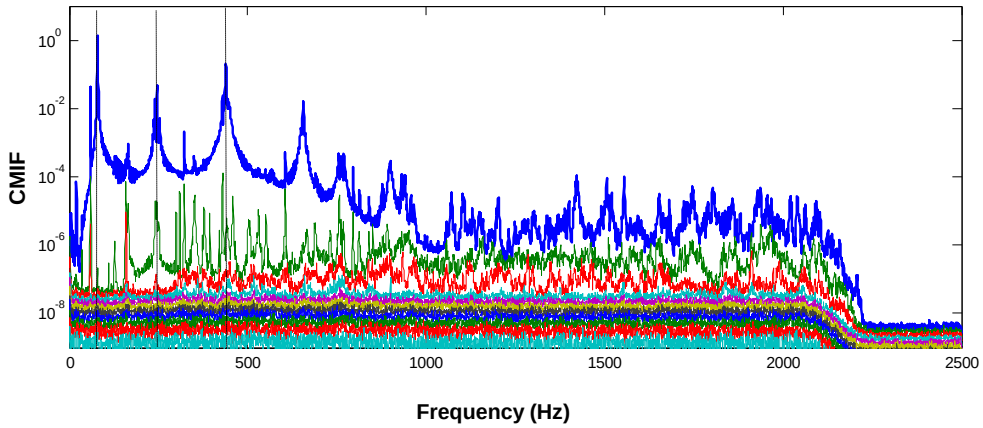

Figure 3-12: The singular values of the spectrum matrix as a function of the frequency. The first three local maxima are shown as dash vertical lines which correspond to the first three true natural frequencies of the beam respectively.

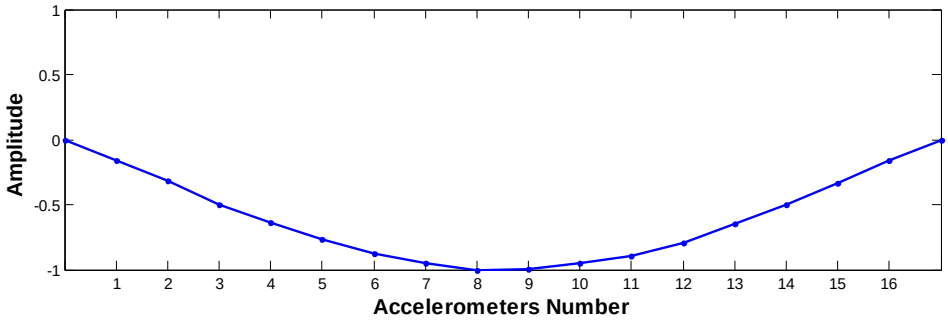

Figure 3-13: The first vibration mode of the beam corresponding to the first natural frequency.

The MAC function that compares the reference mode shape $\{\varphi_u\}$ and the selected mode shape $\{\varphi_d\}$ is defined as:

$$MAC\ (u,d) = \frac{\left|\{\varphi_u\}_r^T \{\varphi_d\}_r\right|^2}{\left(\{\varphi_u\}_r^T \{\varphi_u\}_r\right)\left(\{\varphi_d\}_r^T \{\varphi_d\}_r\right)} \tag{3.5}$$

where the subscript r and the superscript T correspond to the mode number and the transpose of the vector respectively (Ewins 2000).

3-3-2 Extrapolation and Interpolation

Mathematical optimizations such as extrapolation and interpolation functions are implemented to the mode shapes prior to the wavelet analysis. To reduce edge effects of mode shapes that might cause discrepancies in the wavelet coefficients and mask the effect of damage near boundaries, the mode shapes are extended over each extremity using a cubic extrapolation function of 32 extra points. Because of sparse sampling of measurement points in experimental mode shapes the wavelet analysis may interpret many points of displacement modes as singularities which can compromise the detection of damage (Loutridis, Douka et al. 2004). Therefore, an oversampling technique is implemented to the mode shape using a spline interpolation function resulting in a total of 316 nodes/sampling points over the length.

3-3-3 Continuous Wavelet Transform (CWT)

The selection of an appropriate type of a wavelet and the choice of its vanishing moment are key elements for effective use of the application of the wavelet analysis in damage detection. As the wavelet coefficients represents the correlation between the mode shape and the selected wavelet, in the presence of no damage the best wavelet is expected to exhibit a zero (or near zero) wavelet coefficient value. In other words, wavelets that are more similar to the signal shape are considered as the best candidates. In this study, according to several trial-error sensitivity analyses, it was concluded that Gaussian and Symlet wavelets with four vanishing moments are the most powerful wavelets in detecting structural singularities while using mode shape. However, for structural responses that are similar to polynomial of order higher than 4, wavelets with a higher number of vanishing moments provide more stable performance to detect abnormalities of mode shapes (Alvandi, Bastien et al. 2009).

A measured mode shape can be treated as a spatially distributed signal which contains the important information regarding the dynamic characteristics of the structure. To perform the analysis on spatial signals as it is the case in this study, the time t in Eq.2.8 can be replaced by the spatial coordinate x, indicating the location (or sampling node) of the displacement mode shape:

$$CWT = \frac{1}{\sqrt{s}} \int_{-\infty}^{+\infty} f(x)\psi^{*}\left(\frac{x-u}{s}\right)dx \tag{3.6}$$

where $f(x)$ refer to the main function in the space-domain, ψ^{*} is the complex conjugate of the mother function $\psi(x)$, s and u are scale and transition indices respectively. A sudden change or peak in the analyzed wavelet coefficients can be interpreted as an indicator of the location of damage or structural modification. The mode shape is typically measured over the entire length of the structure and, for a structure with a significant width, it can be obtained according to several measuring lines parallely implemented during measurements. In this study, a CWT has been applied on mode shapes extracted separately from each measurement and a wavelet coefficient is computed for each node (or pseudo-sensor) along the length of the beam. Next, by collecting the wavelet coefficients corresponding to each set of measurements, a large set of data containing the results of the wavelet analysis in a matrix format is generated. The matrix is constructed based on our observations in an ascending order, meaning that the first few rows corresponds to the repeated measurements in the first level of damage (E0), the next series indicates the wavelet coefficients in the next level of incremental damage (E2), and similarly in this way the last few rows are in accordance with the most extreme level (E4). The wavelet coefficients have been normalized relative to the maximum value observed in the observations (Alvandi, Bastien et al. 2009).

Despite popularity of the wavelet transform for damage detection in structures, a high noise to signal ratio at small levels of damage patterns may lead to either false indication of actual damage location or misinterpretation of the results. The latter emphasises the need for the development of a robust statistical pattern recognition technique to determine the patterns that are highly correlated with damage.

3-3-4 Principal Component Analysis (PCA)

User-defined functions are further developed in MATLAB platform to filter out noise from the wavelet coefficients and to replace these coefficients with a few new features that contribute most to the overall variance of the variations of the wavelet coefficients. The wavelet coefficients from the first two successive surveys are combined in a single matrix [X] and are used as variables for the PCA model.

$$X = \begin{bmatrix} x_{11} & x_{12} & x_{13} & . & . & . & . & x_{1n} \\ x_{21} & x_{22} & x_{23} & . & . & . & . & x_{2n} \\ . & . & . & . & . & . & . & \\ x_{m1} & x_{m2} & x_{m3} & . & . & . & . & x_{mn} \end{bmatrix} \tag{3.7}$$

where m indicates the total number of measurements ($m = N_1 + N_2$), n denotes the total number of sampling nodes or variables observed at equally spaced locations along the beam, and N is the sample size for each set of measurements. Note that the selection of the variables can be done for any two surveys from the available inspections. However, since the primary focus of this study is to detect damage at small damage patterns, only the first two successive surveys are studied in this dissertation. The PCA analysis is performed by centering the sample matrix [X] and computing the covariance matrix [C] of dimensions $n \times n$:

$$[C] = \frac{[X]^T [X]}{n-1} \tag{3.8}$$

where T represents the transpose of [X]. To extract the components that contain maximum variability of data due to damage and to determine percentage of variance observed by each component, the Singular Value Decomposition (SVD) algorithm is first applied on the centered matrix [X] as follows (Jackson 2005):

$$[X] = [U]\,[\Lambda]\,[V]^T \tag{3.9}$$

where [U] is an orthogonal $m \times m$, $[\Lambda]$ is an $m \times n$ rectangular diagonal matrix, and $[V]^T$ is an orthogonal $n \times n$ matrix transposed by the superscript T. Next, the eigenvalue decomposition of the sample covariance matrix [C] is defined by:

$$[C] = [V]\,[\Lambda]^2 [V]^T \tag{3.10}$$

while the columns of [V] are defined as the eigenvectors (or Principal Components PC) of [C], the square root of the diagonal entries of $[\Lambda]$, that are ranked in descending order, correspond to the eigenvalues (λ) of [C]. As a result, the percentage of variance explained (η) by the i^{th} principal component is given by:

$$\eta = 100\% \cdot \left(\lambda_i \Big/ \sum_{i=1}^{n} \lambda_i \right) \tag{3.11}$$

The analysis is performed in a way that the first few components are found to explain most of the variability observed in the wavelet coefficients. Finally, one can extract the score matrix [S] by linear transformation of the data into the new subspace of *n* variables which are introduced as new damage-sensitive features in this study:

$$[S] = [X]\,[V] \tag{3.12}$$

The elements of the [S] can be expressed by:

$$S = \begin{bmatrix} s_{11}^{\ 1} & s_{12}^{\ 2} & s_{13}^{\ 3} & . & . & . & . & s_{1n}^{\ pc} \\ s_{21}^{\ 1} & s_{22}^{\ 2} & s_{23}^{\ 3} & . & . & . & . & s_{2n}^{\ pc} \\ . & . & . & . & . & . & . & \\ s_{m1}^{\ 1} & s_{m2}^{\ 2} & s_{m3}^{\ 3} & . & . & . & . & s_{mn}^{\ pc} \end{bmatrix} \tag{3.13}$$

where *m*, *n*, and the superscript *pc* represent the number of observations, variables, and the given Principal Component (PC) respectively. The scores are sorted in a way that the first few columns of [S] correspond to the scores of the first few PCs while filtering out noise in the scores of higher components (Dackermann, Li et al. 2008). Therefore, performing statistical investigations on the scores associated with the first few components may improve damage detection at small levels of damage despite low signal to noise ratios.

3-3-5 Hypothesis Testing

The damage detection criterion investigated in this study is derived by analyzing the distribution of scores for increasing levels of damage (Shahsavari, Chouinard, 2017). Due to statistical uncertainty and variability in experimental measurements, the criterion is formulated in the form of a statistical test of hypothesis. Tests are performed to compare the equality of some specific statistics such as the mean or median value. Under laboratory or environmentally controlled conditions, the change in the distribution of scores can be attributed to the change in the state of

the beam caused by damage. A classical hypothesis test may be generally expressed by two hypotheses (Montgomery and Runger 2012):

$$H_0 : \mu_1 - \mu_2 = 0 \qquad \text{(null hypothesis-undamaged)} \qquad (3.14)$$

$$H_1 : \mu_1 - \mu_2 \neq 0 \qquad \text{(alternative hypothesis-damaged)} \qquad (3.15)$$

where subscripts 1 and 2 corresponds to different states of the beam respectively. The null hypothesis (H_0) in this application is that there is no incremental damage and the average difference in mean values does not significantly differ from zero when comparing data from two sets of measurements. Note that the same principal can be performed to compare the full distributions of the dynamic parameters or other statistics. The alternative hypothesis (H_1) is that the mean values for the dynamic properties are not equal between two sets of measurements, corresponding to a scenario of incremental damage since all other conditions (notably environmental conditions) were kept constant in the laboratory. The significance level (α) of the test is defined as the probability to reject the null hypothesis (no incremental damage) and corresponds to the probability of false detection of an incremental damage. For given samples from two populations, the p-value (P) can also be calculated as a measure of the power of the test to the reject the null hypothesis, which is the lowest level of significance that would provide the rejection limit of the null hypothesis. The null hypothesis is rejected if the p-value is smaller than the significance level selected for the test. In statistics, the significance level is often set to 5%; however, in the context of SHM, the latter may result in a large number of false alarms. Hence, lower significance levels of 1% or even 0.1% may be more appropriate. At given significance level (α), the result of the test returns either the logical value of H=1, indicating the rejection of the null hypothesis, or H=0 a failure to reject the null hypothesis.

In this application, to conclude statistically the existence of incremental damage, the t-test (Abramowitz and Stegun 1966) and Mann-Whitney U-tests (Gibbons and Chakraborti 2011) are used to compare whether the average difference of dynamic properties between two groups of measurements is significant. The t-test (Abramowitz and Stegun 1966) is performed for the equality of means for two random populations (e.g., $[\underline{S}_1]$ and $[\underline{S}_2]$) that follow the normal

distribution when the variance is unknown but equal. To achieve the best estimate of the variances, the pooled estimate of the common variance (ν_p^2) is defined as:

$$\nu_p^{\,2} = \frac{(N_1 - 1)\nu_1^{\,2} + (N_2 - 1)\nu_2^{\,2}}{N_1 + N_2 - 2} \tag{3.16}$$

where ν_1 and ν_1 are sample standard deviations and N_1 and $N2$ are the corresponding sample sizes. The test statistic (T) for the test has a t-distribution with N1 + N2 – 2 degrees of freedom:

$$T = \frac{\overline{S}_1 - \overline{S}_2}{\sqrt{\nu_p^{\,2}\left(\frac{1}{N_1} + \frac{1}{N_2}\right)}} \tag{3.17}$$

where $\overline{S}_1$ and $\overline{S}_2$ are the sample means from data from the two populations. The P-value (P) of the test is determined from the t-distribution for the corresponding values of the test statistic (T). A P-value below the significance level ($P < \alpha$) represents enough evidence against the null-hypothesis (H_0) at the significance level (α), thus H=1 indicating the existence of incremental damage in the beam, whereas a P-value greater than the significance level ($P > \alpha$) fails to reject H_0, thereby H=0, rejecting the alternative hypothesis (H_1) for the existence of the incremental damage between the two sets of measurements.

Unlike the t-test which is based on the assumption that the observations are normally distributed random variables, the Mann-Whitney U-test (Gibbons and Chakraborti 2011) is suitable for non-normally distributed data sets. The U-test follows a same principle as with the t-test for damage detection. However, unlike the t-test that is based on the equality of the means between two populations, the null hypothesis (H_0) in the U-test assumes that the two samples come from the same distributions with equal medians. In order to calculate the U statistic, the data for both samples is combined first into one set from lowest to highest score and numeric ranks are assigned to all observations, with the smallest observation given rank 1, the second smallest rank 2, etc. The tied scores (the ones with the same value) receive a rank equal to the average of unadjusted rankings. For example, given that AB=(2,3,4,5,6,6,7) is the combined set of the two samples A=(7,5,6) and B=(3,6,4,2) ordered in ascending order, A=(4,5.5,7) and B=(1,2,3,5.5) are defined as the adjusted ranks calculated for each group respectively. For two independent

samples ([$\underline{S}_1$] and [$\underline{S}_2$]) with lengths (N_1 and N_2), the test statistic for the Mann-Whitney U-Test (U) is determined as the smaller value of $U1$ and $U2$:

$$U_1 = N_1 N_2 + \frac{N_1(N_1+1)}{2} - R_1 \tag{3.18}$$

$$U_2 = N_1 N_2 + \frac{N_2(N_2+1)}{2} - R_2 \tag{3.19}$$

$$U = \min(U_1 \ , \ U_2) \tag{3.20}$$

where R_1 and R_2 are the sum of the ranks in each sample respectively. Following the same approach used in parametric testing, the observed U must be determined if support or reject the null hypothesis (H_0). In U-test, the z-statistic (Z) is used to approximate the P-value (P). For large sample sizes (N_1 or $N_2 > 10$), normal approximation is used while computing the P-value:

$$Z = \frac{U - \left(\frac{N_1 N_2}{2}\right)}{\sqrt{\frac{N_1 N_2 (N_1 + N_2 + 1)}{12}}} \tag{3.21}$$

For two-sided tests, the double value of Z gives the P-value. The lower is the P-value, the smaller is the risk of being wrong to reject the null hypothesis (H_0). If ($P < \alpha$), one has statistically significant evidence to reject H_0 between two groups of random variables and can conclude the existence of incremental damage in the beam.

3-3-6 Likelihood Test

Given the statistical detection of damage, the next step of the data analysis is to detect the most likely locations of damage along the beam. A novel detection algorithm is developed based on an adaptation of the Likelihood Ratio (LR) test often used in statistics to measure the fitness of good between two models (Kendall and Stuart 1979). Assuming that the damage has been occurred at one location, the LR test compares the likelihood of two different models relative to the scores measured in the damaged state at each location (or sampling node) along the length of the beam and selects the model with the highest likelihood. The two models are generated with a simple

assumption that the scores follow a normal distribution. The reference model (also referred to a full or complete model) is a model that the scores are computed in the damaged state (state 2), having their own mean μ and standard deviation σ. Against the full model, the scores of the alternative or nested model are computed sequentially at each location along the beam by removing the data at that location during the computation of the scores, as if one location or pseudo sensor is removed at that location. The vector of scores in the reference model $\{S_R\}$ is given by:

$$S_R = \{[X]_{m\times n} \,.\, [V]^{pc}_{n\times 1}\} \qquad ;m = N_1 + N_2 \tag{3.22}$$

where N_1 and N_2 are the sample sizes for each set of measurements, m and n are the total number of observations and variables in the original wavelet coefficient matrix [X], and $[V]^{pc}$ is a given set of eigenvector corresponding to the selected principal component (PC). The scores for the alternative (leave-a-node-out) model $\{S_i\}$ are generated sequentially for each location (or sampling node) along the beam such that, in each iteration, the component corresponding to the current node is set to zero:

$$S_i = \{\ [X]_{m\times n} \,.\, [V]^{pc}_{n\times 1} \,|\, V(i) = \underline{0}\} \qquad ;(i = 1,\ 2,\ 3,....,\ n) \tag{3.23}$$

$$S_{ALT} = \left[\{S_1\} \quad \{S_2\} \quad ... \quad \{S_n\}\right]_{m\times n} \tag{3.24}$$

Given the scores for the alternative model $[S_{Alt}]$, the latter is used to calculate the location parameters (μ and σ) of the scores of the alternative model. Finally, for each location or sampling node along the beam, the LR test is simply computed as the ratio of the likelihood (L) between the reference and alternative model at a given location:

$$LR(i) = \frac{L(S_R \,|\, \mu_R, \sigma_R)}{L(S_i \,|\, \mu_i, \sigma_i)} \qquad ;(i = 1,\ 2,\ 3,....,\ n) \tag{3.25}$$

with,

$$L(S_R \,|\, \mu_R, \sigma_R) = \sum_{j=N_1+1}^{m} \left(2\pi\sigma_R^2\right)^{-\frac{1}{2}} e^{\frac{-(S_R(j)-\mu_R)^2}{2\sigma_R^2}} \tag{3.26}$$

$$L(S_i \mid \mu_i, \sigma_i) = \left\{ \sum_{j=N_1+1}^{m} \left(2\pi\sigma_i^2\right)^{-\frac{1}{2}} e^{\frac{-(S_i(j)-\mu_i)^2}{2\sigma_i^2}} \right\}_i \qquad ;(i = 1,\ 2,\ 3,....,\ n) \tag{3.27}$$

Assuming that the model with the removed node (alternative model) is least informative or likely close to the damage location, one can expect that the LR achieves its maximum value in this location. In the presence of temperature effects, since a change in the temperature may affect reversibly the likelihood result, a correction algorithm is suggested to correct for the reversible effect of the temperature before performing the LR test. In real field test, a temperature correction factor should be established by making measurements at different temperatures in the early life of a structure before some damage is either introduced or increased. In this application, the correction for temperature is obtained from measurements at the two reference temperatures (5°C and 25°C) for the initial state of damage (E0). For the combined effect of the temperature and incremental damage between two surveys, an increase in the temperature from one survey to another one may amplify the average difference of scores between two sets of measurements. The latter can be adjusted by subtracting the value corresponding to the temperature correction factor from the average difference of scores between two surveys. However, while incremental damage is coincides with a decrease in temperature, the scores can be adjusted by adding the correction value to the average difference of scores.

CHAPTER 4 : AVANT-PROPOS

Auteurs et affiliation :

- Vahid Shahsavari : Étudiant au doctorat, Université Laval, Faculté des sciences et de génie, Département de génie civil et de génie des eaux.
- Josée Bastien : Professeur, Université Laval, Faculté des sciences et de génie, Département de génie civil et de génie des eaux.
- Luc Chouinard : Professeur, Université McGill, Faculté de génie, Département de génie civil et de mécanique appliquée.
- Antoine Clément: Étudiant au post-doctorat, Université Laval, Faculté des sciences et de génie, Département de génie civil et de génie des eaux.

État : publié en ligne

Date d'acceptation: 10 février 2017

Revue : Journal of Civil Structural Health Monitoring

Titre français : Tests basés sur la vraisemblance des coefficients d'ondelettes pour la détection des dommages dans les structures de faisceaux

Résumé français : La détection précoce de dommage a émergé comme préoccupation importante pour les ingénieurs impliqués dans l'évaluation des structures. Cet article présente une approche de détection de dommage qui combine différentes techniques pour améliorer la détection et la localisation de petits incréments de dommage en utilisant des modes propres dérivées de tests de vibration sur une structure. Une étude expérimentale est réalisée sur une poutre à deux assemblages (joints) qui peuvent simuler l'endommagement incrémentiel avec un système de plaques et de boulons. La condition initiale est définie comme l'état lorsque les plaques sont entièrement assemblées. Dans cet état, la poutre comprend deux zones plus faibles à l'emplacement de chaque ensemble d'assemblage (joint) en raison d'une réduction de la raideur

de 12% par rapport à une poutre intacte. La configuration d'essai est utilisée pour simuler d'endommagement incrémentiel en modifiant la masse et la rigidité de la poutre à chaque joint. La méthode de détection proposée s'avère plus efficace que les autres méthodes actuelles pour détecter de petits incréments de dommage et provoquer moins de fausses alarmes. La procédure de détection comprend quatre étapes: 1) une transformée en ondelette continue (CWT) pour détecter des anomalies locales du premier mode propre; 2) une analyse de composantes principales (PCA) des coefficients d'ondelettes pour extraire les modèles dominants les plus fortement corrélés avec l'endommagement incrémentiel 3) des tests statistiques de l'hypothèse sur les scores des composantes principales pour détecter l'endommagement incrémentiel statistiquement significatif, et 4) un test du rapport de probabilité (LR) pour déterminer l'emplacement le plus probable d'endommagement incrémentiel le long de la poutre.

Mots-clés : Détection et localisation d'endommagement, Poutre, Mode propre, Ondelette, Analyse des composantes principales, Rapport de probabilité

4. Likelihood-Based Testing of Wavelet Coefficients for Damage Detection in Beam Structures

4-1 Abstract

Early detection of damage has emerged as an important concern for engineers involved in structural condition assessments. This paper presents a damage detection approach that combines different techniques to improve detection and localization of small increments of damage using mode shapes derived from vibration tests on a structure. An experimental study is carried out on a beam with two assemblies (joints) that can simulate incremental damage with a system of plates and bolts. The initial condition is defined as the state when the plates are fully assembled. In this state, the beam comprises two weaker zones at the location of each joint assembly due to a 12% reduction in stiffness in comparison to an intact beam. The test setup is used to simulate incremental damage by modifying the mass and stiffness of the beam at each joint. The proposed method of detection is shown to outperform current alternative methods in detecting small increments of damage and to result in fewer false alarms. The detection procedure comprises four steps: 1) A Continuous Wavelet Transform (CWT) to detect local anomalies in the first mode shape, 2) A Principal Component Analysis (PCA) of wavelet coefficients to extract dominant patterns that are most highly correlated with incremental damage and to reduce noise, 3) Statistical tests of hypothesis on the scores of principal components to detect statistically significant incremental damage, and 4) A Likelihood Ratio (LR) test to determine the most likely location of incremental damage along the beam.

Key-words: Damage Detection and Localization, Beam, Mode Shape, Wavelet, Principal Component Analysis, Likelihood Ratio

4-2 Introduction

Ageing of existing civil engineering structures and the associated problems of deterioration have increased the interest in monitoring the structural health of structures (Sohn, Farrar et al. 2001). Structural Health Monitoring (SHM) systems have been used extensively for mechanical systems (e.g. rotating machines (Farrar and Duffey 1999, Sanz, Perera et al. 2007, Lei, Lin et al. 2013)); however, the application of SHM to large civil infrastructures such as bridges, has not progressed as rapidly (Taha, Noureldin et al. 2006). Currently, health monitoring of bridge structures relies mostly on visual inspections and low-level localized nondestructive investigations that are limited to portions of the structures that are easily accessible. In addition, inspections, monitoring and investigations are costly, which limits the ability to continuously monitor specific structures. The limitations of these localized monitoring methods have promoted the development of remote surveillance systems as well as global monitoring methods (Salawu and Williams 1995).

Among global monitoring methods, the measurement of vibrations has been found to provide valuable information on the dynamic properties of structures. Vibration-based techniques have been used to monitor bridge structures since the early 1980's. The methods are mostly based on the detection of changes in the natural frequencies and mode shapes of the structures (Sun and Chang 2004, Alvandi and Cremona 2006). These parameters are sensitive to localized structural damage that affect the mass or stiffness of the structure. However, these parameters are poor indicators of low-level damage and cannot be used stand-alone (Sun and Chang 2004, Taha, Noureldin et al. 2006, Alvandi, Bastien et al. 2009). For example, in tests performed on 40 highway bridges (Farrar, Baker et al. 1994), no changes were detected in the natural frequencies and their associated mode shapes until severe damage (e.g. a cut through the bottom mid-height of the web and entire flange of the main plate girder of a bridge). In addition, changes in natural frequencies do not provide information on the localization of damage (Doebling, Farrar et al. 1998).

Localization of damage using mode shapes has been investigated extensively in recent years; however, comparative studies have shown that mode shapes are not efficient for the detection of low levels of damage (Kim, Ryu et al. 2003). To improve the effectiveness of damage detection, techniques based on Artificial Neural Network (ANN) models have been proposed by using the

differences between modal shapes of intact and damaged structures and demonstrated on numerical models of a simple beam and a multi-girder bridge (Lee, Lee et al. 2005). These techniques require large training data sets from both intact and damaged states of a given structure, which is rarely available for real structures (Sohn, Farrar et al. 2004). Various measures based on modal properties have also been used for damage detection. The Modal Assurance Criterion (MAC) and Coordinate Modal Assurance Criterion (COMAC) factors compare modal shapes between two states but in most cases they fail to provide conclusive evidence of damage compared with other existing techniques (Ndambi, Vantomme et al. 2002).

Mode Shape Curvature (MSC) based methods have been proposed as a means to improve damage detection and localization (Pandey, Biswas et al. 1991). MSC has been proposed for detecting the location of damage in beam-type structures and was demonstrated with numerical simulations for a cantilever and a simply supported beam to demonstrate the sensitivity of higher derivatives of the mode shapes to damage (Pandey, Biswas et al. 1991). Using similar concepts, the changes in the modal flexibility matrix and its derivatives have been used to localize damage in beam-like structures (Catbas, Gul et al. 2007). Modal strain energy based methods, which are based on similar principles as MSC methods, form another group of damage detection techniques (Catbas, Gul et al. 2007). However, several studies indicate that curvature methods can amplify noise present in field measurements and mask changes due to small increments of damage (Chance, Tomlinson et al. 1994, Maeck, Abdel Wahab et al. 2000, Alvandi and Cremona 2006, Cao and Qiao 2008, Perera and Huerta 2008).

Small changes in modal parameters due to damage are difficult to detect without post-processing to enhance the signals (Chen, Spyrakos et al. 1995, Sun and Chang 2004). The CWT has been used for this purpose on mode shapes from measurements on beams and plates to detect damage and its location (Gentile and Messina 2003, Rucka and Wilde 2006, Alvandi, Bastien et al. 2009, Solís, Algaba et al. 2013) and on the displacement response of Euler-Bernoulli beams under various loading conditions (Spanos, Failla et al. 2006). The WT provides a means to analyze localized areas of a signal at different scales of time and space (Wang and Deng 1999). The wavelet analysis can be performed as the Discrete Wavelet Transform (DWT) or the Continuous Wavelet Transform (CWT). The DWT is most suitable for decomposition, compression, and feature extraction of signals, while the CWT is better adapted for the continuous monitoring of signals over the entire record. The WT provides a wavelet coefficient which is an indicator of

local anomalies in signals (Liew and Wang 1998). For example, Jaiswal and Pande (2015) use a numerical model of a beam to demonstrate damage localization by using the DWT on mode shapes. DWT has been used on mode shapes in combination with neural networks to detect and quantify damage in a numerical model of a cantilever beam (Vafaei, Alih et al. 2015) and a numerical model and experimental tests on a simply supported beam (Zhong and Oyadiji 2007, Zhong and Oyadiji 2011). Both DWT and CWT have been used on numerical models of a fixed-beam and a simple frame to detect cracks from deflected shapes (Ovanesova and Suarez 2004). Finally, CWT was used to detect damage experimentally from the deflected shape of a beam using laser measurements (Okafor and Dutta 2000, Cao and Qiao 2008, Wu and Wang 2011).

The performance of CWT applied to mode shapes is investigated numerically as a function of the location and depth of cracks for a beam in (Montanari, Spagnoli et al. 2015) and the effect of sampling intervals are found to be an important factor for wavelet analysis. Successful applications of the wavelet analysis are mostly performed on numerical models with significant levels of damage (Gentile and Messina 2003, Loutridis, Douka et al. 2004). However, CWT can fail to detect and indicate the location of damage and produce multiple false detections when the measurements are noisy and the level of damage is low (Salgado, Cruz et al. 2006, Shahsavari, Bastien et al. 2015). Statistical pattern recognition techniques are proposed in this study to improve the efficiency of CWT for the latter conditions.

The Principal Component Analysis (PCA) is a statistical analysis method which was first developed for data compression and feature extraction from large multivariate data sets (Pearson 1901). PCA has previously been used in the context of SHM for various purposes, and applied to different types of variables. For example, PCA has been used as a means to normalize data (either dynamic or static) by removing effects associated with varying environmental or loading conditions (Sohn, Czarnecki et al. 2000, Yan, Kerschen et al. 2005a, Yan, Kerschen et al. 2005b), to filter out noise (Moutinho, Caetano, et al. 2012), and for data reduction, and feature extraction (Santos, Crémona et al. 2016, Santos, Crémona et al. 2013, Santos, Crémona et al. 2016, Wang, Xiang, et al. 2015). The use of PCA in this application is to reduce the effect of noise and for extracting features that are highly correlated with the level of damage. The application of PCA to wavelet coefficients was shown to be efficient for that purpose and is novel in the context of SHM. In this application, PCA is applied to wavelet coefficients obtained at a set of locations along a beam for two successive surveys. The PCA identifies the patterns of

variation that explain most of the variance and in the process filters out noise that may be present in the measurements (Shahsavari, Bastien et al. 2015). The scores associated with the first few components of the PCA are shown to be highly correlated with the occurrence of incremental damage.

Statistical tests of hypothesis are used on the scores of the components to detect statistically significant changes in the distribution of scores between sets of measurements, which is associated with incremental damage. In this application, tests are performed on location parameters with the t-test for the comparison of mean values and the Mann-Whitney U-test for the comparison of medians (Abramowitz and Stegun 1966, Gibbons and Chakraborti 2011). Given that statistically significant incremental damage is detected, a Likelihood Ratio (LR) test is then proposed for the localization of damage (Kendall and Stuart 1979). The likelihood ratio is used in statistics as a goodness-of-fit measure for comparing nested models (Vuong 1989). It has also been used in the context of medicine to determine the diagnostic value of performing or not various tests (Zandbergen, Haan et al. 2001). The likelihood ratio as presented in the paper is a novel adaptation of this procedure by evaluation sequentially a series of nested models along the length of the beam in order to evaluate the relative likelihood of damage by comparing a full model with nested models that remove information from sensor position sequentially.

To summarize, the methodology used in this work has four steps: 1) Wavelet coefficients are computed using CWT on the first vibration mode shape of an experimental beam for two states of damage, 2) A PCA is performed on the wavelet coefficients computed at equal intervals along the beam to filter out noise from the measurements and identify the principal patterns of variation of the coefficients as they are affected by damage, 3) Statistical tests of hypothesis on equality of location parameters between the two states are performed to detect significant changes in the distribution of scores, and 4) Given that statistically significant damage is detected, a Likelihood Ratio (LR) procedure is used to determine the most likely location of damage. The procedure is demonstrated for a beam with two distinct locations of damage where the location and degree of damage can be controlled. The proposed procedure is validated by performing tests under controlled conditions in the laboratory and its performance is compared to other commonly used methods of damage detection, quantification and localization. Given the good results obtained with the proposed procedure, the next step is its application to an existing bridge and the evaluation of the robustness of the procedure to variability in climatic exposure conditions.

4-3 Experimental Setup

This study is performed under laboratory conditions by using a test setup that can simulate damage at two locations, different boundary conditions and different levels of damage for a beam. The original specimen is a steel I-beam (W150x37) consisting of three sections connected by several bolts and plates. Figure 4-1 illustrates the experimental setup in its initial state showing a discontinuity at the location of the two joint assemblies. The initial state of the beam corresponds for our purposes to the beam in its fully bolted configuration. Note that the beam is homogenous throughout its length and has a 12% reduction in stiffness relative to an intact I beam at the simulated damage locations in the fully assembled configuration. Each damage location consists of a 0.002 m notch across half of the depth (top half portion) of the beam. Levels of damage are simulated by adding or removing a set of bolted connections at the damage locations (Figure 4-2).

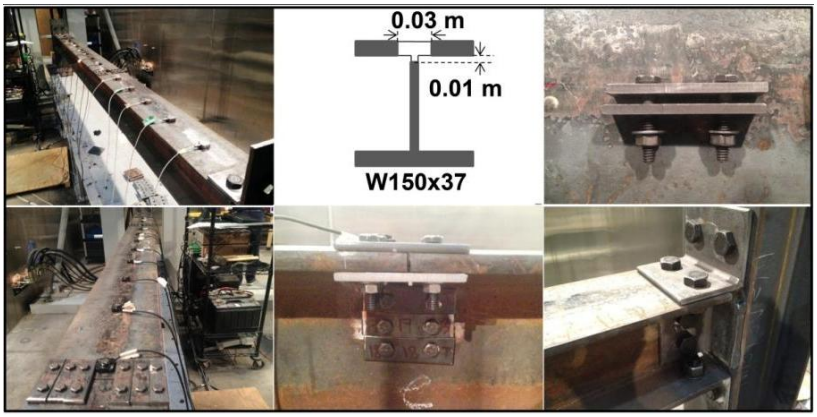

Figure 4-1: Test setup in its fully bolted configuration state indicating a small discontinuity at the location of joint assembly.

Figure 4-2: Damage increase from the initial state to the next increased level of damage.

Damage locations are at distances of 0.17L (0.5 m) and 0.65L (1.95 m) from the left end of the beam, where L (3 m) is the total length of the beam (Figure 4-3). The test setup consists of sixteen equally spaced sensors installed along the top flange of the beam. A large number of sensors are selected in order to test the accuracy of the algorithms for damage location. Lower levels of instrumentation could be investigated but is beyond the scope of this paper. To minimize the sampling interval from one instrument to the other, a spline function (De Boor 1978) is used to introduce 20 interpolation points between each instrument resulting in a total of 316 sampling points (nodes) for the experimental mode shapes.

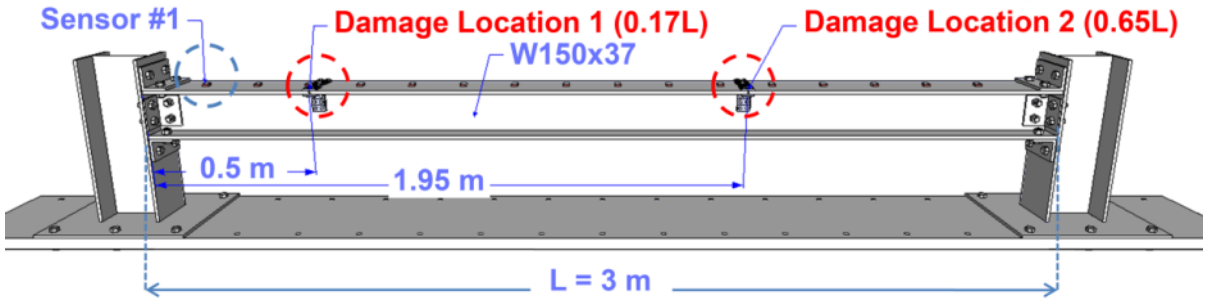

Figure 4-3: Schematic representation of the setup with relevant dimensions.

Two types of accelerometers with relatively similar specifications (Kistler model 8305B2SP4M and 8310A25A1M11SP15M) are used to measure accelerations at the sixteen nodal points. Random dynamic input excitations are applied by impact with a hammer; which is adequate to engage the structure over a wide range of frequencies for the estimation of first few mode shapes. Several measurements are performed in each damage state of the beam to account for uncertainties associated with the input motions. The test setups used in this experiment consists of introducing incremental damage at only one of the two locations at a time. The locations at 0.17L and 0.65L are used to compare the effect of damage location on the detectability of damage. In all cases, the beam is considered to be in an initially damaged state (E0) at the locations of the plates but with only one location where damage is increased incrementally.

Figure 4-4 shows an example of modal superposition for a beam with fixed supports and incremental damage at location 0.17L and illustrates the lack of sensitivity of modal shapes for small increments of damage. In this work, only the first fundamental mode shape is used since it is the mode shape that can be measured most accurately and its extraction is more convenient than higher modes in field applications. This is because the amount of energy required to engage

the natural frequency associated with the first mode shape is much smaller than for higher modes, which may be restrictive when investigating large-scale structures (Reynders 2012). However, the use of higher modes for damage detection in bridges has been considered in previous studies (Lee and Yun 2006, Chang and Kim 2016). Higher modes (longitudinal, torsional and transversal) can be identified in actual bridges and are important in detecting and localizing damage by deploying sensors at multiple locations. For the experimental beam used in this case, sensors could only be used to detect longitudinal modes of vibration. As the order of vibration modes increases, the number of nodal points where displacement is null or small increases. Although higher modes are in theory more sensitive to damage due to higher curvature, the latter can limit detectability near these regions (Rucka 2011). Nevertheless, the application of the proposed approach is not limited only to the first mode of vibration and the contribution of higher modes (e.g. second bending mode) could be considered in future applications for more complex structures. Combining observations for several modes could improve detectability in the latter case.

The next section evaluates several current procedures for the detection, quantification and localization of damage with the experimental setup. The results are presented as a function of damage location and damage level, designated as initial or extra low (E0), low (E1), medium (E2), high (E3) and very high (E4) (Figure 4-5).

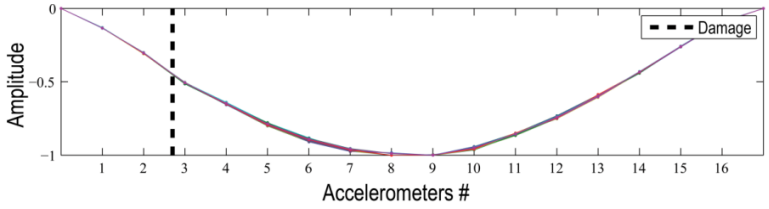

Figure 4-4: Modal superposition of several measurements for a small increase in the size of damage at 0.17L (or near the accelerometer #3).

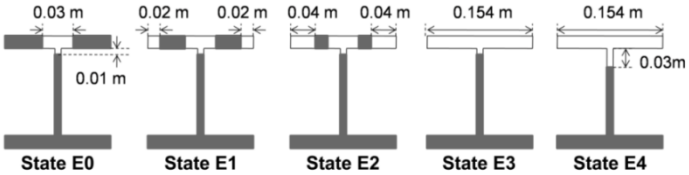

Figure 4-5: Different patterns of damage evolving sequentially from state E0 to E4.

Table 4-1 represents the ratio of damaged to undamaged moment of inertia (I/Io), the stiffness reduction (%), the equivalent crack height (a) for a rectangular section (%), and the number of measurements as a function of the level of damage for both damage locations. Note that the measurements taken from the initial state E0 are common in both cases (0.17L and 0.65L). The calculation of the moment of inertia is performed at the centroidal axis of the remaining section at each damage level. The choice of the centroidal axis is for the purpose of defining the reference state for pure bending. For each state/level of damage, the percentage reduction in stiffness ($St._{red.}$) is calculated in relation to the intact cross-section as expressed below:

$$St._{red.} = (1 - \frac{I}{I_o}) \times 100\ \% \tag{4.1}$$

where I and I_o denote the moment of inertia for the damaged and intact cross-section respectively. The percentage of crack height for an equivalent rectangular section is then obtained proportional to the cube root of the ratio of damaged to undamaged moment of inertia:

$$a = \left(1 - \sqrt[3]{\frac{I}{I_o}}\right) \times 100\ \% \tag{4.2}$$

Table 4-1: Damage scenarios corresponding to damage locations 1 and 2.

Damage Level (E)	I/Io*	Stiffness Reduction (%)	Equivalent Crack Height (%)	Measurements # (location 1: 0.17L)	Measurements # (location 2: 0.65L)
E0	0.88	12	4	1 to 48	1 to 48
E1	0.72	28	10	49 to 116	49 to 99
E2	0.52	48	19	117 to 214	100 to 199
E3	0.21	79	39	215 to 312	200 to 281
E4	0.14	86	47	313 to 510	282 to 374

*Io= Moment of Inertia for an original homogeneous section.

4-4 Comparative Study of Damage Detection Techniques

In this section, the principles, general formulations, and performance of various damage detection techniques are presented and compared to highlight their potential shortcomings.

4-4-1 Techniques Based on the Natural Frequency

The basic premise in using global modal parameters for damage detection is that these parameters are affected by changes in physical properties of structures that are associated with stiffness and mass. Consequently, a decrease in the natural frequencies can be an indication of structural damage (Ndambi, Vantomme et al. 2002).

Figure 4-6 and Figure 4-7 show respectively the distribution of natural frequencies as a function of damage level at each location of damage (0.17L and 0.65L). In both cases, the histograms show that the mean frequency decreases with the damage level but are very similar for the first three levels of damage (E0, E1, and E2). Note that these results are obtained under controlled laboratory conditions and that much more variability is expected under field conditions, which may compromise detection at low levels of damage. In general, difficulties associated with the measurement of natural frequencies and the adverse effects of environmental conditions hamper the application of frequency-based methods for damage detection (Vafaei, Alih et al. 2015).

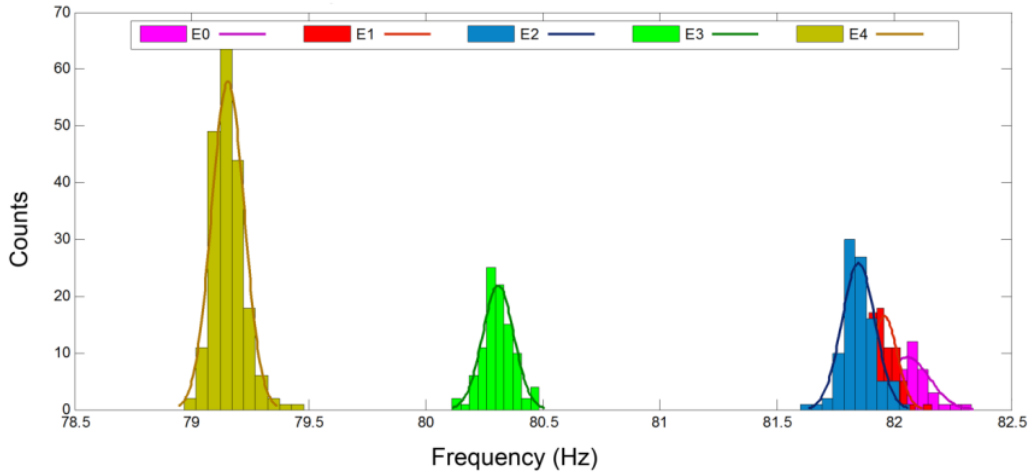

Figure 4-6: Histogram of changes in the distribution of natural frequencies as a function of damage level located at 0.17L.

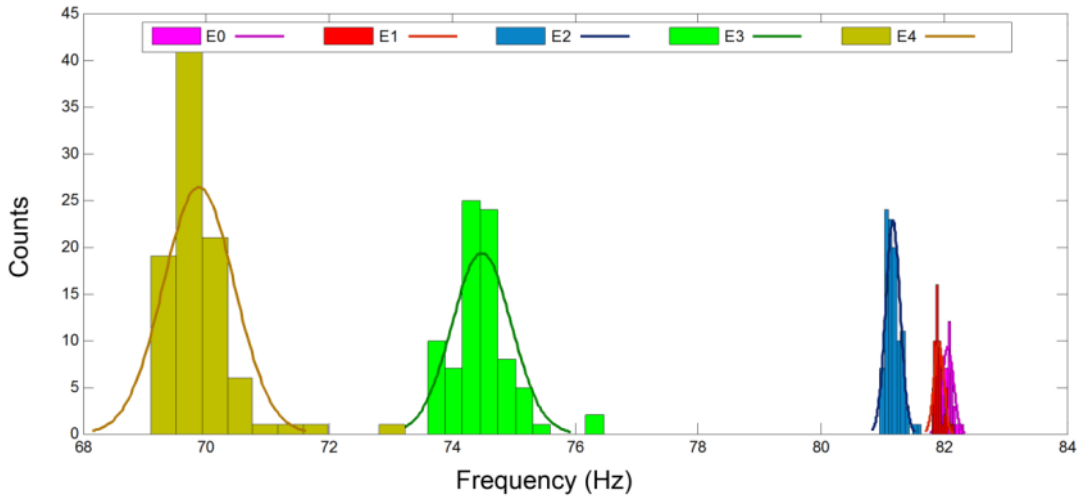

Figure 4-7: Histogram of changes in the distribution of natural frequencies as a function of damage level located at 0.65L.

4-4-2 Modal Assurance Criterion (MAC)

The MAC factor (Ewins 2000) can also be used for damage detection purposes. This parameter is a measure of the correlation between two mode shapes in the form of a scalar quantity that is equal to 1 if two modes are perfectly correlated and is equal to zero if they are completely uncorrelated. In theory, the MAC values higher than 0.98 confirm the fact that the two modes are nearly identical while the values lower than 0.98 can be interpreted as an indicator of damage in the structure (Huth, Feltrin et al. 2005). The MAC function that compares the undamaged mode $\{\varphi_u\}$ and the damaged mode $\{\varphi_d\}$ is defined as:

$$MAC\ (u,d) = \frac{\left|\{\varphi_u\}_r^T \{\varphi_d\}_r\right|^2}{\left(\{\varphi_u\}_r^T \{\varphi_u\}_r\right)\left(\{\varphi_d\}_r^T \{\varphi_d\}_r\right)} \tag{4.3}$$

where the subscript r and the superscript T denote the mode number and the transpose of the vector respectively. Table 4-2 shows the result of the MAC function between the average of mode shapes computed from the initial state of damage (E0) and the next states with increased level of damage (E1, E2, E3, and E4) respectively. For the two locations of damage (0.17L and 0.65L), the MAC indicates that the mode shapes are highly correlated with the reference mode shape (E0). Since the MAC does not vary significantly with the level of damage, it cannot be used reliably to detect incremental damage, even for the higher states E3 and E4.

Table 4-2: Damage identification with MAC method.

Damage Location	(E1,E0)	(E2,E0)	(E3,E0)	(E4,E0)
0.17L	0.999	0.999	0.995	0.994
0.65L	0.999	0.999	0.988	0.984

4-4-3 Mode Shape Curvature (MSC)

Mode shapes derivatives, such as curvature (Pandey, Biswas et al. 1991), can be used as an alternative to displacement mode shapes to detect local changes associated with damage. Mode shape curvature is inversely proportional to the flexural stiffness (EI) of the beam cross section. Hence, in the presence of damage, a reduction in this parameter results in an increase in curvature. The curvature $MSC(x)$ at location x along the beam is defined as:

$$MSC(x) = \frac{M(x)}{EI} \tag{4.4}$$

where $\mathrm{M}(\mathrm{x})$ is the bending moment at location x, I is the moment of inertia and E is Young's modulus. Local modal curvatures can be obtained numerically using a central difference approximation on experimental mode shapes (Jaiswal and Pande 2015):

$$MSC(x) = \frac{\varphi_{x+1} - 2\varphi_x + \varphi_{x-1}}{h^2} \tag{4.5}$$

where φ_x is the mode shape displacement at point x and h is the distance between two successive measured locations. The largest computed MSC value can be interpreted as an indicator of damage location along the length of the beam after applying the interpolation function on experimental displacement mode shapes. Figure 4-8 shows absolute values in mode shape curvature (MSC) for each level of damage. In this figure, the dashed lines indicate the damage locations (nodes number 42 and 212) along the beam. The mean of mode shapes is used to compute the MSC at each damage level. For both cases (damage located at 0.17L and 0.65L), significant changes in MSC are obtained for the higher levels of damage E3 and E4. However, for small levels of damage (E0, E1 and E2) MSC fails to detect damage at its actual position. Large values are also obtained at locations away from the actual damage location resulting in

multiple false alarms. The latter may be due to the amplification of noise in the computation of curvature.

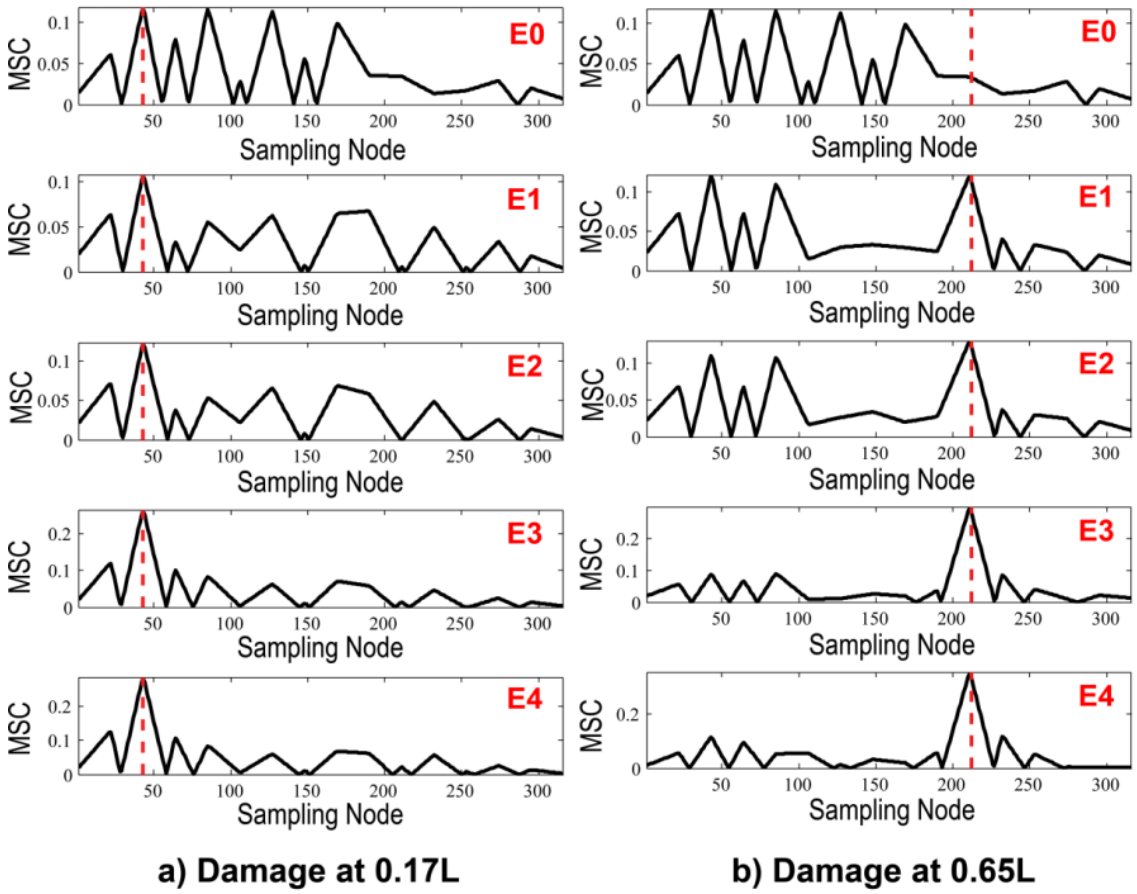

Figure 4-8: Changes in the MSC coefficients as a function of damage level.

4-4-4 Discrete Wavelet Transform (DWT)

The application of the Wavelet Transform (WT) on vibration measurements for damage detection has been addressed by many authors (Liew and Wang 1998, Ovanesova and Suarez 2004, Zhong and Oyadiji 2007, Zhong and Oyadiji 2011, Jaiswal and Pande 2015, Vafaei, Alih et al. 2015). Since mode shapes have finite lengths, discrepancies of wavelet coefficients, known as edge effects, may occur at the beginning and at the end of the structural element and mask potential damage in these regions. The width of this region at each end is estimated as the half-width of the wavelet with the largest scale. This issue can be addressed by adding nodes beyond the two extremities of the beam over a region extending at least half of the largest scale number

assigned to the wavelet (Rucka and Wilde 2006). In this study, the mode shapes were extended over these nodes by using a cubic extrapolation function (Strang and Nguyen 1996).

Wavelets are defined as oscillatory, real or complex-valued functions with zero mean value and finite length. The mother wavelet $\psi(x)$, as the basis of signal decomposition, must satisfy the following two conditions:

$$\int_{-\infty}^{+\infty} \psi(x)\, dx = 0 \tag{4.6}$$

$$\int_{-\infty}^{+\infty} |\psi(\omega)|^2 \frac{d\omega}{\omega} < \infty \tag{4.7}$$

where $\psi(\omega)$ is the Fourier transform of the mother function $\psi(x)$. From the mother function $\psi(x)$, a set of analyzing wavelets can be obtained as function of scale s and position u parameters:

$$\psi(x) = \frac{1}{\sqrt{s}} \psi\left(\frac{x-u}{s}\right) \tag{4.8}$$

Scaling a wavelet changes its width through either compression or extension while shifting a wavelet means translating the beginning of the wavelet along the length of the signal. Applying a Wavelet Transform (WT) results in wavelet coefficients which are a function of scale and position parameters. The magnitude of these coefficients is related to the similarity between the wavelet and the shape of the signal at a given position along the beam. In general, the wavelet type is selected to maximize the wavelet coefficient at the location of damage along the beam (Alvandi, Bastien et al. 2009).

The Discrete Wavelet Transform (DWT) (Ovanesova and Suarez 2004) decomposes the analyzed signal into low frequency (large scale) and high frequency (small scale) components using two different filtering algorithms called Approximation (A) and Detail (D). The data contained in the approximation part is iteratively split into higher levels of approximation and detail until covering a desired level of decomposition. Since this process may produce twice as much data as the initial data set, the DWT mostly uses the dyadic scales:

$$s = 2^j \ , \ u = k2^j \ ; \ j,k \in Z \tag{4.9}$$

where Z, s, and u denote a set of positive integers, scale and position indices respectively. While the low frequency components represent the general patterns of deformations in a signal, the high frequency components contained in the detail function are appropriate to reveal singularities and break-down points caused by damage. Hence, the detail functions are considered for damage detection in this study. For the wavelet analysis of signals in the space-domain, such as mode shapes, the argument of the function is the spatial coordinate x (i.e. $f(x)$). For the given one-dimensional function $f(x)$, the level J detail function $D_J(x)$ is expressed by:

$$D_J(x) = \sum_{k=-\infty}^{+\infty} cD_J(k)\, \psi_{J,k}(x) \tag{4.10}$$

$$cD_J(k) = \int_{-\infty}^{+\infty} f(x)\, \psi_{J,k}(x) dx \tag{4.11}$$

where $cD_J(k)$ is the level J detail coefficients. Many wavelets have been developed with different features and properties. The selection of a type of wavelet and the level/scale of decomposition for a particular application is a function of the characteristics of the signal to be analyzed. The selection process is presented in detail in (Taha, Noureldin et al. 2006) and (Ovanesova and Suarez 2004). For our purposes, the bio-orthogonal wavelet (bior6.8) was identified as the best candidate to perform the DWT.

Figure 4-9 shows the third level of detail coefficients for the first mode shapes obtained from each state of damage. For each level of damage, the mean mode shape is used for the analysis. The dashed lines indicate the damage locations at node 42 and 212 for each group respectively. Damage is detectable for the states E3 and E4 when the beam is subjected to significant reductions in stiffness at two locations of damage. However, high values of DWT coefficients are also observed in the vicinity of damage locations. The fluctuations of wavelet coefficients are more evident for small levels of damage, indicating a higher noise to signal ratio in these states. For damage located at 0.17L (states E1 and E2), although the maximum absolute value of wavelet coefficients is consistent with the location of damage, one cannot conclude confidently if it is due to damage or related to a low signal to noise ratio. The latter becomes important when

the damage is located at 0.65L for the states E1 and E2. In addition, for both cases, the DWT fails to detect damage in the initial state E0.

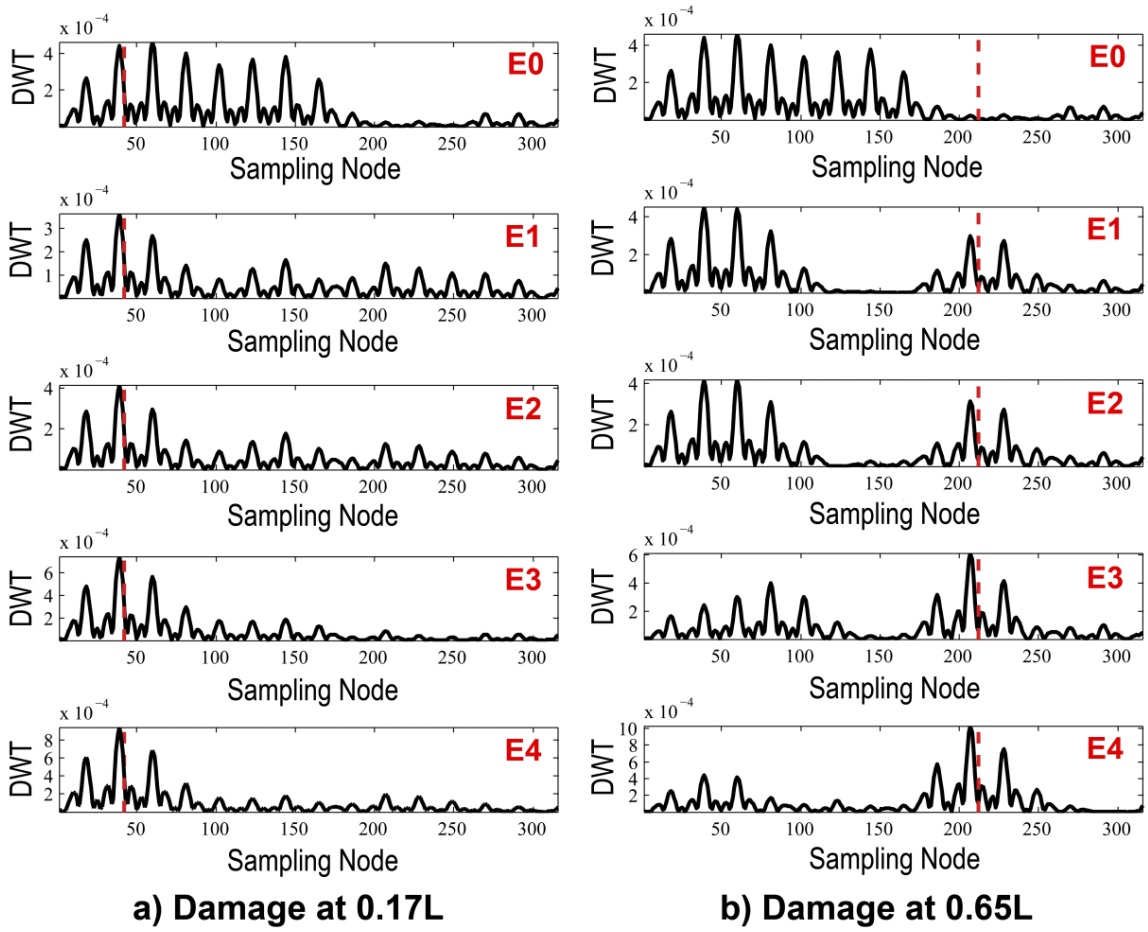

Figure 4-9: Detail coefficients of the DWT as a function of damage level.

The shortcoming of the DWT can be explained by the fact that this method is mainly considered for compression and decomposition of continuous signals with a large amount of information contained in the higher frequency components. Therefore, each level of decomposition may exhibit much more information contained in the signal that was not visible in lower frequency components. However, in the case of experimental displacement mode shapes derived from a limited number of measuring points, the decomposition procedure may result in a loss of information contained in the mode shape.

4-4-5 Continuous Wavelet Transform (CWT)

In general, the DWT is more efficient for the decomposition and compression of the functions while the Continuous Wavelet Transform (CWT) is more appropriate for continuous monitoring of signals using a set of functions modified by the dilation and translation of the mother wavelet $\psi(x)$. For the given one-dimensional function $f(x)$, the CWT (Daubechies 1992) is defined as:

$$CWT\ (s,u) = \frac{1}{\sqrt{s}} \int_{-\infty}^{+\infty} f(x) \psi^* \left(\frac{x-u}{s} \right) dx \tag{4.12}$$

where x, ψ^*, s, u are spatial coordinate, the complex conjugate of the mother function $\psi(x)$, the scale and the position indices respectively. $CWT(s,u)$ is defined as the wavelet coefficient and is the scalar value associated with the wavelet transform. The expression is used to calculate the variation of the signal in the vicinity of u whose size is proportional to s. For a specific scale, the scaled wavelet is shifted over the entire length of the beam and the wavelet coefficients are computed at each individual location. In the presence of damage, high values of the wavelet coefficient indicate a strong similarity between the signal and the wavelet and is interpreted as an indicator for damage (Alvandi, Bastien et al. 2009). In this study, in order to detect local anomalies of the mode shapes caused by damage, the Gaussian wavelet (Daubechies 1992) was used as the basis of wavelet function for the CWT analysis (Figure 4-10).

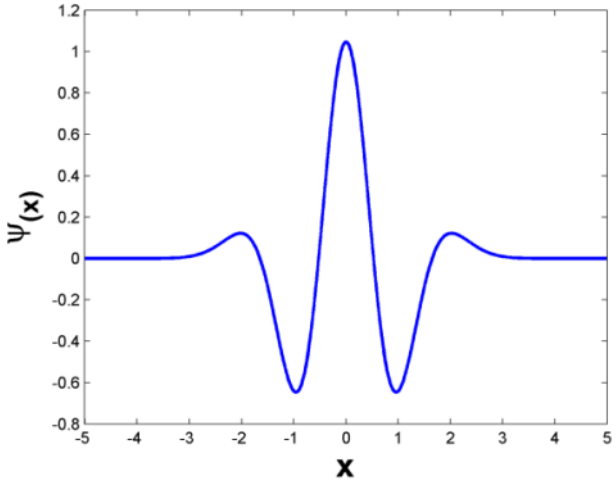

Figure 4-10: Gaussian wavelet function with zero mean value and finite length.

The symmetric and oscillatory shapes of the Gaussian wavelet results in a better description of local features contained in the mode shapes (Misiti, T. Misiti et al. 1996, Gentile and Messina 2003). A more detailed discussion about wavelets and damage detection using the CWT can be found in (Rucka and Wilde 2006).

For a given mode shape, the wavelet coefficients are computed for each location or sampling node along the entire length of the beam. Figure 4-11 shows the wavelet coefficients as a function of location along the beam for each of the (first) mode shape obtained from repeat measurements at each damage level (E0 to E4) using the Gaussian wavelet at scale 32. The dashed lines represent the location of incremental damage for each case. Note that the scale is a crucial parameter and a tradeoff has to be considered in the selection of this parameter. Large scales may miss small variations on the mode shapes while a smaller scale may be too sensitive to noise associated with experimental measurements at the location of the sensors. For this study, the scale of 32 was selected after performing the wavelet analysis for a wide range of scales and was selected as the best compromise considering the noise to signal ratio from the experimental measurements.

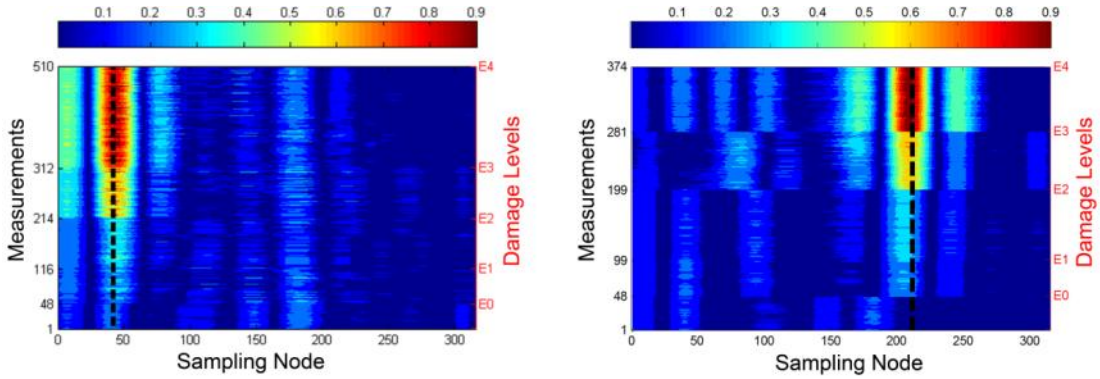

Figure 4-11: CWT coefficients for all measurements at all damage levels (E0 to E4).

The results are obtained for the experimental beam for increasing levels of damage located at 0.17L and 0.65L (Figure 4-3). The measurement numbers represent repeat measurements at each level of damage (Table 4-1). In Figure 4-11a, observations numbered from 1 to 48 are for the initial condition (E0) while observations numbered from 49 to 116 relate to damage level E1 and so forth. In Figure 4-11b, observations are numbered for five damage levels, from E0 to E4 where measurements number 48, 99, 199, and 281 indicate the last measurement for increasing

levels of damage. As shown, the wavelet coefficients increase at locations of damage with increasing levels of damage, confirming that they are good indicators of damage, especially at higher levels (E2, E3 and E4). However, damage detection is not as apparent between the first two levels of damage (E0 and E1).

To address issues related to the application of the CWT for damage detection at low damage levels, this study proposes a novel statistical pattern recognition technique to derive new features from the wavelet coefficients such that they are more highly correlated with damage. In this application, the wavelet coefficients exhibit oscillatory shapes as a function of location along the beam. These oscillatory shapes are the result of the shape of the wavelet, which result in higher coefficients when the damage location coincides with peaks and throughs of the wavelet.

4-5 Damage Detection and Localization Algorithm

The current techniques described throughout the comparative study in Section 3 are limited in their ability to detect low levels of damage in the presence of high noise to signal ratios. Hence, the emphasis in this section is the development of analysis procedures to improve detection between the first two levels of damage while reducing the probability of false detection.

4-5-1 Principal Component Analysis (PCA)

To improve the detection of low levels of damage, a Principal Component Analysis (PCA) is first used to improve the signal over noise ratio and to develop an objective statistical test for the detection of damage. The wavelet coefficients computed for the first mode of vibration at each location along the beam are considered as the variables for the PCA. The matrix of observations is partitioned and is comprised of the wavelet coefficients for the two initial states E0 and E1. The columns correspond to locations along the beam while the rows represent the repeat measurements at each level of damage.

Singular Value Decomposition (SVD) is one of the popular forms of Principal Component Analysis (PCA) which is based on the eigen-decomposition of the sample covariance (or correlation) matrix for a vector of random variables (Pearson 1901, Jackson 2005). In this case since the coefficients are related to the level of damage, the analysis is performed on the

covariance matrix. For a mean-centered matrix $[X]$ of dimensions m by n, where m is the total number of observations or experimental trials and n is the number of random variables, the SVD of the data matrix $[X]$ is given by:

$$[X]=[U]\,[\Lambda]\,[V]^T \tag{4.13}$$

where $[U]$ is an orthogonal $m\times m$ matrix (meaning that $[U]^T[U]=[I]$ where $[I]$ is the identity matrix), $[\Lambda]$ is an $m\times n$ rectangular diagonal matrix, and $[V]^T$ (the transpose of $[V]$) is an orthogonal $n\times n$ matrix. The diagonal elements of $[\Lambda]$ are non-negative real numbers which are known as the singular-values of $[X]$. The columns of $[U]$ and the columns of $[V]$ are defined as the left-singular-vectors and right-singular-vectors respectively. PCA performs the eigenvalue decomposition of the sample covariance matrix $[X]^T[X]$ as follows:

$$[X]^T[X]=\left([V]\,[\Lambda]\,[U]^T\right)\left([U]\,[\Lambda]\,[V]^T\right) \tag{4.14}$$

$$[X]^T[X]=[V]\,[\Lambda]^2[V]^T \tag{4.15}$$

The diagonal entries of $[\Lambda]^2$, ordered in decreasing order from the upper left to lower right, are equal to the eigenvalues (λ) of the covariance matrix, while the columns of the right-singular-vectors $[V]$ are defined as the its corresponding eigenvectors. The eigenvector (or loading) matrix $[V]$ resulting from the diagonalization of the covariance matrix is also known as the Principal Components (PC) matrix. Each eigenvalue (λ_i) is a measure of the variance for the i^{th} principal component. The percentage of variance explained (η) by the i^{th} principal component is expressed by:

$$\eta=100\%\cdot\left(\lambda_i/\sum_{i=1}^{n}\lambda_i\right) \tag{4.16}$$

where λ_i corresponds to the associated eignevalue of the i^{th} principal component. The first few eigenvectors (principal components) with the highest eigenvalues explain most of the variance observed in the wavelet coefficients while relegating noise in the higher components. The linear

projection of the data into the subspace of $q \leq n$ variables results in an $m \times q$ score matrix $[S]$ which is extracted as a new feature for damage detection:

$$[S] = [X]\,[V] \tag{4.17}$$

Therefore, each column of $[S]$ corresponds to the scores for the sequence of eigenvectgors. By discarding components that contribute least to the overall variance, a reduction in dimension is achieved without a significant loss of information in relation to the original data. This results in a linear combination of wavelet coefficients with a higher signal to noise ratio. The scores obtained for the first few components are used next for detecting small increments of damage.

4-5-2 Statistical Detection of Damage

Since the covariance matrix of the wavelet coefficients is defined from multiple observations from two consecutive states, the variance of coefficients is due to the variance that is associated with each sensor under stationary conditions as well as the variance associated with incremental damage. The portion of the variance that is sensor specific is uncorrelated between sensors while the damage related portion will be correlated. The principal components are linear combinations of the original random variables that explain the highest percentage of the variance observed in a given data set. The coefficients of the principal components are a function of the variance of each variable as well as the correlation between the variables, which is associated with increments of damage. The scores computed for each component are a function of the similarity between the component and a set of observations and can be used as an indicator for the occurrence of incremental damage.

A statistical test is used to determine if the change in the distribution of scores is statistically significant between two sets of observations as a means to objectively determine if incremental damage is present or not. In this application, the wavelet coefficients between states E0 and E1 are used to form the covariance matrix for the PCA. Figure 4-12 shows the scree plot for the first few components. The scree plot shows, in decreasing order, the percentage contribution of the variance explained by each component and can be used to select the set of components that explains most of the observed variance.

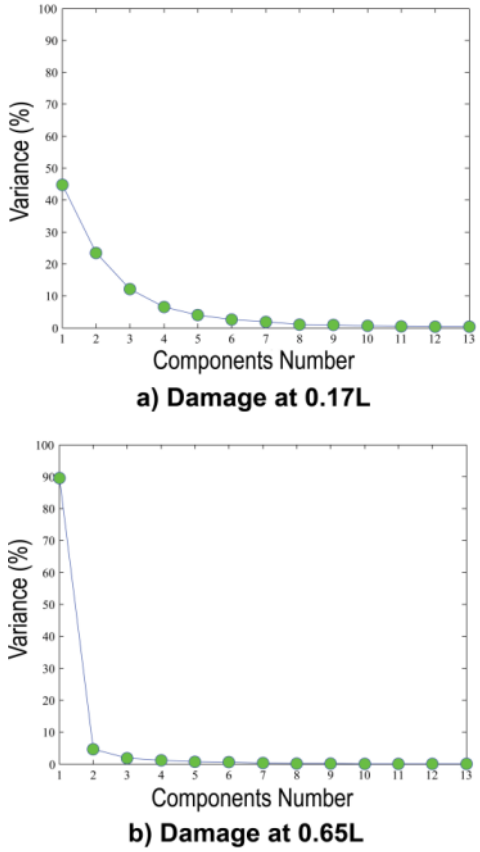

Figure 4-12: Scree plot of Principal Components (PCs) for states E0 and E1.

Figure 4-12a and Figure 4-12b show the scree plots for data sets when incremental damage is located at 0.17L and 0.65L respectively. In Figure 4-12a, the first three components explain 80% of the overall variability while Figure 4-12b indicates that the first two components explain 95% of total variance. The lower percentage of variance explained for the first data set can be partially explained by the lower signal to noise ratio on the first mode of vibration when damage is located near one of the supports. Various objective rules can be used to select the optimal number of principal components. The rules are used in the context of data reduction by replacing the original data set by a reduced but representative set of new uncorrelated variables that are linear combinations of the original variables. In summary, most of the rules stop when the variance explained by a component is close to the variance associated with noise, which is uncorrelated by definition. For our purposes, the first component was found to be most informative for damage detection and localization since it is the most highly correlated with the level of damage. Statistical detection procedures are investigated next for both data sets to compare the robustness of the proposed procedure as a function of damage location.

Figure 4-13 shows the first few components corresponding to the analyses for the two damage scenarios located at 0.17L and 0.65L for incremental damage between levels E0 and E1. The horizontal axis corresponds to locations (or sampling nodes) along the beam while the vertical axis provides the values of the eigenvectors for each component. The dashed lines correspond to the location of incremental damage. Although, the nodes near the damage location have high values, other nodes where there is no damage have equally large values, which indicate that eigenvectors by themselves are not very informative as to the location of damage. In this case, the components are related to the dominant patterns observed in the spatial variation of the wavelet coefficients for the damage levels E0 and E1 observed in Figure 4-11. For each PC, a set of scores can be computed with Eq. 4.17 for each set of measurements.

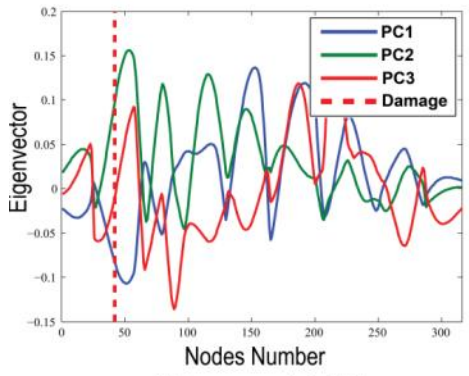

a) Damage at 0.17L

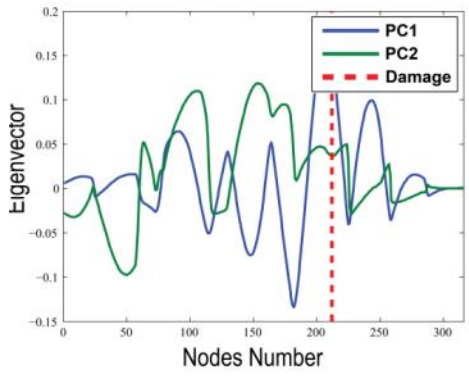

b) Damage at 0.65L

Figure 4-13: Plot of the first few Principal Components (PCs) for states E0 and E1

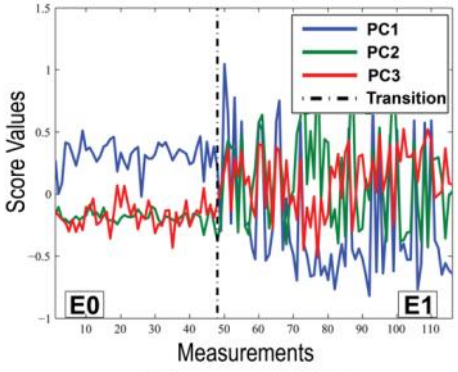

a) Damage at 0.17L

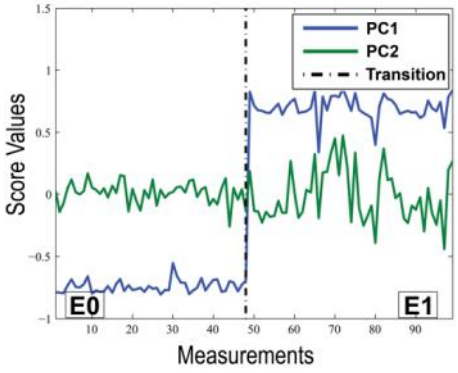

b) Damage at 0.65L

Figure 4-14: Observed scores corresponding to the first few components for states E0 and E1.

The scores are largest when the pattern of measurements matches the shape of a PC. In this case, the scores are computed across the states E0 and E1 (Figure 4-14). In both cases (damage at 0.17L and 0.65L), the scores from measurements 1 to 48 correspond to the initial state (E0) while the remaining scores correspond to the state E1. In the presence of no damage, the scores for repeat records are expected to follow the normal distribution with a given mean and variance. Figure 4-14a indicates a change in both the mean value and the standard deviation of the scores for the first three components between states E0 and E1 for damage at location 0.17L. This difference is more evident between the two states for the first component for damage at location 0.65L (Figure 4-14b).

Descriptive statistics such as Box and Whisker plots (Montgomery and Runger 2012) are well suited for a visual comparison of the distribution of scores between the two states (E0 and E1) (Figure 4-15). On each box, the central horizontal line, the top/bottom edges of the box, the extended vertical lines, and the individual points correspond to the median, the first/third quartiles, the extreme points (whiskers), and the outliers in the distribution of scores respectively. For damage located at 0.17L, the first three components indicate a change in the location parameters as well as in the dispersion of scores between states E0 and E1. For damage located at 0.65L, the difference in the location of scores is much larger for the first component and less for the second component.

Statistical tests can be used to determine if these differences are statistically significant. The tests that are favored are those for the equality of location parameters (e.g. mean, median) since a shift in the distribution of scores is expected with increasing damage. Two location tests are investigated, the t-test (Abramowitz and Stegun 1966) and the Mann-Whitney U-test (Gibbons and Chakraborti 2011). The t-test is exact for normally distributed random variables while the second test is non-parametric. The latter is more useful when data do not meet the assumption of normality or in the case when the normality of data is uncertain. The assumption of normality is verified in this application through normal probability plots (Figure 4-16) and histograms of the scores (Figure 4-17) (Montgomery and Runger 2012). The scores for state E0 are mostly normally distributed while the scores under E1 exhibit more variability and multi-model behaviour.

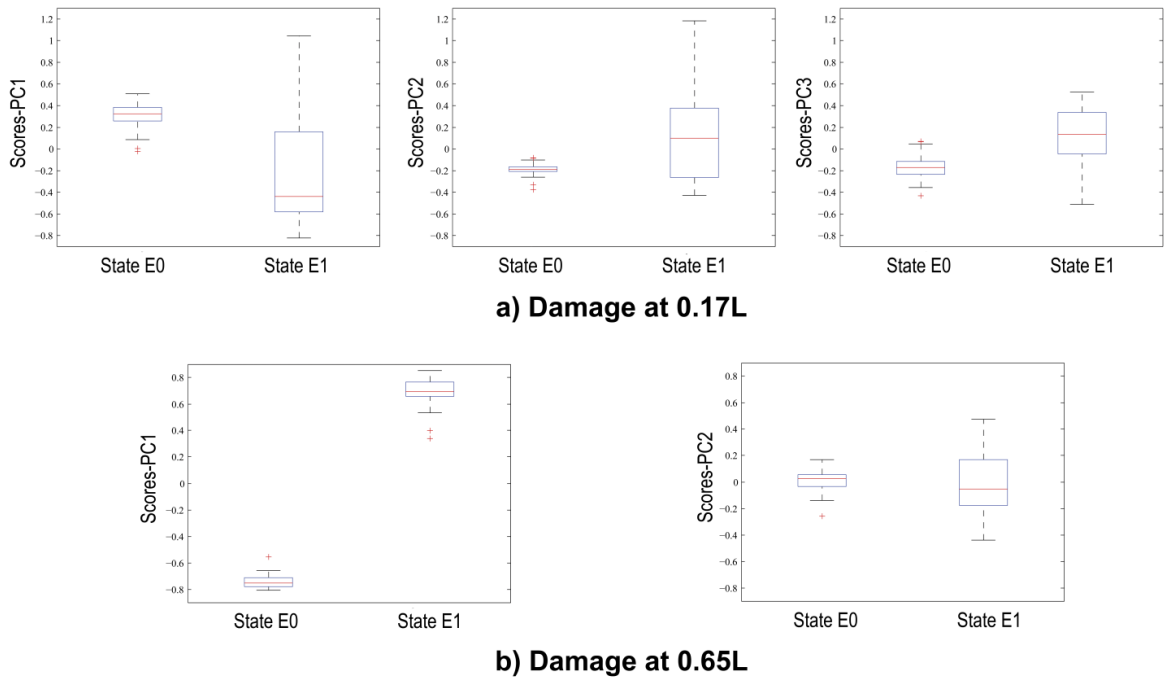

Figure 4-15: Box and Whisker plots for scores of PCs between states E0 and E1.

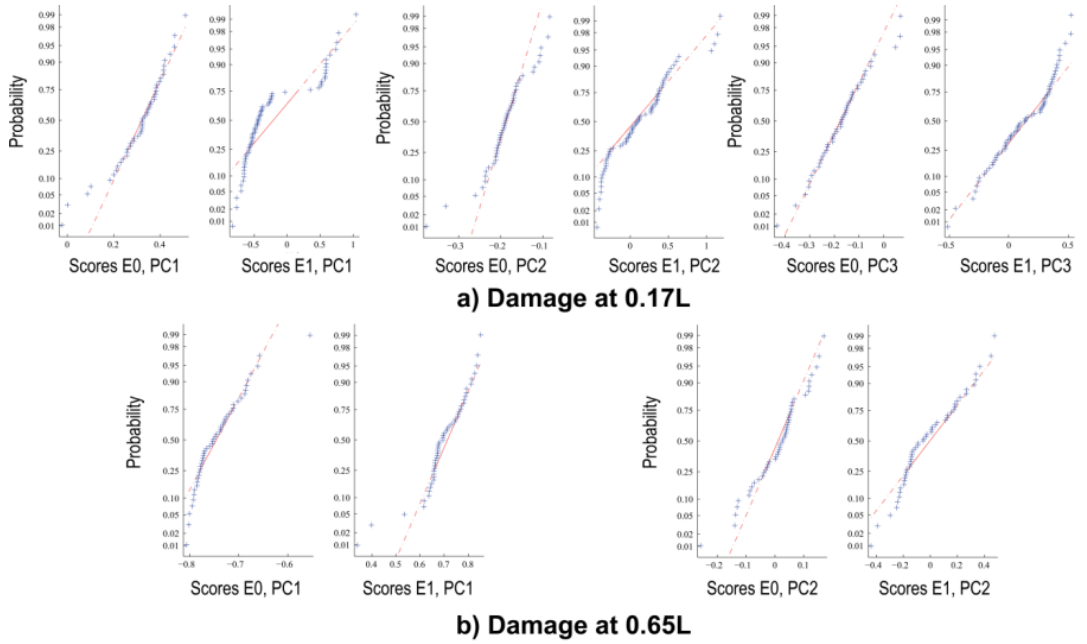

Figure 4-16: Analysis of the distribution of scores for states E0 and E1, normal probability plot.

Both parametric and non-parametric tests (t-test and U-test) are performed in this application. Under the null hypothesis (H), the location parameter (either mean or median) is assumed to be

equal for the two populations, while the alternative hypothesis is that they are different. Given the null hypothesis, the distribution of the test statistic (sample mean or median) is derived, and the sample statistic is computed and compared to the theoretical distribution. In the cases of a double-sided alternative, the null hypothesis is not rejected if the test statistic is within the limits defined by the significance level of the test (α). The level of significance of the test corresponds to the probability of rejecting the null hypothesis when it is true or equivalently, a false alarm. Alternatively, the P-value (P) of the test statistic can be computed and compared to the significance level.

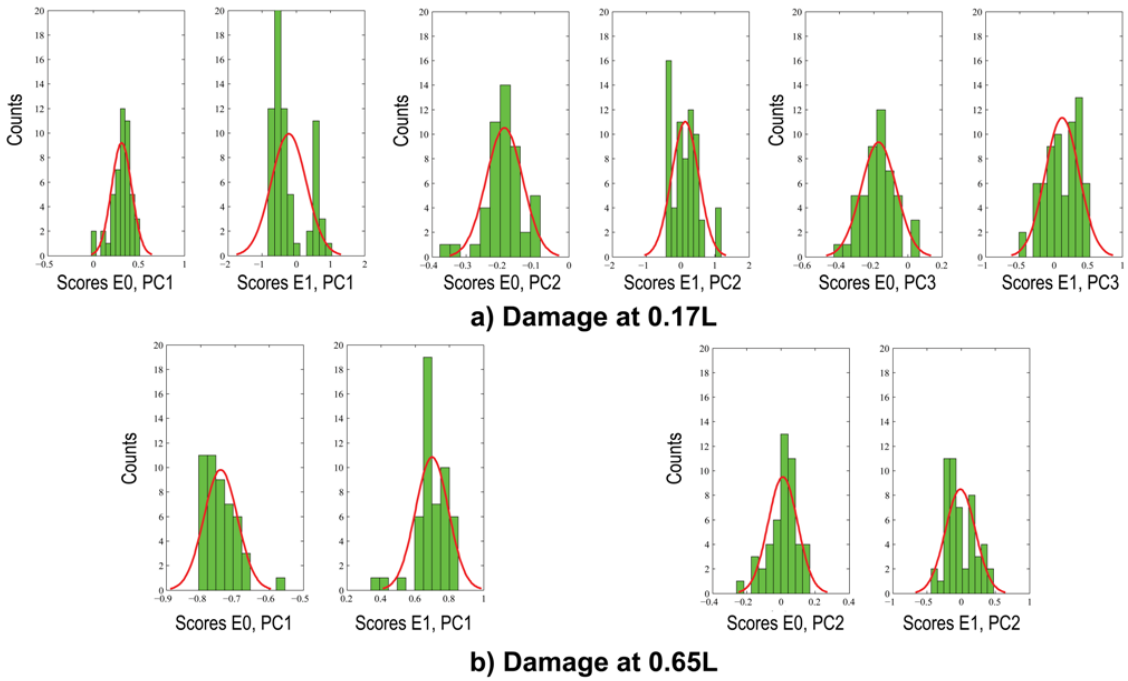

Figure 4-17: Analysis of the distribution of scores for states E0 and E1, histogram.

The result of the test returns either the logical value of H=0 or H=1. A P-value less than or equal to the significance level $(P \leq \alpha)$ represents statistical evidence to reject the null hypothesis at the significance level α, thereby H=0, while if $P > \alpha$ the test shows strong evidence against the null hypothesis (H=1) (Abramowitz and Stegun 1966, Gibbons and Chakraborti 2011). The t-test can be applied when the underlying distributions are assumed normal for the cases where the variances from the two samples are equal or unequal. Table 4-3 shows the results of the t-test for all the cases considered in this application.

Table 4-3: Summary of results for the t-test between two independent samples (E0-E1).

Damage	PC	$\bar{x}_{E0}$	$\bar{x}_{E1}$	σ_{E0}	σ_{E1}	H	P	N_{E0}	N_{E1}	Dof*	α
0.17L	1	0.3115	-0.2198	0.1104	0.5227	1	1.17E-10	48	68	114	0.01
0.17L	2	-0.1882	0.1328	0.0534	0.3919	1	1.82E-07	48	68	114	0.01
0.17L	3	-0.1709	0.1206	0.1024	0.2480	1	5.61E-12	48	68	114	0.01
0.65L	1	-0.7420	0.6983	0.0491	0.0930	1	1.07E-96	48	51	97	0.01
0.65L	2	0.0115	-0.0108	0.0864	0.2111	0	5.12E-01	48	51	97	0.1

*Dof = Degree of freedom (N_{E0}+N_{E1}- 2) where N defines the number of samples.

In all cases, the P-values are very small, indicating that the null hypothesis for the equality of means is rejected for significance levels greater than the P-value. For damage located at 0.17L (all components) and 0.65L (only the first component), the test indicates that the difference is significant with a P-value below 0.01. However, the result of the test for damage location at 0.65L (second component) is less significant with a P-value above 0.1 of significance level. However, the latter component explains less than 5% of the total variance and can be neglected. Alternatively, the non-parametric Mann-Whitney U-test can be used. Table 4-4 shows the results for the test and represents similar results to those of the t-test except for PC2 for damage at location 0.65L. In the latter case, the P-value is approximately 0.13. In summary, results from both tests are efficient in detecting incremental damages between states E0 and E1 and that the assumption of normality is not critical for the outcome of the t-test.

Table 4-4: The results of the Mann-Whitney U-test between two independent samples (E0-E1).

Damage	PC	R_{E0}*	R_{E1}	U	H	P	N_{E0}	N_{E1}	α
0.17L	1	3644	3142	796	1	2.82E-06	48	68	0.01
0.17L	2	2066	4720	890	1	3.23E-05	48	68	0.01
0.17L	3	1666	5120	490	1	1.57E-10	48	68	0.01
0.65L	1	1176	3774	0	1	1.07E-17	48	51	0.01
0.65L	2	2615	2335	1009	1	1.33E-01	48	51	0.14

*R = Sum of ranks for the assigned group of data.

4-5-3 Likelihood-Based Localization of Damage

Given that a statistically significant level of damage is detected, the next issue is to determine as accurately as possible its location along the beam. The localization procedure that is proposed is based on an adaptation of the Likelihood Ratio (LR) test (Kendall and Stuart 1979) often used in statistics for comparing the goodness of fit between two nested models. In this case, the LR test is used to compare the likelihood of two models (reference and alternative) for a given data set at each location x_i (or sampling node) along the beam and selecting the model with the highest likelihood. Therefore, the LR test is defined as follows:

$$LR(x_i) = \frac{L(S_R \mid \mu_R, \sigma_R)}{L(S_i \mid \mu_i, \sigma_i)} \qquad ;\ i = 1\ ,\ 2\ ,\ 3\ ,\ ....\ ,\ 316 \tag{4.18}$$

where $\mathrm{L}(\mathrm{S} \mid \mu, \sigma)$ represents the likelihood function for a set of scores (S) when these are assumed to be normally distributed with a given mean (μ) and standard deviation (σ). The subscripts R and i refer to the scores for the reference and alternative model respectively. The scores observed for the damaged state E1 are used to compute the parameters for the reference and alternative models.

For a given Principal Component (PC) or eigenvector $V = \{V_1 \quad V_2 \quad .... \quad V_n\}^T$ with $n = 316$ nodes (pseudo-sensors), the scores { S_{pc} } are computed using Eq. 4.17:

$$S_{pc} = \{[X]_{m \times n} \cdot [V]_{n \times 1}^{pc}\}_{m \times 1} \tag{4.19}$$

$$S_{pc} = \{s_1 \quad s_2 \quad .... \quad s_m\} \qquad ;\ m = N_{E0} + N_{E1} \tag{4.20}$$

where the pc denotes the number of selected component, $[X]$ represents the original wavelet coefficients matrix while the subscripts m and n are the total number of observations and variables in $[X]$, and N_{E0} and N_{E1} are the number of repeat measurements (sample size) for the states E0 and E1 respectively. The scores associated with the reference model are computed with the scores that correspond to the damage state E1 only:

$$S_R = \left\{ \; N_{E0} < j \le m \; : \; S_{pc}\left(s_j\right) \; \right\} \qquad ; \; m = N_{E0} + N_{E1} \tag{4.21}$$

where j is a real positive integer number and s_j is the j^{th} element of the score vector $\{S_{pc}\}$. Assuming that the principal components are not changed significantly by removing one node, alternative models are produced as a sequence of models at the location of each node. The scores for the alternative model (damage located at x_i) are computed by removing the variable corresponding to location x_i. This is equivalent of removing the sensor (or node) at the given location and assumes that the principal components are not affected (one variable is removed out of 316):

$$S_i = \left\{ \; [X]_{m\times n} \; . \; [V]^{pc}_{n\times 1} \; | \; V(i) = 0 \right\}_{m \times 1} \qquad ; \; i = 1 \; , \; 2 \; , \; 3 \; , \; .... \; , \; 316 \tag{4.22}$$

$$S_{ALT} = \left[\{S_1\} \quad \{S_2\} \quad ... \quad \{S_n\} \right]_{m\times n} \tag{4.23}$$

where $V(n) = 0$ defines the n^{th} element of the eigenvector $\{V\}$ corresponding to the node that is removed. The application of the procedure provides a sequence of n models $[S_{ALT}]$, which are used to calculate location parameters for the alternative models. The likelihood function of each model can be obtained as the product of the normal probability density function evaluated for each score in the damaged state E1.

$$L\left(S_R \; | \; \mu_R, \sigma_R\right) = \sum_{j=1}^{N_d} \left(2\pi\sigma^2\right)^{-\frac{1}{2}} \; e^{\frac{-\left(S(j)-\mu\right)^2}{2\sigma^2}} \tag{4.24}$$

$$L\left(S_i \; | \; \mu_i, \sigma_i\right) = \left\{ \sum_{j=1}^{N_d} \left(2\pi\sigma_i^2\right)^{-\frac{1}{2}} \; e^{\frac{-\left(S(j)-\mu_i\right)^2}{2\sigma_i^2}} \right\}_i \qquad ; \; i = 1 \; , \; 2 \; , \; 3 \; , \; .... \; , \; 316 \tag{4.25}$$

where Eq. 4.24 defines the likelihood function of the reference model as a function of the corresponding scores $\{S_R\}$ and the location parameters (μ_R and σ_R). The likelihood function for the alternative model $\{S_i\}$ in Eq. 4.25 is computed at each node along the beam. Finally, the LR for each node is obtained by substituting Eq. 4.25 and Eq. 4.25 into Eq. 4.18 and the node with the highest LR is identified as the node closest to the damage.

Figure 4-18 and Figure 4-19 show the likelihood ratios for states E0 to E1 for the first three PCs when damage is located at 0.17L, and when damage is located at 0.65L for the first two PCs.

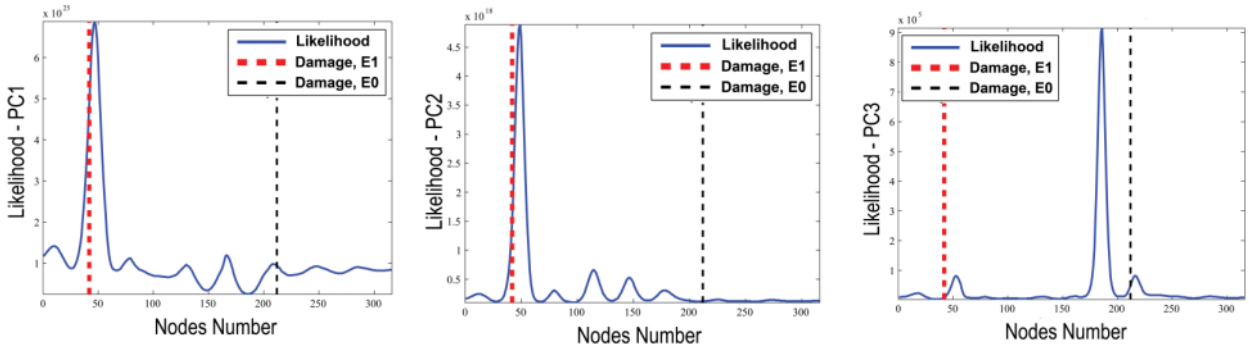

Figure 4-18: Damage detection based on likelihood of scores for damage evolving from states E0 to E1 at 0.17L.

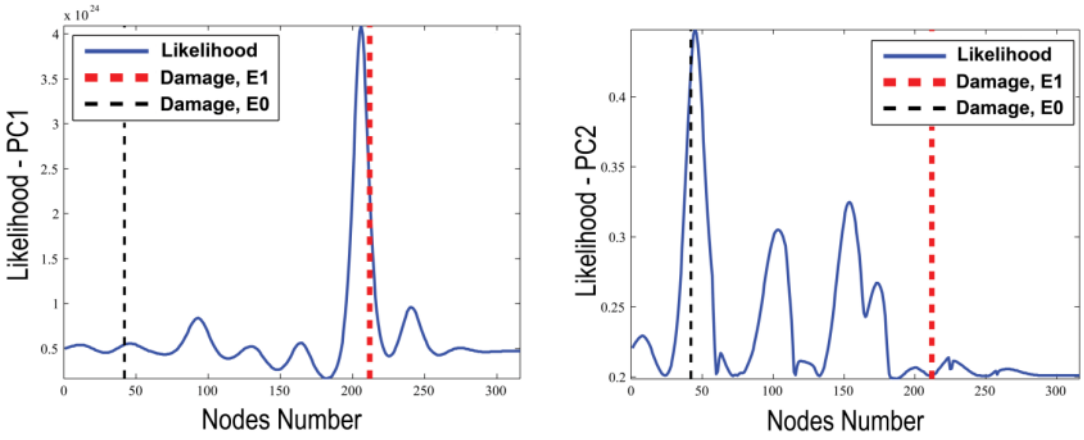

Figure 4-19: Damage detection based on likelihood of scores for damage evolving from states E0 to E1 at 0.65L.

Figure 4-18 shows that when damage is located at 0.17L (node 42), the LR test is very efficient with the first two components in detecting the location of incremental damage (red dashed line). The third component, which is associated with a much lower percentage of the total variance, is relatively successful in identifying the location of the joint assembly at 0.65L (node 212), indicated by a black dashed line. In the latter case, the location corresponds to an existing discontinuity at 0.65L (joint assembly) in its initial state E0 that did not increase in size. This can be explained by an increase in displacements near the location of an existing joint assembly when damage is introduced at another location along the beam. According to Table 4-1, the equivalent

crack height for this discontinuity, which is fully assembled by bolted connections (state E0), is 4% of a rectangular section. Similarly, Figure 4-19 indicates that the LR applied to the first component is successful in localizing damage at 0.65L. The second component explains a much smaller percentage of the total variance and successfully detects the location of the assembly at 0.17L which is fully bolted for this configuration.

In conclusion, for both damage locations, the components with largest variance are correlated with the incremental damage, while the components with less variability correlate with an existing discontinuity outside the zone of incremental damage. Compared to the alternative techniques, which failed to localize the incremental damage, the proposed likelihood algorithm provides accurate results for the localization of incremental damage as well as for the localization of existing defects. This methodology exemplifies a likelihood-based damage detection criterion for a beam with damage at two locations. Concrete surface defects may cause stiffness and/or mass reduction in bridge composite girders or beam-type structures and hence, would result in changes or anomalies in mode shapes, which can be detected through the statistical tests on component scores with the proposed approach. Similarly, the Likelihood Ratio (LR) test can determine if the damage is localized or distributed, as may occur with corrosion of steel reinforcement in concrete. The source of excitation can be any device currently used to perform modal analysis or ambient noise. The current results are limited to longitudinal mode shapes given the size of test structure but the approach could be extended to analyze also transversal and torsional mode shapes for properly instrumented structures. The spatial resolution for detecting damage is related to the spacing between sensors. For example, scaling the spacing between two adjacent sensors could be determined such that 10 to 12 pairs of sensors are used to define the dominant longitudinal, transversal and torsional modes of vibration.

4-6 Conclusions

This paper proposes a novel statistical procedure for the detection and localization of damage in beams using vibration data. The proposed approach is demonstrated for a beam in a laboratory experiment with a set of sensors equally spaced along its length. Various levels of damage can be simulated by removing sets of connections at two locations along the beam. The detection procedure can be performed in beam-type structures prone to any local change in their dynamic characteristics (e.g. mass, stiffness). Due to difficulties and limitations to obtain higher vibration modes of structures by modal testing methods, the experiments are adapted for the first vibration mode of the beam through random excitations by means of a hammer. Although impact methods are easy to implement and have the ability to provide a broad range of frequencies required for an accurate estimation of the mode shapes, their applications are restricted to light weight bridges. For large bridges that cannot be taken out of service and because of technical difficulties associated with the implementation of impact methods, ambient excitation sources (such as ground vibrations caused by traffic loads, wind, waves, etc.) can be used as the most practical method for exciting the structure.

Several sets of measurements are obtained at each damage level to account for uncertainties associated with experimental measurements. A comparative study is carried using various existing detection algorithms to investigate their performance for small increments of damage in the presence of experimental noise. The results indicate that the existing methods fail to clearly locate low levels of incremental damage when the signal to noise ratio is weak. The Continuous Wavelet Transform (CWT) is found to be a promising avenue to detect slight changes in mode shapes due to damage. In this application, the CWT is applied to the first mode of vibration of the beam. The analysis of the wavelet coefficients as a function of location along the beam show a high degree of correlation with higher levels of damage but fails to detect damage at lower levels of damage while indicating potential damage at undamaged locations.

A sequence of statistical procedures is proposed which improves the delectability and localization of low level damage. The use of statistical tests decreases considerably the risk of false detections. The first step of the procedure is to perform a Principal Component Analysis (PCA) on the wavelet coefficients. The first few PCs are found to represent most of the

variability of the data and to eliminate noise. The scores associated with dominant components are then calculated for the initial state (E0) and the first damage level (E1) of the beam. In the presence of damage, the distribution of the scores of the PCs is significantly modified. Statistical tests of location (t-test and Mann-Whitney U-test) are used to detect if the distribution are significantly different for a specified significance level (α). The significance level of the test is selected to minimize false detections while preserving the power of the test. In this application, the significance level could be set at low level (0.01) while still preserving adequate power for the lowest level of damage. The tests are performed for two locations of damage along the length of the beam. Given that statistically significant damage has been detected, the next step of the procedure is to detect the most likely location of damage. Given a series of sensors (or nodes) along the beam, the Likelihood Ratio (LR) algorithm is applied to the scores of a PC to determine the node that contributes the most to the change in scores introduced by the damaged state. The LR is applied to the first few PCs for the two locations of damage in the experimental setup. In both cases, the LR correctly identifies the location of damage at both locations with a high degree of accuracy.

This study exhibits promising results to achieve a high degree of confidence for damage detection in a relatively large experimental beam subjected to damage at two locations while maintaining different levels of stiffness reduction (E0 and E1). The results of the study are obtained under controlled environmental conditions. The next step in this research is to investigate the performance of the detection procedures under field conditions for an existing bridge when environment conditions (mainly temperature) are not constant and the structure is more complex.

Acknowledgement

This study is supported through a CREATE grant from the Natural Sciences and Engineering Research Council of Canada (NSERC) and the CRIB Research Center (Université Laval). The authors would also like to acknowledge the many useful comments from the reviewers.

4-7 Nomenclatures

r	Mode shape number (subscript)
ω_r	Natural frequency of the r^{th} mode
h	Distance between two nodes
u	Undamaged (subscript)
d	Damaged (subscript)
{ϕ}	Mode shape displacement vector
MAC(*u*,*d*)	MAC value between two mode shapes
MSC(*x*)	Mode shape curvature at location *x*
f(t)	Time-domain function
t	Time variable
F(ω)	Fourier Transform of *f*(t)
f(*x*)	Space-domain function
x	Spatial coordinate
Ψ(*x*)	Wavelet function
Ψ(*ω*)	Fourier Transform of Ψ(*x*)
u	Wavelet function position parameter
s	Wavelet function scale parameter
j	Positive integer
k	Positive integer
D_j	j^{th} level of the Detail coefficient
A_j	j^{th} level of the Approximation coefficient
CWT(*x*)	Wavelet coefficient at location *x*
m	Number of observations
n	Number of variables/nodes
[X]	Wavelet coefficients matrix
[U]	Left-singular values of [X]
[Λ]	Singular-values of [X]
[V]	Right-singular values of [X]
[C]	Covariance matrix of [X]

PC_i	i^{th} principal component
λ_i	i^{th} eigenvalue
η_i	Percentage of variance for the i^{th} PC
[S]	Score matrix
$[S_1]$	Scores for the 1st set of measurements
$[S_2]$	Scores for the 2nd set of measurements
pc	Selected component (subscript)
$\{V\}_{pc}$	Selected eigenvector or PC
$\{S\}_{pc}$	Score vector for the selected component
$\{S_R\}$	Scores for the reference model
$\{S_i\}$	Scores for the alternative model
$LR(x_i)$	Likelihood Ratio at i^{th} location
$L(S_R \mid \mu, \sigma)$	Likelihood of reference scores
$L(S_i \mid \mu_i, \sigma_i)_i$	Likelihood of alternative scores at i^{th} node
μ	Population mean
σ	Standard deviation
ν^2	Variance
P	P-value
H	Hypothesis testing
H0	Null hypothesis
H1	Alternative hypothesis
α	Type I error and/or significance level
β	Type II error
R	Sum of ranks
Dof	Hypothesis testing degree of freedom
$\bar{x}$	Sample mean
N	Sample size

4-8 References

Abramowitz, M. and I. A. Stegun (1966). "Handbook of mathematical functions." Applied mathematics series 55: 62.

Alvandi, A., J. Bastien, E. Gregoire and M. Jolin (2009). "Bridge integrity assessment by continuous wavelet transforms." International Journal of Structural Stability and Dynamics 9(1): 11-43.

Alvandi, A. and C. Cremona (2006). "Assessment of vibration-based damage identification techniques." Journal of Sound and Vibration 292(1): 179-202.

Cao, M. and P. Qiao (2008). "Integrated wavelet transform and its application to vibration mode shapes for the damage detection of beam-type structures." Journal of Smart Materials and Structures 17(5): 055014.

Catbas, F., M. Gul and J. Burkett (2007). "Damage assessment using flexibility and flexibility-based curvature for structural health monitoring." Journal of Smart Materials and Structures 17(1): 015024.

Chance, J., G. Tomlinson and K. Worden (1994). "A simplified approach to the numerical and experimental modelling of the dynamics of a cracked beam." Proceedings-SPIE the International Society for Optical Engineering, Citeseer.

Chang, K.-C. and C.-W. Kim (2016). "Modal-parameter identification and vibration-based damage detection of a damaged steel truss bridge." Journal of Engineering Structures 122: 156-173.

Chen, H., C. Spyrakos and G. Venkatesh (1995). "Evaluating structural deterioration by dynamic response." Journal of Structural Engineering 121(8): 1197-1204.

Daubechies, I. (1992). "Ten lectures on wavelets," Society for Industrial and Applied Mathematics.
De Boor, C. (1978). "A practical guide to splines," Springer-Verlag New York.

Doebling, S. W., C. R. Farrar and M. B. Prime (1998). "A summary review of vibration-based damage identification methods." Journal of Shock and Vibration Digest 30(2): 91-105.

Ewins, D. (2000). "Modal Testing: Theory, Practice, and Application," Research Studies Press.

Farrar, C. R., W. Baker, T. Bell, K. Cone, T. Darling, T. Duffey, A. Eklund and A. Migliori (1994). "Dynamic characterization and damage detection in the I-40 bridge over the Rio Grande," Los Alamos National Lab., NM (United States).

Farrar, C. R. and T. A. Duffey (1999). "Vibration-based damage detection in rotating machinery." Key Engineering Materials, Trans Tech Publ.

Gentile, A. and A. Messina (2003). "On the continuous wavelet transforms applied to discrete vibrational data for detecting open cracks in damaged beams." International Journal of Solids and Structures 40(2): 295-315.

Gibbons, J. D. and S. Chakraborti (2011). "Nonparametric statistical inference," Springer.

Huth, O., G. Feltrin, J. Maeck, N. Kilic and M. Motavalli (2005). "Damage identification using modal data: Experiences on a prestressed concrete bridge." Journal of Structural Engineering 131(12): 1898-1910.

Hu W-H, Moutinho C, Caetano E, Magalhães F, Cunha Á (2012). "Continuous dynamic monitoring of a lively footbridge for serviceability assessment and damage detection." Journal of Mechanical Systems and Signal Processing, 33:38-55.

Jackson, J. E. (2005). "A user's guide to principal components," John Wiley & Sons.

Jaiswal, N. and D. Pande (2015). "Sensitizing The Mode Shapes Of Beam Towards Damage Detection Using Curvature And Wavelet Transform." International Journal Of Scientific & Technology Research Volume 4(4).

Kendall, M. and A. Stuart (1979). "The advanced theory of statistics." Statistical Inference and Relationship. London, Charles Griffin.

Kim, J. T., Y. S. Ryu, H. M. Cho and N. Stubbs (2003). "Damage identification in beam-type structures: frequency-based method vs mode-shape-based method." Journal of Engineering Structures 25(1): 57-67.

Lee, J. J., J. W. Lee, J. H. Yi, C. B. Yun and H. Y. Jung (2005). "Neural networks-based damage detection for bridges considering errors in baseline finite element models." Journal of Sound and Vibration 280(3): 555-578.

Lee, J. J. and C. B. Yun (2006). "Damage diagnosis of steel girder bridges using ambient vibration data." Journal of Engineering Structures 28(6): 912-925.

Lei, Y., J. Lin, Z. He and M. J. Zuo (2013). "A review on empirical mode decomposition in fault diagnosis of rotating machinery." Journal of Mechanical Systems and Signal Processing 35(1): 108-126.

Liew, K. and Q. Wang (1998). "Application of wavelet theory for crack identification in structures." Journal of Engineering Mechanics 124(2): 152-157.

Loutridis, S., E. Douka and A. Trochidis (2004). "Crack identification in double-cracked beams using wavelet analysis." Journal of Sound and Vibration 277(4–5): 1025-1039.

Maeck, J., M. Abdel Wahab, B. Peeters, G. De Roeck, J. De Visscher, W. De Wilde, J.-M. Ndambi and J. Vantomme (2000). "Damage identification in reinforced concrete structures by dynamic stiffness determination." Journal of Engineering Structures 22(10): 1339-1349.

Misiti, M., T. Misiti, G. Oppenheim and J.M. Poggi (1996). "Wavelet Toolbox, User's Guide (Matlab)." The Mathworks, Inc.

Montanari, L., A. Spagnoli, B. Basu and B. Broderick (2015). "On the effect of spatial sampling in damage detection of cracked beams by continuous wavelet transform." Journal of Sound and Vibration 345: 233-249.

Montgomery, D. C. and G. C. Runger (2012). "Applied Statistics and Probability for Engineers," John Wiley & Sons.

Ndambi, J.-M., J. Vantomme and K. Harri (2002). "Damage assessment in reinforced concrete beams using eigenfrequencies and mode shape derivatives." Journal of Engineering Structures 24(4): 501-515.

Okafor, A. C. and A. Dutta (2000). "Structural damage detection in beams by wavelet transforms." Journal of Smart Materials and Structures 9(6): 906.

Ovanesova, A. and L. Suarez (2004). "Applications of wavelet transforms to damage detection in frame structures." Journal of Engineering structures 26(1): 39-49.

Pandey, A., M. Biswas and M. Samman (1991). "Damage detection from changes in curvature mode shapes." Journal of Sound and Vibration 145(2): 321-332.

Pearson, K. (1901). "LIII. On lines and planes of closest fit to systems of points in space." Journal of Philosophical Magazine Series 6 2(11): 559-572.

Perera, R. and C. Huerta (2008). "Identification of damage in RC beams using indexes based on local modal stiffness." Journal of Construction and Building Materials 22(8): 1656-1667.

Reynders, E. (2012). "System identification methods for (operational) modal analysis: review and comparison." Archives of Computational Methods in Engineering 19(1): 51-124.

Rucka, M. (2011). "Damage detection in beams using wavelet transform on higher vibration modes." Journal of Theoretical and Applied Mechanics 49(2): 399-417.

Rucka, M. and K. Wilde (2006). "Application of continuous wavelet transform in vibration based damage detection method for beams and plates." Journal of Sound and Vibration 297(3): 536-550.

Salawu, O. S. and C. Williams (1995). "Bridge assessment using forced-vibration testing." Journal of Structural Engineering 121(2): 161-173.

Salgado, R., P. J. S. Cruz, L. F. Ramos and P. B. Lourenço (2006). "Comparison between damage detection methods applied to beam structures." CEC-EST - Comunicações a Conferências Internacionais : [129].

Sanz, J., R. Perera and C. Huerta (2007). "Fault diagnosis of rotating machinery based on auto-associative neural networks and wavelet transforms." Journal of Sound and Vibration 302(4): 981-999.

Santos JP, Cremona C., Orcesi, AD, Silveira (2016). "Early Detection Based on Pattern Recognition and Data Fusion." Journal of Structural Engineering, Doi: 10.1061/(ASCE)ST.1943-541X.0001643

Santos JP, Crémona C., Orcesi, AD, Silveira (2013). "Multivarite Statistical Analysis for Early Damage Detection." Journal of Engineering Structures, 56: 273-285

Santos J, Crémona C, Silveira P, Calado L (2016). "Real-time damage detection based on pattern recognition." Journal of Structural Concrete, 17(3): 338-354

Shahsavari, V. (2011). "Applying the MASW method to estimate the thickness of superficial layers in concrete," Dissertation, Université de Sherbrooke.

Shahsavari, V., J. Bastien, L. Chouinard and A. Clément (2015). "A Novel Response-Based Approach to Localize Low Intensity Damage of Beam-Like Structures." Proc. of the 5th International Conference on Smart Materials and Nanotechnology in Engineering Vancouver, BC, Canada: 99-109.

Shahsavari, V., L. Chouinard and J. Bastien (2017). "Wavelet-based analysis of mode shapes for statistical detection and localization of damage in beams using likelihood ratio test." Journal of Engineering Structures 132: 494-507.

Sohn, H., C. R. Farrar, F. M. Hemez, D. D. Shunk, D. W. Stinemates, B. R. Nadler and J. J. Czarnecki (2004). "A review of structural health monitoring literature: 1996-2001," Los Alamos National Laboratory Los Alamos, New Mexico.

Sohn, H., C. R. Farrar, N. F. Hunter and K. Worden (2001). "Structural health monitoring using statistical pattern recognition techniques." Journal of Dynamic Systems, Measurement, and Control 123(4): 706-711.

Sohn H, Czarnecki JA, Farrar CR (2000). "Structural health monitoring using statistical process control." Journal of Structural Engineering, 126 (11):1356-1363

Solís, M., M. Algaba and P. Galvín (2013). "Continuous wavelet analysis of mode shapes differences for damage detection." Journal of Mechanical Systems and Signal Processing 40(2): 645-666.

Spanos, P. D., G. Failla, A. Santini and M. Pappatico (2006). "Damage detection in Euler–Bernoulli beams via spatial wavelet analysis." Journal of Structural Control and Health Monitoring 13(1): 472-487.

Strang, G. and T. Nguyen (1996). "Wavelets and filter banks," Wellesley-Cambridge Press, Wellesley, USA

Sun, Z. and C. Chang (2004). "Statistical wavelet-based method for structural health monitoring." Journal of Structural Engineering 130(7): 1055-1062.

Taha, M., A. Noureldin, J. Lucero and T. Baca (2006). "Wavelet transform for structural health monitoring: a compendium of uses and features." Journal of Structural Health Monitoring 5(3): 267-295.

Vafaei, M., S. C. Alih, A. B. A. Rahman and A. b. Adnan (2015). "A wavelet-based technique for damage quantification via mode shape decomposition." Journal of Structure and Infrastructure Engineering 11(7): 869-883.

Vuong QH (1989). "Likelihood ratio tests for model selection and non-nested hypotheses." Econometrica: Journal of the Econometric Society, 57(2):307-333.

Wang, Q. and X. Deng (1999). "Damage detection with spatial wavelets." International journal of Solids and Structures 36(23): 3443-3468.

Wu, N. and Q. Wang (2011). "Experimental studies on damage detection of beam structures with wavelet transform." International Journal of Engineering Science 49(3): 253-261.

Yan A-M, Kerschen G, De Boe P, Golinval J-C (2005). "Structural damage diagnosis under varying environmental conditions—part I: a linear analysis." Journal of Mechanical Systems and Signal Processing, 19 (4):847-864

Yan A-M, Kerschen G, De Boe P, Golinval J-C (2005). "Structural damage diagnosis under varying environmental conditions—part II: local PCA for non-linear cases." Journal of Mechanical Systems and Signal Processing, 19 (4):865-880

Zandbergen E, Haan R, Hijdra A (2001). "Systematic review of prediction of poor outcome in anoxic-ischaemic coma with biochemical markers of brain damage." Journal of Intensive care medicine, 27 (10):1661-1667

Zhong, S. and S. O. Oyadiji (2007). "Crack detection in simply supported beams without baseline modal parameters by stationary wavelet transform." Journal of Mechanical Systems and Signal Processing 21(4): 1853-1884.

Zhong, S. and S. O. Oyadiji (2011). "Crack detection in simply supported beams using stationary wavelet transform of modal data." Journal of Structural Control and Health Monitoring 18(2): 169-190.

CHAPTER 5 : AVANT-PROPOS

Auteurs et affiliation :

- Vahid Shahsavari: Étudiant au doctorat, Université Laval, Faculté des sciences et de génie, Département de génie civil et de génie des eaux.
- Luc Chouinard : Professeur, Université McGill, Faculté de génie, Département de génie civil et de mécanique appliquée.
- Josée Bastien : Professeur, Université Laval, Faculté des sciences et de génie, Département de génie civil et de génie des eaux.

État : publié en ligne

Date d'acceptation: 29 novembre 2016

Revue : Journal of Engineering Structures

Titre français : Analyse par ondelettes des modes propres pour la détection statistique et la localisation de l'endommagement dans des poutres en utilisant le test de rapport de probabilité

Résumé français : Cet article présente une étude de cas sur les procédures statistiques pour la détection et la localisation de l'endommagement le long d'une poutre. Les essais sont effectués, en laboratoire, sur une poutre spécialement constituée de trois sections boulonnées entre elles à deux endroits (assemblages) le long de la poutre servant à simuler différents niveaux d'endommagement incrémentiel. L'endommagement incrémentiel est simulé en éliminant séquentiellement les éléments de plaque à chacun des deux assemblages. Dans ce travail, les algorithmes de détection de dommage sont testés pour détecter de faibles niveaux d'endommagement incrémentiel, ce qui est habituellement difficile compte tenu du rapport bruit à signal élevé. La poutre est testée pour deux conditions de retenue, rotulé-rotulé et ancastré-ancastré. L'algorithme de détection combine diverses techniques statistiques avec une méthode de détection de dommage par vibration à ondelettes pour améliorer la détection de faibles

niveaux d'endommagement incrémentiel et propose une nouvelle approche basée sur la probabilité pour localiser le dommage le long de la poutre. Une analyse par transformée d'ondelette continue (CWT) est appliquée au premier mode de vibration de la poutre obtenu à partir d'un ensemble de 16 accéléromètres unidirectionnels à espacement égal mesurant la réponse d'accélération dynamique de la poutre. Une analyse de composantes principales (PCA) est effectuée sur les coefficients d'ondelettes afin d'extraire les principaux motifs de variation et de filtrer le bruit. Les scores de la première composante principale se sont montrés très corrélés aux niveaux de dommage comme démontré par des tests statistiques sur les changements du paramètre de localisation des scores dans les états d'endommagement successifs. Étant donné qu'un dommage statistiquement significatif est détecté, un test de probabilité (LR) est proposé pour déterminer l'emplacement le plus probable d'endommagement incrémentiel le long de la poutre. Les résultats indiquent que l'algorithme est très efficace pour détecter le dommage à plusieurs endroits et pour les deux conditions de retenue étudiées.

Mots-clés : Détection et localisation des dommages, Mode propre, Ondelette, Analyse des composantes principales, Ratio de probabilité.

5. Wavelet-Based Analysis of Mode Shapes for Statistical Detection and Localization of Damage in Beams Using Likelihood Ratio Test

5-1 Abstract

This paper presents a case study on statistical procedures for the detection and localization of damage along a beam. Tests are performed on a specially designed beam consisting of an assembly of three bolted sections under laboratory conditions to simulate various levels of incremental damage at two possible locations along the beam. Incremental damage is simulated by sequentially removing plate elements at each location. In this work, damage detection algorithms are tested to detect low levels of incremental damage which is usually challenging given the high noise to signal ratio. The beam is tested for two end restraint conditions, pinned-pinned and fixed-fixed. The detection algorithm combines various statistical techniques with a wavelet-based vibration damage detection method to improve the detection of low levels of incremental damage and further proposes a novel likelihood-based approach for the localization of damage along the beam. A Continuous Wavelet Transform (CWT) analysis is applied to the first mode of vibration of the beam obtained from a set of 16 equally spaced unidirectional accelerometers measuring dynamic acceleration response of the beam. A Principal Component Analysis (PCA) is performed on the wavelet coefficients in order to extract the main patterns of variation of the coefficients and to filter out noise. The scores of the first principal component are shown to be highly correlated with damage levels as demonstrated by statistical tests on changes on the location parameter of the scores in successive damage states. Given that statistically significant damage is detected, a Likelihood Ratio (LR) test is proposed to determine the most likely location of incremental damage along the beam. The results indicate that the algorithm is very efficient to detect damage at multiple locations and for the two end restraint conditions investigated.

Key-words: Damage Detection and Localization, Mode Shape, Wavelet, Principal Component Analysis, Likelihood Ratio.

5-2 Introduction

In recent years, Structural Health Monitoring (SHM) has received considerable attention in the literature as a means of monitoring the safety and reliability of important civil engineering structures such as bridges (Alvandi and Cremona 2006). Visual inspections or low-level localized nondestructive investigations are costly and labor intensive when applied to large-scale structures and provide partial information of the global state of the structure. To complement this information, vibration-based surveys are becoming more popular due to the efficiency in deploying the instrumentation and the wealth of resulting data on the dynamic properties of the structures. Local damage identification techniques such as ultrasonic and X-ray methods are not applicable to inspect concealed and inaccessible portions of structures and the data cannot be extrapolated to uninspected portions of the structures. Structural condition assessments based on visual observations and local damage identification techniques also vary greatly as a function of the personal experience and technical expertise of the inspector. In view of these limitations, vibration-based surveys can provide a good assessment of the global structural condition by performing measurements at a relatively small number of accessible points (Fan and Qiao 2011).

Incremental damage can be identified from changes in the dynamic characteristics of the structure, which are influenced, by changes in mass, stiffness, boundary conditions, and geometric properties. Modal parameters such as natural frequencies and mode shapes are the most popular global parameters used for damage detection. However, these have been found to perform poorly to detect low levels of incremental damage for tests performed on existing bridges without some form of pre and/or post-treatment (Farrar, Baker et al. 1994). A recent review on the use of natural frequencies for the detection of damage indicates that damage can be detected for large structures only when the level of damage is significant and measurements are done precisely (Salawu 1997). Modal damping ratio is very sensitive to environmental conditions and there is no consistent correlation between system damping and damage (Farrar and Jauregui 1998, Li, Li et al. 2010, Zhang, Bao et al. 2012). Hence, this parameter is not as reliable for damage detection. Both natural frequencies and damping can only provide information on the presence of damage and cannot provide information on its likely location.

In-situ applications of global modal-based damage detection techniques applied to bridges indicate that natural frequencies are less sensitive to low levels of damage than mode shapes (Mazurek and DeWolf 1990, Farrar, Baker et al. 1994). The selection of mode shapes and/or the derivatives of the mode shapes have been used by several researchers as a means to detect and locate damage. Localization of damage is based on either direct or indirect use of mode shapes. Direct or traditional use of mode shapes is based on a direct comparison of modal shapes for intact and damaged states as demonstrated through finite element models or experimental tests (Messina, Williams et al. 1998). In the latter case when data from the intact state is unavailable, the baseline data is usually generated using a finite element model (Fan and Qiao 2011).The indirect use of mode shape is based on modern signal processing techniques such as wavelet analysis applied to the mode shapes (Rucka and Wilde 2006). Artificial Neural Network (ANN) models have also been used to predict the extent and location of damage using modal shape differences from numerical models of a simple beam and a multi-girder bridge (Lee, Lee et al. 2005). However, this method has limited applicability given that it requires data in damaged and undamaged states in order to train the neural network model, which is not possible for ageing structures (Sun and Chang 2002).

Changes in mode shape curvature have also been used to increase the sensitivity of mode shapes for damage detection and localization in beams (Pandey, Biswas et al. 1991), a prestressed concrete bridge (Wahab and De Roeck 1999), and structural damage in beams and plates (Abdo and Hori 2002). The investigation of curvature has been further employed in modal flexibility-based techniques as a supplementary index to assess simulated damage in a steel grid structure (Catbas, Gul et al. 2007). Changes in the modal flexibility have also been used to detect and localize damage in finite element models of simple beams (Pandey and Biswas 1994). Modal strain energy based methods are another group of widely used damage identification techniques that can be considered an extension of the mode shape curvature (MSC) method (Ndambi, Vantomme et al. 2002). In most curvature-based damage identification techniques, the difference operator is used to compute the curvature of mode shapes, which can magnify noise present in the original mode shape and mask actual changes due to small levels of damage (Cao and Qiao 2008). A comparative study of detection methods based on the Modal Assurance Criterion (MAC), the Coordinate Modal Assurance Criterion (COMAC), modal flexibility, and strain energy concludes that changes in modal strain energy could detect damage more precisely

(Ndambi, Vantomme et al. 2002). MAC and COMAC are used to correlate two mode shapes but since damage does not affect significantly mode shapes these methods cannot provide enough evidence of low levels of damage (Pandey, Biswas et al. 1991). Stiffness-based differential techniques (Lin 1990) are another group of damage detection methods that are highly dependent on the number of higher modes used in the calculation of the stiffness matrix. However, these methods have limited applicability because of the difficulty in obtaining accurate data for higher modes of vibration (Pandey and Biswas 1994).

In general, most modal-based damage detection techniques are not efficient for the detection of low levels of damage in the presence of noise or in the case of multiple damage scenarios. Signal processing and pattern recognition techniques have been proposed to improve damage detection, quantification and localization (Fan and Qiao 2011). The Fourier Transform (FT) is used to convert functions from the time to the frequency domains. For vibration-based applications where the signals are nonlinear and non-stationary, such as in damage detection, the evolving nature of the time-series data is best analyzed with the Short-Time Fourier transform (STFT) (Gabor 1946, Sun and Chang 2002). However, a tradeoff between time and frequency resolution with STFT limits the ability of achieving a high resolution analysis simultaneously in the time and frequency domains (Robertson, Camps et al. 1996). Fractal Dimension (FD) algorithms have also been proposed to estimate the localized FD of the fundamental mode shape to locate cracks in beams (Hadjileontiadis, Douka et al. 2005). The damage features are detected by moving a fixed-size window across the fundamental mode shape, which is identified as a peak on the FD curve. However, the contribution of higher modes may provide misleading information on damage. The Hilbert-Huang Transform (HHT) is an innovative energy-frequency-time distribution of the signals that relies on an empirical mode decomposition (EMD) of the data, which allows to decompose a signal into a set of basic functions called Implicit Mode Functions (IMF) before implementing the Hilbert spectral analysis (Yang, Lei et al. 2004, Roveri and Carcaterra 2012). HHT has the disadvantage that the first IMF may cover a wide frequency range and fail to reflect the true frequency pattern of the signal which may cause misinterpretation of the result (Peng, Peter et al. 2005).

Recently, the Wavelet Transform (WT) has been favored over other traditional methods because of its capacity to analyze a signal over a wide range of scales (Daubechies 1992). Basically, WTs

are classified into two categories: Discrete Wavelet Transform (DWT) and Continuous Wavelet Transform (CWT). Even though the DWT has good computing efficiency, its main applications are often limited to data decomposition, compression and noise removal (Peng, Peter et al. 2005). A technique that has been quite efficient to detect localized damage-induced modifications in mode shapes is the CWT. Since mode shapes are more sensitive to local features than natural frequencies, the information contained in the measured mode shapes can be treated as a signal in the spatial domain for processing by the wavelet analysis. A "wavelet coefficient" is calculated in the form of a scalar value at each point of a signal which can be used as an indicator to identify local anomalies, break-down points or discontinuities in the mode shapes (Rucka and Wilde 2006). To extend the applicability of CWT to real structures, several authors (Okafor and Dutta 2000, Cao and Qiao 2008, Wu and Wang 2011) demonstrated the results of their experimental studies by identifying small perturbations in the deflection profile of a beam obtained from high resolution laser-based measurements. However, for an actual bridge where a fixed reference point and a stationary environmental condition are required to derive precisely the real deflection shape of the structure, the efficiency of the laser-based scanning technology is limited by its high sensitivity to exposure conditions and ambient vibrations.

Several authors have applied the WT to a variety of structural problems to demonstrate its effectiveness and versatility. Analyses with CWT can be optimized by varying the number of sampling intervals (Montanari, Spagnoli et al. 2015) and by applying it to a set of vibration modes in the intact and damaged states (Solís, Algaba et al. 2013). In this application, only the first fundamental mode shape is used since it is the most accurate mode when using standard modal testing methods. In large scale structures, since the amount of energy required for exciting the first natural mode is smaller than for higher modes, the first mode is the most easily and accurately identified (Reynders 2012). Wavelet analysis provides promising results for the detection and localization of damage compared to other methods; however, its performance can be affected by the presence of noise or of multiple damage locations, which may result in multiple false detections along the structural element. To address these issues quantitatively, the detection of damage can be analyzed using statistical principles. The detection for the presence of damage is formulated as a test of hypothesis (Montgomery and Runger 2012) where the null hypothesis corresponds to no damage and the alternative hypothesis corresponds to the presence of damage. The test is performed for a significance level (α) which corresponds to the probability

of type I error or the probability of rejecting the null hypothesis when the latter is true (i.e., the probability of false detection). The decision rule associated with the significance level of the test must also be evaluated for the probability of the type II error (β) which is the probability of accepting the null hypothesis when it is false (i.e., concluding to no damage when damage is actually present). Alternative approaches such as Neural Networks based methods have also been proposed to implement tests for the detection of damage. In all cases, training data sets from both damaged and undamaged states are required to derive the decision rule.

Shahsavari el al. (Shahsavari, Bastien et al. 2015) proposed a novel pre-processing statistical procedure to minimize the effects of experimental noise on wavelet coefficients obtained from the first fundamental vibration modes of a beam with fixed-fixed end conditions. Noise reduction as well as aggregate characteristics were obtained by performing a Principal Component Analysis(PCA) (Pearson 1901) on the wavelet coefficients at regularly spaced nodes along the structural element corresponding to the location of the sensors. The first few principal components were found to capture most of the variability in the coefficients and to isolate the noise to higher components that were not used for the analysis. In this paper, the PCA scores corresponding to the first few principal components are shown to be good indicators of low levels of incremental damage and an objective detection criterion is proposed using statistical hypothesis testing. When statistically significant damage is detected at the given significance level, a second algorithm is proposed to determine the most likely location of damage. Both procedures are demonstrated and validated for a data set on an experimental beam for two end conditions (pinned-pinned and fixed-fixed) and two distinct damage locations.

5-3 Damage Detection Algorithm

The level of uncertainty on mode shapes derived from vibration tests increases with the order of the mode shapes which reduces the effectiveness of higher modes for damage detection at low levels of damage (Reynders 2012). The procedure that is proposed in this paper is demonstrated only for the first mode shape of the experimental beam. The applicability or the need to include higher modes is outside the scope of the current paper. Given the first mode shape, wavelet coefficients are calculated at each point corresponding to the location of sensors along the length of the beam. In the present work, dynamic vibrations are induced using an impact hammer at

different points along the beam. To obtain good estimates of the coefficients, the measurements are repeated several times (~50 to 100 times). These measurements are used to obtain the distribution of the wavelet coefficients under homogenous conditions at each location along the beam. The mean value (or median) of the distribution is a measure of the average degree of agreement between the wavelet shape and the mode shape at the location of each sensor while the standard deviation represents the variability in the mode shapes due to measurement errors and noise. A change between surveys in the mean value of the wavelets at a given location is interpreted as an anomaly in the mode shape, which is linked to damage while a change in the standard deviation indicates a change in the noise level, or variability in the mode shapes which can also be to a lesser degree linked to damage.

For low levels of incremental damage, the signal to noise ratio in the observations and wavelet coefficients can compromise detection. This issue is addressed by preprocessing the wavelet coefficients with a Principal Component Analysis (PCA) which is a procedure used for feature extraction, de-noising and compression of data by extracting the main patterns of variation for a set of random variables (Pearson 1901). PCA has been used in damage detection applications to determine the distribution of a given set of structural parameters affected by an undetermined number of environmental factors that can result in false detection of damage (Sohn, Worden et al. 2002, Yan, Kerschen et al. 2005, Yan, Kerschen et al. 2005, Li, Li et al. 2010). PCA has also been used in the analysis of dynamic data from the Pedro e Inês footbridge to remove the effect of changes in environmental conditions on modal frequencies (Hu, Moutinho et al. 2012). In the present work, PCA is applied to the set of wavelet coefficients for the first mode shape of the beam. The set of observations corresponds to the repeat measurements (~ 50 to 100 times) performed for two successive levels of damage. Results from the PCA indicate that most of the variability is explained by the first few components that are related to damage while the remaining components are mainly associated with noise, which exhibits low correlation between variables. Given a component, scores can be calculated for each observation of the data set and classified into each of the two sessions of measurements. Statistical tests are performed on the distribution of PCA scores between the two states (or two inspections) to detect statistically significant change in the distributions. Tests can be performed either on the entire distribution or on a parameter of the distribution such as the mean value, the median or the variance. Tests on the full distribution are more sensitive to outliers while the tests on the mean or median are more

robust. The tests are used to determine objectively and statistically if the parameters are different at a given significance level using classical hypothesis (H) testing methods (Montgomery and Runger 2012).

The following sub-sections summarizes the main features of the Continuous Wavelet Transform (CWT) for damage detection, followed by the Principal Components Analysis (PCA) for data compression and noise reduction, the statistical hypothesis testing for minimizing false alarms, and the Likelihood Ratio (LR) approach for the localization of damage.

5-3-1 Continuous Wavelet Transform (CWT)

Unlike Fourier Transform (FT) in which sine and cosine functions are the basis of signal decomposition, the CWT (Daubechies 1992) applies the wavelets as oscillatory, real or complex-valued functions with zero mean value and finite length. To cover the entire range of a signal, the basic wavelet function, called the mother function $\psi(x)$, generates a set of basis wavelet functions by changing the scale (stretching or compressing) of the wavelet along the entire length of the signal formulated as (Rucka and Wilde 2006, Wu and Wang 2011):

$$\psi(x)=\frac{1}{\sqrt{s}}\psi\left(\frac{x-u}{s}\right) \tag{5.1}$$

where s and u denote the scale and the position indices respectively. The CWT is defined as a convolution product of a one-dimensional function $f(x)$ (mode shapes in this application) with a set of functions formed by the dilation and translation of basic wavelet function $\psi(x)$ as follows:

$$CWT=\frac{1}{\sqrt{s}}\int_{-\infty}^{+\infty} f(x)\psi^{*}\left(\frac{x-u}{s}\right)dx \tag{5.2}$$

where x and ψ^{*} refer to the spatial coordinate of the function $f(x)$ and the complex conjugate of the mother function $\psi(x)$ respectively. CWT is a scalar quantity defined as the wavelet coefficient in the vicinity of location u and show how well a wavelet function correlates with the signal being analyzed. Sharp or sudden irregularities in the mode shapes create coefficients with large magnitudes, which form the basis of damage detection using wavelet theory. The basic wavelet must comply to the following two conditions:

$$\int_{-\infty}^{+\infty} \psi(x)\, dx = 0 \tag{5.3}$$

$$\int_{-\infty}^{+\infty} |\psi(\omega)|^2 \frac{d\omega}{|\omega|} < \infty \tag{5.4}$$

where $\psi(\omega)$ is the Fourier transform of $\psi(x)$ and ω is the angular frequency. These conditions guarantee the reproduction of the signal in the inverse transform (Wu and Wang 2011). Since wavelets are functions with finite length, vibration mode shapes with abrupt ends may result in large wavelet coefficients at both extremities, which can mask the effect of damage in these regions. To reduce edge-effects of mode shapes, the mode shapes are extended by cubic extrapolation (Strang and Nguyen 1996) using 32 extra points at each extremity (Alvandi, Bastien et al. 2009). To obtain a meaningful scalogram from the analysis of mode shapes, a high number of measurement points uniformly distributed along the length of the mode shapes are often required by the wavelet transform (Rucka and Wilde 2006). Therefore, to enhance the performance of the damage detection using wavelets and to smooth the sampling interval from one instrument to the other, a spline function (De Boor 1978) is used to introduce 20 interpolation nodes between each measuring point resulting in a total of 316 sampling nodes for the wavelet transform. In general, different types of wavelets can be used for damage detection. The selection of a particular wavelet is itself an open issue which is beyond the scope of this work but is discussed extensively in the literature (Ovanesova and Suarez 2004). In this study, preliminary analyses indicate that the Symlet wavelet is a good option to identify irregularities associated with damage in the mode shapes.

5-3-2 Principal Component Analysis (PCA)

The variables used in the principal component analysis are defined as the wavelet coefficients observed at equally spaced locations along the length of the beam. A large number of repeat observations (~ 50 to 100) are recorded in each state to account for the variability in the dynamic response due to the input impact excitation. The wavelet coefficients from two successive surveys (N_1 and N_2 measurements respectively) are combined in a single matrix [X]:

$$X = \begin{bmatrix} x_{11} & x_{12} & x_{13} & . & . & . & . & x_{1n} \\ x_{21} & x_{22} & x_{23} & . & . & . & . & x_{2n} \\ . & . & . & . & . & . & . & \\ x_{m1} & x_{m2} & x_{m3} & . & . & . & . & x_{mn} \end{bmatrix} \tag{5.5}$$

$$X = \begin{bmatrix} \underline{\mathbf{X}}_1 \\ \hline \underline{\mathbf{X}}_2 \end{bmatrix} \tag{5.6}$$

where *m* is the total number of observations ($m = N_1 + N_2$) and *n* is the number of locations (or sampling nodes) where wavelet coefficients are evaluated along the beam. The matrix [X] can also be partitioned in submatrices $[\underline{\mathbf{X}}_1]$ and $[\underline{\mathbf{X}}_2]$ which separates the observations for the two sets of observations. The PCA can be performed on either the correlation or the covariance matrix. The analysis in this application is performed on the covariance matrix. For the latter, the observations are first centered as:

$$[X] = \left[x_{mn} - \overline{X} \right] \tag{5.7}$$

$$\overline{X} = \left\{ \frac{1}{m} \sum_{j=1}^{m} x_{jn} \right\} \tag{5.8}$$

where $\{\overline{X}\}$ is a vector of size *n* denoting the vector of mean values of [X]. The sample covariance matrix [C] of dimensions $n \times n$ is then:

$$[C] = \frac{[X]^T [X]}{n-1} \tag{5.9}$$

where the uppercase superscript T means the transpose. The PCA consists in computing the eigenvalues and eigenvectors for the covariance matrix using the Singular Value Decomposition (SVD) algorithm given below (Jackson 2005):

$$[X] = [U] \, [\Lambda] \, [V]^T \tag{5.10}$$

where [U] is an orthogonal $m \times m$ matrix (such that $[U]^T[U]=[I]$ where [I] is the identity matrix), [Λ] is an $m \times n$ rectangular diagonal matrix, and [V] is an orthogonal $n \times n$ matrix. Using this decomposition, the eigenvalue decomposition of the covariance matrix [C] can be defined as:

$$[C] = \left([V] [\Lambda] [U]^T \right) \left([U] [\Lambda] [V]^T \right) \tag{5.11}$$

$$[C] = [V] [\Lambda]^2 [V]^T \tag{5.12}$$

where the diagonal entries of [Λ] are equal to the square root of the eigenvalues (λ) of the covariance matrix [C], while the corresponding columns of [V] are defined as the eigenvectors (or Principal Components PC) of [C]. In PCA, each eigenvalue (λ_i) is a measure of the amount of variance explained by the corresponding eigenvector and these are ranked in decreasing order. Accordingly, the percentage of variance explained (η) by the i^{th} principal component is expressed by the associated eigenvalue (λ_i) of that component divided by the sum of all eigenvalues:

$$\eta = 100\% \cdot \left(\lambda_i \Big/ \sum_{i=1}^{n} \lambda_i \right) \tag{5.13}$$

The first few components are found to explain most of the variance observed in the wavelet coefficients while relegating noise in the higher components. The final step in PCA is the projection of the data into the new subspace of n variables which are uncorrelated over the dataset:

$$[S] = [X] [V] \tag{5.14}$$

where [S] is defined as the score matrix essential for damage detection in this study. Each row and column of [S] corresponds to scores computed respectively for a given set of observations and a principal component:

$$S = \begin{bmatrix} s_{11}^{1} & s_{12}^{2} & s_{13}^{3} & . & . & . & . & s_{1n}^{pc} \\ s_{21}^{1} & s_{22}^{2} & s_{23}^{3} & . & . & . & . & s_{2n}^{pc} \\ . & . & . & . & . & . & . & \\ s_{m1}^{1} & s_{m2}^{2} & s_{m3}^{3} & . & . & . & . & s_{mn}^{pc} \end{bmatrix} \tag{5.15}$$

$$S = \begin{bmatrix} \underline{S}_1 \\ \hline \underline{S}_2 \end{bmatrix} \tag{5.16}$$

where the superscript pc represents the number of corresponding principal component in score matrix [S] and $[\underline{S}_1]$ and $[\underline{S}_2]$ are the scores for the separate sets of measurements. In summary, the first column of [S] corresponds to the scores of the first principal component and so on for the next principal components. By discarding components that contribute least to the overall variance, a reduction in dimension is achieved while retaining as much of the variance in the data set as possible. Since the first few components reach a higher signal to noise ratio, dimension reduction is also very useful to deal with variables in noisy data sets (Dackermann, Li et al. 2008). If incremental damage occurs between the two states (i.e., inspections), the latter is expected to be reflected in a change in the wavelet coefficients. In consequence, the first few components of the PCA analysis are related to the patterns of variation of the wavelet coefficients that explain most of the variance observed between the two states.

The scores for the first few components are calculated for the two states and their distribution are compared. If the component is associated with a state of increasing damage, the scores increase for the second state since the pattern of wavelet coefficients has a higher correlation with the component. A statistical test can be performed to determine if the differences in the distributions are statistically significant. In this work, statistical tests based on the t-test (Abramowitz and Stegun 1966) and the Mann-Whitney U-test (Gibbons and Chakraborti 2011) are performed to determine if the damage is statistically significant between selected states.

5-3-3 Hypothesis Testing

Hypothesis testing has been used in different applications in order to accept or reject statistically the existence of damage (Nair, Kiremidjian et al. 2006, Mujica, Ruiz et al. 2013). Under

laboratory and environmentally controlled conditions, differences are attributed to changes in the state of the beam due to damage. A statistical test of hypothesis on the equality of the means between two sets of random variables (damaged/undamaged) may be generally expressed by two hypotheses (Montgomery and Runger 2012):

$$H_0 : \mu_1 - \mu_2 = 0 \qquad \text{(null hypothesis-undamaged)} \qquad (5.17)$$

$$H_1 : \mu_1 - \mu_2 \neq 0 \qquad \text{(alternative hypothesis-damaged)} \qquad (5.18)$$

where subscripts 1 and 2 define the damaged or undamaged states of the structure respectively. The null hypothesis (H_0) in Eq. 5.17 states that the mean values of the two distributions are not significantly different from zero (no damage) while the inequality of means in the alternative hypothesis (H_1) states that there is statistically significant evidence to reject the null hypothesis (H_0). In statistical hypothesis testing, the choice of the significance level (α) is arbitrary. This parameter is most often set to 0.05 or 0.01 (i.e., 5% or 1%). The test decision returns either the logical value of H=1, indicating the rejection of H_0, or H=0 a failure to reject H_0 at given significance level (α). The t-test (Abramowitz and Stegun 1966) and Mann-Whitney U-tests (Gibbons and Chakraborti 2011) are most commonly used hypothesis tests to compare whether the average difference between two groups of random variables is significant or if it is due to random chance.

Assuming equal variances for two groups of normally distributed random variables (e.g., $[\underline{S}_1]$ and $[\underline{S}_2]$ as it is the case in this study) with unknown means and standard deviations, the two-sample t-test statistic (T) (Abramowitz and Stegun 1966) is defined as:

$$T = \frac{\overline{\underline{S}}_1 - \overline{\underline{S}}_2}{\sqrt{\nu_p{}^2 \left(\frac{1}{N_1} + \frac{1}{N_2} \right)}} \qquad (5.19)$$

$$\nu_p{}^2 = \frac{(N_1 - 1)\nu_1{}^2 + (N_2 - 1)\nu_2{}^2}{N_1 + N_2 - 2} \qquad (5.20)$$

Where $\overline{\underline{S}}$, ν, and N are respectively the samples mean, variance, and size for each group respectively. The P-value (P) of the test is determined from the t-distribution for the

corresponding values of the test statistic (T) with N_1+N_2 -2 degrees of freedom. A P-value below the significance level ($P < \alpha$) represents enough evidence against the null-hypothesis (H_0) at the significance level α, thus indicating the existence of some damage in the structure, whereas a P-value greater than the significance level ($P > \alpha$) fails to reject H_0, thereby rejecting the alternative hypothesis (H_1) and the presence of damage.

Unlike the parametric t-test, which is based on the assumption that the observations are normally distributed random variables, the Mann-Whitney U-test (also known as rank-sum test) (Gibbons and Chakraborti 2011) is a non-parametric analysis suitable for non-normally distributed and ordinal data sets. In this test, the null hypothesis (H_0) assumes that the two samples come from the same distributions with equal medians, against the alternative hypothesis (H_1) that they differ. As with the test on the equality of means, the null hypothesis is rejected if the P-value is smaller than the significance level selected for the test and concludes for the presence of incremental damage in the structure.

5-3-4 Likelihood Ratio (LR)

When a significant difference in the distribution of scores is detected, the next step is to determine the most likely location of damage along the beam. The most likely location is identified by performing a Likelihood Ratio (LR) test at each location (or sampling node) along the whole length of the beam (Kendall and Stuart). The LR test compares the likelihood of two different models and selects the model with the highest likelihood. In this work, the likelihood for the models is computed relative to the scores measured in the damaged state. Assuming a normal distribution for the scores, the reference model follows a normal distribution with the mean μ and standard deviation σ for the scores computed in the damaged state (state 2). The alternate models are computed sequentially at each location along the beam by removing the data at the location of the current model as if the corresponding sensor is missing. The location that provides the highest likelihood ratio (or contrast) corresponds to the sensor that is most informative for damage location.

For the given set of eigenvector $V = \begin{bmatrix} V_1 & V_2 & \dots & V_n \end{bmatrix}^T$, the scores for the reference model $\{S_R\}$ are obtained as:

$$S_R = \{[X]_{m\times n} \cdot [V]^{pc}_{n\times 1}\} \qquad ; m = N_1 + N_2 \tag{5.21}$$

where N is the sample size, *m* and n are the number of observations and variables in the original wavelet coefficient matrix [X], $\{S_R\}$ is an array of size m, and the superscript pc denotes the number of selected principal component (PC). The vector of scores $\{S_R\}$ is used to compute the mean μ_R and the standard deviation σ_R of the reference model. Since the PCs are not significantly altered by removing one variable (i.e., node), the scores for the alternative (leave-a-node-out) model $\{S_i\}$ are generated by multiplying the matrix of observation [$\underline{X}$] by the set of eigenvectors {V} where the components for the current node is set to zero. Repeating the operation for each node, results in a sequence of *n* alternative models from which $[S_{ALT}]$ is derived. The latter is used to calculate the mean μ_i and standard deviation σ_i of the scores for the alternative models.

$$S_i = \{\ [X]_{m\times n} \cdot [V]^{pc}_{n\times 1} \mid V(i) = \underline{0}\} \qquad ; (i = 1,\ 2,\ 3,....,\ n) \tag{5.22}$$

$$S_{ALT} = \left[\{S_1\}\quad \{S_2\}\quad ...\quad \{S_n\}\right]_{m\times n} \tag{5.23}$$

The Likelihood Ratio (LR) is calculated for each of the n alternate as:

$$LR(i) = \frac{L(S_R \mid \mu_R, \sigma_R)}{L(S_i \mid \mu_i, \sigma_i)} \qquad ; (i = 1,\ 2,\ 3,....,\ n) \tag{5.24}$$

with,

$$L(S_R \mid \mu_R, \sigma_R) = \sum_{j=N_1+1}^{m} \left(2\pi\sigma_R^2\right)^{-\frac{1}{2}}\ e^{\frac{-(S_R(j)-\mu_R)^2}{2\sigma_R^2}} \tag{5.25}$$

$$L(S_i \mid \mu_i, \sigma_i) = \left\{ \sum_{j=N_1+1}^{m} \left(2\pi\sigma_i^2\right)^{-\frac{1}{2}}\ e^{\frac{-(S_i(j)-\mu_i)^2}{2\sigma_i^2}} \right\}_i \qquad ; (i = 1,\ 2,\ 3,....,\ n) \tag{5.26}$$

Since the model with the removed node that is closest to the damage is expected to be least informative (or likely) in comparison to the full model, the LR achieves its maximum value

which is identified as the likely location of damage. The LR is computed to the scores of the first three principal components in this work which explain most of the variance.

5-4 Experimental Setup

The experimental setup is designed to easily vary boundary conditions and the levels of damage. The specimen is a bolted-beam assembly with a total length (L) of 3 m, consisting of three steel I sections (W150*37). The experimental tests are performed for the beam with pinned-pinned and fixed-fixed end conditions (Figure 5-1). Simulated damage locations are located at 0.17L and 0.65Lmeasured from the left end of the beam (Figure 5-2). Damage is introduced by sequentially removing a set of bolts and plates at the damage locations to change the mass and stiffness of the beam.

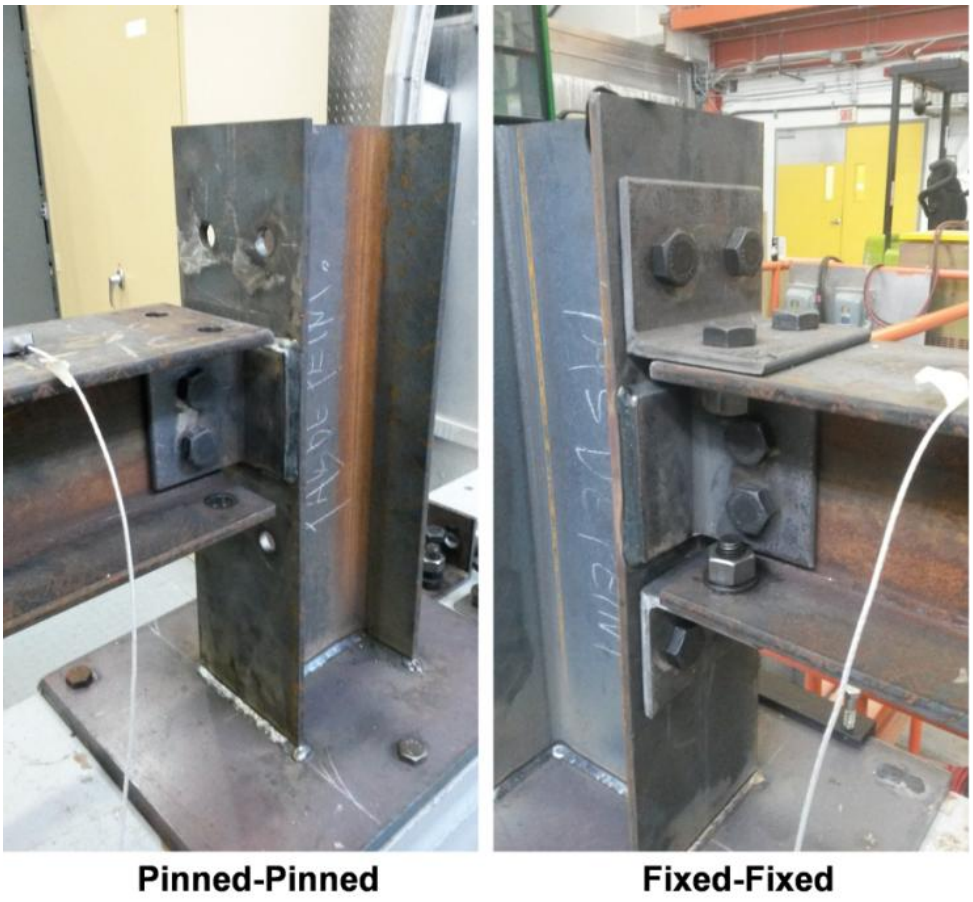

Figure 5-1: Experimental setup with different end support conditions.

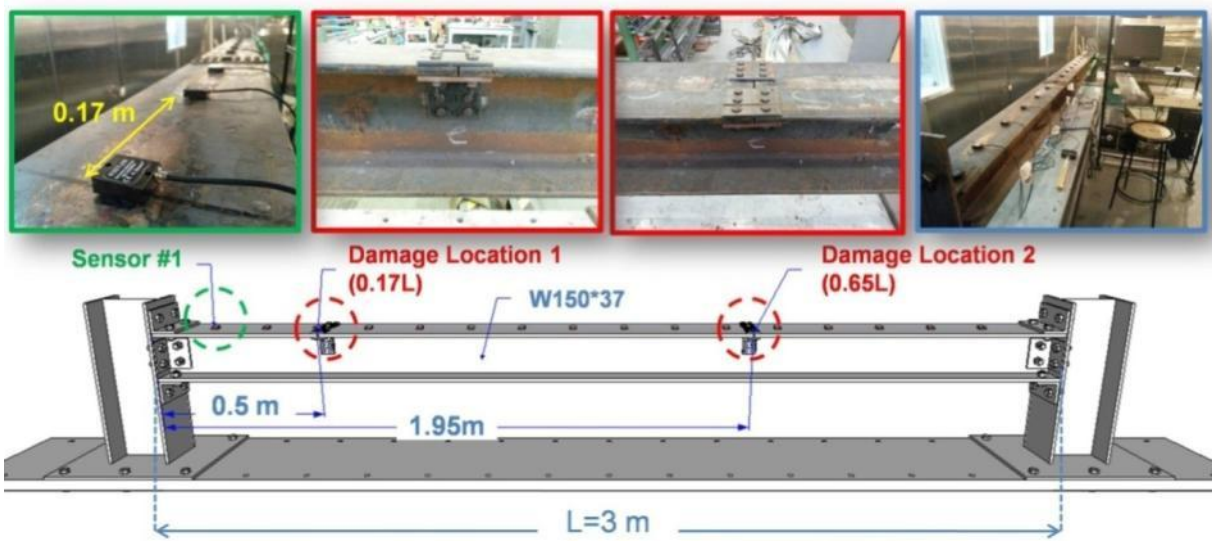

Figure 5-2: Test setup in its fully bolted configuration showing damage locations at 0.17L and 0.65L.

As shown in Figure 5-3, the beam is not homogenous in its fully bolted configuration. The presence of the bolted sections locally reduces the stiffness of the beam by 12% in the fully assembled configuration. The latter corresponds to an equivalent crack of 4% of the height for an equivalent rectangular section. Figure 5-3 indicates the cross-section dimensions of the beam in its fully assembled (initial) state as well as the next possible level of incremental damage considered in this work. Since the main purpose of this study is the early detection of the onset of damage, the damage states are limited to a comparison between the initial state (E0) of damage and the next level state (E1) where the damage is introduced by loosening bolted connections at the damage locations. The state E0 corresponds to the fully assembled system of plates whereas the state E1 corresponds to the case when the first set of plates is removed. In this case, the difference between damage states E0 and E1 is equivalent to a 16% reduction in stiffness or 6% increase in crack height for an equivalent rectangular section.

A relatively large number of sensors were selected in order to properly test the accuracy of the algorithms for the detection and localization of damage. Data acquisition is done under laboratory conditions using sixteen sensors equally spaced along the beam. This number of sensors was selected in order to obtain accurate estimates of the mode shape to be analyzed. In actual bridges, the spacing between sensors affects both the probability of detection of anomalies in mode shapes as well as the level of resolution for damage localization. In this instance, using

16 equally spaced sensors on an actual bridge would provide similar levels of performance for the analysis of the first mode of vibration of the bridge, though reducing the spatial resolution in the localization of damage.

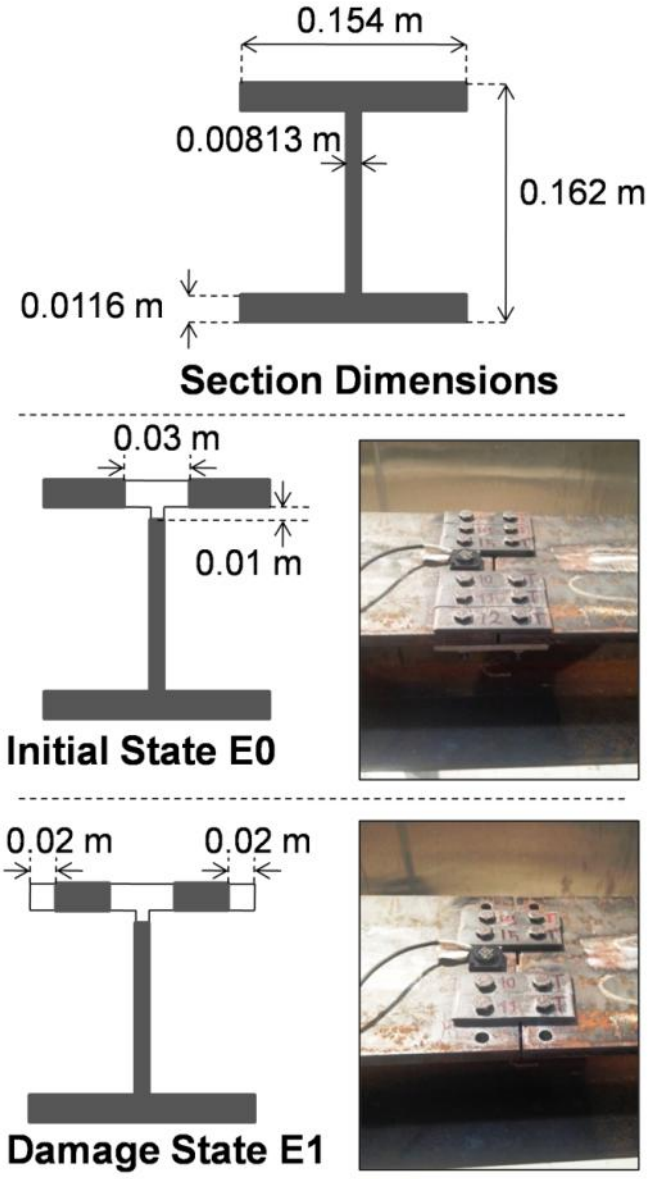

Figure 5-3: Section dimensions, initial (E0) and first (E1) damage states.

The sensors comprise three types of accelerometers (PCP model 3711D1FB3G, Kistler model 8305B2SP4M and 8310A25A1M11SP15M) with share similar specifications. The use of sensors from different suppliers is not considered a major source of uncertainty or bias for the purpose of

damage detection since the sensors are always kept at the same location. Table 5-1 represents the characteristics of the beam for each setup: the centroidal moment of inertia (mm^4) for the intact I-beam (Io) and for each state of damage (I), the ratio of the moments of inertia in the damaged and undamaged states (I/Io), the reduction in stiffness (%), the equivalent crack height for a rectangular section (m), and the number of measurements as a function of the level of damage for both damage locations.

Table 5-1: Parameters for test setups for the experimental program.

Pinned-Pinned End Conditions

Damage Level	I *(mm^4)	I/Io**	Stiffness Reduction (%)	Equivalent Crack Height (m)	Measurements # (location 1: 0.17L)	Measurements # (location 2: 0.65L)
E0	1.952E+07	0.88	12	0.04 h	1 to 97	1 to 97
E1	1.596E+07	0.72	28	0.10 h	98 to 191	98 to 192

Fixed-Fixed End Conditions

Damage Level	I	I/Io	Stiffness Reduction (%)	Equivalent Crack Height	Measurements # (location 1: 0.17L)	Measurements # (location 2: 0.65L)
E0	1.952E+07	0.88	12	0.04 h	1 to 48	1 to 48
E1	1.596E+07	0.72	28	0.10 h	49 to 96	49 to 93

*I= Centroidal moment of inertia for the beam cross-section under damage states E0 and E1.

**Io= Centroidal moment of inertia for an original homogeneous section W150*37 (2.205E+07 mm^4).

Random excitations are mechanically induced using an impact hammer at different points on the top flange of the beam to vary the amplitude and frequency content of each impulse load. Providing an appropriate excitation force with a wide range of frequency bandwidth is essential to detect accurately the mode shapes by the monitoring system. In order to provide a sufficient number of observations for statistical analysis and account for uncertainties in experimental measurements, several measurements are performed at each damage level. It should be noted that the measurements are done for increasing levels of damage at a single damage location in each setup. The experimental setup is designed to simulate a complex structure with two existing damage locations in which incremental damage is introduced at only one location.

5-5 Results and Discussion

The wavelet transform analysis on the first fundamental mode shape was performed using the Symlet wavelet at a scale of 64. Note that the scale is a crucial parameter and a tradeoff exists always for an appropriate selection of this parameter. Large scales may ignore small variations on the mode shapes due to damage and therefore large variations of the mode shapes will only be visible in the results. However, in spite of the interpolation, since experimental mode shapes are not signals with smooth or perfect continuous curves, many discontinuities exist along the mode shapes that may cause fluctuations in the results of the wavelet analysis. Hence, too small scales may produce too much noise and only reveal the position of the sensors. For this study, the scale is selected in a way that exhibit sudden variations of the mode shapes as a result of damage while mitigating the appearance of noise as to the location of measurement points at smaller scales.

The results for the two experimental setups (pinned-pinned and fixed-fixed end conditions) are illustrated in Figure 5-4 and Figure 5-5 respectively. In each figure, the Y-axis corresponds to the label of observations for the damage states (E0) and (E1). The transition of damage level occurs at measurement number 97 in Figure 5-4 and 48 in Figure 5-5. In all cases, the black dashed line represents the location of damage, which corresponds to an equivalent crack of 4% of the cross-section for an equivalent rectangular section for state E0 and 10% for state E1. The data in Figure 5-4 was collected using a combination of different types of sensors, while the data in Figure 5-5 was measured with a new set of similar sensors.

Uncertainties and variability due to experimental conditions can result in false detections of damage due to high noise to signal ratios. The data in Figure 5-4 exhibits more variability than that of Figure 5-5. Differences in the level of variability between Figure 5-4 and Figure 5-5 are attributed to experimental conditions (unequal length of cables, differences in types of sensors, etc).

The results for the two experimental setups demonstrate that the wavelet transform alone is not sufficient to clearly detect and locate damage since no clear and consistent pattern can be deduced from the wavelet coefficients for damage initiation and location.

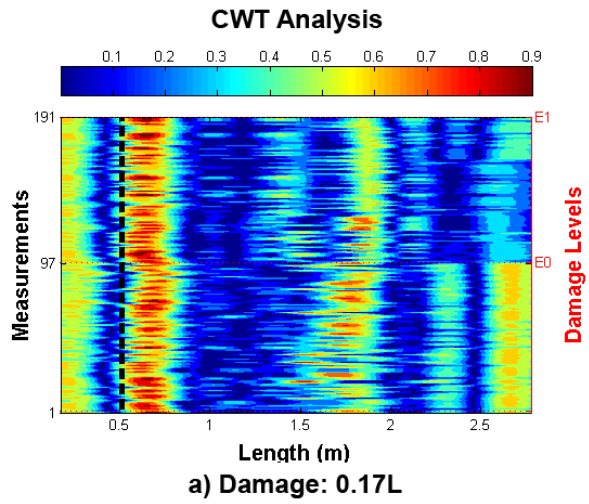

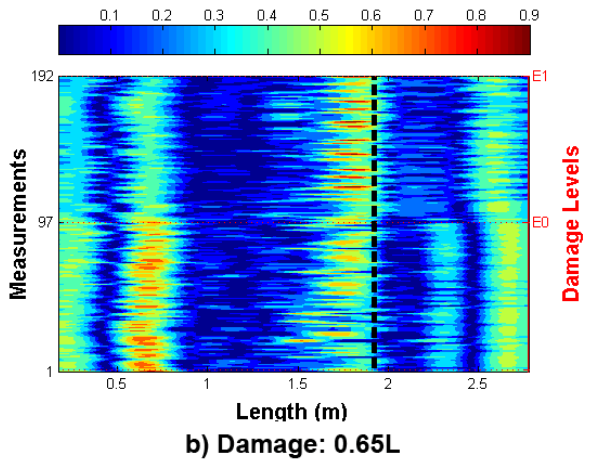

Figure 5-4: CWT coefficients for a pinned beam at damage levels E0 to E1.

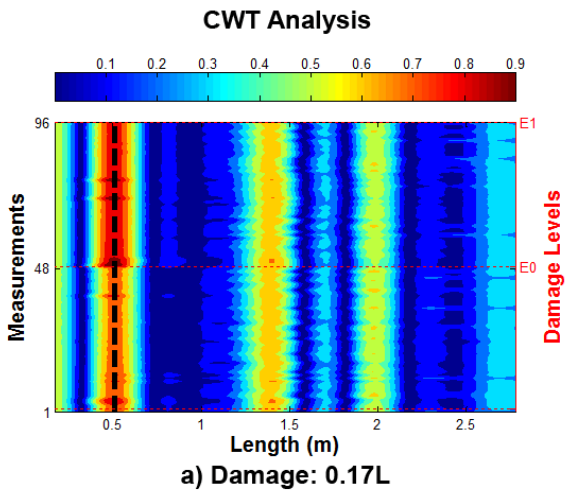

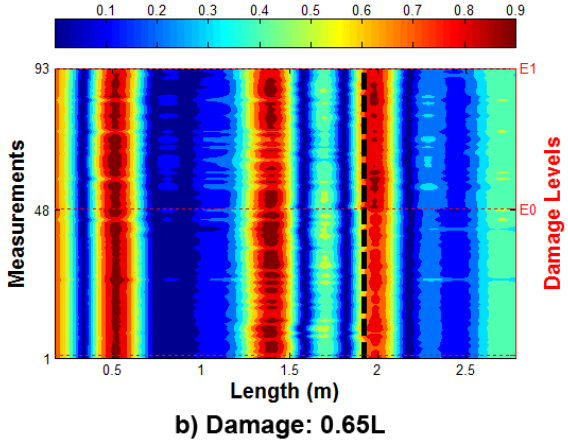

Figure 5-5: CWT coefficients for a fixed beam at damage levels E0 to E1.

To improve the signal to noise ratio, a Principal Component Analysis (PCA) is performed on the data set for observations in states E0 and E1. Figure 5-6 and Figure 5-7 show the scree plot of principal components for the beam with pinned-pinned and fixed-fixed end conditions respectively. As shown, the first few components explain most of the variability. Assuming that dominant patterns in the wavelet coefficients are correlated with changes in damage state, the scores of the first few principal components are compared across the two states E0 and E1. For the pinned-pinned end conditions, the percentage of the variance explained by the first three components is 67% and 66% for the two damage locations, while the percentage is 90% and 77% for the fixed-fixed conditions which is indicative of a higher signal to noise ratio for the fixed-fixed end conditions.

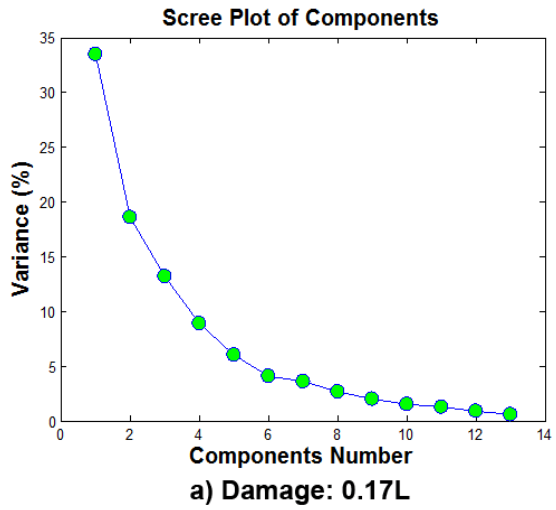

Figure 5-6: Scree plot for PCA for a pinned beam.

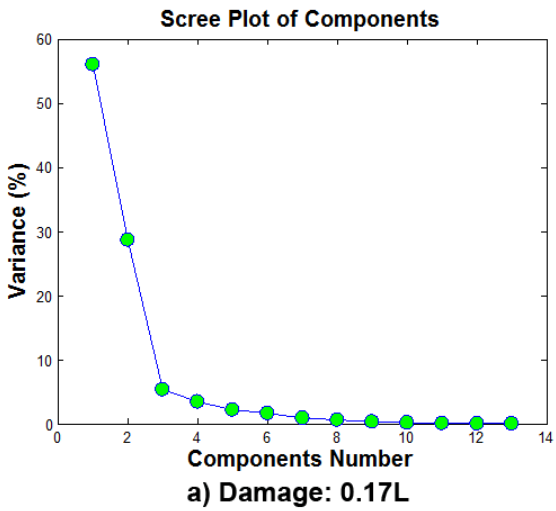

Figure 5-7: Scree plot for PCA for a fixed beam.

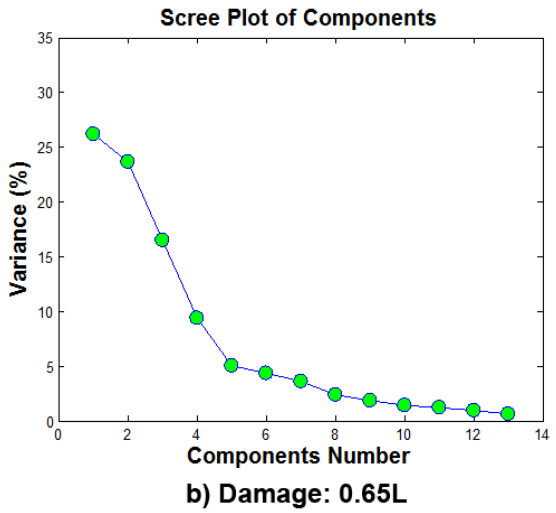

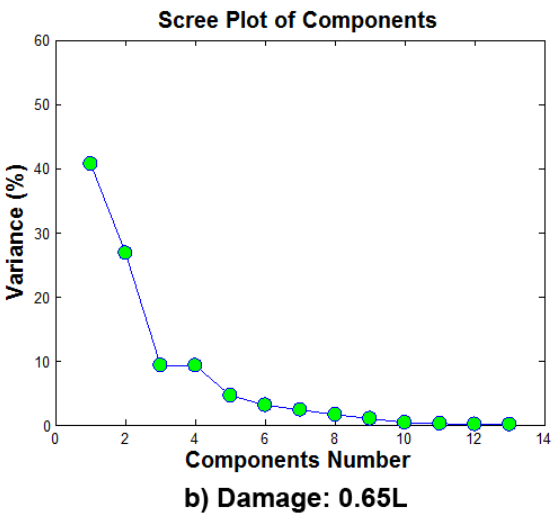

Figure 5-8 and Figure 5-9 show the first three principal components for the various cases analyzed. In each of these figures, the location where an increase of damage is introduced is indicated by a dotted red line. These indicate that the components by themselves are not informative as to the presence or location of damage. Hence, for each PC, the score are computed across the states E0 and E1 with Eq. 5.14 (Figure 5-10 and Figure 5-11). The vertical line separates the scores between the states E0 and E1. For each component, a change in the mean value (and/or the variance) of scores between the two states is attributed to a change in the level of damage. In all cases, this difference in scores is more pronounced for the first component. However, for a better visualization of the distribution of scores, Figure 5-12 and

Figure 5-13 show box and whisker plots for the scores between the two states E0 and E1. On each box, the central horizontal line (red) is the median, the edges of the box (blue) correspond to the first and third quartiles, the whiskers (black lines extending vertically from the boxes) indicate the most extreme data points that are not outliers, and outliers (+ red) are plotted as individual points.

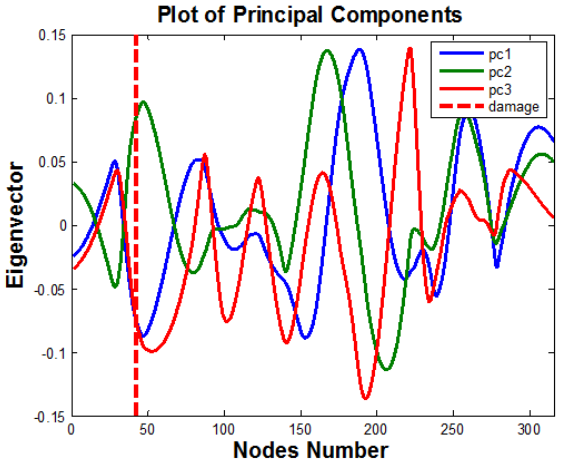

Figure 5-8: Plot of the first three Principal Components (PCs) for a pinned beam.

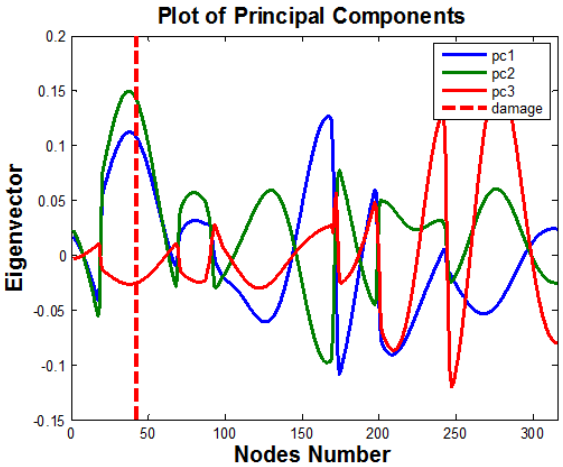

Figure 5-9: Plot of the first few Principal Components (PCs) for a fixed beam.

A change in the distribution of scores is expected with increasing levels of damage and statistical tests based on the equality of location parameters are used to determine if these differences are statistically significant. Table 5-2 and Table 5-3 show the results of the t-test and the Mann-Whitney U-test between the scores at levels E0 and E1. The results of the two tables indicate that

the two statistical tests are efficient in detecting the change of location parameters between the two states of damage. For the first and second components, the results of the two tests indicate that the null hypothesis is rejected (H=1) at a significance level (α) of 1% (or 0.01). However, for both tests, the null hypothesis on the third component for damage at 0.17L (pinned beam) fails to reject the equality of means (H=0) at a significance level of 1%. According to Table 5-2 and Table 5-3, the tests on the first two components are conclusive on the presence of damage and there is no need to use the third component.

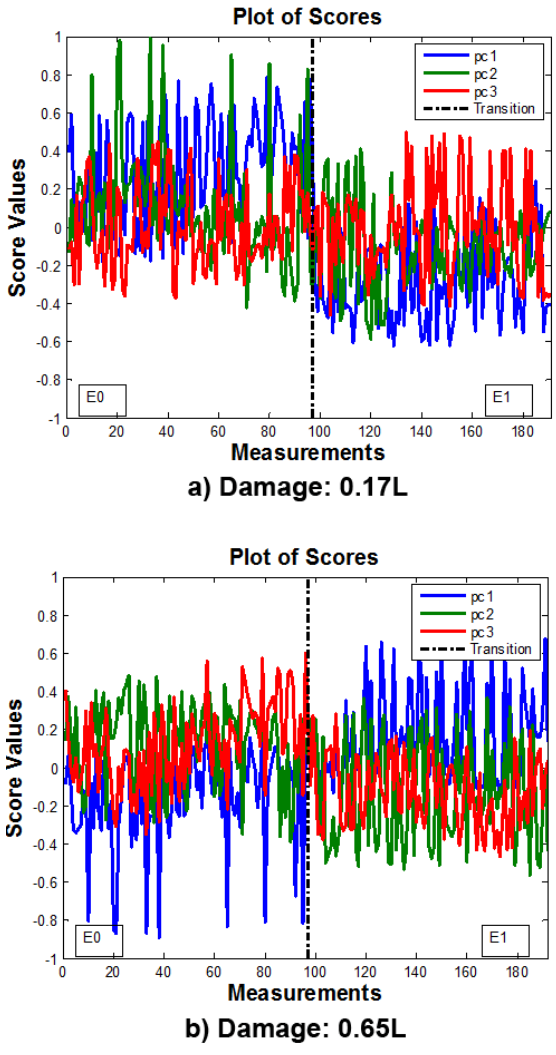

Figure 5-10: PC scores for a pinned beam.

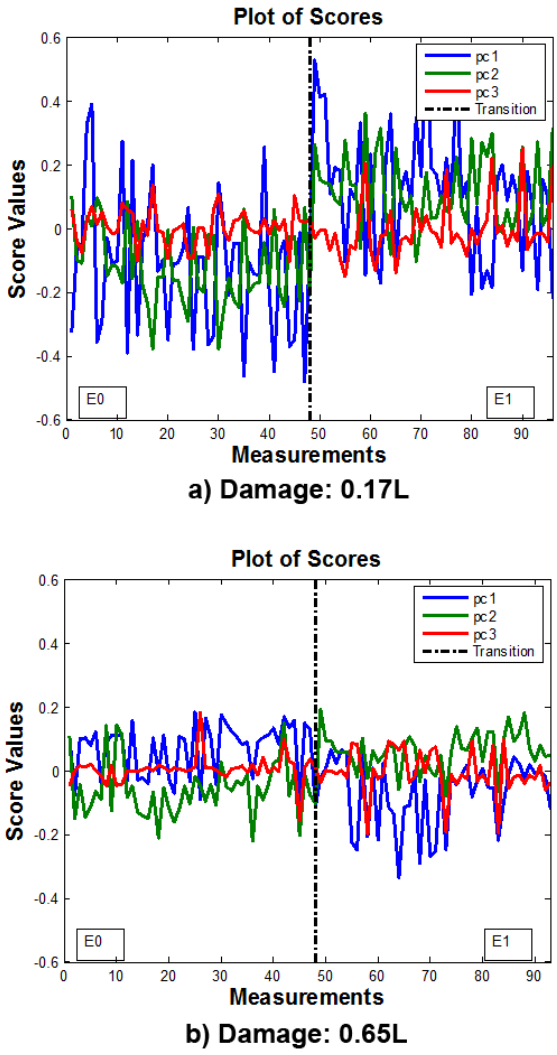

Figure 5-11: PC scores for a fixed beam.

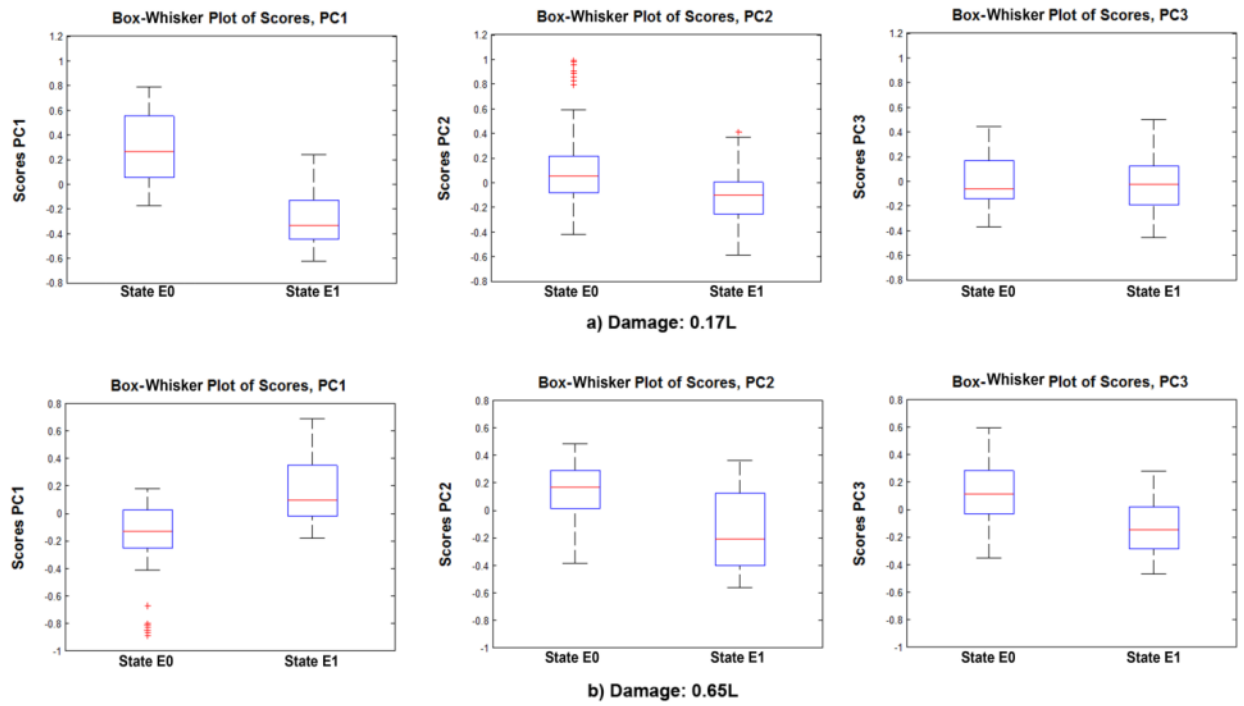

Figure 5-12: Box and Whisker plot for the scores of a pinned beam.

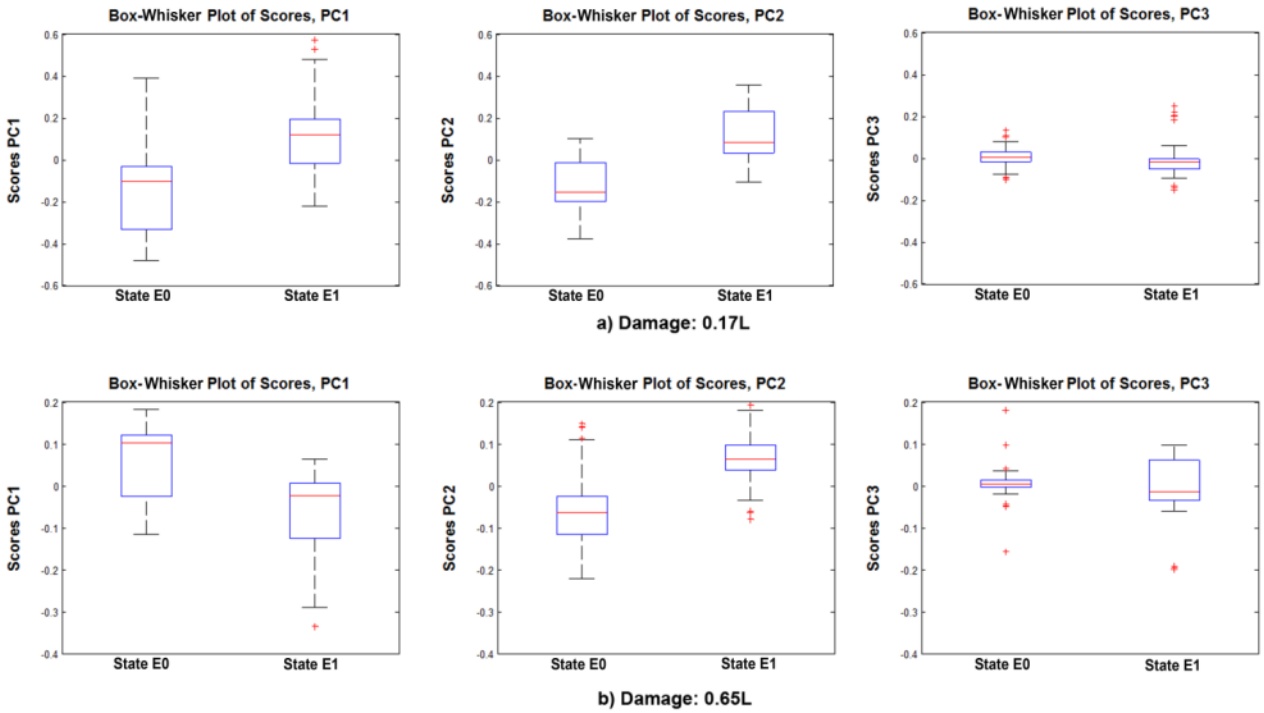

Figure 5-13: Box and Whisker plot for the scores of a fixed beam.

Table 5-2: Summary of results for the t-test between two scores at levels E0 and E1.

Pinned-Pinned End Conditions

Damage	PC	$\bar{x}_{E0}$	$\bar{x}_{E1}$	σ_{E0}	σ_{E1}	H	P	N_{E0}	N_{E1}	Dof*	α
0.17L	1	0.2831	- 0.2922	0.2773	0.2223	1	1.46E-36	97	94	189	1%
0.17L	2	0.1037	- 0.1070	0.3012	0.2185	1	1.24E-07	97	94	189	1%
0.17L	3	0.0065	- 0.0067	0.2247	0.2512	0	7.03E-01	97	94	189	1%
0.65L	1	- 0.1652	0.1687	0.2582	0.2424	1	6.01E-17	97	95	190	1%
0.65L	2	0.1330	- 0.1358	0.2215	0.2798	1	5.66E-12	97	95	190	1%
0.65L	3	0.1242	- 0.1269	0.2219	0.1827	1	4.50E-15	97	95	190	1%

Fixed-Fixed End Conditions

Damage	PC	$\bar{x}_{E0}$	$\bar{x}_{E1}$	σ_{E0}	σ_{E1}	H	P	N_{E0}	N_{E1}	Dof	α
0.17L	1	- 0.1148	0.1148	0.2128	0.1985	1	3.73E-07	48	48	94	1%
0.17L	2	- 0.1175	0.1175	0.1231	0.1173	1	1.46E-15	48	48	94	1%
0.17L	3	0.0058	- 0.0058	0.0548	0.0875	0	4.34E-01	48	48	94	1%
0.65L	1	0.0668	- 0.0713	0.0844	0.1078	1	9.67E-10	48	45	91	1%
0.65L	2	- 0.0586	0.0625	0.0874	0.0608	1	1.48E-11	48	45	91	1%
0.65L	3	0.0047	- 0.0051	0.0420	0.0677	0	4.12E-01	48	45	91	1%

*Dof = Degree of freedom ($N_{E0} + N_{E1} - 2$) where N defines the number of samples.

Given that statistically significant differences in the mean or median scores are detected, the Likelihood Ratio (LR) is applied to the scores of the first few PCs to identify the nodes that contribute the most to the change in scores in the damaged state. In this case, since the term at the numerator in Eq. 5.24 is common for all nodes along the beam, the likelihood can be computed only for a set of scores obtained from the leave-a-node-out method in Eq. 5.26. Note that when the damage level is increased from the initial state (E0) to the next state (E1) in one location (e.g., 0.17L), the state of damage remains unchanged (E0) at the other location (e.g., 0.65L).

Table 5-3: The results of the Mann-Whitney U-test between two scores at levels E0 and E1.

Pinned-Pinned End Conditions

Damage	PC	R_{E0}*	R_{E1}	U	H	P	N_{E0}	N_{E1}	α
0.17L	1	13348	4988	8595	1	4.31E-26	97	94	1%
0.17L	2	11297	7039	6544	1	2.04E-07	97	94	1%
0.17L	3	9423	8913	4670	0	7.72E-01	97	94	1%
0.65L	1	6361	12167	1608	1	6.70E-15	97	95	1%
0.65L	2	11803	6725	7050	1	2.25E-10	97	95	1%
0.65L	3	12132	6396	7379	1	6.12E-13	97	95	1%

Fixed-Fixed End Conditions

Damage	PC	R_{E0}	R_{E1}	U	H	P	N_{E0}	N_{E1}	α
0.17L	1	1714	2942	1766	1	6.94E-06	48	48	1%
0.17L	2	1384	3272	2096	1	4.72E-12	48	48	1%
0.17L	3	2680	1976	800	0	1.00E-02	48	48	1%
0.65L	1	2956	1415	1780	1	7.55E-08	48	45	1%
0.65L	2	1470	2901	294	1	1.55E-09	48	45	1%
0.65L	3	2523	1848	1347	0	4.05E-02	48	45	1%

*R= The sum of the ranks in each group of data.

Figure 5-14 shows the results of the LR test for the pinned-pinned end conditions. In these figures, the red dashed line corresponds to the location of incremental damage, whereas the black dashed line corresponds to the location of the other discontinuity (joint assembly in its initial state E0) where the damage level remains constant. For the damage at location 0.17L, the results indicate the first component (34% of the total variance) identifies correctly the location of incremental damage. The second component (19% of the total variance) identifies the location of the other bolted connected where damage was not increased. This can be explained by an increase in the displacements at the location of an existing weakness when damage is introduced

at another location along the beam. The third component (13% of the variance) is less significant and identifies both of the previous locations but the statistical tests for damage detection are not significant at 1% significance level. For the damage at 0.65L, the results indicate that the first component (26% of the variance) identifies correctly the location of incremental damage. The second component (24% of the variance) also identifies the location of incremental damage but not as clearly. The third component (16% of the variance) is less significant and identifies the location of the other bolted connection where damage was not increased. The damage detection and localization algorithm performs well at both location of incremental damage.

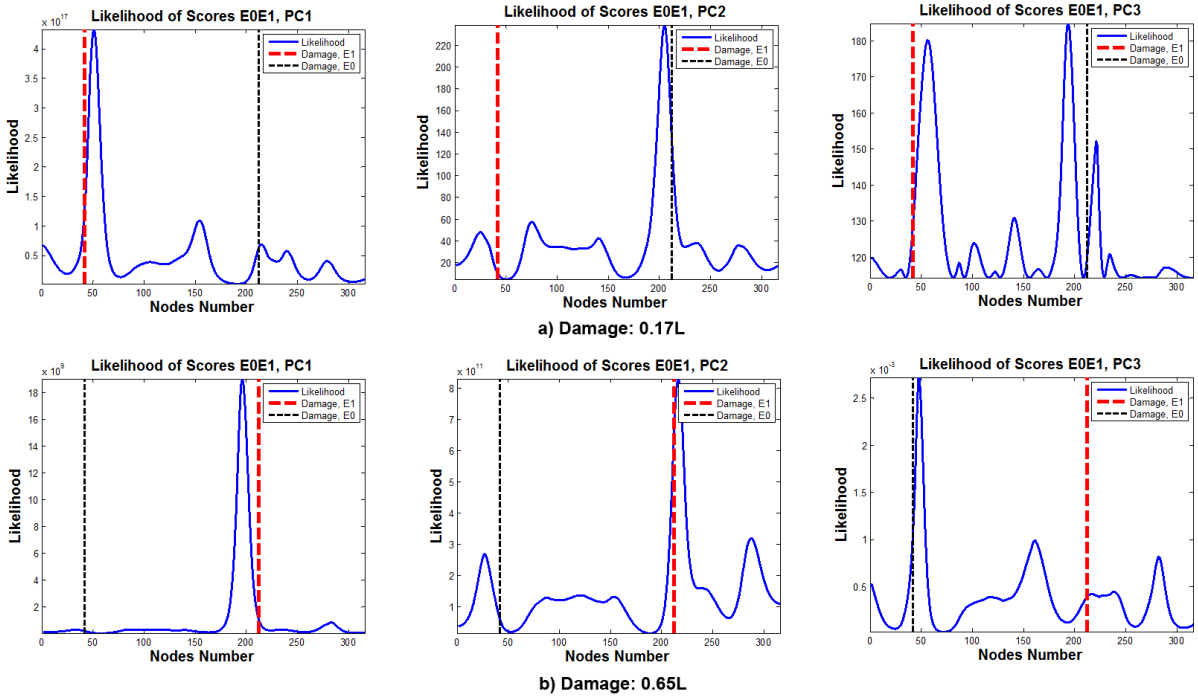

Figure 5-14: Likelihood for damage evolving from states E0 to E1, Pinned beam.

Figure 5-15 shows the results for the case with fixed-fixed end conditions. As mentioned previously, the signal to noise ratio is much higher for this set since the same type of instrument is used for measurements as shown by the first three principal components which explain a much greater percentage of the total variance. For the damage located at 0.17L, the first (56% of the variance) and second (29% of the variance) components identify very clearly the location of incremental damage along the beam. The third component (5% of the variance) is less significant and identifies the location of the other bolted section where damage was not increased. For the incremental damage at 0.65L, the first (41% of the variance) and second (27% of the variance)

components identify very clearly the location of increased damage along the beam. The third component (10% of the variance) identifies the location of the other bolted section where damage was not increased; however, the test for the detection of damage is not significant at the 1% significance level.

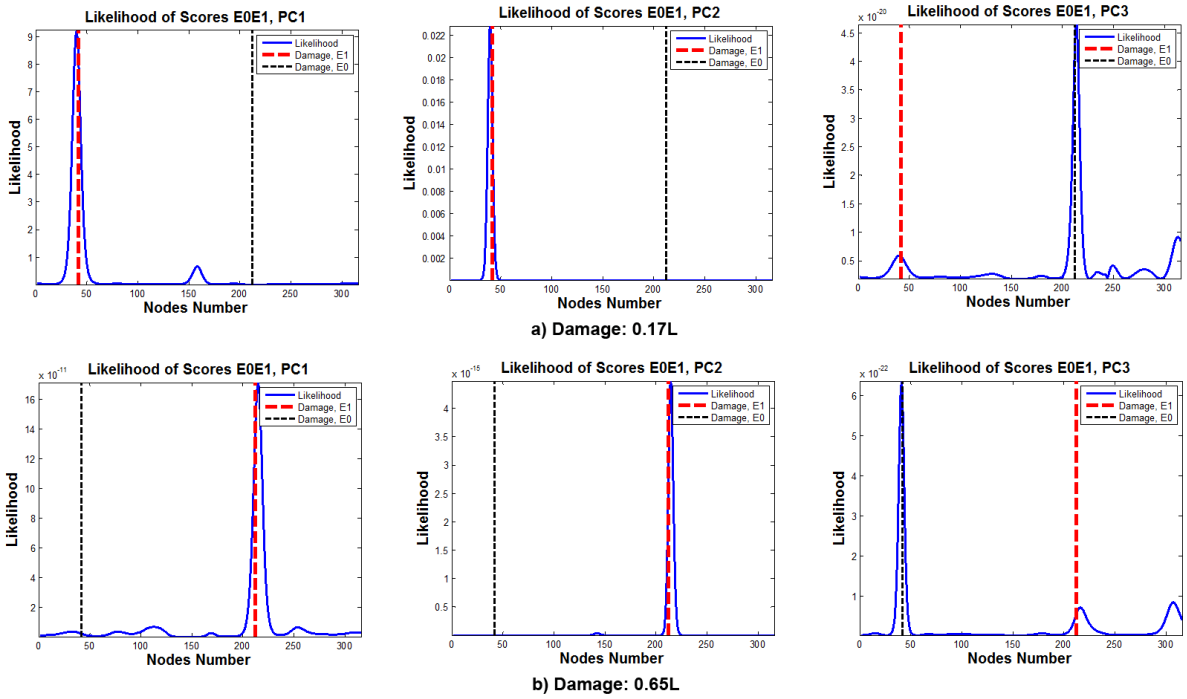

Figure 5-15: Likelihood for damage evolving from states E0 to E1, fixed beam.

In summary, the proposed procedure properly identifies the incremental damage as well as its location under the fixed end conditions when the same type of sensor is used for the entire beam. The first two principal components can accurately detect statistically significant incremental damage as well as its location. The third component, which is associated with a much lower percentage of the total variance, does not result in statistically significant damage at the 1% significance level but can be used to detect the second area of weakness in the beam where assembly plates have not been removed. The results for the two incremental damage locations (0.17L and 0.65L) give similar results. The results obtained for the pinned end conditions are obtained with a set of sensors from different suppliers which introduces more variability in the measurements. Nonetheless, the first principal component can be used to correctly detect the incremental damage as well as its location. The second principal component also detects and

locates the incremental damage at 0.65L while for the incremental damage introduced at 0.17L the second component identifies the existing weakness at 0.65L.

5-6 Conclusions

An experimental program was performed on a beam assembly to test and validate a new detection and localization of damage algorithm. The damage detection algorithm used wavelet coefficients to detect anomalies in mode shapes of the beam. To obtain a good estimate of the wavelet coefficients and minimize the effects of experimental uncertainties, the measurements were repeated several times for each state of damage. For real field tests, since the lowest, or fundamental, resonance frequency associated with the first mode shape is most accurately determined by a limited number of sensors, in this study only the first mode of vibration was analyzed for the detection of damage. To do so, dynamic vibrations were induced by applying random excitations using an impact hammer.

Since wavelet coefficients could not deduce clearly the location of damage in a clear and consistent pattern, a principal component analysis was first performed to identify the most important patterns of variation in the wavelet coefficients and to minimize the effect of noise. Assuming that dominant patterns in the wavelet coefficients are correlated with changes in damage state, the scores of the components were then used to detect significant changes in their distribution when damage was introduced. Tests of location parameters based on the t-test and the Mann-Whitney U-test were proposed for this purpose. Given that significant damage has been detected, a Likelihood Ratio (LR) test is further used to determine its most likely location along the beam.

The results were performed on a beam with two bolted connecting sections that can be modified to simulate increasing levels of damage with 16 equally spaced sensors. For an actual bridge, given that the cost of sensors is relatively minor in comparison to the annualized maintenance costs on a large bridge, the number and the spacing of sensors can be scaled up to obtain the desired degree of resolution. The parameters that were varied in the beam are the location of damage (0.17L and 0.65L) and the end conditions (pinned-pinned or fixed-fixed). The results indicate that the proposed procedures are efficient at detecting both the occurrence and location of damage.

Future work should investigate the effect of environmental conditions such as temperature on the distribution of scores. To minimize the effect of reversible temperature effects in field

applications, measurements should be performed under similar temperature conditions or measurements can be corrected by estimating and correcting for the reversible temperature effects. Another difficulty to be addressed is the applicability of wavelets to mode shapes derived from ambient noise excitations since impact input motions are not feasible easily for large structures. The next step will be to adapt and investigate the proposed procedure for field applications to a bridge. Issues that need to be addressed are the effects of varying exposure conditions as well as spatially distributed damage on wavelet scores. Another issue is to determine how the procedure performs with ambient noise as the source of excitation.

Acknowledgement

This study is supported through a CREATE grant from the Natural Sciences and Engineering Research Council of Canada (NSERC) and the CRIB Research Center (Université Laval).

5-7 Nomenclatures

r	Mode shape number (subscript)
ω_r	Natural frequency of the r^{th} mode
u	Undamaged (subscript)
d	Damaged (subscript)
$f(x)$	Space-domain function
x	Spatial coordinate
$\Psi(x)$	Wavelet function
$\Psi(\omega)$	Fourier Transform of $\Psi(x)$
u	Wavelet function position parameter
s	Wavelet function scale parameter
CWT(x)	Wavelet coefficient at location x
m	Number of observations
n	Number of variables/nodes
[X]	Wavelet coefficients matrix
[U]	Left-singular values of [X]
[Λ]	Singular-values of [X]
[V]	Right-singular values of [X]
[C]	Covariance matrix of [X]
PC_i	i^{th} principal component
λ_i	i^{th} eigenvalue
η_i	Percentage of variance for the i^{th} PC
[S]	Score matrix
$[S_1]$	Scores for the 1st set of measurements
$[S_2]$	Scores for the 2nd set of measurements
pc	Selected component (subscript)
$\{V\}_{pc}$	Selected eigenvector or PC
$\{S\}_{pc}$	Score vector for the selected component
$\{S_R\}$	Scores for the reference model
$\{S_i\}$	Scores for the alternative model

$LR(x_i)$	Likelihood Ratio at i^{th} location
$L(S_R \mid \mu, \sigma)$	Likelihood of reference scores
$L(S_i \mid \mu_i, \sigma_i)_i$	Likelihood of alternative scores at i^{th} node
μ	Population mean
σ	Standard deviation
ν^2	Variance
P	P-value
H	Hypothesis testing
H0	Null hypothesis
H1	Alternative hypothesis
α	Type I error and/or significance level
β	Type II error
R	Sum of ranks
Dof	Hypothesis testing degree of freedom
$\bar{x}$	Sample mean
N	Sample size
T	t-test statistic

5-8 References

Abdo, M.-B. and M. Hori (2002). "A numerical study of structural damage detection using changes in the rotation of mode shapes." Journal of Sound and vibration 251(2): 227-239.

Abramowitz, M. and I. A. Stegun (1966). "Handbook of mathematical functions." Applied mathematics series 55: 62.

Alvandi, A., J. Bastien, E. Gregoire and M. Jolin (2009). "Bridge integrity assessment by continuous wavelet transforms." International Journal of Structural Stability and Dynamics 9(1): 11-43.

Alvandi, A. and C. Cremona (2006). "Assessment of vibration-based damage identification techniques." Journal of Sound and Vibration 292(1): 179-202.

Cao, M. and P. Qiao (2008). "Integrated wavelet transform and its application to vibration mode shapes for the damage detection of beam-type structures." Journal of Smart Materials and Structures 17(5): 055014.

Catbas, F., M. Gul and J. Burkett (2007). "Damage assessment using flexibility and flexibility-based curvature for structural health monitoring." Journal of Smart materials and structures 17(1): 015024.

Dackermann, U., J. Li and B. Samali (2008). "Structural damage identification utilising PCA-compressed frequency response functions and neural network ensembles." 20th Australasian Conference on the Mechanics of Structures and Materials, Toowoomba, Australia.

Daubechies, I. (1992). "Ten lectures on wavelets," Society for Industrial and Applied Mathematics.

De Boor, C. (1978). "A practical guide to splines," Springer-Verlag New York.

Fan, W. and P. Qiao (2011). "Vibration-based damage identification methods: a review and comparative study." Structural Health Monitoring 10(1): 83-111.

Farrar, C. R., W. Baker, T. Bell, K. Cone, T. Darling, T. Duffey, A. Eklund and A. Migliori (1994). "Dynamic characterization and damage detection in the I-40 bridge over the Rio Grande," Los Alamos National Lab., NM (United States).

Farrar, C. R. and D. A. Jauregui (1998). "Comparative study of damage identification algorithms applied to a bridge: I. Experiment." Journal of Smart materials and structures 7(5): 704-719.

Gabor, D. (1946). "Theory of communication. Part 1: The analysis of information." Electrical Engineers-Part III: Radio and Communication Engineering," Journal of the Institution of 93(26): 429-441.

Gibbons, J. D. and S. Chakraborti (2011). "Nonparametric statistical inference," Springer.

Hadjileontiadis, L., E. Douka and A. Trochidis (2005). "Fractal dimension analysis for crack identification in beam structures." Journal of Mechanical Systems and Signal Processing 19(3): 659-674.

Hu, W.-H., C. Moutinho, E. Caetano, F. Magalhães and Á. Cunha (2012). "Continuous dynamic monitoring of a lively footbridge for serviceability assessment and damage detection." Journal of Mechanical Systems and Signal Processing 33: 38-55.

Jackson, J. E. (2005). "A user's guide to principal components," John Wiley & Sons.

Kendall, M. and A. Stuart (1979). "The advanced theory of statistics. Statistical Inference and Relationship." London, Charles Griffin.

Lee, J. J., J. W. Lee, J. H. Yi, C. B. Yun and H. Y. Jung (2005). "Neural networks-based damage detection for bridges considering errors in baseline finite element models." Journal of Sound and Vibration 280(3): 555-578.

Li, H., S. Li, J. Ou and H. Li (2010). "Modal identification of bridges under varying environmental conditions: temperature and wind effects." Journal of Structural Control and Health Monitoring 17(5): 495-512.

Lin, C. S. (1990). "Location of modeling errors using modal test data." AIAA journal 28(9): 1650-1654.

Mazurek, D. F. and J. T. DeWolf (1990). "Experimental study of bridge monitoring technique." Journal of Structural Engineering 116(9): 2532-2549.

Messina, A., E. Williams and T. Contursi (1998). "Structural damage detection by a sensitivity and statistical-based method." Journal of sound and vibration 216(5): 791-808.

Montanari, L., A. Spagnoli, B. Basu and B. Broderick (2015). "On the effect of spatial sampling in damage detection of cracked beams by continuous wavelet transform." Journal of Sound and Vibration 345: 233-249.

Montgomery, D. C. and G. C. Runger (2012). "Applied Statistics and Probability for Engineers," John Wiley & Sons.

Mujica, L., M. Ruiz, F. Pozo, J. Rodellar and A. Güemes (2013). "A structural damage detection indicator based on principal component analysis and statistical hypothesis testing." Journal of Smart Materials and Structures 23(2): 025014.

Nair, K. K., A. S. Kiremidjian and K. H. Law (2006). "Time series-based damage detection and localization algorithm with application to the ASCE benchmark structure." Journal of Sound and Vibration 291(1): 349-368.

Ndambi, J.-M., J. Vantomme and K. Harri (2002). "Damage assessment in reinforced concrete beams using eigenfrequencies and mode shape derivatives." Journal of Engineering Structures 24(4): 501-515.

Okafor, A. C. and A. Dutta (2000). "Structural damage detection in beams by wavelet transforms." Journal of Smart Materials and Structures 9(6): 906.

Ovanesova, A. and L. Suarez (2004). "Applications of wavelet transforms to damage detection in frame structures." Journal of Engineering Structures 26(1): 39-49.

Pandey, A. and M. Biswas (1994). "Damage detection in structures using changes in flexibility." Journal of Sound and Vibration 169(1): 3-17.

Pandey, A., M. Biswas and M. Samman (1991). "Damage detection from changes in curvature mode shapes." Journal of Sound and Vibration 145(2): 321-332.

Pearson, K. (1901). "LIII. On lines and planes of closest fit to systems of points in space." Journal of Philosophical Magazine Series 6 2(11): 559-572.

Peng, Z., W. T. Peter and F. Chu (2005). "An improved Hilbert–Huang transform and its application in vibration signal analysis." Journal of Sound and Vibration 286(1): 187-205.

Reynders, E. (2012). "System identification methods for (operational) modal analysis: review and comparison." Archives of Computational Methods in Engineering 19(1): 51-124.

Robertson, D. C., O. I. Camps, J. S. Mayer and W. B. Gish (1996). "Wavelets and electromagnetic power system transients." Power Delivery, IEEE Transactions on 11(2): 1050-1058.

Roveri, N. and A. Carcaterra (2012). "Damage detection in structures under traveling loads by Hilbert–Huang transform." Journal of Mechanical Systems and Signal Processing 28: 128-144.

Rucka, M. and K. Wilde (2006). "Application of continuous wavelet transform in vibration based damage detection method for beams and plates." Journal of Sound and Vibration 297(3): 536-550.

Salawu, O. (1997). "Detection of structural damage through changes in frequency: a review." Journal of Engineering Structures 19(9): 718-723.

Shahsavari, V., J. Bastien, L. Chouinard and A. Clément (2015). "A Novel Response-Based Approach to Localize Low Intensity Damage of Beam-Like Structures." Proc. of the 5th International Conference on Smart Materials and Nanotechnology in Engineering Vancouver, BC, Canada: 99-109.

Sohn, H., K. Worden and C. R. Farrar (2002). "Statistical damage classification under changing environmental and operational conditions." Journal of Intelligent Material Systems and Structures 13(9): 561-574.

Solís, M., M. Algaba and P. Galvín (2013). "Continuous wavelet analysis of mode shapes differences for damage detection." Journal of Mechanical Systems and Signal Processing 40(2): 645-666.

Strang, G. and T. Nguyen (1996). "Wavelets and filter banks," Wellesley-Cambridge Press, Wellesley, USA

Sun, Z. and C. Chang (2002). "Structural damage assessment based on wavelet packet transform." Journal of Structural Engineering 128(10): 1354-1361.

Wahab, M. A. and G. De Roeck (1999). "Damage detection in bridges using modal curvatures: application to a real damage scenario." Journal of Sound and Vibration 226(2): 217-235.

Wu, N. and Q. Wang (2011). "Experimental studies on damage detection of beam structures with wavelet transform." International Journal of Engineering Science 49(3): 253-261.

Yan, A.-M., G. Kerschen, P. De Boe and J.-C. Golinval (2005). "Structural damage diagnosis under varying environmental conditions—part I: a linear analysis." Journal of Mechanical Systems and Signal Processing 19(4): 847-864.

Yan, A.-M., G. Kerschen, P. De Boe and J.-C. Golinval (2005). "Structural damage diagnosis under varying environmental conditions—part II: local PCA for non-linear cases." Journal of Mechanical Systems and Signal Processing 19(4): 865-880.

Yang, J. N., Y. Lei, S. Lin and N. Huang (2004). "Hilbert-Huang based approach for structural damage detection." Journal of Engineering Mechanics 130(1): 85-95.

Zhang, D., Y. Bao, H. Li and J. Ou (2012). "Investigation of temperature effects on modal parameters of the China National Aquatics Center." Journal of Advances in Structural Engineering 15(7): 1139-1153.

CHAPTER 6 : AVANT-PROPOS

Auteurs et affiliation :

- Vahid Shahsavari: Étudiant au doctorat, Université Laval, Faculté des sciences et de génie, Département de génie civil et de génie des eaux.
- Luc Chouinard : Professeur, Université McGill, Faculté de génie, Département de génie civil et de mécanique appliquée.
- Josée Bastien : Professeur, Université Laval, Faculté des sciences et de génie, Département de génie civil et de génie des eaux.

État : soumis à la revue

Date de soumission : 16 décembre 2016

Revue : Journal of Structural Health Monitoring

Titre français : Détection d'endommagement structural dans des conditions environnementales variables

Résumé français : Les changements des conditions environnementales, en particulier la température de l'air, ont un effet significatif sur les résultats des essais dynamiques sur les structures. Lorsque ces tests sont utilisés dans le but de la détection et la localisation de dommages, ces effets peuvent facilement masquer les changements dans les propriétés dynamiques associées aux dommages. Le but de ce projet est d'effectuer une série d'essais dans des conditions contrôlées pour estimer les contributions relatives des effets des dommages et de température sur les propriétés dynamiques d'une poutre et proposer des procédures pour améliorer la détection de dommages à des températures variables. Dans ce cas, une poutre instrumentée est soumis à des variations de température entre 5°C et 25°C et deux niveaux de dommage en deux endroits le long de sa longueur. Les deux niveaux d'endommagement correspondent à un dommage incrémentiel de 12% par rapport au moment d'inertie de la poutre. Pour cette application, la détection de dommage est basée sur l'analyse des coefficients

d'ondelettes appliqués sur le premier mode de vibration de la poutre. Une analyse des composantes principales (PCA) des coefficients d'ondelettes est utilisée pour filtrer le bruit en ne retenant que les premiers composants qui expliquent la plus grande partie de la variance observée dans les coefficients d'ondelettes. Les scores du premier composant sont fortement corrélés avec le niveau de dommage. Étant donné la présence du dommage, un test de probabilité (LR) est effectué pour trouver les endroits les plus probables d'endommagement le long de la longueur de la poutre. Les résultats indiquent que pour une plage de températures de 20°C, les effets de température peuvent affecter les modes propres et peuvent masquer l'endommagement incrémentiel correspondant à une réduction de 12% de la rigidité.

Mots-clés : Température, Dommage, Mode propre, Ondelettes, Analyse des composants principaux, Rapport de probabilité.

6. Detection of Structural Damage under Varying Environmental Conditions

6-1 Abstract

Changes in environmental conditions, especially air temperature, have a significant effect on results from dynamic tests on structures. When these tests are used for the purpose of damage detection and damage localization, these effects can easily mask changes in dynamic properties associated with damage. The purpose of this project is to perform a series of tests under controlled conditions to estimate the relative contributions of damage and temperature effects on the dynamic properties of a beam and to propose procedures to improve damage detection under varying temperatures. In this instance, an instrumented beam is subjected to temperature variations between 5^{o}C and 25^{o}C and two levels of damage at two locations along its length. The two levels of damage correspond to incremental damage of 12% relative to the moment of inertia of the beam. For this application, the detection of damage is based on the analysis of the wavelet coefficients applied on the first mode of vibration of the beam. A Principal Component Analysis (PCA) of the wavelet coefficients is used to filter noise by retaining only the first few components that explain most of the variance observed in the wavelet coefficients. The scores of the first component are found to be highly correlated with the damage level. Given damage, a Likelihood Ratio (LR) test is performed to find the most likely locations of damage along the length of the beam. The results indicate that for a temperature range of 20^{o}C, temperature effects can affect mode shapes and mask incremental damage corresponding to a 12% reduction in stiffness.

Key-word: Temperature, Damage, Mode Shape, Wavelet, Principal Component Analysis, Likelihood Ratio.

6-2 Introduction

Vibration-based damage detection techniques rely mainly on identifying statistically significant changes in modal characteristics of structures and more specifically bridges. Natural frequencies and mode shapes are the most popular global parameters of bridges that are typically used for damage detection. However, changes in these global properties can also be induced by changing environmental conditions. Most notably, variations in air temperature can induce changes in the state of expansion joints, boundary conditions or deflections of the bridges, which affect the stiffness and measured vibration responses (Mosavi, Seracino et al. 2012). In order to achieve reliable structural assessments, an effective Structural Health Monitoring (SHM) program needs to discriminate between irreversible changes in dynamic properties due to structural damage to those from reversible thermal effects. In real structures, a practical difficulty occurs when damage-induced changes in frequencies or mode shapes at small damage levels are of the same order of magnitude as those due to environmental conditions (Huth, Feltrin et al. 2005, Wenzel and Pichler 2005).

Several investigators have previously investigated the effect of temperature on the natural frequencies and mode shapes of bridge structures. Mosavi et al. (2012) present results on a two-span steel-concrete highway bridge over a 24-hour period and found no significant changes in the first five natural frequencies between midnight (21.1°C) and morning (21.7°C) measurements, while a 1-2% change is observed for measurements between midnight (21.1°C) and noon (36.9°C). Cornwell et al. (1999) found that the frequencies of the Alamosa Canyon Bridge for the first three modes varied by approximately 4.7%, 6.6% and 5.0% respectively during a 24-h test period in the Summer. In the latter case, changes in modal frequencies are related to temperature differentials of more than 25°C across the bridge deck. Cross et al. (2013) analyses the effect of environmental and operational conditions on the first five modal frequencies of the Tamar suspension bridge during a three year period and reports a maximum change of 4.5% in the frequency of the first mode for a 20°C variation. Huh et al. (2005) perform experimental modal analysis on a pre-stressed concrete highway bridge with a yearly temperature variations of 40°C and report changes in frequency of 0.3 Hz, 0.35 Hz, and 0.5 Hz for the first three bending modes respectively. The tests were performed also under different incremental damage scenarios and the authors report changes in the first three bending modes

frequencies of 0.11 Hz, 0.11 Hz, and 0.02 Hz when the largest load (4800 KN) is applied at mid-span and note that these changes are smaller than those associated with temperature effects. Although the temperature effect on natural frequencies has been studied widely, few studies have investigated the effect of temperature on mode shapes. Xu and Wu (2007) perform the numerical analysis of a cable-stayed bridge and conclude that changes in the two mode shape curvatures of the bridge due to 10% reduction in stiffness of the girder are smaller than those caused by temperature gradients of 40°C. In addition, the results for the first ten natural frequencies subject to different distributions of temperature effects (40°C in cables, 35°C in towers, 30°C in girder, and 25°C in piers) show a maximum of 1.7% change in frequencies and demonstrate that the temperature effect is mostly associated with vertical mode shapes. Balmes et al. (2008) report that the frequencies for the first four modes of an intact beam are affected by temperature gradients of 20°C and that the effect is most significant at lower frequency modes, indicating a frequency change of 16%, 8%, 5%, and 3% respectively, whereas the variations of mode shapes for the damaged state of the beam (simulated by increasing the stiffness of a spring attached to the beam in its intact state in order to induce 1% deviations from the undamaged state) and under temperature effect are less than 1%. In theory, the latter can be explained by the fact that mode shapes are more resistant to temperature changes when it comes to an undamaged structure or an intact beam with regular cross-section, except if there are defects that already exist in the structure which can be affected by the effect of temperature. In actual structures, since higher mode shapes are difficult to identify and the level of uncertainty increases for these modes (Reynders 2012), only the first mode shape is considered for this study.

In general, an increase in ambient temperature affects the stiffness matrix of a structure and results in a decrease in natural frequencies. Note that changes in the damping ratio are not considered in this work since they are poor indicators of low levels of damage given that measured values exhibit much greater levels of variability as compared to frequencies and mode shapes (Farrar, Cornwell et al. 2000, Huth, Feltrin et al. 2005, Li, Li et al. 2010, Xia, Chen et al. 2012, Zhang, Bao et al. 2012). In order to discriminate between temperature and damage-related changes in modal properties, observations are required over a range of temperatures at known states of damage. Classical statistical methods can then be used to estimate a relation between temperature and frequencies (Xia, Chen et al. 2012). Sohn et al. (1999) use a linear regression models to predict the first two natural frequencies as a function of temperature for a concrete

bridge and reported a 5% change in frequencies over 24 hour time periods with temperature gradients of 28°C. The tests were conducted over a two day period. The data from the first day was used to train the adaptive filter while the data from the second day was used for prediction purposes. The maximum error for the validation data set was 3.95% for the predicted frequency as a function of temperature, which is of the same order as the temperature effect. Cury et al. (2012) use neural networks to predict temperature effects on the first three modal frequencies of a girder bridge. The results indicate that the proposed method is not quite efficient in filtering the effects of temperature and the comparison between corrected and non-corrected average natural frequencies. In addition, a comparison of natural frequencies before and after strengthening the bridge decks (six months monitoring in each state) shows only an increase of 0.1%. Neural networks usually require a larger training data set as compared to data requirements for regression models which make the latter more appropriate for typical structures. For both types of models, the data should be collected for the structure when there is no evolution in the state of structural damage.

Kerschen et al. (2005a, 2005b) use Principal Component Analysis (PCA) to analyse the first four natural frequencies of a concrete box girder bridge as a function of temperature and damage level (concrete spalling, settlement of pier, anchor failure, etc) over a one year period. The analysis is performed on the covariance matrix of measured frequencies and the PCA models are estimated for the reference (undamaged) state for varying environmental conditions. Assuming that the residual error of reconstruction of the input data remains small in the presence of no damage, significant increases in the latter are associated with damage. Hu et al. (2012) develop a damage detection novelty index based on the residual errors of the reconstructed data from natural frequencies identified at different times. PCA analysis is performed on the frequencies for the eight vertical bending modes of the Pedro e Inês footbridge using three years of continuous monitoring with temperature variations of 35°C. The results indicate that the maximum changes in the natural frequencies vary between 2.7-3.9% and the correlation analysis of the natural frequencies with temperature reveals that frequencies tend to decrease linearly with temperature. This damage detection technique is based on the comparison of principal components with those for the structure in an undamaged state. However, since the bridge was new, the approach could not be validated for damage detection. The authors also used a finite element model of the bridge and introduced damage by reducing spring constants at the supports

by 5% and 30%, which was detected by the change in the novelty index and validates the procedure.

In conclusion, the detection of damage through changes in the natural frequencies can easily get masked due to the influence of environmental conditions, especially for low levels of incremental damage. The techniques reviewed above are not always applicable since they require a large amount of observations on frequencies over a wide range of temperatures under steady state conditions to form the covariance matrix. In addition, the procedures are mainly addressing the variability in the measured frequencies and no formal test is proposed to determine if the changes that are observed in the residuals of the reconstructed data are statistically significant. Finally, the tests only address changes in natural frequencies and cannot be used for damage localization.

In the following section, the effect of temperature is investigated in relation to the detection of damage based on the use of wavelets on modal shapes. The wavelets offer a higher probability of damage detection than changes in frequencies, as well as a means of localizing damage (Shahsavari, Bastien et al. 2015, Shahsavari, Bastien et al. 2017). Very limited research has been performed on the effect of temperature on mode shapes. Mode shapes can be affected by temperature depending on the restraint conditions, the condition of expansion joints, and the presence of damage.

6-3 Methodology

This section summarizes the main features of the detection procedure used in this work (Shahsavari, Chouinard et al. 2017).

6-3-1 Continuous Wavelet Transform (CWT)

The Continuous Wavelet Transform (CWT) (Daubechies 1992) is a common signal processing tool which has been used initially for the analysis of time series but that can also be applied to any sequence of observations. In the case of damage detection, CWT has been applied to mode shapes in order to detect small anomalies that can be correlated to damage (Rucka and Wilde 2006, Spanos, Failla et al. 2006, Alvandi, Bastien et al. 2009, Solís, Algaba et al. 2013,

Montanari, Spagnoli et al. 2015). The CWT of a one-dimensional function f(x) (mode shape in this application) is defined as:

$$CWT(x) = \frac{1}{\sqrt{|s|}} \int_{-\infty}^{+\infty} f(x) \psi^* \left(\frac{x-u}{s} \right) dx \tag{6.1}$$

where ψ*(x) represents the complex conjugate of the wavelet mother function ψ(x), s and u denote the scale and the position parameters of the mother wavelet, and CWT(x) is defined as the wavelet coefficient in the vicinity of location x. The function ψ(x) is defined such that:

$$\int_{-\infty}^{+\infty} \psi(x)\, dx = 0 \tag{6.2}$$

$$\int_{-\infty}^{+\infty} |\psi(\omega)|^2 \frac{d\omega}{|\omega|} < \infty \tag{6.3}$$

where ψ(ω) is the Fourier transform of ψ(x). In this paper, the Symlet wavelet (Daubechies 1992) of scale 64 complies with the admissibility conditions to perform the wavelet analysis. Wavelets at large scales are appropriate to characterize the overall pattern of the mode shape while smaller scales may be too sensitive to noise present in the signal. For this study, after several trials and errors in selecting the best candidate, the Symlet wavelet of scale 64 was found a suitable option to analyze the given mode shape.

For a given mode shape, wavelet coefficients are calculated at each point/node corresponding to the locations of sensors installed along the length of the beam. One should note that high values of wavelet coefficients in the vicinity of the ends of the structure can occur due to discontinuity of the signal at both ends and may mask structural damage in those locations. In addition, since experimental mode shapes are not smooth perfectly, the latter may restrict meaningful extraction of wavelet scalograms. To minimize both effects, the mode shapes are extended and smoothed by cubic extrapolation (Strang and Nguyen 1996) and spline interpolation (De Boor 1978) prior to the wavelet analysis.

Wavelets have been used with success for damage detection in several applications (Rucka and Wilde 2006, Alvandi, Bastien et al. 2009, Wu and Wang 2011) but were found to be sensitive to

the presence of noise and varying environmental conditions for detecting low levels of incremental damage. The wavelet coefficients are displayed as a function of location along the mode shape and large values are used as indicators of local damage. The most common procedure is to select a threshold value on wavelet coefficients to identify locations of damage. This procedure is usually effective but also produces many false positives for the presence of damage. Optimal selection procedures for the threshold level have been proposed based on statistical tests and machine learning algorithms using training data sets from both damaged and undamaged states (Sohn, Dzwonczyk et al. 1999, Cury, Cremona et al. 2012).

In the event of no incremental damage and under constant environmental conditions, the wavelet coefficients at each node along the beam for a given mode shape are assumed to be random variables with a given probability distribution function. Descriptive statistics such as Box and Whisker plots can be used to describe location and dispersion parameters (e.g. mean value, standard deviation) of the wavelet distributions. A change in the mean value of the wavelets is attributed to the presence of an anomaly in the mode shape at the given location while a change in the standard deviation indicates variability from noise. Damage detection can be implemented through statistical tests on location parameters to determine objectively if the mean (or median) coefficients between two measurement sessions are different at a given significance level. For low levels of damage, damage detection can be compromised due to a low signal to noise ratio in the observations. In those cases, a Principal Component Analysis (PCA) is performed to reduce noise.

6-3-2 Principal Component Analysis (PCA)

The Principal Component Analysis (PCA) (Pearson 1901) is mostly used for noise reduction, data compression and the meaningful extraction of information in large data sets. The input data set of the PCA model contains the wavelet coefficients for the given mode shape. Each location/node corresponds to one variable (n in total) while observations (m in total) are comprised of the number of repeat measurements. In multivariate data analysis, the PCA of the centered data matrix [X] of dimensions m by n is defined as the eigenvalue decomposition of the sample covariance (or correlation matrix) using the Singular Value Decomposition (SVD) algorithm:

$$[X]=[U]\,[\Lambda]\,[V]^T \tag{6.4}$$

where [U] is an orthogonal m×m matrix, $[\Lambda]$is an m×n diagonal matrix containing eigenvalues of the covariance matrix $[X]^T[X]$ sorted in a descending order, and [V] is an orthogonal n×n matrix respectively. In terms of this factorization, the eigenvalue decomposition of the covariance matrix is defined as:

$$[X]^T[X]=\left([V]\,[\Lambda]\,[U]^T\right)\left([U]\,[\Lambda]\,[V]^T\right) \tag{6.5}$$

$$[X]^T[X]=[V]\,[\Lambda]^2[V]^T \tag{6.6}$$

The columns of matrix [V] are the corresponding eigenvectors or Principal Components (PCs) of $[X]^T[X]$. In PCA, the amount of variance for each eigenvector (or PC) is measured by its corresponding eignevalue. In consequence, the explained variance of the i^{th} principal component is expressed by dividing the corresponding eigenvalue (λ_i) of the given component to the sum of eigenvalues:

$$\eta=100\%\cdot\left(\lambda_i \Big/ \sum_{i=1}^{n}\lambda_i\right) \tag{6.7}$$

The score matrix [S] is obtained by linear transformation of the original data matrix into the new subspace of q≤ n variables as a new variable for damage detection:

$$[S]=[X]\,[V] \tag{6.8}$$

where q represents the number of principal components. Finally, [S] is an m×q matrix where m returns the number of observations in [X]. This transformation is defined in such a way that the first PC accounts for highest variance possible in the data, and each succeeding component in turn contains the variables with the largest variance under the constraint that it is orthogonal to the preceding components. Therefore, the first few components reach a higher signal to noise ratio since noise between variables is uncorrelated.

6-3-3 Likelihood Ratio (LR) Test

Assuming that the scores associated with the first principal component are highly correlated with damage, a damage localization procedure has been proposed using a modified Likelihood Ratio (LR) test (Kendall and Stuart 1979). For a given data set that comprises two sets of observations for an increasing level of damage, the LR test compares the likelihood of the scores for the reference or full model with the likelihood of the scores for the alternative model by removing sequentially one of the nodes. Removing one of the nodes is equivalent to removing one instrument from the monitoring network. The node that is the closest to the damaged area has the most influence on the likelihood function. For two groups of observations (undamaged, damaged) with random variables, the LR test is performed relative to the scores measured in the damaged state. The scores associated with the reference model {SR} are computed using Eq. 6.8:

$$S_R = \{[X]_{m\times n} \,.\, [V]^{pc}_{n\times 1}\} \qquad ; m = N_1 + N_2 \tag{6.9}$$

where [X] represents the original wavelet coefficients matrix, m and n are the total number of observations and variables in [X], pc denotes the number of selected eigenvector {V} or principal component. N_1 and N_2 are the sample sizes for the undamaged and damaged states respectively. Assuming that principal components are not affected significantly by removing one node, the scores for the alternative model {Si} are generated by multiplying the matrix of observation [X] by the set of eigenvectors {V} where the components for the current node is set to zero (as one node/sensor is removed). The repetition of this procedure for each node, results in a sequence of n models from which $[S_{ALT}]$ is derived:

$$S_i = \{\, [X]_{m\times n} \,.\, [V]^{pc}_{n\times 1} \,|\, V(i) = 0\}_{m\times 1} \qquad ;\; i = 1\,,\, 2\,,\, 3\,,\, ...\,,\, n \tag{6.10}$$

$$S_{ALT} = [\{S_1\} \quad \{S_2\} \quad ... \quad \{S_n\}]_{m\times n} \tag{6.11}$$

Lastly, the mean (μ) and standard deviation (σ) for both models are obtained accordingly to compute the Likelihood Ratio (LR) at each location x_i along the length of the beam.

$$LR(x_i) = \frac{L(S_R \mid \mu_R, \sigma_R)}{L(S_i \mid \mu_i, \sigma_i)} \qquad ;(i = 1,\ 2,\ 3,....,\ n) \tag{6.12}$$

with,

$$L(S_R \mid \mu_R, \sigma_R) = \sum_{j=N_1+1}^{m} \left(2\pi\sigma_R^2\right)^{-\frac{1}{2}}\ e^{\frac{-(S_R(j)-\mu_R)^2}{2\sigma_R^2}} \tag{6.13}$$

$$L(S_i \mid \mu_i, \sigma_i) = \left\{ \sum_{j=N_1+1}^{m} \left(2\pi\sigma_i^2\right)^{-\frac{1}{2}}\ e^{\frac{-(S_i(j)-\mu_i)^2}{2\sigma_i^2}} \right\}_i \qquad ;(i = 1,\ 2,\ 3,....,\ n) \tag{6.14}$$

where subscripts R and i are used to indicate the reference and alternative (leave-a-node-out) models, N is the sample size for each model, n is the number of variables or pseudo-sensors along the beam, μ and σ are the parameters of the normal distribution.

The result of the LR test is shown as a function of node position and since the model with the removed node close to the damage location is expected to be least informative (or likely) in comparison to the full model, the LR reaches its maximum value at this location. In field applications, the results of the LR test could be less reliable due to temperature effects. Therefore, statistical investigations to correct for the effect of the temperature are important for a robust damage detection decision rule.

6-4 Experimental Setup and Protocol

An experimental bolted-beam of length L = 3m and uniform cross section (W150×37) is used for this study in an environmentally-controlled room. The beam comprises three assembled sections where damage can be simulated by adding or removing sets of plates and bolts (Figure 6-1). The damage locations are fully assembled and bolted for the reference or initial state. A novelty of this work is the versatile design of the test setup which allows various conditions by removing/stiffening bolts at the damage locations and by changing support conditions. The first or initial state of damage (known as state E0 in this paper) corresponds to the beam in its fully bolted configuration at each joint. The incremental level of damage (state E1) is induced by removing a set of bolts and plates at the two damage locations (Figure 6-2).

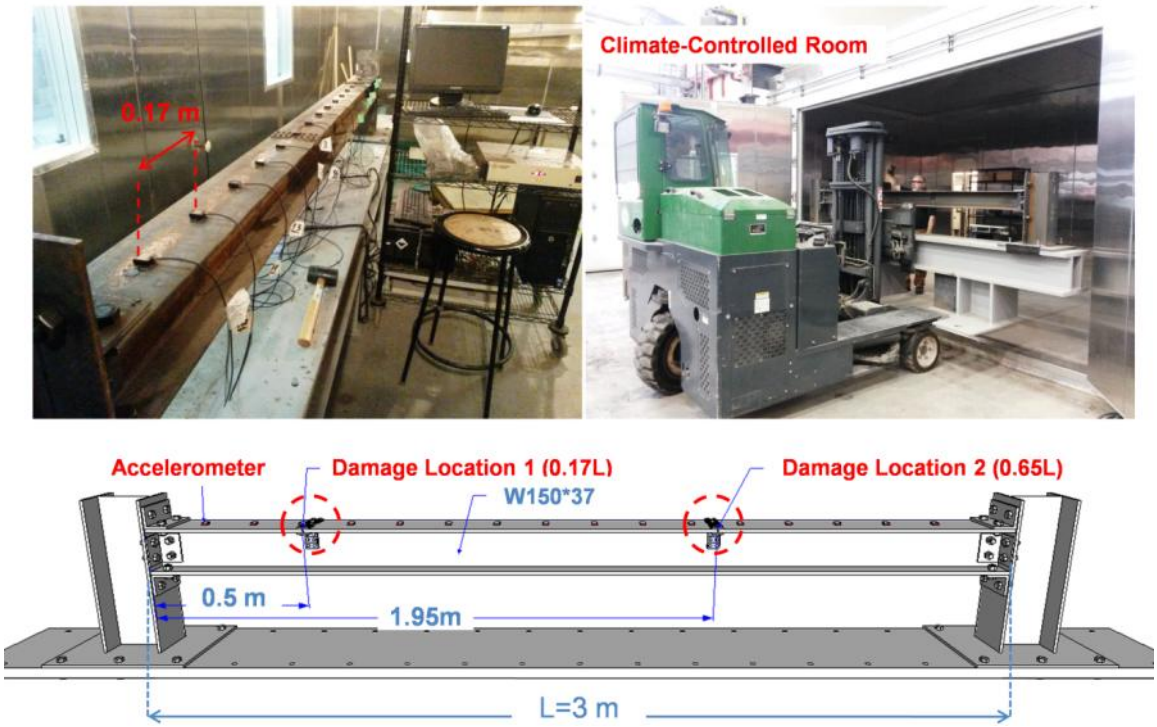

Figure 6-1: Experimental test setup in a climate-controlled room.

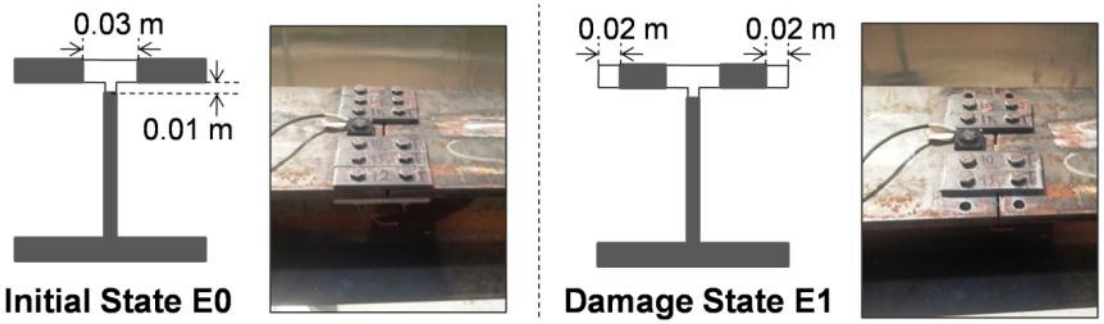

Figure 6-2: Damage-induced modifications in the beam at the initial state E0 and the damage state E1.

The reduction of rigidity corresponds to an equivalent crack of 4% (state E0) and 10% (state E1) of the cross-section for an equivalent rectangular section. Each set of vibration measurements are repeated 25 times under random excitations using sixteen sensors equally spaced along the length of the beam. This large number of sensors improves the signal to noise ratio and the estimation of the wavelet coefficients.

The measurements are performed in an environmentally-controlled room at two reference temperatures (5°C and 25°C) and the two damage levels (E0 and E1). The experimental protocol is defined as follows:

- Setup 1: Damage state E0 at 5°C.
- Setup 2: Damage state E0 at 25°C.
- Setup 3: Damage state E1 at 5°C.
- Setup 4: Damage state E1 at 25°C.

Table 6-1 describes the parameters for each experimental setup. The setups are used to evaluate: 1) the effect of temperature, 2) the effect of incremental damage, and 3) the combined effect of damage and temperature.

Table 6-1: Parameters for test setups for the experimental program.

Data	Damage Level (E)	I/Io	Stiffness Reduction (%)	Damage Locations	Equivalent Crack Height (m)	Measurements #	Temperature (°C)
Setup1	E0	0.88	12	0.17L and 0.65L	0.04 h	25	5
Setup2	E0	0.88	12	0.17L and 0.65L	0.04 h	25	25
Setup3	E1	0.72	28	0.17L and 0.65L	0.10 h	25	5
Setup4	E1	0.72	28	0.17L and 0.65L	0.10 h	25	25

Io= Moment of Inertia for an intact section.

6-5 Correction of Wavelet Coefficients for Thermal Effects

In this work, the wavelet coefficients obtained at locations along the beam for the first mode shape are used to perform a Principal Component Analysis (PCA) (Shahsavari, Bastien et al. 2015, Shahsavari, Chouinard et al. 2017). Table 6-2 presents the percentage of explained variance computed by the PCA analysis of the wavelet coefficients for various combinations of experimental as a function of temperature and damage level. The four setups represent all possible outcomes for two consecutive surveys on the beam. Previous work with the wavelets was limited to the detection of damage between states at constant temperatures (i.e. setups 1 and 3). In all cases, the first Principal Component (PC) explains most of the variance observed in the wavelet coefficients. The percentage of variance explained by the first component varies as a function of the state of the beam. Since temperature and damage effects tend to increase

anomalies present in the first mode shape, the highest percentage of variance explained corresponds to the case when a damage increment is combined with an increase in temperature while the lowest percentage is when a damage increment is combined with a decrease in temperature.

Table 6-2: The percentage of explained variance (%) for the first four Principal Components (PCs) at different experimental conditions.

Group	Experimental Conditions	Data Sets	PC1	PC2	PC3	PC4
A	Temperature Effect	Set1 (E0 at 5°C) - Set2 (E0 at 25°C)	57%	12%	9%	6%
	Temperature Effect	Set3 (E1 at 5°C) - Set4 (E1 at 25°C)	73%	12%	7%	2%
B	Damage Effect	Set1 (E0 at 5°C) - Set3 (E1 at 5°C)	72%	13%	4%	4%
	Damage Effect	Set2 (E0 at 25°C) - Set4 (E1 at 25°C)	78%	8%	6%	4%
C	Damage and Temperature Effect	Set1 (E0 at 5°C) - Set4 (E1 at 25°C)	85%	6%	3%	2%
	Damage and Temperature Effect	Set2 (E0 at 25°C) - Set3 (E1 at 5°C)	50%	23%	11%	6%

Figure 6-3a illustrates the first principal component corresponding to an increase of temperature from 5^{o}C to 25^{o}C in the state E0 to the one for an increment of damage from the state E0 to E1 at constant temperature (5^{o}C) and indicates that the temperature effect does not produce a significantly different first component compared to incremental damage. Note that the dashed lines correspond to the two locations of defects along the beam. The principal components by themselves are not very informative as to the locations of damage. However, the values are larger for the damage location near the center of the beam (0.65L), which is attributed to a higher signal to noise ratio at this location. Figure 6-3b shows the effect of temperature (from 5^{o}C to 25^{o}C) in the state E1 compared to the effect of incremental damage at constant temperature (25^{o}C). Again, the effects of temperature and incremental damage on the principal component appear similar. Figure 6-3c and Figure 6-3d compare the first principal components for the combined effects of temperature and incremental damage to an increment of damage at constant temperature (5^{o}C and 25^{o}C respectively). Again, the results indicate that the first principal component provides similar patterns for the temperature and damage effects. Previous studies performed at constant temperature indicate that changes in the scores of the first component are good indicators of incremental damage.

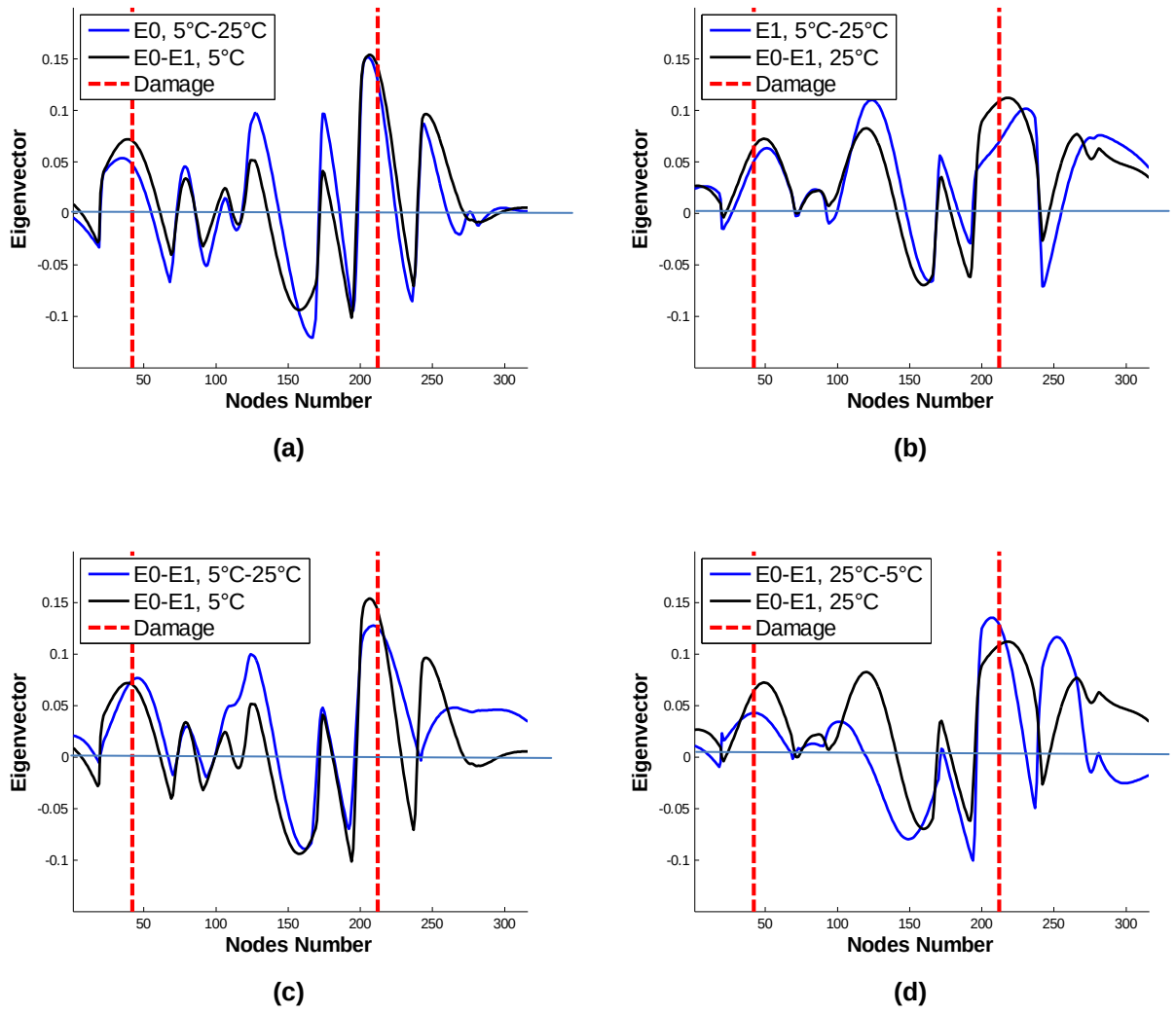

Figure 6-3: The first principal component corresponding to: a) the effect of temperature increasing from 5°C to 25°C in state E0 and the effect of damage evolving from states E0 to E1 at 5°C, b) the effect of temperature increasing from 5°C to 25°C in state E1 and the effect of damage evolving from states E0 to E1 at 25°C, c) the combined effects of temperature and incremental damage from state E0 at 5°C to state E1 at 25°C and the effect of damage evolving from states E0 to E1 at 5°C, d) the combined effects of temperature and incremental damage from state E0 at 25°C to state E1 at 5°C and the effect of damage evolving from states E0 to E1 at 25°C.

The first set of results compares surveys performed at different temperatures first for the damage level E0 and second for the damage level E1 (Figure 6-4a and Figure 6-5a). In both cases, the tests are performed at 5°C and 25°C and show statistically significant changes in the scores

between the two temperatures when there is no incremental damage. In the case of a beam with a regular cross-section, changes in temperature affect the natural frequency but should not modify significantly the mode shapes, and in consequence the wavelet coefficients.

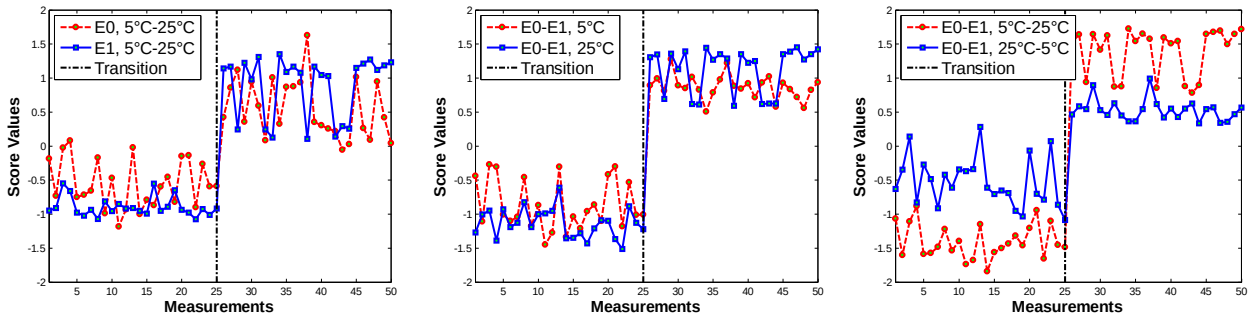

Figure 6-4: a) Scores for the temperature effect (5°C to 25°C) for damage levels E0 (red) and E1 (blue), b) Scores for incremental damage (E0 to E1) at constant temperature (5°C in red, 25°C in blue), c) Scores as a function of both temperature and incremental damage (E0 at 5°C to E1 at 25°C in red, E1 at 25°C to E1 at 5°C in blue).

In the presence of discontinuities, such as in the case of the experimental beam, due to presence of the bolt and plate assemblies at two locations, mode shapes (and wavelet coefficients) are affected by changes in temperature. In this case, the anomalies in the mode shapes at the location of the assemblies are amplified with an increase in temperature and are greater for the damage level E1. This increase in the scores could be wrongly interpreted as incremental damage if the latter are not corrected properly for the reversible temperature effect. In addition, this correction appears to be dependent on the current state of the beam.

The Likelihood Ratio (LR) (Figure 6-6a) correctly identifies the locations of the defects that account for the increase in the second set of scores, which correspond to the location of the bolt and plate assemblies indicated by a red dashed line. The two locations of damage are located simultaneously with a higher likelihood at 0.65L. This can be attributed to the higher signal to noise ratio near the center of the beam.

The second set of results compares surveys performed at constant temperature in the presence of incremental damage (first for the state E0 and second for the state E1). Figure 6-4b and Figure 6-5b show a statistically significant increase in the scores due to incremental damage which is

similar in magnitude to the temperature effect. The Likelihood Ratio (LR) correctly identifies the locations of the defects that account for the increase in the second set of scores, which correspond to the location of incremental damage (Figure 6-6b).

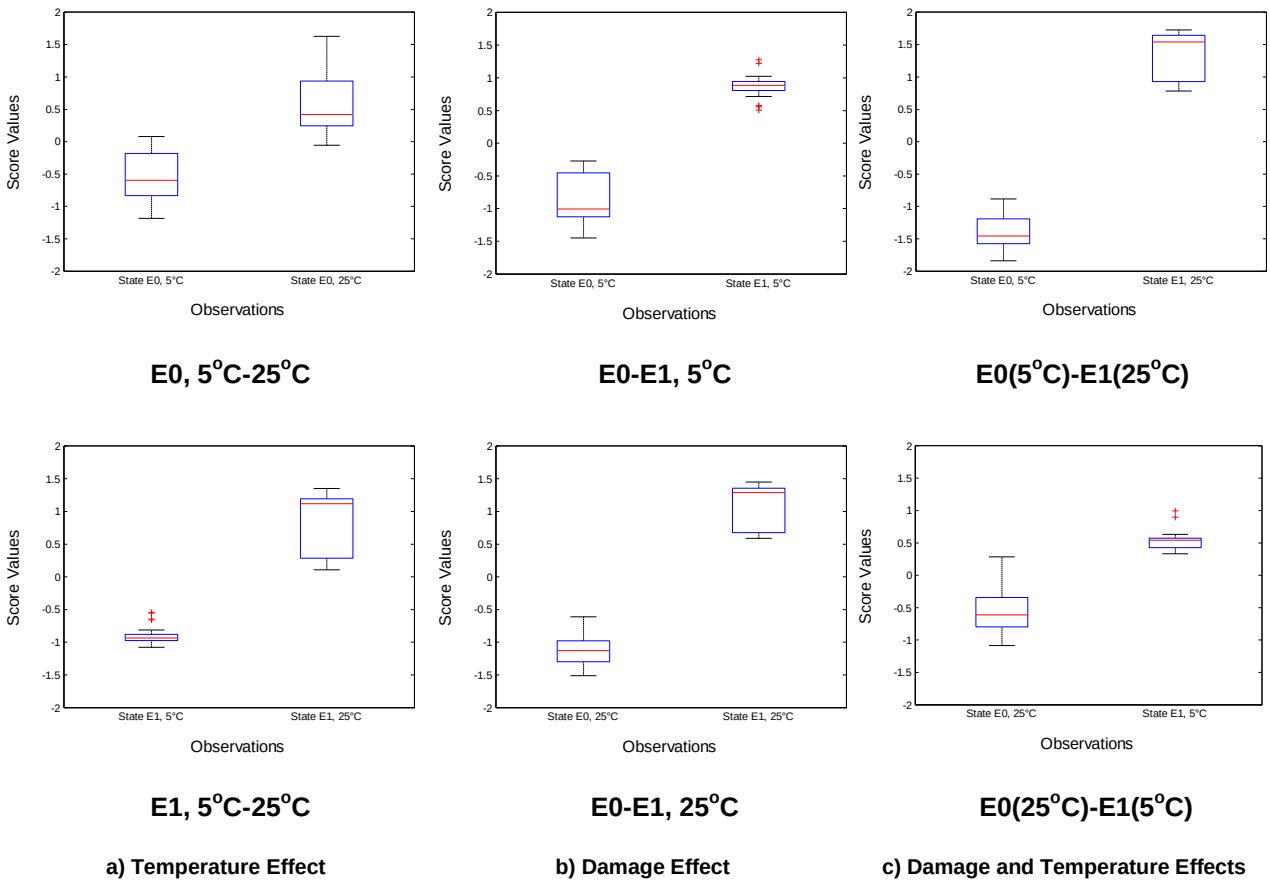

Figure 6-5: Box-Whisker plot for comparing the location parameters in the distribution of scores.

The final set of results compares the combined effects of temperature and incremental damage (Figure 6-4c and Figure 6-5c). The first case corresponds to an increase in both temperature and damage level, while the second case corresponds to an increase in damage level combined to a decrease in temperature. In the first case, both temperature and incremental damage contribute to an increase in the scores between the two surveys which amplifies the differences between the two distributions. The Likelihood Ratio (LR) correctly identifies the locations of the two locations of incremental damage (Figure 6-6c). For the second case, the decrease in temperature has an opposite effect on the scores as compared to incremental damage. The combination of the

two effects is to decrease the difference between the two distributions and the probability of detection of incremental damage. A similar effect is noted for the likelihood ratio which fails to detect with high certainty the location of damage at 0.17L.

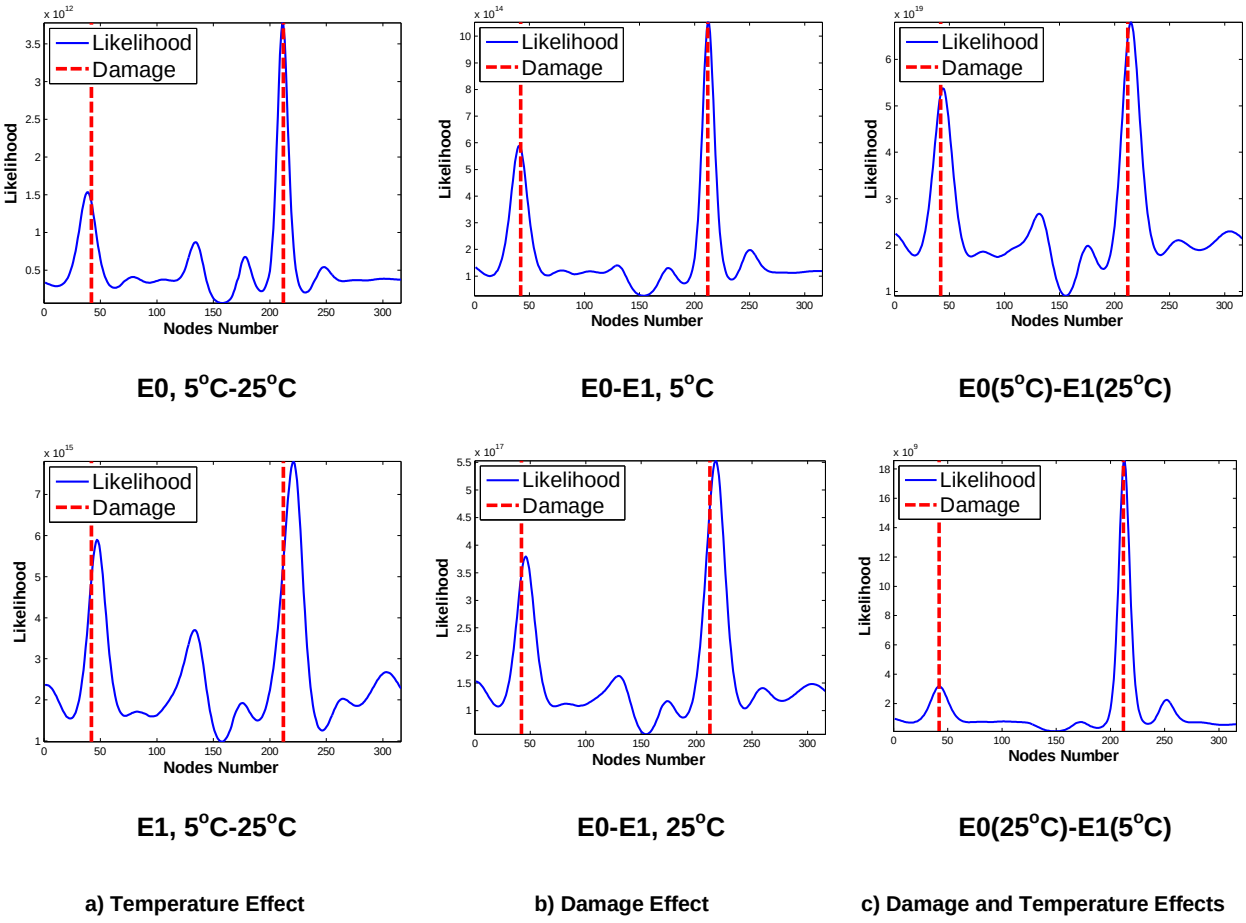

Figure 6-6: Likelihood Ratio (LR) test applied to the scores of the first component for the localization of damage locations.

Effects associated with temperature are assumed to be perfectly reversible while those associated with damage are irreversible, which can be used to estimate a correction factor for temperature given that data is collected for the initial state of damage over a range of temperatures. In order to estimate the temperature correction, it is required that scores are computed in relation to the same principal component that accounts for both temperature effects and incremental damage. A comparison of wavelet scores for the 4 setups shows similarity (Figure 6-7), which justifies performing the PCA for the entire set of observations.

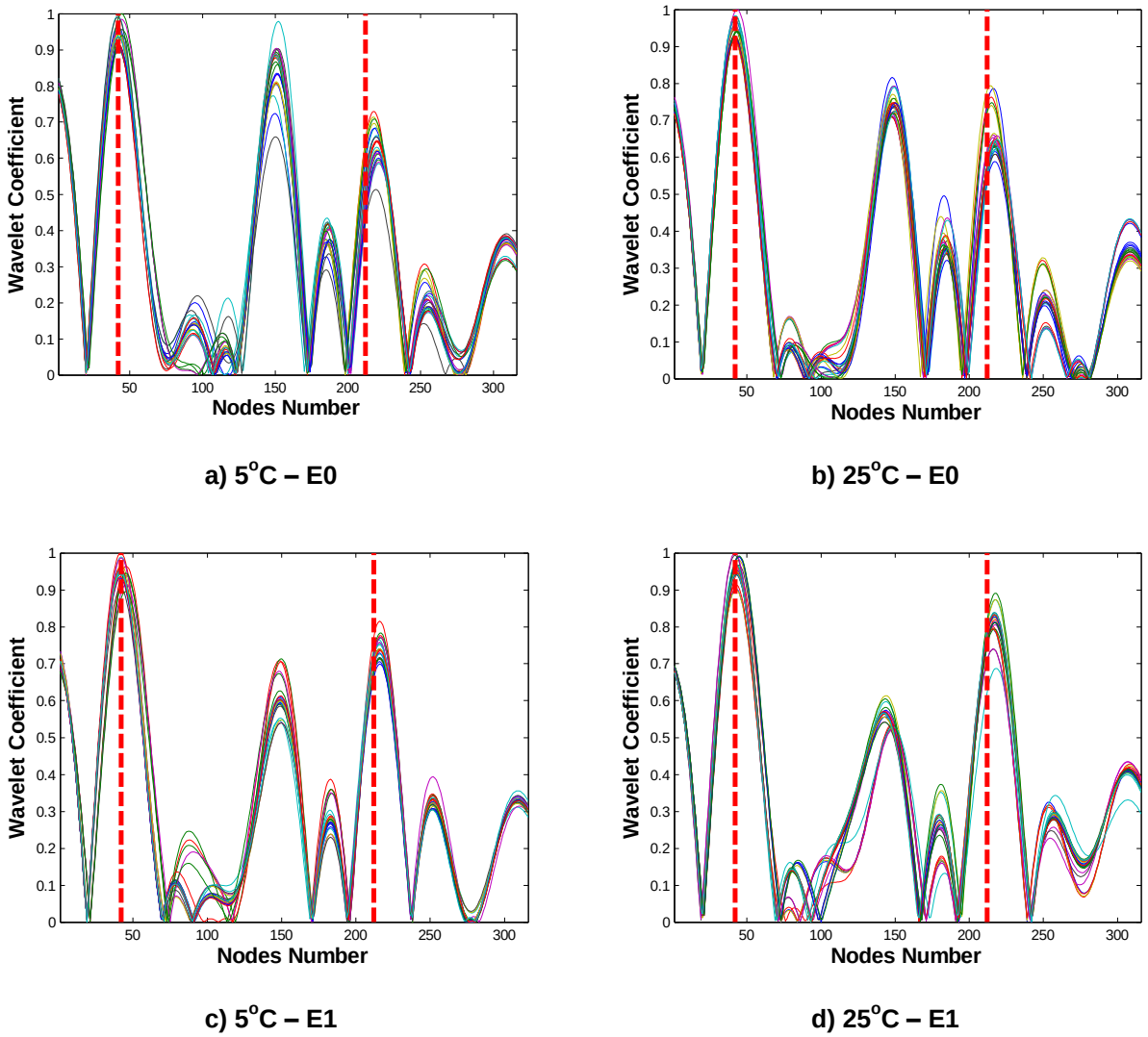

Figure 6-7: Wavelet coefficients for the first mode shape and for each of the first four setups.

The similarity between setups may partly be due to the fact that the damage locations are the same in all cases and this may not be true if incremental damage occurs at a previously undamaged location. The corresponding PCA scores associated with the first principal component for the combined data set are shown in Figure 6-8 for each setup. Table 6-3 summarizes the characteristics of the scores for each setup and indicates significant differences associated with changes in temperature and damage level.

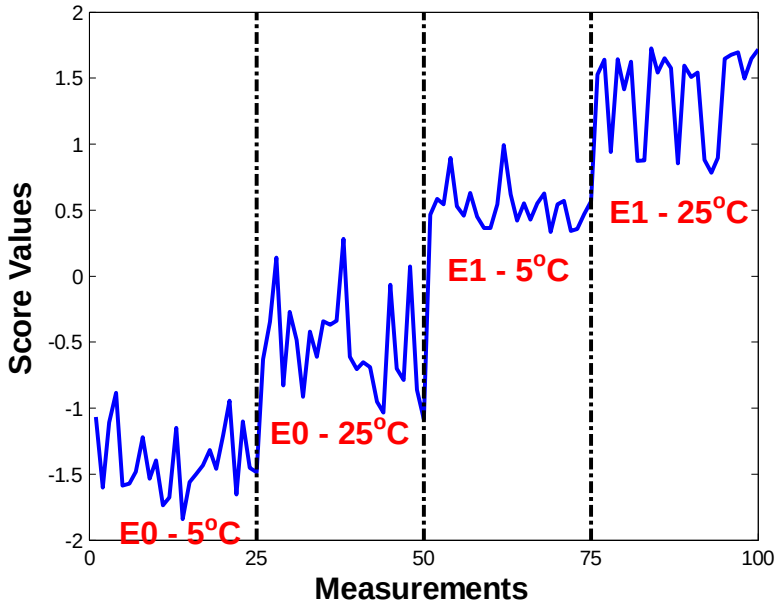

Figure 6-8: Corresponding scores for each setup indicating significant differences in the average scores due to changes in temperature and damage level.

Table 6-3: Average scores and standard deviation for each setup.

Setup		Scores	
Temperature	Damage Level	Average	Standard Deviation
5°C	E0	-1.40	0.25
25°C	E0	-0.53	0.36
5°C	E1	0.53	0.16
25°C	E1	1.40	0.34

The correction for temperature is obtained from measurements at the two reference temperatures (5^oC and 25^oC) for the initial state of damage. In the latter, the difference in scores for a temperature increase of 20^oC is on average equal to 1.12. It should be noted that damage detection is not affected significantly in this case due to temperature effects since the effect of damage and temperature both contribute to an increase in scores. For example, given that there is no incremental damage for the two cycles of inspections (E0 at 5^oC and E0 at 25^oC), damage would be detected at the next inspection cycle if incremental damage occurred (E1 at 5^oC) given that the scores did not return to their original level. The relevance of the temperature correction is primarily to relate changes in scores to the degree of damage at the same reference temperature

(Shahsavari, Chouinard et al. 2017). In this instance, if the results of the surveys correspond to setups 1-4, the difference in scores is attributed to both an increase in temperature and incremental damage. The average difference in scores between the two surveys is amplified and is equal to 2.80. Hence, the corrected difference in average scores due to incremental damage is obtained by subtracting the effect of temperature for the initial state of damage (2.80 - 1.12 = 1.68). The likelihood test corresponding to adjusted scores compared to the one computed before correcting for the scores (Figure 6-9) indicates that the proposed procedure has been efficient to minimize false alarms due to temperature effect and to correct for the reversible effect of the temperature. In the latter, the magnitude of maximum likelihood value shown in Figure 6-9b corresponds well to the one for the incremental damage effect at constant temperature (5^{o}C) (Figure 6-6b).

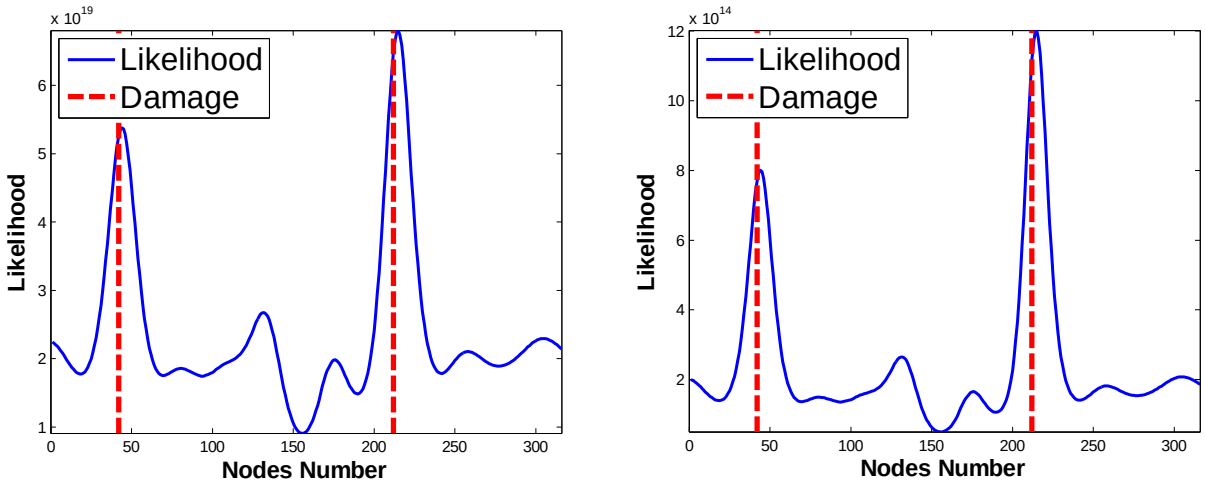

a) E0(5^{o}C)-E1(25^{o}C), before correction **b) E0(5^{o}C)-E1(25^{o}C), after correction**

Figure 6-9: Likelihood test result before (a) and after (b) correction for increasing effect of temperature.

Similarly, if the results of the surveys correspond to setups 2-3, the difference in scores is attributed to a decrease in temperature and incremental damage and is smaller since temperature and incremental damage have opposite effects on scores. The change in scores due to incremental damage is then obtained by taking the difference in the average scores obtained from the survey (1.06) and adding the effect of the difference in temperatures for the initial state of damage to the difference in scores from the surveys (1.06 + 1.12 = 2.18). Figure 6-10 illustrates

the result of the likelihood test for the scores computed before and after correction for the temperature effect indicating that the correction procedure has been able to identify more clearly damage location at 0.17L and to compensate the reversible effect of temperature for damage detection. In the latter, the magnitude of maximum likelihood value shown in Figure 6-10b is in good agreement with the one observed for the incremental damage effect at constant temperature (25^{o}C) (Figure 6-6b).

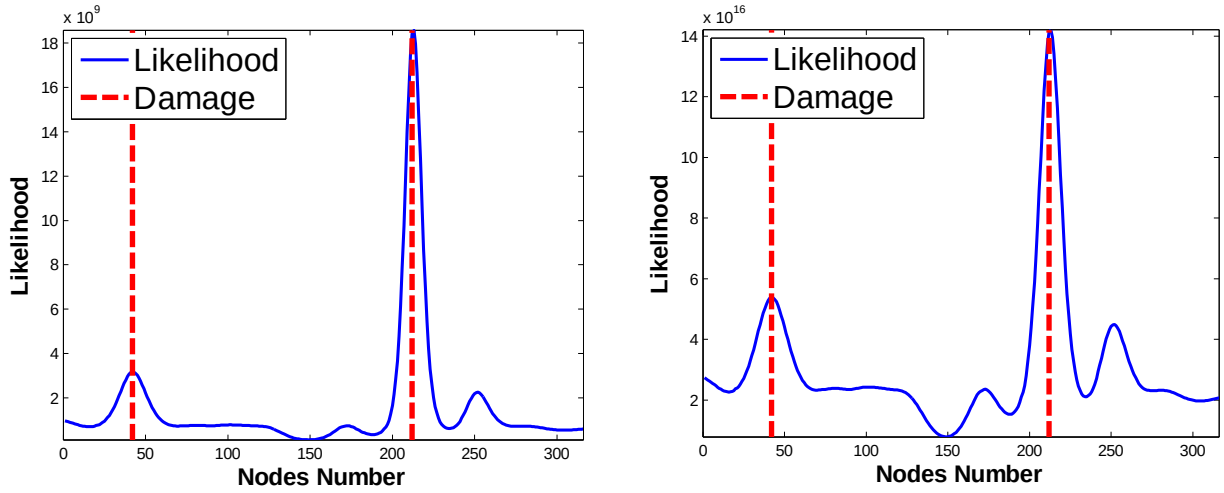

a) E0(25^{o}C)-E1(5^{o}C), before correction **b) E0(25^{o}C)-E1(5^{o}C), after correction**

Figure 6-10: Likelihood test result before (a) and after (b) correction for decreasing effect of temperature.

The results indicate that mode shapes can also be affected by temperature effects, but this effect can be corrected since the effects of temperature and damage are both additive in terms of the scores obtained from the analysis with wavelets. For other temperature differentials, a linear interpolation or extrapolation procedure can be used for the correction. Since the temperature effect is important, the correction for temperature should be established by making measurements at different temperatures in the early life of a structure before some damage is either introduced or increased. If records are kept and measurements are done at regular intervals, it may be possible to establish a trend. In addition, since temperature effects are reversible, the distribution of scores should remain the same after each temperature cycle.

6-6 Conclusions

This paper describes a novel data-driven methodology to estimate undesired effect of temperature variations for detecting small levels of damage which is usually challenging given the high noise to signal ratio. An experimental program was performed on a beam under temperature changes uniformly distributed in a climate-controlled room. Experimental conditions were divided in three main groups to study 1) the effect of temperature, 2) the effect of incremental damage and 3) the combined effects of both factors. Wavelet coefficients derived from the first mode of vibration of the beam were used for the statistical model in this work. Damage detection was followed by the application of a Principal Component Analysis (PCA) on wavelet coefficients to determine statistically the components that contribute most strongly to the overall variance of the coefficients and to minimize the effect of noise. Given that the first Principal Component (PC) accounts for highest variance possible in the data, the localization procedure was performed only for this component using the proposed Likelihood Ratio (LR) test to determine most likely locations of damage along the beam.

Assuming a reversible effect of temperature on distribution of scores, statistical investigations were further performed to account for the effect of temperature on the scores. The correction for temperature effect was performed by setting a mathematical solution to discriminate between the effects of temperature and incremental damage in the distribution of scores. The Likelihood Ratio (LR) test was then repeated for the adjusted scores and compared with those computed before the correction. Finally, results indicate that the proposed procedure is efficient to correct for reversible temperature effects, which is important in the estimation of the degree of damage as a function of changes in scores. In this study, the correction algorithm is based on experimental evaluations performed for only two reference temperatures and for two states of damage. However, previous experiments indicate that scores are linearly related to damage level and to temperature and the procedure should be applicable to a wide range of conditions. In addition, the correction algorithm relies only on adjusting the corresponding scores for the first principal component. Further investigations are still required to optimize the solution and to advance the likelihood result under combined effects of the temperature and damage.

Acknowledgement

This study is supported through a CREATE grant from the Natural Sciences and Engineering Research Council of Canada (NSERC) and the CRIB Research Center (Université Laval).

6-7 Nomenclatures

r	Mode shape number (subscript)
ω_r	Natural frequency of the r^{th} mode
u	Undamaged (subscript)
d	Damaged (subscript)
$f(x)$	Space-domain function
x	Spatial coordinate
$\Psi(x)$	Wavelet function
$\Psi(\omega)$	Fourier Transform of $\Psi(x)$
u	Wavelet function position parameter
s	Wavelet function scale parameter
CWT(x)	Wavelet coefficient at location x
m	Number of observations
n	Number of variables/nodes
[X]	Wavelet coefficients matrix
[U]	Left-singular values of [X]
[Λ]	Singular-values of [X]
[V]	Right-singular values of [X]
[C]	Covariance matrix of [X]
PC_i	i^{th} principal component
λ_i	i^{th} eigenvalue
η_i	Percentage of variance for the i^{th} PC
[S]	Score matrix
$[S_1]$	Scores for the 1st set of measurements
$[S_2]$	Scores for the 2nd set of measurements
pc	Selected component (subscript)
$\{V\}_{pc}$	Selected eigenvector or PC
$\{S\}_{pc}$	Score vector for the selected component
$\{S_R\}$	Scores for the reference model
$\{S_i\}$	Scores for the alternative model

$LR(x_i)$	Likelihood Ratio at i^{th} location
$L(S_R \mid \mu, \sigma)$	Likelihood of reference scores
$L(S_i \mid \mu_i, \sigma_i)_i$	Likelihood of alternative scores at i^{th} node
μ	Population mean
σ	Standard deviation

6-8 References

Alvandi, A., J. Bastien, E. Gregoire and M. Jolin (2009). "Bridge integrity assessment by continuous wavelet transforms." International Journal of Structural Stability and Dynamics 9(1): 11-43.

Balmes, É., M. Basseville, F. Bourquin, L. Mevel, H. Nasser and F. Treyssede (2008). "Merging sensor data from multiple temperature scenarios for vibration monitoring of civil structures." Journal of Structural Health Monitoring 7(2): 129-142.

Cornwell, P., C. R. Farrar, S. W. Doebling and H. Sohn (1999). "Environmental variability of modal properties." Journal of Experimental Techniques 23(6): 45-48.

Cross, E., K. Koo, J. Brownjohn and K. Worden (2013). "Long-term monitoring and data analysis of the Tamar Bridge." Journal of Mechanical Systems and Signal Processing 35(1): 16-34.

Cury, A., C. Cremona and J. Dumoulin (2012). "Long-term monitoring of a PSC box girder bridge: Operational modal analysis, data normalization and structural modification assessment." Journal of Mechanical Systems and Signal Processing 33: 13-37.

Daubechies, I. (1992). "Ten lectures on wavelets," Society for Industrial and Applied Mathematics.

De Boor, C. (1978). "A practical guide to splines," Springer-Verlag New York.

Farrar, C. R., P. J. Cornwell, S. W. Doebling and M. B. Prime (2000). "Structural health monitoring studies of the Alamosa Canyon and I-40 bridges." Los Alamos National Laboratory, Los Alamos, NM, Technical Report LA-13635-MS.

Hu, W.-H., C. Moutinho, E. Caetano, F. Magalhães and Á. Cunha (2012). "Continuous dynamic monitoring of a lively footbridge for serviceability assessment and damage detection." Journal of Mechanical Systems and Signal Processing 33: 38-55.

Huth, O., G. Feltrin, J. Maeck, N. Kilic and M. Motavalli (2005). "Damage identification using modal data: Experiences on a prestressed concrete bridge." Journal of Structural Engineering 131(12): 1898-1910.

Kendall, M. and A. Stuart (1979). "The advanced theory of statistics. Statistical Inference and Relationship." London, Charles Griffin.

Li, H., S. Li, J. Ou and H. Li (2010). "Modal identification of bridges under varying environmental conditions: temperature and wind effects." Journal of Structural Control and Health Monitoring 17(5): 495-512.

Montanari, L., A. Spagnoli, B. Basu and B. Broderick (2015). "On the effect of spatial sampling in damage detection of cracked beams by continuous wavelet transform." Journal of Sound and Vibration 345: 233-249.

Mosavi, A. A., R. Seracino and S. Rizkalla (2012). "Effect of temperature on daily modal variability of a steel-concrete composite bridge." Journal of Bridge Engineering 17(6): 979-983.

Pearson, K. (1901). "LIII. On lines and planes of closest fit to systems of points in space." Journal of Philosophical Magazine Series 6 2(11): 559-572.

Reynders, E. (2012). "System identification methods for (operational) modal analysis: review and comparison." Archives of Computational Methods in Engineering 19(1): 51-124.

Rucka, M. and K. Wilde (2006). "Application of continuous wavelet transform in vibration based damage detection method for beams and plates." Journal of Sound and Vibration 297(3): 536-550.

Shahsavari, V., J. Bastien, L. Chouinard and A. Clément (2015). "A Novel Response-Based Approach to Localize Low Intensity Damage of Beam-Like Structures." Proc. of the 5th International Conference on Smart Materials and Nanotechnology in Engineering Vancouver, BC, Canada: 99-109.

Shahsavari, V., J. Bastien, L. Chouinard and A. Clémen (2017). " Likelihood-Based Testing of Wavelet Coefficients for Damage Detection in Beam Structures." Journal of Civil Structural Health Monitoring, 7(1), 79-98.

Shahsavari, V., L. Chouinard and J. Bastien (2017). "Wavelet-based analysis of mode shapes for statistical detection and localization of damage in beams using likelihood ratio test." Journal of Engineering Structures 132: 494-507.

Sohn, H., M. Dzwonczyk, E. G. Straser, A. S. Kiremidjian, K. H. Law and T. Meng (1999). "An experimental study of temperature effect on modal parameters of the Alamosa Canyon Bridge." Journal of Earthquake Engineering & Structural Dynamics 28(8): 879-897.

Solís, M., M. Algaba and P. Galvín (2013). "Continuous wavelet analysis of mode shapes differences for damage detection." Journal of Mechanical Systems and Signal Processing 40(2): 645-666.

Spanos, P. D., G. Failla, A. Santini and M. Pappatico (2006). "Damage detection in Euler–Bernoulli beams via spatial wavelet analysis." Journal of Structural Control and Health Monitoring 13(1): 472-487.

Strang, G. and T. Nguyen (1996). "Wavelets and filter banks," Wellesley-Cambridge Press, Wellesley, USA

Wenzel, H. and D. Pichler (2005). "Ambient vibration monitoring," John Wiley & Sons.

Wu, N. and Q. Wang (2011). "Experimental studies on damage detection of beam structures with wavelet transform." International Journal of Engineering Science 49(3): 253-261.

Xia, Y., B. Chen, S. Weng, Y.-Q. Ni and Y.-L. Xu (2012). "Temperature effect on vibration properties of civil structures: a literature review and case studies." Journal of Civil Structural Health Monitoring 2(1): 29-46.

Xu, Z.-D. and Z. Wu (2007). "Simulation of the effect of temperature variation on damage detection in a long-span cable-stayed bridge." Journal of Structural Health Monitoring 6(3): 177-189.

Yan, A.-M., G. Kerschen, P. De Boe and J.-C. Golinval (2005). "Structural damage diagnosis under varying environmental conditions—part I: a linear analysis." Journal of Mechanical Systems and Signal Processing 19(4): 847-864.

Yan, A.-M., G. Kerschen, P. De Boe and J.-C. Golinval (2005). "Structural damage diagnosis under varying environmental conditions—part II: local PCA for non-linear cases." Journal of Mechanical Systems and Signal Processing 19(4): 865-880.

Zhang, D., Y. Bao, H. Li and J. Ou (2012). "Investigation of temperature effects on modal parameters of the China National Aquatics Center." Journal of Advances in Structural Engineering 15(7): 1139-1153.

CHAPTER 7

7. Conclusion and Future Work

7-1 Conclusion

The uncertainties associated with real field measurements coupled with the complicated and dynamic nature of structures under varying environmental conditions are the main obstacles that impose progress limitations in this field. The research project presented in this dissertation is introduced first under laboratory conditions to assess the sensitivity of the proposed approach prior to any further attempts for damage detection in an actual bridge. The main advantage of this approach, which discriminates it against other methods, is its ability to locate with high likelihood small patterns of incremental damage (e.g. 4% of the height for an equivalent rectangular cross-section) at multiple locations along a beam.

The principal objective in this study is to propose an automated and efficient damage detection methodology for early detection and localization of incremental damage in an instrumented beam before it reaches a critical state. To this end, the modal analysis is performed only for the first mode of vibration of the beam. The exclusive use of the fundamental mode is a key point of the contribution of this approach to extend its applicability to real bridges. A reason is that the uncertainty of higher modes, which are associated with large natural frequency values, increases due to larger measurement errors through modal analysis. One should note that the extraction of higher modes in large-scale structures is practically difficult and requires a huge amount of energy to vibrate the structure in a desired frequency bandwidth. In addition, the extraction of higher modes is costly since a large number of sensors must be integrated for an accurate estimation of these modes.

A repeated number of measurements are performed to account for the uncertainty and the variability in the experimental mode shapes obtained from sixteen accelerometers equally spaced along the beam. Wavelet analysis is used as a promising tool to detect slight changes in mode

shapes caused by damage. However, it is shown that the wavelet analysis alone is not sufficient to clearly detect and locate the initiation of incremental damage in the presence of noise. A sequence of statistical techniques are explored as a complement to the results of the wavelet analysis by substituting the wavelet coefficients with new features which explain most of the variability observed in the coefficients. A PCA is applied on a set of coefficients computed through the CWT. The PCA is used to filter out noise by discarding the scores corresponding to higher Principal Components (PCs). Instead, the scores associated with the first few components are retained for further investigations through statistical tests on location parameters. Classical hypothesis tests are implemented to determine objectively if the mean (or median) scores between two surveys are different considerably at a given significance level. It has been shown that the use of statistical techniques reduce significantly the risk of false detections when dealing with small increments of damage. Given the statistical detection of damage, a novel algorithm is proposed to detect the most likely location of damage using the concept behind the LR test.

The fourth chapter examines the efficiency of the proposed approach through a comprehensive comparative study for a beam with fixed-fixed end restraint conditions and illustrates how the current technique is advantageous over existing methods. The test object is an assembly of three I-beams joined together by bolted stiffeners. Five levels of incremental damage (ranging from 4% to 47% of equivalent crack height) are introduced by weakening the stiffness of the beam at each joint assembly. The localization procedure is performed in the steady-state conditions of the laboratory and is found very efficient to detect damage even for the smallest level of the damage in this case study.

In the fifth chapter, the sensitivity of the approach is tested for a beam with two end restraint conditions (fixed-fixed and pinned-pinned) to detect low levels of incremental damage corresponding to 4% and 10% of crack height for a rectangular section. This study is performed also in a controlled laboratory condition with two distinct locations of damage. It is found that the use of a same type of instruments (e.g. type of sensors, length of cables, etc) in the fixed beam may highly increase the percentage of the overall variance observed in the first three PCs, leading to a higher signal to noise ratio in the results. For both end conditions, the proposed approach identifies simultaneously the location of the incremental damage as well as the other existing discontinuity which is not increased in size.

Changes in environmental conditions, most notably the variations in air temperature, can induce changes in dynamic characteristics of structures, which can affect the detection of damage at high noise to signal ratio situations. The sixth chapter of this dissertation is devoted to the investigatation of the relative contribution of damage and temperature effects in the extracted mode shapes of the beam. The beam is subjected to temperature variations between 5 ^{o}C and 25 ^{o}C in a climate-controlled room. The incremental damage corresponds to an equivalent crack height of 4% and 10% of a rectangular cross-section, which is induced at two locations along the beam. In this case, unlike the previous chapters where an increment in the size of damage was implemented to one location at a time, the incremental damage occurred for both locations at the same time.

The results indicate that the temperature has a reversible effect on the distribution of scores and that the effect is larger when the damage level is higher. The experimental measurements are performed at two reference temperatures and the two damage levels. The comparison of the mean scores represents that an increase in both temperature and damage level can amplify the average difference of scores between two distributions, and consequently can improve the probability of the detection in the likelihood result. An opposite effect in the distribution of scores is noted when the temperature is decreased as compared to incremental damage. In the latter case, the likelihood test fails to detect clearly the location of damage at 0.17L. Assuming a reversible effect of temperature on distribution of scores, a correction factor is established from measurements at two reference temperatures for the initial state of damage. The latter is used to establish mathematically to discriminate between the effects of temperature and incremental damage in the scores. The likelihood test is then repeated for the adjusted scores and the results indicate that the proposed procedure is efficient to correct for reversible temperature effects.

In summary, the novelty of this work is outlined below:

- A sequence of statistical procedures are explored to improve the detection and localization of damaged-induced variations in the mode shapes with respect to current SHM techniques.

- A damage detection methodology is applied on a relatively large instrumented beam raising difficulties due to complicated features of large-scale specimens to deal with high noise to signal ratio at small levels of incremental damage.

- Issues related to the uncertainty and variability in the mode shapes are addressed by performing repeated measurements for each state of induced damage, which is not the case in most previous studies.

- A wavelet-based technique is performed as a means to highlight small irregularities and abnormal events in the mode shapes due to damage.

- Noise reduction and feature classification are achieved by performing a PCA of the wavelet coefficients.

- Parametric and non-parametric statistical tests are performed to assess significant changes in the selected features generated from PCA models.

- A novel likelihood approach relying on an adaptation of the LR test is proposed to detect most likely locations of damage along the beam.

- A mathematical solution is established to correct for reversible temperature effects on the likelihood results when dealing with the combined effects of temperature and damage evolution, while improving both consistency and detectability relative to the localization of damage.

7-2 Future Work

This methodology represents a response-based approach in which the information relative to the reference (or intact) state of the structure is not required. For aging structures where the baseline data for the undamaged state is not available, the method described in this study can be used as a useful tool for real-time monitoring of the given structure. The damage in this case is simulated

as a reduction of both the mass and stiffness of a bridge girder, though other measures can be considered. The sensor networks can be embedded separately in each girder of a bridge without interrupting or suspending the serviceability of the monitored structure. This exemplifies the possibility of the proposed methodology for long-term monitoring of a structure.

In recent years, the advances of SHM technologies in a variety of aspects, especially Wireless Sensor Networks (WSN), have emerged as a promising means for the remote monitoring of structures. If the sensors are kept in place and the measurements are performed at regular intervals of time, records can be used to establish a trend in terms of damage evolution. Since the evolution of damage is defined in relation to the moment of inertia of the cross-section around its neutral axis, the mean change of scores can be used as an inductive to the size of damage. In consequence, investigations can be used also to create a novel index to assess accurately the extent of damage. However, one may require a rich source of database to approximate as closely as possible the quantity of damage. Alternatively, a theoretical development of a numerical model well correlated with the structure to be analyzed can enhance, in a parallel manner, the efficiency of expectations. But, the difficulties associated with accurate simulations of complicated structures enforce the applicability of this technique to simple structures mostly.

A classical statistical test based on equality of the means can be performed to develop estimates for the probability of detection and the probability of false alarms. For a given significance level, the results obtained from statistical measurements can be used to derive the probability of detection either as a function of damage level or the mean difference of the scores between two states. Results can be drawn to indicate how a decrease in the significance level will decrease the power of the test for the probability of detection with the aim of reducing false alarms.

The extraction of mode shapes explained through this dissertation relies on random dynamic input excitations by an impact hammer. One should note that the implementation of impact testing methods to large-scale structures (e.g. long-span bridges) is a difficult task and causes suspension of the serviceability of the bridge during testing. To measure the response of medium to long span bridges (e.g. spans > 70 m), the use of ambient operating excitations (e.g. traffic loading, wind, etc) is favored due to the ease of implementation. Therefore, a significant practical challenge that remains is to determine how the proposed procedure performs with ambient noise as the source of excitation. At the same time, comparative studies can be

conducted to identify how the weight/speed of traffic affects the result of dynamic tests through field testing and to find which source of excitation may produce better repeatability or readability for modal parameters.

Damage scenarios in this case study are defined as small increments of damage at localized regions along a steel beam. However, issues remain to be addressed for more complex indeterminate structures such as multiple-girder bridges or multiple-span continuous beams, as well as other types of damage such as distributed damage due to corrosion of rebar in reinforced concrete bridges, or concrete deteriorations due to surface spalling and cracks commonly observed in cold regions. Further investigations are required to examine the potential of the proposed procedure for lower levels of damage with the purpose of improving its sensitivity to detect and locate the initiation of damage at the earliest possible stage. It is important to note that the correction for the temperature effect is obtained only for two temperature values in the laboratory. The accuracy of the correction value and subsequently the optimization solution can be improved by making measurements for a broader range of temperatures at the same level of damage. For real cases, performing the measurements in the early life of a structure before some damage is either introduced or increased is highly recommended.

In particular, parametric studies can be conducted further to examine specifically the performance of the statistical procedures with respect to various parameters such as: a) the number of embedded sensors to capture the displacement mode shapes properly, b) the impact of extrapolation and interpolation algorithms to resolve wavelets border distortion problem and to obtain a more accurate estimate of the mode shapes, and c) the selection of the type and/or the scale of the mother wavelet to find the best match for amplifying trivial changes in the mode shapes due to damage while mitigating noise at small levels.

APPENDIX A

A. Modal Excitation Methods for Real Field Testing of Bridges

This section reviews the relative advantages and limitations of different excitation methods for conducting modal tests on bridges. Vibration-based tests are encountered in real field measurements for measuring the dynamic response of a bridge to some applied loading. The latter may be caused by either deterministic (e.g. shaker) or random (e.g. ambient vibrations) sources of excitation (Felber 1994).

AI. Forced Vibration Testing Methods

Forced vibration tests are applied through controlled forces to induce vibration with the aim of measuring the structure's response to these known forces.

AI-1 Shaker Tests

Shakers are used to excite dynamically structures in a controlled manner. For large bridges, a shaker must produce sufficiently large forces to excite a structure in the desired range of frequency required to extract the mode shape of interest. Shakers are usually excited by a sinusoidal forcing function with a varying range of peak since forces. However, the range of maximum forces that can be imposed by a shaker is limited. The use of shakers with other excitations methods can be used to measure most accurately the important frequencies of the bridge. However, shakers are expensive to construct and their heavy weight is a big problem to move them to different locations on the bridge (Felber 1994, Cunha and Caetano 2006).

AI-2 Impact Tests

Impact testing methods are another type of forced vibration testing methods which are suitable for the excitation of short span bridges (e.g. < 30 m span). However, a number of problems arises when the impact hammer is implemented to excite large bridges. The lager is the size of the

bridge, the bigger is the mass of the impact hammer and thus, the more stronger is the impact maximum force. Aside from the difficulties associated with the instrumentation of the impact methods in large-scale bridges, the hammers with heavier masses could cause considerable local damage in the bridge. However, impact hammers are attractive for many researchers since they are inexpensive, portable, and can be implemented easily in experimental studies (Felber 1994).

There are different types of impact devices such as impulse hammers, Eccentric mass vibrators, and Electro-dynamic shakers. Although impulse hammers can provide a wide-band input to simulate different modes of vibration, they preclude the accurate estimation of modal damping factors. Moreover, these hammers cannot provide sufficient energy to excite some reverent modes of vibration corresponding to the higher frequency modes. Eccentric mass vibrators are other options for the impact testing which can be used to measure the response of the structure to sinusoidal forcing over a range of frequencies. However, these devices produce low force amplitude at low frequencies. Electro-dynamic shakers are defined as an alternative with a large variety of input force functions (e.g. random, multi-sine, etc), which may allow for the excitation of the structure at resonance frequencies and, consequently, for a direct identification of mode shapes. Special impulse devices are also designed to overcome the limitations of impulse hammers (Cunha and Caetano 2006).

AI-3 Pullback Tests

Pullback testing methods generally induce a free vibration motion in a bridge by displacing the bridge using an external force and quickly release the applied force. Examples include hydraulic rams, cables, bulldozers, tug boats, and chain blocks. These methods are also known as displacement-release excitation methods. The mass-release displacements are frequently occurred by hanging suddenly a heavy mass from the deck of a bridge. The Vasco da Gama cable-stayed bridge subjected to a free vibration test using a mass of 60.8 tons suspended from the deck (Felber 1994, Cunha and Caetano 2006). When the load is released, the structure tries to return to its position of static equilibrium. In this stage, the free vibration motion of the structure can be recorded to determine the modal parameters of the excited structure. To apply this method to a bridge, special care must be taken into account prior to any attempts to displace the structure. This is because access, jacking locations, budgets, and jurisdictions vary from one case to another. To completely control the forced vibration tests by this method the bridge must be

temporarily taken out of service. In general, displacement-release excitation methods are not very versatile and their implementation requires massive and expensive equipments (Felber 1994, Cunha and Caetano 2006).

AII. Ambient Vibration Testing Method

Ambient vibration testing methods are the simplest method of exciting long-span bridges, which are inherently difficult to excite using forced vibration testing methods. Modal tests based on ambient vibration measurements are best suited to bridges that cannot be taken out of service during the test. In particular, these methods can be considered as an efficient means to estimate accurately modal properties in a timely and cost-effective manner. Unlike forced vibration methods that require force generation apparatus, ambient vibrations results from natural sources of vibration such as wind, wave action, pedestrian and vehicular traffic, construction, etc (Felber 1994).

Although ambient vibration tests are beneficial over forced vibration methods, they encounter with some challenges in practice. It has to be noted that ambient vibration measurements are a combination of the dynamic characteristics of the monitored bridge as well as the vehicles passing over the bridge. Therefore, if the bridge is relatively short, the ratio of the mass and damping characteristics of the vehicles proportional to those of the bridge become significant and may lead to bias the results. Since the excitation is initially unknown and unmeasured in ambient vibration tests, certain assumptions are required in order to perform modal analysis. The forcing input function is assumed to contain all frequencies within the frequency spectrum; in other words the ambient vibration is assumed to be random having a constant power of excitation in the frequency domain. Assuming that the structure behaves linear, the response of the structure is a linear combination of individual force inputs. It is also assumed that that the response at a natural frequency is dominated by the corresponding mode shape, thereby the modes of interest are well separated and lightly damped (Felber 1994, Heerah 2009).

REFERENCES

Abdo, M.-B. and M. Hori (2002). "A numerical study of structural damage detection using changes in the rotation of mode shapes." Journal of Sound and vibration 251(2): 227-239.

Abramowitz, M. and I. A. Stegun (1966). "Handbook of mathematical functions." Applied mathematics series 55: 62.

Allen, M. S. and D. M. Aguilar (2009). "Model validation of a bolted beam using spatially detailed mode shapes measured by continuous-scan laser doppler vibrometry." AIAA structures, structural dynamics, and materials conference.

Alvandi, A., J. Bastien, E. Gregoire and M. Jolin (2009). "Bridge integrity assessment by continuous wavelet transforms." International Journal of Structural Stability and Dynamics 9(1): 11-43.

Alvandi, A. and C. Cremona (2006). "Assessment of vibration-based damage identification techniques." Journal of Sound and Vibration 292(1): 179-202.

Amezquita-Sanchez, J. P. and H. Adeli (2016). "Signal processing techniques for vibration-based health monitoring of smart structures." Archives of Computational Methods in Engineering 23(1): 1-15.

Amiri, G. G., A. Bagheri and S. A. S. Razaghi (2009). "Generation of multiple earthquake accelerograms compatible with spectrum via the wavelet packet transform and stochastic neural networks." Journal of Earthquake Engineering 13(7): 899-915.

Artba (2016). "The American Road and Transportation Builders Association annual report." data released from Department of Transportation Federal Highway Administration National Bridge Inventory, 2015 data. http://www.asce.org/magazine/20160315-analysis-reveals-58,495-u-s--bridges-are-structurally-deficient/

Avitabile, P. (2001). "Experimental modal analysis." Journal of Sound and vibration 35(1): 20-31.

Bajaba, N. and K. Alnefaie (2005). "Multiple damage detection in structures using wavelet transforms." Emirates Journal for Engineering 10: 35-40.

Balageas, D., C. P. Fritzen and A. Güemes (2006). "Structural health monitoring." Wiley Online Library.

Balmes, É., M. Basseville, F. Bourquin, L. Mevel, H. Nasser and F. Treyssede (2008). "Merging sensor data from multiple temperature scenarios for vibration monitoring of civil structures." Journal of Structural Health Monitoring 7(2): 129-142.

Banejad, M. and G. Ledwich (2002). "Correlation based mode shape determination of a power system." Acoustics, Speech, and Signal Processing (ICASSP), 2002 IEEE International Conference on, IEEE.

Banerjee, A. and G. Pohit (2014). "Crack investigation of rotating cantilever beam by fractal dimension analysis." Procedia Technology 14: 188-195.

Bentley, J. P. (1999). "Introduction to reliability and quality engineering." Addison Wesley Longman.

Beskhyroun, S., Wegner, L. D., & Sparling, B. F. (2012). "New methodology for the application of vibration-based damage detection techniques." Journal of Structural Control and Health Monitoring, 19(8), 632-649.

Bernal, D. (2000). "Damage localization using load vectors." European COST F3 Conference.

Bosela, P. A., P. A. Brady, N. J. Delatte and M. K. Parfitt (2013). "Failure Case Studies in Civil Engineering: Structures Foundations and the Environment." Civil and Environmental Engineering Department Books. Book 3, ASCE.

Brasiliano, A., G. N. Doz and J. L. V. de Brito (2004). "Damage identification in continuous beams and frame structures using the Residual Error Method in the Movement Equation." Nuclear engineering and design 227(1): 1-17.

Burton, T., C. Farrar and S. Doebling (1998). "Two methods for model updating using damage Ritz vectors." Proceedings-Spie the International Society for Optical Engineering.

CIRC, (2016), "Canadian Infrastructure Report Card." http://www.canadianinfrastructure. ca/ en/index.html.

Cao, M. and P. Qiao (2008). "Integrated wavelet transform and its application to vibration mode shapes for the damage detection of beam-type structures." Journal of Smart Materials and Structures 17(5): 055014.

Carden, E. P. and J. M. Brownjohn (2008). "ARMA modelled time-series classification for structural health monitoring of civil infrastructure." Journal of Mechanical Systems and Signal Processing 22(2): 295-314.

Casas, J. R. and A. C. Aparicio (1994). "Structural damage identification from dynamic-test data." Journal of Structural Engineering 120(8): 2437-2450.

Catbas, F., M. Gul and J. Burkett (2007). "Damage assessment using flexibility and flexibility-based curvature for structural health monitoring." Journal of Smart Materials and Structures 17(1): 015024.

Chance, J., G. Tomlinson and K. Worden (1994). "A simplified approach to the numerical and experimental modelling of the dynamics of a cracked beam." Proceedings-SPIE the International Society for Optical Engineering, Citeseer.

Chandrashekhar, M. and R. Ganguli (2009). "Damage assessment of structures with uncertainty by using mode-shape curvatures and fuzzy logic." Journal of Sound and Vibration 326(3): 939-957.

Chang K-C, Kim C-W (2016). "Modal-parameter identification and vibration-based damage detection of a damaged steel truss bridge." Journal of Engineering Structures 122:156-173

Chen, H., C. Spyrakos and G. Venkatesh (1995). "Evaluating structural deterioration by dynamic response." Journal of Structural Engineering 121(8): 1197-1204.

Cheng, J. and R.-c. Xiao (2007). "Probabilistic free vibration analysis of beams subjected to axial loads." Advances in Engineering Software 38(1): 31-38.

Chopra, A. K. (2007). "Dynamics of structures—theory and applications to earthquake engineering." Earthquake Spectra 23: 491.

Cornwell, P., C. R. Farrar, S. W. Doebling and H. Sohn (1999). "Environmental variability of modal properties." Experimental Techniques 23(6): 45-48.

Cornwell, P., C. R. Farrar, S. W. Doebling and H. Sohn (2008). "Environmental variability of modal properties." Experimental Techniques 23(6): 45-48.

Cross, E., K. Koo, J. Brownjohn and K. Worden (2013). "Long-term monitoring and data analysis of the Tamar Bridge." Journal of Mechanical Systems and Signal Processing 35(1): 16-34.

Grosso, A. D., & Lanata, F. (2014). "A long-term static monitoring experiment on RC beams: damage identification under environmental effect." Journal of Structure and Infrastructure Engineering, 10(7), 911-920.

Cunha, A. and E. Caetano (2006). "Experimental modal analysis of civil engineering structures." Journal of Sound and Vibration 40(6): 12-20.

Cunha, A., E. Caetano, R. Calgada and R. Delgado (1999). "Modal identification and correlation with finite element parameters of Vasco Da Gama Bridge." Society for Experimental Mechanics, Inc, 17 th International Modal Analysis Conference.

Curadelli, R., J. Riera, D. Ambrosini and M. Amani (2008). "Damage detection by means of structural damping identification." Journal of Engineering Structures 30(12): 3497-3504.

Cury, A., C. Cremona and J. Dumoulin (2012). "Long-term monitoring of a PSC box girder bridge: Operational modal analysis, data normalization and structural modification assessment." Journal of Mechanical Systems and Signal Processing 33: 13-37.

Dackermann, U., J. Li and B. Samali (2008). "Structural damage identification utilising PCA-compressed frequency response functions and neural network ensembles." 20th Australasian Conference on the Mechanics of Structures and Materials, Toowoomba, Australia.

Daubechies, I. (1992). "Ten lectures on wavelets." Society for Industrial and Applied Mathematics.

De Boor, C. (1978). "A practical guide to splines." Springer-Verlag New York.

Delaunay, D., G. Grillaud, J. Bietry and C. Sacre (1999). "Wind response of long-span bridges: in-situ measurements and modal analysis." SPIE proceedings series, Society of Photo-Optical Instrumentation Engineers.

Deraemaeker, A., A. Preumont and J. Kullaa (2006). "Modeling and removal of environmental effects for vibration based SHM using spatial filtering and factor analysis." Proceedings of IMAC XXIV, S.E.M., St. Louis, USA.

Ding, Q. and W. Ding (2006). "Stress wavelets: Multi-scale and multi-resolution assessment of soil structure by the drop-shatter method." Soil and Tillage Research 88(1): 168-179.

Doebling, S. W., C. R. Farrar and M. B. Prime (1998). "A summary review of vibration-based damage identification methods." Journal of Shock and Vibration Digest 30(2): 91-105.

Doebling, S. W., C. R. Farrar, M. B. Prime and D. W. Shevitz (1996). "Damage identification and health monitoring of structural and mechanical systems from changes in their vibration characteristics: a literature review." Los Alamos National Lab., NM (United States).

Douka, E., S. Loutridis and A. Trochidis (2003). "Crack identification in beams using wavelet analysis." International Journal of Solids and Structures 40(13): 3557-3569.

Douka, E., S. Loutridis and A. Trochidis (2004). "Crack identification in plates using wavelet analysis." Journal of Sound and Vibration 270(1): 279-295.

E976, A. "10 Standard Guide for Determining the Reproducibility of Acoustic Emission Sensor Response." ASTM International, West Conshohocken, PA, 2010.

Ewins, D. (2000). "Modal Testing: Theory, Practice, and Application." Research Studies Press.

Fan, W. and P. Qiao (2011). "Vibration-based damage identification methods: a review and comparative study." Journal of Structural Health Monitoring 10(1): 83-111.

Farrar, C. R., W. Baker, T. Bell, K. Cone, T. Darling, T. Duffey, A. Eklund and A. Migliori (1994). "Dynamic characterization and damage detection in the I-40 bridge over the Rio Grande." Los Alamos National Lab., NM (United States).

Farrar, C. R., P. J. Cornwell, S. W. Doebling and M. B. Prime (2000). "Structural health monitoring studies of the Alamosa Canyon and I-40 bridges." Los Alamos National Laboratory, Los Alamos, NM, Technical Report LA-13635-MS.

Farrar, C. R., S. W. Doebling and D. A. Nix (2001). "Vibration–based structural damage identification." Philosophical Transactions of the Royal Society of London. Series A: Mathematical, Physical and Engineering Sciences 359(1778): 131-149.

Farrar, C. R. and T. A. Duffey (1999). "Vibration-based damage detection in rotating machinery." Key Engineering Materials, Trans Tech Publ.

Farrar, C. R. and D. A. Jauregui (1998). "Comparative study of damage identification algorithms applied to a bridge: I. Experiment." Journal of Smart Materials and Structures 7(5): 704-719.

Farrar, C. R. and K. Worden (2012). "Structural health monitoring: a machine learning perspective." John Wiley & Sons.

Felber, A. J. (1994). Development of a hybrid bridge evaluation system, PhD. Dissertation, University of British Columbia, Canada.

Figueiredo, E., G. Park, J. Figueiras, C. Farrar and K. Worden (2009). "Structural health monitoring algorithm comparisons using standard data sets." Los Alamos National Laboratory (LANL), Los Alamos, NM (United States).

Foufoula-Georgiou, E. and P. Kumar (1994). "Wavelets in geophysics." Academic Pr.

Gabor, D. (1946). "Theory of communication. Part 1: The analysis of information." Electrical Engineers-Part III: Radio and Communication Engineering, Journal of the Institution of 93(26): 429-441.

Gentile, A. and A. Messina (2003). "On the continuous wavelet transforms applied to discrete vibrational data for detecting open cracks in damaged beams." International Journal of Solids and Structures 40(2): 295-315.

Gibbons, J. D. and S. Chakraborti (2011). "Nonparametric statistical inference." Springer.

Grégoire, É. (2011). "Utilisation De L'analyse Par Ondelettes Pour Un Suivi Automatisé D'endommagement De Structures Par L'analyse Des Modes Propres." Dissertation, Université Laval.

Hadjileontiadis, L., E. Douka and A. Trochidis (2005). "Fractal dimension analysis for crack identification in beam structures." Journal of Mechanical Systems and Signal Processing 19(3): 659-674.

Han, J. G., W. X. Ren and Z. S. Sun (2005). "Wavelet packet based damage identification of beam structures." International Journal of Solids and Structures 42(26): 6610-6627.

Harik, I. E., Shaaban, A. M., Gesund, H., Valli, G. Y. S., & Wang, S. T. (1990). "United States bridge failures, 1951–1988." Journal of Performance of Constructed Facilities, 4(4), 272-277.

Heerah, A. R. P. (2009). "Field investigation of fundamental frequency of bridges using ambient vibration measurements." Dissertation, McGill University, Canada.

Herrmann, A. W. (2013). "ASCE 2013 Report Card for America's Infrastructure. In IABSE Symposium Report." International Association for Bridge and Structural Engineering 99(33): 9-10

Hu W-H, Moutinho C, Caetano E, Magalhães F, Cunha Á (2012). "Continuous dynamic monitoring of a lively footbridge for serviceability assessment and damage detection." Journal Mechanical Systems and Signal Processing 33:38-55

Hu, N., X. Wang, H. Fukunaga, Z. Yao, H. Zhang and Z. Wu (2001). "Damage assessment of structures using modal test data." International Journal of solids and structures 38(18): 3111-3126.

Hu, W.-H., C. Moutinho, E. Caetano, F. Magalhães and Á. Cunha (2012). "Continuous dynamic monitoring of a lively footbridge for serviceability assessment and damage detection." Journal of Mechanical Systems and Signal Processing 33: 38-55.

Huth, O., G. Feltrin, J. Maeck, N. Kilic and M. Motavalli (2005). "Damage identification using modal data: Experiences on a prestressed concrete bridge." Journal of Structural Engineering 131(12): 1898-1910.

Iyama, J. and H. Kuwamura (1999). "Application of wavelets to analysis and simulation of earthquake motions." Earthquake Engineering & Structural Dynamics 28(3): 255-272.

Jackson, J. E. (2005). "A user's guide to principal components." John Wiley & Sons.

Jaiswal, N. and D. Pande (2015). "Sensitizing The Mode Shapes Of Beam Towards Damage Detection Using Curvature And Wavelet Transform." International Journal Of Scientific & Technology Research Volume 4(4).

Jiang, X. and H. Adeli (2007). "Pseudospectra, MUSIC, and dynamic wavelet neural network for damage detection of highrise buildings." International Journal for Numerical Methods in Engineering 71(5): 606-629.

Kendall, M. and A. Stuart (1979). "The advanced theory of statistics. Statistical Inference and Relationship." London, Charles Griffin.

Kim, C.-Y., D.-S. Jung, N.-S. Kim, S.-D. Kwon and M. Q. Feng (2003). "Effect of vehicle weight on natural frequencies of bridges measured from traffic-induced vibration." Earthquake Engineering and Engineering Vibration 2(1): 109-115.

Kim, H. and H. Melhem (2004). "Damage detection of structures by wavelet analysis." Journal of Engineering Structures 26(3): 347-362.

Kim, J.-T. and N. Stubbs (2003). "Nondestructive crack detection algorithm for full-scale bridges." Journal of Structural Engineering 129(10): 1358-1366.

Kim, J. T., Y. S. Ryu, H. M. Cho and N. Stubbs (2003). "Damage identification in beam-type structures: frequency-based method vs mode-shape-based method." Journal of Engineering Structures 25(1): 57-67.

Kreyszig, E. (2007). "Advanced engineering mathematics." John Wiley & Sons.

Law, S., X. Li and Z. Lu (2006). "Structural damage detection from wavelet coefficient sensitivity with model errors." Journal of Engineering Mechanics 132(10): 1077-1087.

Law, S., X. Li, X. Zhu and S. Chan (2005). "Structural damage detection from wavelet packet sensitivity." Journal of Engineering Structures 27(9): 1339-1348.

Lee JJ, Yun CB (2006). "Damage diagnosis of steel girder bridges using ambient vibration data." Journal of Engineering Structures 28 (6):912-925

Lee, J. and S. Kim (2007). "Structural damage detection in the frequency domain using neural networks." Journal of Intelligent Material Systems and Structures.

Lee, J. J., J. W. Lee, J. H. Yi, C. B. Yun and H. Y. Jung (2005). "Neural networks-based damage detection for bridges considering errors in baseline finite element models." Journal of Sound and Vibration 280(3): 555-578.

Lee, U. and J. Shin (2002). "A frequency-domain method of structural damage identification formulated from the dynamic stiffness equation of motion." Journal of Sound and Vibration 257(4): 615-634.

Lei, Y., J. Lin, Z. He and M. J. Zuo (2013). "A review on empirical mode decomposition in fault diagnosis of rotating machinery." Journal of Mechanical Systems and Signal Processing 35(1): 108-126.

Li, H., S. Li, J. Ou and H. Li (2010). "Modal identification of bridges under varying environmental conditions: temperature and wind effects." Journal of Structural Control and Health Monitoring 17(5): 495-512.

Liew, K. and Q. Wang (1998). "Application of wavelet theory for crack identification in structures." Journal of Engineering Mechanics 124(2): 152-157.

Lin, C. S. (1990). "Location of modeling errors using modal test data." AIAA journal 28(9): 1650-1654.

Lin, J. and M. Zuo (2003). "Gearbox fault diagnosis using adaptive wavelet filter." Journal of Mechanical Systems and Signal Processing 17(6): 1259-1269.

Liou, C. Y. and T. S. Jeng (1989). "The determination of mode shapes from modern cross-spectral estimates." Journal of Mechanical Systems and Signal Processing 3(3): 291-303.

Liu, C. and J. T. DeWolf (2006). "Effect of temperature on modal variability for a curved concrete bridge." Proceedings of SPIE–The International Society for Optical Engineering.

Liu, P. C. (1994). "Wavelet spectrum analysis and ocean wind waves." Wavelets in geophysics 4: 151-166.

Loutridis, S., E. Douka, L. Hadjileontiadis and A. Trochidis (2005). "A two-dimensional wavelet transform for detection of cracks in plates." Journal of Engineering structures 27(9): 1327-1338.

Loutridis, S., E. Douka and A. Trochidis (2004). "Crack identification in double-cracked beams using wavelet analysis." Journal of Sound and Vibration 277(4–5): 1025-1039.

Lucas, J.-M., et al. (2003). "Thermal actions on a steel box girder bridge." Proc., Institution of Civil Engineers: Journal of Structures and Buildings, SB2, 175–182.

Maeck, J., M. Abdel Wahab, B. Peeters, G. De Roeck, J. De Visscher, W. De Wilde, J.-M. Ndambi and J. Vantomme (2000). "Damage identification in reinforced concrete structures by dynamic stiffness determination." Journal of Engineering Structures 22(10): 1339-1349.

Maia, N., J. Silva, E. Almas and R. Sampaio (2003). "Damage detection in structures: from mode shape to frequency response function methods." Journal of Mechanical Systems and Signal Processing 17(3): 489-498.

Mallat, S. G. (1989). "A theory for multiresolution signal decomposition: the wavelet representation." Pattern Analysis and Machine Intelligence, IEEE Transactions on 11(7): 674-693.

Mazurek, D. F. and J. T. DeWolf (1990). "Experimental study of bridge monitoring technique." Journal of Structural Engineering 116(9): 2532-2549.

Melhem, H. and H. Kim (2003). "Damage detection in concrete by Fourier and wavelet analyses." Journal of Engineering Mechanics 129(5): 571-577.

Messina, A. (2004). "Detecting damage in beams through digital differentiator filters and continuous wavelet transforms." Journal of Sound and Vibration 272(1): 385-412.

Messina, A., E. Williams and T. Contursi (1998). "Structural damage detection by a sensitivity and statistical-based method." Journal of Sound and Vibration 216(5): 791-808.

Micro-Measurements "Vishay Precision Group." http://www.micro-measurements.com.

Misiti, M., Y. Misiti, G. Oppenheim and J. Poggi (1996). "Matlab Wavelet Toolbox User\'s Guide. Version 1." The MathWorks Inc., Natick, MA.

Montanari, L., A. Spagnoli, B. Basu and B. Broderick (2015). "On the effect of spatial sampling in damage detection of cracked beams by continuous wavelet transform." Journal of Sound and Vibration 345: 233-249.

Montgomery, D. C. and G. C. Runger (2012). "Applied Statistics and Probability for Engineers." John Wiley & Sons.

Moore, M., B. Phares, B. Graybeal, D. Rolander and G. Washer (2001). "Reliability of visual inspection for highway bridges." volume I: Final report.

Mosavi, A. A., R. Seracino and S. Rizkalla (2012). "Effect of temperature on daily modal variability of a steel-concrete composite bridge." Journal of Bridge Engineering 17(6): 979-983.

Moyo, P. and J. M. W. Brownjohn (2001). "Bridge health monitoring using wavelet analysis." Proceedings of SPIE· The International Soci—ety for Optical Engineering.

Mujica, L., M. Ruiz, F. Pozo, J. Rodellar and A. Güemes (2013). "A structural damage detection indicator based on principal component analysis and statistical hypothesis testing." Smart Materials and Structures 23(2): 025014.

Nair, K. K., A. S. Kiremidjian and K. H. Law (2006). "Time series-based damage detection and localization algorithm with application to the ASCE benchmark structure." Journal of Sound and Vibration 291(1): 349-368.

Ndambi, J.-M., J. Vantomme and K. Harri (2002). "Damage assessment in reinforced concrete beams using eigenfrequencies and mode shape derivatives." Engineering Structures 24(4): 501-515.

Ocak, H., K. A. Loparo and F. M. Discenzo (2007). "Online tracking of bearing wear using wavelet packet decomposition and probabilistic modeling: A method for bearing prognostics." Journal of Sound and Vibration 302(4): 951-961.

Ohkami, T., J. Nagao and S. Koyama (2006). "Identification of elastic materials using wavelet transform." Journal of Computers & Structures 84(29): 1866-1873.

Okafor, A. C. and A. Dutta (2000). "Structural damage detection in beams by wavelet transforms." Smart Materials and Structures 9(6): 906.

Olund, J. and J. DeWolf (2007). "Passive structural health monitoring of Connecticut's bridge infrastructure." Journal of Infrastructure Systems 13(4): 330-339.

Osornio-Rios, R. A., J. P. Amezquita-Sanchez, R. J. Romero-Troncoso and A. Garcia-Perez (2012). "MUSIC-ANN Analysis for Locating Structural Damages in a Truss-Type Structure by Means of Vibrations." Journal of Computer-Aided Civil and Infrastructure Engineering 27(9): 687-698.

Ovanesova, A. and L. Suarez (2004). "Applications of wavelet transforms to damage detection in frame structures." Journal of Engineering Structures 26(1): 39-49.

Pakrashi, V., A. O'Connor and B. Basu (2008). "A study on the effects of damage models and wavelet bases for damage identification and calibration in beams." Journal of Computer-Aided Civil and Infrastructure Engineering 22(8): 555-569.

Pandey, A. and M. Biswas (1994). "Damage detection in structures using changes in flexibility." Journal of Sound and Vibration 169(1): 3-17.

Pandey, A., M. Biswas and M. Samman (1991). "Damage detection from changes in curvature mode shapes." Journal of Sound and Vibration 145(2): 321-332.

Parloo, E., P. Guillaume and M. Van Overmeire (2003). "Damage assessment using mode shape sensitivities." Journal of Mechanical Systems and Signal Processing 17(3): 499-518.

Pearson K. (1901). "LIII. On lines and planes of closest fit to systems of points in space." Journal of Philosophical Magazine Series 6 2(11): 559-572.

Peeters, B. (2000). "System Identification and Damage Detection in Civil Engeneering." Department of Civil Engineering, PhD dissertation, Katholieke Universiteit Leuven, Leuven, Belgium.

Peeters, B., J. Maeck and G. De Roeck (2001). "Vibration-based damage detection in civil engineering: excitation sources and temperature effects." Journal of Smart Materials and Structures 10(3): 518.

Peeters, B. and C. Ventura (2003). "Comparative study of modal analysis techniques for bridge dynamic characteristics." Journal of Mechanical Systems and Signal Processing 17(5): 965-988.

Peng, Z., W. T. Peter and F. Chu (2005). "An improved Hilbert–Huang transform and its application in vibration signal analysis." Journal of Sound and Vibration 286(1): 187-205.

Perera, R. and C. Huerta (2008). "Identification of damage in RC beams using indexes based on local modal stiffness." Journal of Construction and Building Materials 22(8): 1656-1667.

Poudel, U., G. Fu and J. Ye (2005). "Structural damage detection using digital video imaging technique and wavelet transformation." Journal of Sound and Vibration 286(4): 869-895.

Quek, S. T., P. Tua and Q. Wang (2003). "Detecting anomalies in beams and plate based on the Hilbert–Huang transform of real signals." Journal of Smart materials and Structures 12(3): 447.

Reiff, A. J., M. Sanayei and R. M. Vogel (2016). "Statistical bridge damage detection using girder distribution factors." Engineering Structures 109: 139-151.

Reynders, E. (2012). "System identification methods for (operational) modal analysis: review and comparison." Archives of Computational Methods in Engineering 19(1): 51-124.

Rezaei, D. and F. Taheri (2010). "Damage identification in beams using empirical mode decomposition." Journal of Structural Health Monitoring.

Robertson, A. N., C. R. Farrar and H. Sohn (2003). "Singularity detection for structural health monitoring using holder exponents." Mechanical Systems and Signal Processing 17(6): 1163-1184.

Robertson, D. C., O. I. Camps, J. S. Mayer and W. B. Gish (1996). "Wavelets and electromagnetic power system transients." Power Delivery, IEEE Transactions on 11(2): 1050-1058.

Rosales, M. B., C. P. Filipich and F. S. Buezas (2009). "Crack detection in beam-like structures." Journal of Engineering Structures 31(10): 2257-2264.

Roveri, N. and A. Carcaterra (2012). "Damage detection in structures under traveling loads by Hilbert–Huang transform." Journal of Mechanical Systems and Signal Processing 28: 128-144.

Rucka M (2011). "Damage detection in beams using wavelet transform on higher vibration modes." Journal of Theoretical and Applied Mechanics 49 (2):399-417

Rucka, M. and K. Wilde (2006). "Application of continuous wavelet transform in vibration based damage detection method for beams and plates." Journal of Sound and Vibration 297(3): 536-550.

Rucka, M. and K. Wilde (2006). "Crack identification using wavelets on experimental static deflection profiles." Journal of Engineering Structures 28(2): 279-288.

Rytter, A. (1993). "Vibrational based inspection of civil engineering structures." Aalborg University.

Santos JP, Crémona C., Orcesi, AD, Silveira (2016). "Early Detection Based on Pattern Recognition and Data Fusion." Journal of Structural Engineering Doi: 10.1061/(ASCE)ST.1943-541X.0001643

Santos JP, Crémona C., Orcesi, AD, Silveira (2013). "Multivarite Statistical Analysis for Early Damage Detection." Journal of Engineering Structures 56: 273-285

Santos J, Crémona C, Silveira P, Calado L (2016). "Real-time damage detection based on pattern recognition." Journal of Structural Concrete 17(3): 338-354

Sahin, M. and R. Shenoi (2003). "Quantification and localisation of damage in beam-like structures by using artificial neural networks with experimental validation." Journal of Engineering Structures 25(14): 1785-1802.

Salawu, O. (1997). "Detection of structural damage through changes in frequency: a review." Journal of Engineering Structures 19(9): 718-723.

Salawu, O. and C. Williams (1994). "Damage location using vibration mode shapes." Proceedings of the 12th International Modal Analysis.

Salawu, O. S. and C. Williams (1995). "Bridge assessment using forced-vibration testing." Journal of Structural Engineering 121(2): 161-173.

Salgado, R., P. J. S. Cruz, L. F. Ramos and P. B. Lourenço (2006). "Comparison between damage detection methods applied to beam structures." CEC-EST - Comunicações a Conferências Internacionais : [129].

Sanz, J., R. Perera and C. Huerta (2007). "Fault diagnosis of rotating machinery based on auto-associative neural networks and wavelet transforms." Journal of Sound and Vibration 302(4): 981-999.

Shahsavari, V. (2011). "Applying the MASW method to estimate the thickness of superficial layers in concrete." Dissertation, Université de Sherbrooke, Canada.

Shahsavari, V., J. Bastien, L. Chouinard and A. Clément (2015). "A Novel Response-Based Approach to Localize Low Intensity Damage of Beam-Like Structures." Proc. of the 5th International Conference on Smart Materials and Nanotechnology in Engineering Vancouver, BC, Canada: 99-109.

Shahsavari, V., J. Bastien, L. Chouinard and A. Clémen (2017). " Likelihood-Based Testing of Wavelet Coefficients for Damage Detection in Beam Structures." Civil Structural Health Monitoring, 7(1), 79-98.

Shahsavari, V., L. Chouinard and J. Bastien (2017). "Wavelet-based analysis of mode shapes for statistical detection and localization of damage in beams using likelihood ratio test." Engineering Structures 132: 494-507.

Sohn H, Czarnecki JA, Farrar CR (2000) Structural health monitoring using statistical process control. Journal of Structural Engineering 126 (11):1356-1363

Sohn, H., J. A. Czarnecki and C. R. Farrar (2000). "Structural health monitoring using statistical process control." Journal of Structural Engineering 126(11): 1356-1363.

Sohn, H., M. Dzwonczyk, E. G. Straser, A. S. Kiremidjian, K. H. Law and T. Meng (1999). "An experimental study of temperature effect on modal parameters of the Alamosa Canyon Bridge." Earthquake Engineering & Structural Dynamics 28(8): 879-897.

Sohn, H., C. R. Farrar, F. M. Hemez, D. D. Shunk, D. W. Stinemates, B. R. Nadler and J. J. Czarnecki (2004). "A review of structural health monitoring literature: 1996-2001." Los Alamos National Laboratory Los Alamos, New Mexico.

Sohn, H., C. R. Farrar, N. F. Hunter and K. Worden (2001). "Structural health monitoring using statistical pattern recognition techniques." Journal of Dynamic Systems, Measurement, and Control 123(4): 706-711.

Sohn, H., C. R. Farrar, N. F. Hunter and K. Worden (2001). "Structural health monitoring using statistical pattern recognition techniques." Transactions-American Society of Mechanical Engineers Journal of Dynamic Systems Measurement And Control 123(4): 706-711.

Sohn, H., K. Worden and C. R. Farrar (2002). "Statistical damage classification under changing environmental and operational conditions." Journal of Intelligent Material Systems and Structures 13(9): 561-574.

Solís, M., M. Algaba and P. Galvín (2013). "Continuous wavelet analysis of mode shapes differences for damage detection." Journal of Mechanical Systems and Signal Processing 40(2): 645-666.

Spanos, P. D., G. Failla, A. Santini and M. Pappatico (2006). "Damage detection in Euler–Bernoulli beams via spatial wavelet analysis." Journal of Structural Control and Health Monitoring 13(1): 472-487.

Staszewski, W. J. and A. N. Robertson (2007). "Time–frequency and time–scale analyses for structural health monitoring." Philosophical Transactions of the Royal Society A: Mathematical, Physical and Engineering Sciences 365(1851): 449-477.

Strang, G. and T. Nguyen (1996). "Wavelets and filter banks." Wellesley-Cambridge Press, Wellesley, USA

Sun, Z. and C. Chang (2002). "Structural damage assessment based on wavelet packet transform." Journal of Structural Engineering 128(10): 1354-1361.

Sun, Z. and C. Chang (2004). "Statistical wavelet-based method for structural health monitoring." Journal of Structural Engineering 130(7): 1055-1062.

Taha, M., A. Noureldin, J. Lucero and T. Baca (2006). "Wavelet transform for structural health monitoring: a compendium of uses and features." Journal of Structural Health Monitoring 5(3): 267-295.

Taha, M. M. R., A. Noureldin, A. Osman and N. El-Sheimy (2004). "Introduction to the use of wavelet multiresolution analysis for intelligent structural health monitoring." Canadian Journal of Civil Engineering 31(5): 719-731.

Tedesco, J. W., W. G. McDougal and C. A. Ross (1999). "Structural dynamics." Addison Wesley.

Thyagarajan, S., M. Schulz, P. Pai and J. Chung (1998). "Detecting structural damage using frequency response functions." Journal of Sound and Vibration 210(1): 162-170.

Torrence, C. and G. P. Compo (1998). "A practical guide to wavelet analysis." Bulletin of the American Meteorological society 79(1): 61-78.

Fourier Transform. "http://pgfplots.net. Published on 2014-03-15."

Umesha, P., R. Ravichandran and K. Sivasubramanian (2009). "Crack detection and quantification in beams using wavelets." Computer-Aided Civil and Infrastructure Engineering 24(8): 593-607.

Vafaei, M., S. C. Alih, A. B. A. Rahman and A. b. Adnan (2015). "A wavelet-based technique for damage quantification via mode shape decomposition." Journal of Structure and Infrastructure Engineering 11(7): 869-883.

Vakil-Baghmisheh, M.-T., M. Peimani, M. H. Sadeghi and M. M. Ettefagh (2008). "Crack detection in beam-like structures using genetic algorithms." Applied Soft Computing 8(2): 1150-1160.

Vuong QH (1989). "Likelihood ratio tests for model selection and non-nested hypotheses." Econometrica: Journal of the Econometric Society 57(2):307-333

Wahab, M. A. and G. De Roeck (1999). "Damage detection in bridges using modal curvatures: application to a real damage scenario." Journal of Sound and Vibration 226(2): 217-235.

Wahalathantri, B. L., D. Thambiratnam, T. H. T. Chan and S. Fawzia (2010). "An improved modal strain energy method for damage assessment." Proceedings of the Tenth International Conference on Computational Structures Technology, Civil-Comp Press.

Wang, Q. and X. Deng (1999). "Damage detection with spatial wavelets." International journal of Solids and Structures 36(23): 3443-3468.

Wang D, Xiang W, Zeng P, Zhu H (2015) Damage identification in shear-type structures using a proper orthogonal decomposition approach, Journal of Sound and Vibration 355 (2015) 135-149

Wardhana, K., & Hadipriono, F. C. (2003). "Analysis of recent bridge failures in the United States." Journal of performance of constructed facilities, 17(3), 144-150.

Wenzel, H. and D. Pichler (2005). "Ambient vibration monitoring." John Wiley & Sons.

Wu, C., C. Lu and Y. Han (2013). "New algorithm for mode shape estimation based on ambient signals considering model order selection." EURASIP Journal on Advances in Signal Processing 2013(1): 8.

Wu, N. and Q. Wang (2011). "Experimental studies on damage detection of beam structures with wavelet transform." International Journal of Engineering Science 49(3): 253-261.

Xia, Y., B. Chen, S. Weng, Y.-Q. Ni and Y.-L. Xu (2012). "Temperature effect on vibration properties of civil structures: a literature review and case studies." Journal of Civil Structural Health Monitoring 2(1): 29-46.

Xu, Z.-D. and Z. Wu (2007). "Simulation of the effect of temperature variation on damage detection in a long-span cable-stayed bridge." Journal of Structural Health Monitoring 6(3): 177-189.

Yan, A.-M., G. Kerschen, P. De Boe and J.-C. Golinval (2005). "Structural damage diagnosis under varying environmental conditions—part I: a linear analysis." Journal of Mechanical Systems and Signal Processing 19(4): 847-864.

Yan A-M, Kerschen G, De Boe P, Golinval J-C (2005) Structural damage diagnosis under varying environmental conditions—part I: a linear analysis. Journal of Mechanical Systems and Signal Processing 19 (4):847-864

Yan A-M, Kerschen G, De Boe P, Golinval J-C (2005) Structural damage diagnosis under varying environmental conditions—part II: local PCA for non-linear cases. Journal of Mechanical Systems and Signal Processing 19 (4):865-880

Yan, A.-M., G. Kerschen, P. De Boe and J.-C. Golinval (2005). "Structural damage diagnosis under varying environmental conditions—part II: local PCA for non-linear cases." Journal of Mechanical Systems and Signal Processing 19(4): 865-880.

Yang, J. N., Y. Lei, S. Lin and N. Huang (2004). "Hilbert-Huang based approach for structural damage detection." Journal of Engineering Mechanics 130(1): 85-95.

Yesilyurt, I. and H. Gursoy (2013). "Estimation of elastic and modal parameters in composites using vibration analysis." Journal of Vibration and Control: 1077546313486275.

Zandbergen E, Haan R, Hijdra A (2001). "Systematic review of prediction of poor outcome in anoxic-ischaemic coma with biochemical markers of brain damage" Journal of Intensive care medicine 27 (10):1661-1667

Zang, C., M. I. Friswell and M. Imregun (2004). "Structural damage detection using independent component analysis." Journal of Structural Health Monitoring 3(1): 69-83.

Zhang, D., Y. Bao, H. Li and J. Ou (2012). "Investigation of temperature effects on modal parameters of the China National Aquatics Center." Advances in Structural Engineering 15(7): 1139-1153.

Zhang, Z. (1994). "Error study of bridge tests for the purpose of structure identification." Proceedings-Spie_The International Society For Optical Engineering.

Zhang, Z. and A. Aktan (1995). "The damage indices for the constructed facilities." Proceedings-Spie_The International Society For Optical Engineering.

Zhong, S. and S. O. Oyadiji (2007). "Crack detection in simply supported beams without baseline modal parameters by stationary wavelet transform." Journal of Mechanical Systems and Signal Processing 21(4): 1853-1884.

Zhong, S. and S. O. Oyadiji (2011). "Crack detection in simply supported beams using stationary wavelet transform of modal data." Journal of Structural Control and Health Monitoring 18(2): 169-190.

Zhou, Z. (2006). "Vibration-based damage detecton of simple bridge superstructures." Dissertation, University of Saskatchewan, Canada.